ANA ROSALINA PEREIRA RIBEIRO

UNVEILING THYMIC EPITHELIAL CELL ONTOGENY: A ROADMAP TO STUDY THE MICROENVIRONMENT FOR T-CELL GENERATION AND TOLERANCE

Tese de Candidatura ao Grau de Doutor em Ciências Biomédicas, submetida ao Instituto de Ciências Biomédicas Abel Salazar

Orientador – Doutor Nuno Miguel de Oliveira Lages Alves

Categoria – Investigador Principal

Afiliação – Instituto de Investigação e Inovação em Saúde (i3S); Instituto de Biologia Molecular e Celular (IBMC)

Coorientador – Doutor Alexandre Valentim Xavier Mourão do Carmo

Categoria – Investigador Principal

Afiliação – Instituto de Investigação e Inovação em Saúde (i3S); Instituto de Biologia Molecular e Celular (IBMC)

De acordo com o disposto no Decreto Lei nº 74/2006 de 24 de Março, esclarece-se ser da nossa responsabilidade a execução das experiências que estiveram na origem dos resultados apresentados, assim como a sua interpretação, discussão e redacção.

Nesta tese foram utilizados os resultados dos artigos publicados ou submetidos para publicação abaixo indicados:

Ribeiro AR, Rodrigues PM, Meireles C, Di Santo JP and Alves NL, *Thymocyte selection regulates the homeostasis of IL-7-expressing thymic cortical epithelial cells in vivo,* The Journal of Immunology, 2013. 191:1200-1209.

Ribeiro AR, Meireles C, Rodrigues PM and Alves NL, *The intermediate expression of CCRL1 reveals novel subpopulations of medullary thymic epithelial cells that emerge in the postnatal thymus*. European Journal of Immunology, 2014. 44(10):2918-2924.

Table of Contents

Acknowledgments

First of all, I would like to thank my supervisor, Nuno Alves, for the long and intense road that we walked since we arrived at “our one drawer, one bench lab”. I learnt a lot with you, and none of the lines written in this thesis or any of my achievements would be possible without you. Thank you for the opportunity.

I would also like to thank all the people directly involved in this work: my partner in crime (in and out the lab) Catarina Meireles; Pedro Rodrigues; and to the rest of the recently expanded team: Rute, Chiara, Gema, Leonor e Laura, thanks for everything.

This work was possible also with the great help of the IBMC/I3S services, from which I have to highlight some: I would like to thank specially Catarina Leitão, (Advance Flow Cytometry) for the long sortings and long talks. I would like to thank all the people from the Animal Facility (specially Sofia Lamas for the help in surgery procedures). ALM, CCGen and HEMS, thanks for all the technical help.

To the people from CAGE, headed by Alexandre do Carmo, for welcoming us in their lab and teaching me so many things. Apart from all the logistic help that I can never forget, CAGE was the home of really good friends that I will definitely keep for life: Liliana (a post-doc mais linda), Tita (obrigada pela tua força da natureza), Mafalda Santos (serei sempre a tua pirralha, velhota), Vânia (oh Bâaaania, que escândalo), Carine (a mais difícil de conquistar), Mafalda Araújo, Patrícia, Telmo, Catarina.

I am really a lucky girl, and the list of colleagues and friends that I made in the institute that I have to thank for the moments of sanity (or really awesome insanity) is not done yet: Mariana Resende (a tua prima é que agradece!); Marcos Cardoso (o nosso marroquino preferido), Rita Batista (os concertos sem ti não têm piada), Lília (que saudades do breakdance!). I cannot enumerate all of the people that made my walkings through the corridors more pleasant, but your smiles and nice words are all acknowledged in my heart!

To the people that kept me out of the lab, a huge thanks! You are really important in my life: Diana, Diogo, Raúl, Ritinha, Catarina, Telmo, Mi, Vitor: near or far from Porto, you made it my home! Thanks for all the chat conversations,

skype calls, festivals and holidays, dinners and nights out! Brandy, Rita, Ju, Mário, Gu, and Zézica, years won't break this friendship apart and coming back to you and to Amarante will be always my favorite plan for the weekend!

Finalmente, mas não nada menos importante, queria agradecer a toda a minha família pelo apoio que me deram, não só durante esta fase da minha vida, como em cada passo que dei! Não há nada mais importante e melhor que os mimos da família e só posso estar grata por ter a melhor do mundo (e pedir desculpa por nem sempre estar presente). Pai, Ricardo, Márcia, Leo e Guga, vocês são a minha vida. Mãe, esta também é para ti, sempre! PJay, não tenho palavras para agradecer todo o apoio e carinho, nos dias bons e mais ainda nos maus! Não podia ter escolhido melhor a pessoa para partilhar a minha vida!

Vocês sabem que não sou pessoa de muitas palavras, muito menos de muitas lamechices, prefiro sempre estar do que dizer. Durante este tempo aprendi que cada minuto conta, e cada minuto com todos vocês tem ainda um sabor mais especial! Muito obrigada a todos!

"(...) A viagem não acaba nunca. Só os viajantes acabam. E mesmo estes podem prolongar-se em memória, em lembrança, em narrativa. Quando o visitante sentou na areia da praia e disse:"Não há mais o que ver", saiba que não era assim. O fim de uma viagem é apenas o começo de outra. É preciso ver o que não foi visto, ver outra vez o que se viu já, ver na primavera o que se vira no verão, ver de dia o que se viu de noite, com o sol onde primeiramente a chuva caía, ver a seara verde, o fruto maduro, a pedra que mudou de lugar, a sombra que aqui não estava. É preciso voltar aos passos que foram dados, para repetir e para traçar caminhos novos ao lado deles. É preciso recomeçar a viagem. Sempre.(...)"

José Saramago in Viagem a Portugal

Summary

T lymphocytes exhibit a highly diverse T-cell receptor (TCR) repertoire that is crucial for their capacity to recognize and mount specific immune responses against foreign antigens. The thymus harbors a unique stromal cellular network that supports T cell development and education, in which thymic epithelial cells (TECs) are the major components. Thymic epithelium is classically divided in cortical (cTEC) and medullary (mTEC) cells and its proper differentiation is critical for the selection of a diverse and self-tolerant T-cell population. Cortical and medullary TECs derive from a common bipotent precursor that exists in both embryonic and postnatal thymus. Yet, the nature and bioavailability of thymic epithelial progenitors (TEPs), as well as the cellular and molecular mechanisms underlying TEC differentiation pathways downstream of the bipotent progenitor are still poorly understood.

In this thesis, using distinct TEC-specific reporter mouse models, in combination with *in vitro* and *in vivo* fate mapping strategies, we studied the molecular and cellular interactions that govern TEC differentiation pathways. As a crucial thymopoietic factor, Interleukin-7 (IL-7) is highly expressed within the thymus. Here, we showed that high IL-7 expression determines a specialized cTEC population that gradually declines as result of MHC/peptide-TCR-mediated interactions between TECs and thymocytes during selection. Additionally, we showed that this specialized cTEC subset has the capacity to generate both cTECs and mTECs in the embryonic thymus, indicating that epithelial precursors transverse through the cortical lineage before committing into mTEC.

Furthermore, we documented the emergence of novel mTEC subsets sharing cTEC and mTEC markers in the postnatal thymus, suggesting that mTEC differentiation maight follow distinct routes in the embryonic and postnatal thymus and that the bipotent progenitors reside within the cortical compartment after birth. Accordingly, exploiting clonogenic assays that selectively grow cells with stem-cell capacity, we demonstrated that cTECs appear to be enriched for epithelial progenitors with the ability to generate both epithelial lineages and to improve thymopoiesis in IL-7-deficient mice. Nevertheless, the abundance of cortical-residing TEPs declines with aging.

Together, these results indicate that the cortical compartment harbors the niche of bipotent precursors in the embryonic and early postnatal thymus, which

bioavailability declines across life. The homeostasis of this cTEC niche is controlled by continual TCR-mediated lympho-epithelial interactions.

Understanding the mechanisms underlying the establishment of the thymic microenvironment in the early phase of thymic development and its maintenance across life has become one of the major goals to comprehend the generation of a diverse and tolerant T cell population and, ultimately, intervene in cases of disorder.

Resumo

Os linfócitos T exibem um repertório muito diverso do receptor de células T (TCR), essencial para a sua capacidade de reconhecer e montar respostas imunitárias específicas contra antigénios externos. O timo possui um estroma único que suporta o desenvolvimento e a educação de células T, que é maioritariamente composto por células epiteliais do timo (TEC). O epitélio tímico é classicamente dividido em células corticais (cTEC) e medulares (cTEC) e a sua adequada diferenciação torna-se crítica para a selecção de uma população diversa e auto-tolerante de células T. As TEC corticais e medulares derivam de um precursor comum e bipotente que existe tanto no timo embrionário, como pós-natal. No entanto, a identidade e a biodisponibilidade dos progenitores epiteliais tímicos (TEP), bem como os mecanismos celulares e moleculares subjacentes às vias de diferenciação das TEC a jusante dos seus progenitores bipotentes ainda não se encontram completamente entendidas.

Nesta tese, utilizando diversos modelos de ratinho repórter específicos para TEC, e em combinação com estratégias *in vitro* e *in vivo* de mapeamento de descendência, estudamos as interações moleculares e celulares que regulam as vias de diferenciação das TEC. Como um conhecido factor timopoiético fundamental, a interleucina-7 (IL-7) é expressa em elevados níveis no timo. Aqui, mostramos que a expressão de IL-7 determina uma população homogénea de cTECs, cuja representação diminui gradualmente durante o desenvolvimento, como resultado de interações mediadas por complexos MHC/péptido-TCR entre TEC e timócitos, durante processos de selecção. Adicionalmente, mostramos que esta população especializada de cTEC tem a capacidade de originar tanto cTECs mTECs durante o desenvolvimento embrionário, sugerindo que os precursores epiteliais transitam pela linhagem cortical antes de se diferenciar em mTEC.

De forma complementar, documentamos o aparecimento de novas populações de mTEC partilhando marcadores característicos de cTEC e mTEC no timo pós-natal. Este facto sugere que os progenitores bipotentes encontram-se também no compartimento cortical após o nascimento e que a diferenciação medular pode seguir rotas distintas no timo embrionário e pós-natal. Em conformidade, explorando ensaios clonogénicos para crescer de forma selectiva células com capacidade de células-estaminais, demonstramos que as cTECs

estão enriquecidas para células progenitoras com a capacidade de gerar as duas linhagens epiteliais e para melhorar a timopoiese em ratinhos deficientes em IL-7. No entanto, a abundância destes progenitores residentes no córtex diminui com a idade.

Em suma, estes resultados mostram que o compartimento cortical retém uma população de precursores epiteliais bipotentes no timo pós-natal embrionário e pós-natal, cuja biodisponibilidade diminui ao longo da vida. A homeostasia deste nicho de cTECs é controlada por interações linfo-epiteliais contínuas mediadas por TCR.

A compreensão dos mecanismos subjacentes à criação do microambiente tímico na tanto na sua fase inicial de desenvolvimento como a sua manutenção ao longo da vida tornou-se um dos principais objetivos para melhor perceber a geração de células T e a indução da sua tolerância e, ultimamente, intervir em casos de doença.

List of Abbreviations

β5t – Proteasome subunit β5t

γc – common cytokine receptor gamma chain family

Aire – Autoimmune Regulator

APC – Antigen Presenting Cell

BAC – Bacterial Artificial Chromossome

CCL – CC-motif chemokine ligand

CCR – CC-motif chemokine receptor

CCRL – CC-motif chemokine receptor ligand

CD – cluster of differentiation

Cld - Claudin

CMJ – Cortico-Medullary Junction

cTEC – Cortical Thymic Epithelial Cell

CTSL – Cathepsin L

CTSS – Cathepsin S

CXCL – C-XC-motif chemokine ligand

DC – Dendritic cell

dGuo - 2-deoxyguanosine

DLL4 – Delta-like Ligand 4

DN – Double Negative

DP – Double Positive

E – Embryonic day

EGF – Epidermal Growth Factor

EpCAM – Epithelial Cell Adhesion Molecule

Fezf2 – FEZ family Zink Finger 2

FGF – Fibroblast Growth Factor

Foxn1 – Forkhead box protein N1

FTOC – Fetal Thymic Organ Culture

GFP – Green Fluorescent Protein

HSC – Hematopoietic Stem Cell

HSCT – Hematopoietic Stem Cell Transplantation

IL – Interleukin

LTβR – Lymphotoxin β Receptor

Lti – Lymphoid Tissue Inducer

MHC – Major Histocompatibility Complex

mTEC – Medullary Thymic Epithelial Cell

MTS – Mouse Thymic Stromal

Nb - Newborn

NCC – Neural Crest Cell

NK – Natural Killer

OPG – Osteoprotegerin

PDPN – Podoplanin

Plet-1 – Placenta Expressed Transcript 1

RAG – Recombination-activating Genes

RANK – Receptor Activator of NF-κB

RANKL – Receptor Activator of NF-κB Ligand

RFP – Red Fluorescent Protein

RTOC – Reaggregate Thymic Organ Culture

Sema3E – Semaphorin

SP – Single Positive

SSEA-1 – Stage-specific Embryonic Antigen 1

TCR – T-cell receptor

TEC – Thymic Epithelial Cell

TEP – Thymic Epithelial Progenitor

Tg - Transgenic

TNFRSF – Tumour Necrosis Factor Receptor Superfamily

TRA – Tissue-restricted Antigen

TRAF6 – Tumour Necrosis Factor Receptor Activator Factor 6

Treg – Regulatory T cell

TSSP – Thymus-specific serine protease

UEA-1 – Ulex Europaeus Agglutinin 1

YFP – Yellow Fluorescent Protein

Introduction

The capacity of our body to resist and fight pathogens, such as bacteria, parasites and virus, relies on the proper function of the immune system. The immune system comprises multiple and coordinated mechanisms that confer protection and/or infection resolution. It is classically divided in two main branches, the innate and the adaptive systems. While the innate system represents the first line of defense providing early and rapid broad responses, the adaptive system relies on lymphocytes and ensures life-lasting memory against a specific pathogen.

The extensive study of the immune system throughout time has uncovered many of the cellular and molecular interactions that regulate its development, homeostasis and function. However, the complexity of this unique network extends beyond the hematopoietic compartment and includes the active participation of the involving environmental tissue. For instance, lymphocytes within the adaptive system can be divided into two main populations, B and T cells, and despite their common origin, B- and T- cell generation requires distinct stromal instructive niches in the bone marrow and in the thymus, respectively. This thesis focuses on the thymic microenvironment that supports the generation of a broad T cell repertoire and guarantees tolerance induction.

In this introduction, I discuss the general concepts related to the development and differentiation of the thymic microenvironment and its function on the establishment of an accurate T cell repertoire. Further concepts are dissected within the results and discussion chapters.

Establishing the Immune System's accuracy: Recognizing foreign without harming self

One of the most remarkable properties of the immune system is its ability to specifically recognize, respond, and eliminate many foreign (non-self) antigens while not reacting to own (self) antigens. Tolerance to self-components, or self-tolerance, is maintained by several mechanisms, which can already be observed in cells of the innate branch. For instance, complement activation is regulated by a

series of proteins that avoid tissue damage by preventing the inadvertent binding of activated complement components to host cells or of spontaneous activation in plasma [1]. Similarly, Natural Killer (NK) cells possess inhibitory receptors for self-Major Histocompatibility Complex (MHC) molecules that prevent their activation towards healthy cells, being their killing capacity regulated by the balance between activating and inhibitory signals [2]. On the adaptive side of immune responses, while the random generation of a broad repertoire of lymphocytes maximizes the recognition of a diverse spectrum of foreign antigens, it also augments the possible emergence of self-reactive specificities. Therefore, immature B and T lymphocytes are generally probed for autoreactivity before leaving their maturation site, or held in check by a variety of checkpoint mechanisms.

As T cell-mediated responses are routinely associated with the most prevalent autoimmune disorders, such as psoriasis, rheumatoid arthritis, multiple sclerosis or type I diabetes, it is then important to understand the role of T cells in immunological responses.

T cell-mediated immunity

T cells express a unique membrane-bound antigen-recognizing T cell receptor (TCR), which recognizes short peptide fragments presented by MHC molecules on the surface of antigen presenting cells (APCs). Moreover, the restriction of the TCR to the MHC differs in CD4 (helper) and CD8 (cytotoxic) T cells, which recognize peptides bound to MHC class II or I (MHCII/I), respectively. Apart of these differences in antigen recognition, CD4 and CD8 T cells display distinct functions during an immune response. While CD8 T cells predominantly kill cells infected with viruses or other intracellular pathogens, CD4 T cells provide essential additional signals that mediate B cell responses and influence APC activity, in a concerted mechanism to resolve infection.

Upon maturation in the thymus, naïve T cells patrol the peripheral secondary lymphoid organs and are induced to proliferate and differentiate into effector cells upon antigen recognition and in the presence of co-stimulatory signals. Concomitantly, a small fraction of primed T cells differentiate into long-

lived memory T cells that ensure rapid responses against a secondary exposure to their specific antigen, for instance in the context of re-infection or vaccination [3].

Although naïve T cells only complete their maturation in the periphery, the selection of a diverse, self-tolerant and functional T cell pool occurs already within the thymus. The establishment of the unique and specialized thymic microenvironment, together with the mechanisms that mediate T cell development, are further dissected in the following sections.

Generating a diverse and self-tolerant T cell pool: thymic function and architecture

The role of the thymus was not fully understood until 55 years ago, since thymectomy in adult mice had not been associated with any immune defect. It was only with the work of Jacques Miller on thymectomized young mice that the role of the thymus on the generation of T cells was elucidated [4, 5]. The appearance of the thymus in evolution is linked to the emergence of lymphocytes expressing highly diverse antigen-recognition receptors based on DNA recombination of variable (V), diversity (D), and joining (J) elements. Concomitantly, the thymic microenvironment evolved to provide a unique cellular network to generate T cells with a huge diversity of TCR specificities [6]. Additionally, in order to cope with this huge diversity, the thymic microenvironment became dedicated to screen developing T cells for their capacity to recognize self-MHC/peptide complexes and purge or convert into regulatory lineages (Treg) the clones that reveal self-reactivity [7, 8]. This tolerance induction depends on a specialized thymic epithelial cell (TEC) stromal population.

During T cell development, there is an intricate migration of developing T cells through a tridimensional stromal cell network composed of non-hematopoietic cells, including TECs, mesenchymal and endothelial cells, and cells from hematopoietic origin such as dendritic cells (DCs) and macrophages [9]. TECs represent the major stromal component and are classically divided into two main subsets: cortical (cTECs) and medullary (mTEC) cells, which define specialized niches with distinct functions **(Figure I)**. While cTECs form an outer reticular

cellular network that regulates early phases of T cell development, such as attraction of lymphoid progenitors, commitment into T cell lineage and positive selection; mTECs support later stages of thymocyte differentiation and selection [10] **(**more detail in **Figure II and III)**. Proving their function, mice deficient on the TEC master regulator fork-head box N1 (Foxn1) (Nude mice) have a vestigial thymus and therefore display T cell immunodeficiency [11-13]. Additionally, deficiencies in key cTEC mediators of positive selection results in reduced repertoire diversity [14-17] and, in contrast, deficits on medullary compartmentalization are strongly associated with autoimmune syndromes [18-20].

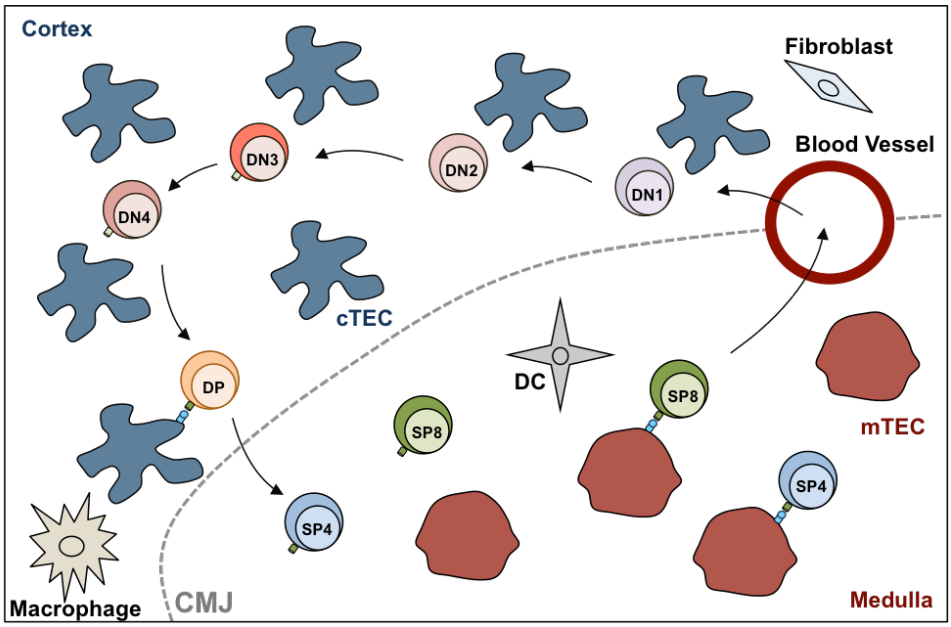

Figure I – General view of the compartment-specific stages of T cell development within the thymic microenvironment. In the differentiated thymus, hematopoietic precursors enter the thymus at the cortical-medullary junction (CMJ) through the blood stream. Within the cortex, cortical TECs (cTECs) support early stages of T cell development, from the commitment to selection of a broad T cell receptor (TCR) repertoire. In the medulla, thymocytes are selected based on their TCR affinities and further matured before leaving the thymus to the peripheral secondary lymphoid organs.

T cell production is also variable throughout life and although thymic function is initiated during embryogenesis, T cell output reaches its peak during early life and slowly declines with aging in a process known as thymic involution [21]. This physiological progress is characterized by both a progressive decrease in thymic cellularity and loss of tissue organization. Consequently, these alterations lead to the age-related decrease in T cell output and function, which ultimately result in more susceptibility to infections, autoimmune disorders and loss

of tumor immune surveillance [21]. Although such defects may be intrinsic to cells of hematopoietic origin, functional and structural alterations in the thymic epithelial compartment affect T cell production and repertoire selection throughout life. This evidence suggests the existence of lymphoid-extrinsic factors, which may derive from the thymic stromal microenvironment [22-25]. The age-associated loss of function is also detrimental for thymic regeneration upon acute damage, for instance, in conditioning treatments for hematopoietic stem cell transplantation (HSCT) or cancer therapy.

All together, this spectrum of pathologies reveals the importance of the correct establishment and maintenance of thymic epithelial compartments to tightly regulate thymocyte development and education throughout life. Therefore, comprehending thymic origin and epithelium differentiation is key to understand the mechanisms underlying T cell development and ultimately intervene in cases of deterioration of the immune system activity.

Thymic foundations: building the T-cell supportive epithelium

Thymic epithelial specification and epithelial progenitors

The development of a functional specialized thymic epithelium starts early in embryogenesis, however, TEC differentiation is a dynamic process that occurs throughout life. Thymic organogenesis starts with the out-budding and growth of the endoderm-derived epithelium of the third pharyngeal pouch between days 9 and 11 of murine embryonic gestation (E9-E11) [11, 12, 26-28]. TEC specification occurs concomitantly with the onset of Foxn1 expression at the ventral region of the newly formed anlagen. Then, epithelial proliferative capacity relies, initially, on signals provided by the surrounding neural crest-derived mesenchymal cells (NCC), such as Fibroblast Growth Factor 7 (FGF7) and 10 (FGF10) [29], and later on the continuous interaction with developing thymocytes [10].

Cortical and medullary thymic epithelial cells share a common progenitor of endodermal origin. Although bipotent thymic epithelial progenitors (TEPs) are maintained in Foxn1-deficient mice [30], this factor is required for the initiation of a

transcriptional program that engages the early TEP differentiation, and for the progression of cTECs and mTECs throughout distinct stages of differentiation [30, 31]. Epithelial precursors with the capacity to rebuild a functional thymus bearing cortical and medullary areas appear to be determinant of the thymic size in the embryonic and postnatal thymus [17, 32-36]. Still, the identity and abundance of TEC progenitors throughout life are not determined. Additionally, the developmental pathways for cTEC and mTEC lineage differentiation from the described bipotent progenitor are still not completely understood. This thesis focuses on the study of transitional stages within cTEC and mTEC developmental pathways.

Cortical epithelium development: establishing the thymic compartment for early T cell development and positive selection

The patterning of the thymic epithelium is initiated concomitantly with thymic colonization by the first hematopoietic cells. Cells displaying $Ly51^{+}CD205^{+}$ $\beta5t^{+}$ cortical phenotype can be found as early as embryonic day 12 (E12) of gestation [10, 37-39] in mice, suggesting that commitment into cTEC lineage occurs early in thymus ontogeny. Although this initial step of cortical development seems to be exclusively dependent on Foxn1 [12,34], the complete acquisition of the cTEC maturation markers MHCII and CD40 is partially impaired in mice exhibiting blocks in T cell development [12,34,[40]]. Thus, the intricate interaction between cTECs and developing thymocytes is not only essential for T cell education, but reciprocally for the correct establishment of the thymic cortical epithelium. Additionally, mesenchymal cells were shown to regulate cTEC homeostasis in a retinoic acid-dependent manner[41].

Attracted by a series of chemotactic factors produced by TECs, such as CC-chemokine ligand 21 (CCL21) and 25 (CCL25) and C-X-C motif chemokine (CXCL12) [42-45], fetal liver- or adult bone marrow- derived hematopoietic precursors seed the thymus from E11.5 throughout adulthood [44, 46, 47]. Upon entry in the thymus these progenitors initiate T-cell differentiation and eventually become irreversibly committed to T cell program. T cell differentiation is a well-

described pathway that can be followed by the expression of the CD4 and CD8 co-receptors. In the cortex, double negative (DN) cells for CD4 and CD8 expression progress through four distinct (DN1 to DN4) stages, identified accordingly to their expression profiles of CD25 and CD44 [9]. During this early phase of T cell development, cortical TECs provide survival and proliferation cues such as interleukin-7 (IL-7) [48-50]. Commitment to T cell-lineage occurs at DN1-DN2 stage transition upon triggering of the Notch signaling pathway, mediated by the cTEC-derived Delta-like 4 (DLL4) [51-54]. The consequent initiation of V(D)J rearrangement of the T-cell receptor (TCR) β-chain (*Tcrb*) or γ- (*Tcrg*) and δ- (*Tcrd*) chain genes at DN2-DN3, mediated by the recombination-activating genes (RAG) enzymes. At this stage, DN thymocytes can commit either into γδ or αβ T-cell lineage [55]. Progression towards the αβ lineage takes only place in DN3 thymocytes that express a functional pre-TCR at the surface, therefore passing β-selection and transiting to further DN4 and double positive (DP) stages **(Figure II)**.

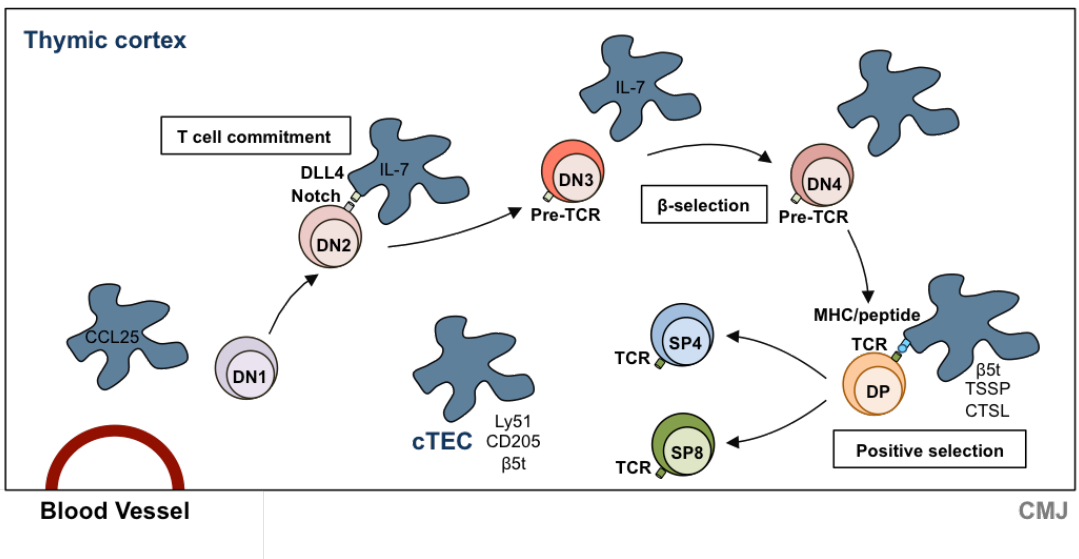

Figure II – Cortical stages of T cell development: from the entry in the thymus to positive selection. $Ly51^{+}CD205^{+}\beta5t^{+}$ cTECs express key factors that mediate the recruitment of hematopoietic precursors (CCL25), thymocyte survival (IL-7) and T cell commitment (Notch ligand DLL4), which drive the initiation of rearrangement of the TCR genes, resulting in the expression at the cell surface of the pre-TCR and, upon β-selection, the complete TCR complex. Positive selection is mediated by the cTEC-specific proteases β5t, TSSP and CTSL, which allow the expression of a range of MHC/peptide complexes. DP thymocytes that are able to recognize these complexes are positively selected and further differentiate into SP4 or SP8 lineage.

Upon successful rearrangement of the TCR α chain gene (*Tcra)*, DP thymocytes express a fully assembled αβ TCR, which is subsequently selected for

its functional capacity to recognize with moderate affinity self-peptide-MHC complexes presented by cTECs, in a process known as positive selection. This key checkpoint ensures the assortment of thymocytes restricted to self-MHC with broad TCR diversity potentially reactive to foreign antigens. Then, positively selected thymocytes can further differentiate into CD4 or CD8 single positive (SP) cells [56, 57]. cTECs are the major mediators of this process, expressing a unique set of selecting self-peptides generated by the particular action of several intracellular proteolytic enzymes. Among those, the cTEC-specific catalytic proteasome subunit β5t (*Psmb11*) is responsible for the profile of MHCI-associated peptides that select SP8s [14, 17, 37]. On the other hand, the thymus-specific serine protease (TSSP) (*Prss16*) and cathepsin L participate in the presentation of peptides that contribute to positive selection of MHCII-restricted SP4s [15, 16, 58-60] **(Figure II)**.

In order to acquire the specialized molecular machinery to proficiently support thymocyte survival, commitment and to process and present antigens that select a highly diverse pool of T cells, a functional and mature cTEC network has to be established. For that, cortical differentiation relies on reciprocal signals from developing thymocytes, resulting from continual lympho-stromal interactions. Apart of inducing cortical differentiation, signals from thymocytes beyond the DN stage negatively regulate the expression of genes associated with cTEC function, such as IL-7 and DLL4, indicating that thymocyte-TEC crosstalk control the homeostasis of a functional cortex [61, 62]. Yet, the nature of the thymocyte-derived molecular signals that mediate these checkpoints in cTEC differentiation is still uncovered.

Thymic medulla differentiation and its role on tolerance induction

The establishment of medullary areas is initiated in the murine embryonic thymus and was shown to derive from the emergence of small clonal islets, deriving from mTEC-committed progenitors [63, 64]. In agreement, cells bearing cortical phenotype are readily detected in the E12 thymus anlagen in distinct areas of cells expressing the medullary-associated claudin (Cld) -3 and -4 [64]. Although

mTEC differentiation starts during embryogenesis, complete compartmentalization of the thymus is only achieved after birth, with the growth of a conspicuous medullary compartment, fostered by the continuous interaction with developing T cells [7]. These findings suggest that TEC differentiation is a dynamic process across life, being the establishment of the epithelial compartment achieved through the expansion and differentiation of cortical and medullary committed cells. Nevertheless, alternative scenarios may be considered in which distinct pathways work in concert to establish the thymic microenvironment.

Thymocytes positively selected in the cortex upregulate their levels of CCR7 and PlexinD1 expression and migrate to the medulla, in response to their respective ligands CCL19/CCL21 and Semaphorin3E (Sema3E), mainly produced by medullary cells [9, 65-67]. There, thymocytes are exposed to a myriad of mTEC-derived self-antigens that represent virtually the whole body [10, 68-70]. For that, mTECs have the capacity to uniquely express clusters of tissue-restricted antigens (TRAs) throughout the medulla [71, 72]. This promiscuous gene expression observed in mTECs is, in part, dependent on Aire[73] and on the newly identified FEZ family zink finger 2 (Fezf2) [74]. Direct presentation of mTEC-derived TRAs or cross-presentation by dendritic cells (DCs) leads to deletion of autoreactive T cells or generation of regulatory T cells (Tregs). The fate of possibly harmful cells seems to depend on their TCR affinity for the self-peptide: strong signals drive apoptosis, while weaker interactions convert these cells into the regulatory lineage [75]. Therefore, only thymocytes that survive negative selection are able to further mature within the medullary cell network and exit to the periphery, where their maturation is completed [76] **(Figure III)**.

In order to be able to fully support the income of positively selected thymocytes and their selection, mTECs also undergo a coordinated differentiation process, which can be followed by the expression levels of co-stimulatory molecule CD80, MHCII and autoimmune regulator (Aire). Acquisition of these markers allows the description of a progenitor-progeny relationship amongst mTECs, in which $mTEC^{low}$ population ($CD80^{lo}MHCII^{lo}Aire^{-}$) contains the progenitors for the mature $mTEC^{high}$ ($CD80^{hi}MHCII^{hi}Aire^{+}$) cells [77, 78]. Nevertheless, terminally differentiated post-Aire stage, defined by involucrin

expression, may exist within mTEC^{low} cells [79-82], which makes the mTEC^{low} population heterogenous **(Figure V)**. Within the mTEC^{high} population, the emergence of Aire^{+} cells occurs at E16 [77, 78, 83] and is highly dependent on signals provided by cells of hematopoietic orgin [84-86].

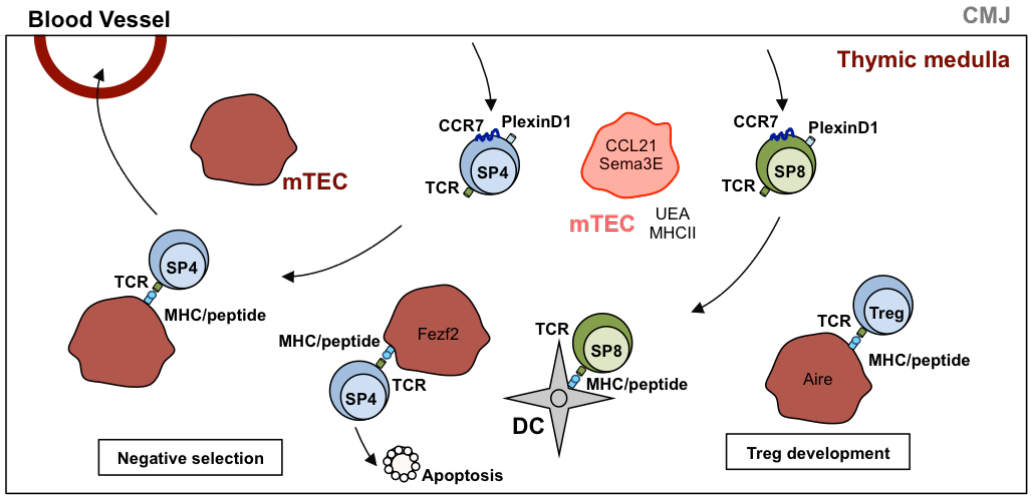

Figure III – T cell development mediated by the thymic medulla. Positively selected thymocytes migrate to the medulla, attracted by mTEC-derived signals such as CCL21 and Sema3E. Here, thymocytes are exposed to a myriad of self-peptides that are presented by MHC complexes. This promiscuous expression of self-antigens is mediated by two known factors: Aire and Fezf2. SP thymocytes bearing autoreactive TCRs undergo apoptosis during negative selection, or diverted into the Treg lineage. Only the cells that pass this selection event are further matured in the medullary compartment and leave the thymus to patrol the periphery.

In contrast to the cTEC lineage, the molecular signals and cellular partners of this TEC-thymocyte crosstalk are better comprehended. Mice displaying impaired NF-κB signaling were shown to have abnormal medullary architecture, including loss of Aire^{+}mTECs, and consequent severe autoimmune syndromes [87-90]. Indeed, the well-known mediators of NF-κB activation at the cell-surface and members of the tumour necrosis factor receptor super family (TNFRSF) are widely expressed in mTECs [91]. Among those, RANK (TNFRSF11a), CD40 (TNFRSF5), lymphotoxin β receptor (LTβR) and OPG (TNFRSF11b) play distinct roles in mTEC development, in which RANK signaling is the pivotal mediator [82, 83, 91, 92]. Nevertheless, RANK and CD40 double deficiency further reduces the frequency of Aire^{+} mTECs, while CD40 only partially compensate RANK absence [91], suggesting hierarchical roles for members of the TNFRSF. Additionally, the intrathymic cellular sources for RANK and CD40 ligands (RANKL and CD40L) and

their availability vary throughout development. In the embryonic thymus, RANKL$^+$ lymphoid tissue inducer (LTi) cells [77] and invariant Vγ5TCR$^+$ thymocytes [93], the first TCR$^+$ cells generated in the thymus, foster the development of the initial medullary areas by triggering maturation of mTEC progenitors. However, medulla expansion occurs only in the postnatal thymus, simultaneously with increased positive selection of CD4$^+$ and CD8$^+$ thymocytes. In particular, CD4$^+$SP act as the major source of CD40L [92] and autoantigen-specific CD4$^+$ thymocytes were shown to strongly interact with mTECs to foster their differentiation and expansion [94, 95]. Overall, these findings provide evidence for the existence of mTEC-restricted progenitor and for direct and linear precursor-product relationship within medullary lineage, in which distinct intrathymic hematopoietic partners participate sequentially in mTEC development [83]. While RANKL$^+$ LTi cells and invariant Vγ5TCR$^+$ thymocytes control embryonic mTEC emergence; CD4$^+$ thymocytes provide RANKL/CD40L for continued medulla maturation in the postnatal thymus **(Figure IV)**.

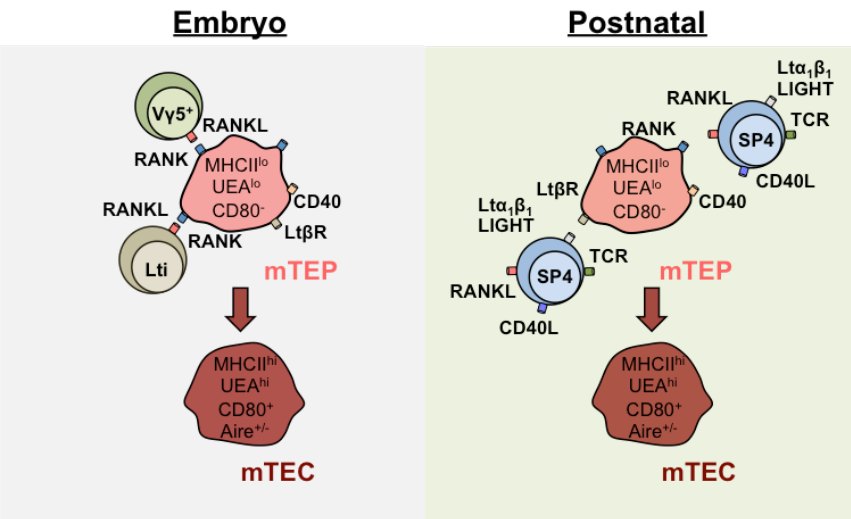

Figure IV – TEC-thymocyte crosstalk in medullary induction at embryonic and postnatal stages. Distinct hematopoietic partners and their TNFRSF ligands act sequentially in the differentiation of the mature medullary cells.

Although our understanding of TEC function and development has greatly increased in the years preceding the initiation of this thesis, we still lack evidence for the pathways that drive lineage commitment into cTEC and mTEC and how the two compartments differentiate downstream of the common bipotent TEP. As

already mentioned, the description of the compartment-restricted precursors [38, 63, 64] led to notion that both lineages would follow distinct and unrelated differentiation pathways, which diverge very early in TEC differentiation (as depicted in **Figure V**). However, it is still not clear how cortical and medullary fates relate to each other.

Furthermore, our knowledge on the nature of precursors and the mechanisms responsible for the establishment of the embryonic thymic epithelium and its maintenance throughout postnatal life remains limited. In the next sections, I describe the work that we conducted to answer some of these fundamental questions and the latest findings on TEC biology that help us to achieve our current view of TEC differentiation and consequent impact on thymus homeostasis.

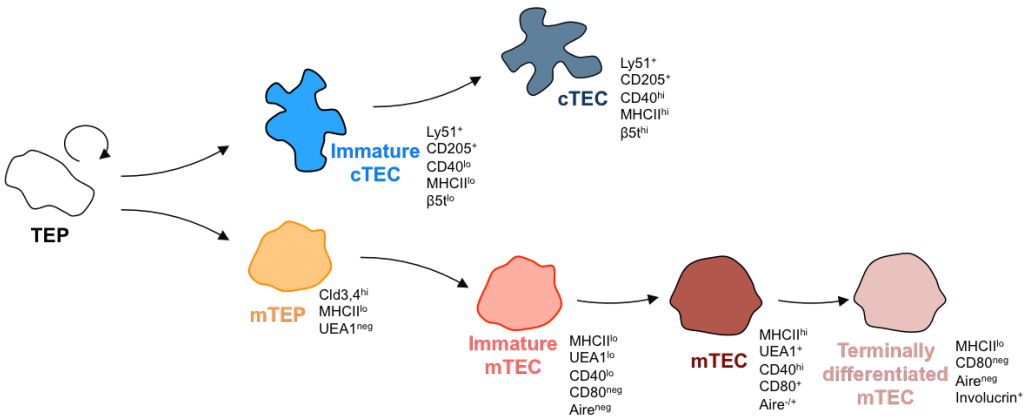

Figure V – TEC differentiation model. cTECs and mTECs derive from a common bipotent precursor (TEP) and follow unrelated differentiation pathways, in which compartment-restricted precursors fuel the respective compartment. Along differentiation, cortical and medullary cells acquire the maturation markers depicted in the figure.

Aims

In this thesis, we proposed to characterize the lineage relationship between cortical and medullary thymic epithelial cells and their progenitors in the embryonic **(Results Chapter I)** and postnatal **(Results Chapter II and III)** thymus. Additionally, we studied the role of TEC-thymocyte interactions and the molecular cues involved in cTEC/mTEC homeostasis and specification **(Results Chapter I and II)** and interrogated how the biovailability of thymic epithelial progenitors is controlled in the postnatal thymus **(Results Chapter III)**.

To address these questions, we combined the use of distinct TEC-specific reporter mouse models in immunocompetent and immunodeficient backgrounds with multiparametric flow cytometry analysis, gene expression profiling, *in vitro* thymic organotypic and TEC clonogenic cultures, as well as *in vivo* thymic transplantations.

We believe that deciphering these queries is of great value to understand the intricacies of thymic epithelium biology and the mechanisms underlying its major role in T cell development, education and, therefore, proper T cell function in the immune system.

Results Chapter I

Thymocyte Selection Regulates the Homeostasis of IL-7 - expressing Thymic Cortical Epithelial Cells In Vivo

Ana R. Ribeiro, Pedro M. Rodrigues, Catarina Meireles, James P. Di Santo and Nuno L. Alves

The Journal of Immunology, 191:1200-1209 (2013)

Abstract

Thymic epithelial cells (TECs) help orchestrate thymopoiesis, and TEC differentiation relies on bidirectional interactions with thymocytes. Although the molecular mediators that stimulate medullary thymic epithelial cell (mTEC) maturation are partially elucidated, the signals that regulate cortical thymic epithelial cell (cTEC) homeostasis remain elusive. Using IL-7 reporter mice, we show that TECs coexpressing high levels of IL-7 (*Il7*$^{YFP+}$TECs) reside within a subset of CD205^{+}Ly51^{+}CD40^{low} cTECs that coexpresses *Dll4*, *Ccl25*, *Ccrl1*, *Ctsl*, *Psmb11*, and *Prss16* and segregates from CD80^{+}CD40^{high} mTECs expressing *Tnfrsf11a*, *Ctss*, and *Aire*. As the frequency of *Il7*$^{YFP+}$TECs gradually declines as mTEC development unfolds, we explored the relationship between *Il7*$^{YFP+}$TECs and mTECs. In thymic organotypic cultures, the thymocyte-induced reduction in *Il7*$^{YFP+}$TECs dissociates from the receptor activator of NF-κB–mediated differentiation of CD80^{+} mTECs. Still, *Il7*$^{YFP+}$TECs can generate some CD80^{+} mTECs in a stepwise differentiation process via YFP^{-}Ly51^{low}CD80^{low} intermediates. *Il7*$^{YFP+}$TECs are sustained in *Rag2*$^{-/-}$ mice, even following *in vivo* anti-CD3ε treatment that mimics the process of pre-TCR β-selection of thymocytes to the double positive (DP) stage. Using Marilyn-*Rag2*$^{-/-}$ TCR transgenic, we find that positive selection into the CD4 lineage moderately reduces the frequency of *Il7*$^{YFP+}$TECs, whereas negative selection provokes a striking loss of *Il7*$^{YFP+}$TECs. These results imply that the strength of MHC/peptide–TCR interactions between TECs and thymocytes during selection constitutes a novel rheostat that controls the maintenance of IL-7-expressing cTECs.

Introduction

Thymic epithelial cells (TECs) provide essential instructive signals for the differentiation of T lymphocytes bearing a diverse TCR repertoire restricted to self-MHCs and tolerant to self-antigens. Cortical thymic epithelial cells (cTECs) and medullary thymic epithelial cells (mTECs) constitute two functionally distinct microenvironments for T cell differentiation [7, 9]. Whereas cTECs mediate early stages of T cell development, including lineage commitment, proliferation, and

positive selection, mTECs are largely responsible for negative selection [9, 96]. These two prototypical TEC subsets derive from a common bipotent precursor [30, 36], although the definition of compartment-specific progenitors remains incomplete.

The complete partitioning into cTECs and mTECs requires reciprocal instructive signals from developing thymocytes, a bidirectional interaction known as “thymic crosstalk” [39, 40, 84]. It has been recently elucidated that the establishment of the medullary epithelial niche relies on the cooperative contribution of members of the TNFR superfamily, including receptor activator of NF-κB (RANK), lymphotoxin β receptor (LTβR), and CD40, whose ligands are differentially expressed by several thymic hematopoietic cell types, namely, lymphoid tissue inducer cells, positively selected double positive (DP) thymocytes, αβ $CD4^+$ single positive thymocytes (SP4), and γδ T cells [10]. Still, our understanding of the molecular nature, as well as the impact, of thymic crosstalk for the homeostasis of cTECs is largely unresolved, owing in part to the paucity of appropriate markers to define checkpoints in their differentiation.

IL-7 is an essential cytokine for T cell development in humans, mice, and jawed fish [49, 97, 98], indicating a high functional conservation of the IL-7 signaling pathway in thymopoiesis. Several reports, including our own, have shown that IL-7 is predominantly produced by TECs within the thymus [50, 99-101]. Using IL-7 reporter transgenic mice, in which YFP expression identifies a subset of YFP^+ TECs that coexpress high levels of *Il7* (referred to as $Il7^{YFP+}$TECs), we documented that $Il7^{YFP+}$TECs gradually decay with age in a thymocyte-dependent manner that correlated inversely with the emergence of CD80-expressing mTECs, suggesting that these cells may define a particular cortical epithelial subset. Of interest, $Il7^{YFP+}$TECs are, conversely, sustained when T cell development is profoundly blocked in $Rag2^{-/-}Il2rg^{-/-}$ mice [50, 62], indicating that the regulation of their homeostasis is coupled to thymocyte–TEC interactions. These findings have raised the hypothesis that lympho-epithelial interactions affect the size and function of cortical epithelial microenvironments while promoting mTEC diversification [61, 62, 102]. Still, identification of the thymocyte-derived signals that modulate the size of the thymic IL-7 epithelial niche remains elusive.

In this article, we study the lineage relationship between *Il7*$^{YFP+}$TECs and other well-defined TEC subsets. In addition, we examine the regulation of *Il7*$^{YFP+}$TECs homeostasis in models of absent, positive, and negative thymocyte selection. We find that *Il7*$^{YFP+}$TECs represent a cortical epithelial subset that is able to give rise to mTECs in reaggregate thymic organ cultures (RTOCs), although less efficiently when compared with YFP^{-} counterparts. *Il7*$^{YFP+}$TECs are maintained in *Rag2*$^{-/-}$ mice, and their homeostasis is not substantially affected by *in vivo* anti- CD3ε treatment, which generates functionally incompetent DP thymocytes to undergo selection. Using TCR transgenic models, we show that thymocyte-TEC interactions during positive selection reduce *Il7*$^{YFP+}$TECs. Of note, negative selection induces a severe depletion of this subset. Our findings indicate that TCR-mediated signals delivered by thymocytes during thymic selection regulate IL-7-expressing TECs.

Materials and Methods

Mice

IL-7 reporter mice [B6.Cg-Tg (Il7-EYFP)5Pas] were backcrossed onto *Rag2*$^{-/-}$ [103] and Marilyn-*Rag2*$^{-/-}$ [104] C57BL/6 background. Dual reporter mice were generated by crossing IL-7 reporter mice with Ccrl1: eGFP reporter mice (CCRL1-reporter) [105]. Marilyn-*Rag2*$^{-/-}$ and CCRL1-reporter mice were kindly provided by Jocelyne Demengeot (Instituto Gulbenkian de Ciência, Oeiras, Portugal) and by Thomas Boehm (Max Planck Institute of Immunobiology and Epigenetics, Freiburg, Germany), respectively. Mice were housed under specific pathogen-free conditions, and experiments were performed in accordance with institutional guidelines. For fetal studies, the day of vaginal plug detection was designated embryonic day (E) 0.5.

Isolation and flow cytometry analysis of TECs

TECs were isolated as described [106]. Single-cell suspensions were stained with anti-CD4, anti-CD80, and anti-Ly51 (PE) Abs (BD Biosciences); anti-I-A/I-E (Alexa 780); anti-CD40 (PE); anti-CD45.2 (PerCP-Cy5.5); anti- EpCAM, anti-CD8 (APC); anti-CD205 (biotin), anti-EpCAM (eFluor 450) Abs, and streptavidin (PE-Cy7)

(eBioscience). Analysis was made with the FACSCanto II (BD Biosciences) and FlowJo software. Cell sorting was performed using the FACSAria I (BD Biosciences), with sort purities. 95%. A 510/10-nm band pass filter (502LP dichroic mirror) and 542/27-nm band pass filter (525LP dichroic mirror) were used to discriminate the GFP from the YFP signal.

Gene expression

For quantitative PCR, mRNA from sorted cells was purified using the RNeasy Micro Kit (QIAGEN). RNA was reverse transcribed to cDNA, using the SuperScript III First-Strand Synthesis System for RT-PCR (Invitrogen) and Random Hexamers (Fermentas), and then subjected to real-time PCR using either TaqMan Universal PCR Master Mix (Applied Biosystems) and primers for *Hprt*, *18s*, *Il7*, *Prss16*, *Ctsl*, *Aire*, *Dll4*, *Ccl25*, *Tnfrsf11a*, and *Psmb11* (also from Applied Biosystems); or iQ SYBR Green Supermix (Bio-Rad), using primers specific for *Actb* (forward: 59-CGTGAAAAGA- TGACCCAGATACA-39; reverse: 59-TGGTACCAGCAGAGGCATACAG-39), Ctss (forward: 59-CCATTGGGATCTCTGGAAGAAAA-39; reverse: 59-TC-ATGCCCACTTGGTAGGTAT-39), and *Ccrl1* (forward: 59-AGGTCCTCTG-ATTTCCTCTGC-39; reverse: 59-GCAGGAAGACTTTTGCGAAC-39). All samples were analyzed as triplicates, and the ΔΔCt method was used to calculate relative levels of target mRNA compared with *Hprt*, *18s*, or *Actb*. Procedures were done according to the manufacturer's protocols. Real-time PCR was performed in an iCycler iQ5 Real-Time PCR thermocycler (Bio- Rad). Data were analyzed using iQ5 Optical System software (Bio-Rad).

Fetal thymic organ culture

Freshly isolated E14.5 thymic lobes were used to establish fetal thymic organ cultures (FTOCs), as described [77]. Three to four lobes were used per condition to normalize intrathymic variations. FTOCs were cultured for 4 d in DMEM (Life Technologies), supplemented with 10% FCS, 2 mM L-glutamine (Life Technologies), and 360 mg/l 2-deoxyguanosine (dGuo) (Sigma-Aldrich). The dGuo-treated FTOCs were cultured with 5 mg/ml anti-RANK (αRANK) (R&D Systems) and/or with 10 mg/ml anti-LTbR mAb AC.H6 (kindly provided by Jeff

Browning, Biogen Idec, Weston, MA). For blocking experiments, anti-RANKL Ab (PeproTech) was added on days 0 and 4 of FTOC at a final concentration of 10 mg/ml. After 8 d in culture, stromal cells were isolated and analyzed by flow cytometry.

RTOC

Freshly isolated E14.5 thymic lobes were used to establish RTOCs, as described [77]. *Il7*$^{YFP+}$ and YFP^{-} TECs (CD45^{-}EpCAM^{+}) were sorted to high purity (>95%) using a FACSAria. RTOCs were established from mixtures of 100,000–150,000 TECs, with CD4^{+}CD8^{+} and CD4^{+} thymocytes at 1:1:1 ratio. After 8 d in culture, RTOCs were dissociated, and single-cell suspensions were analyzed by flow cytometry.

In vivo anti-CD3ε treatment

Neonatal 3- to 4-d-old *Rag2*$^{-/-}$ mice were injected i.p. with 10 mg/g (body weight) of purified anti-CD3ε mAb [107] (clone 1452C11; kindly provided by Dr. Benedita Rocha, Hôpital Necker, Paris, France). Mice thymi were collected and analyzed 12 d after treatment.

Immunohistological analysis

Thymic lobes were prepared as described [50]. Briefly, samples were fixed in 4% paraformaldehyde (Electron Microscopy Sciences), and 8-mm sections were stained with rabbit anti-GFP, biotinylated anti-CD205, anti-CD8, anti-MTS10, and rat anti-MHCII Alexa Fluor 647 as primary Abs, with Alexa Fluor 488 anti-rabbit, Alexa Fluor 647 anti-rat, and streptavidin Alexa 555 as secondary Abs (Invitrogen). MTS10 was kindly provided by Dr. R. Boyd (Monash Immunology and Stem Cell Laboratories, Monash University, Melbourne, Australia). Vectashield mounting medium with DAPI (Vector Laboratories) was used to prepare the slides. Analysis was performed in an AxioImager.Z1 (Zeiss). Images were processed with AxioVision (Zeiss) and Fiji Software.

Statistical analysis

Statistical analysis of the results was made using GraphPad Prism Software. The two-tailed Mann–Whitney U test was used for analysis between groups. A 95%

confidence interval was applied in the calculations, and samples with p values < 0.05 were considered significant (marked with *).

Results

Il7^{YFP+}*TECs identify a subset of cortical epithelial cells throughout development*

In IL-7 reporter mice, the expression of YFP identifies TECs (*Il7*$^{YFP+}$TECs) that arise early in embryonic development, gradually declining in proportion postnatally (Fig. 1A, 1C) in a thymocyte-dependent manner [50, 62]. We first examined how the development of *Il7*$^{YFP+}$TECs correlated with the differentiation of distinct thymic epithelial subsets. Both *Il7*$^{YFP+}$ and YFP^{-} TECs were phenotypically indistinguishable at E13.5–14.5, having the Ly51^{low}CD205^{low} phenotype. However, from E15.5 onward, although the majority of *Il7*$^{YFP+}$TECs retained a cortical Ly51^{high}CD205^{high} phenotype, a fraction of Ly51^{low}CD205^{low} cells emerged exclusively within the YFP^{-} fraction [Fig. 1B, top; age-matched wild- type (WT) thymi are shown in Supplemental Fig. 1]. It has been previously shown that the differential expression of CD205, CD40, and MHCII define distinct stages during cTEC development [38]. We found that *Il7*$^{YFP+}$ and YFP^{-} subsets gradually expressed CD205 and CD40 between E13.5 and 16.5. Noticeably, and in contrast to some YFP^{-} cells that progressively acquired higher levels of CD40 and decreased the expression of CD205, the majority of *Il7*$^{YFP+}$ TECs continually expressed CD205 and intermediate levels of CD40 (Fig. 1B, middle). The emergence of CD80^{+} mature mTECs occurred exclusively within the YFP^{-}CD40^{high} TEC subset and continually segregated from *Il7*$^{YFP+}$ TECs (Fig. 1B, bottom). Proportionally, *Il7*$^{YFP+}$ TECs made up 60% of the cortical-enriched TEC compartment about E13–15, identifying a cTEC subset that gradually declined as mTEC differentiation unfolded from E16 onward (Fig. 1C). Quantitatively, the initial rise in mature mTECs (E16-Nb) preceded the conspicuous drop in *Il7*$^{YFP+}$ TECs numbers observed from 1–2 postnatal wk onward (Fig. 1C and as shown previously in Ref. 13), implying that YFP^{-}TECs may be enriched in direct

precursors of mTECs. As such, we further investigate the mechanisms underlying the decay in *Il7*$^{YFP+}$ TECs and its relationship to the developing mTEC compartment.

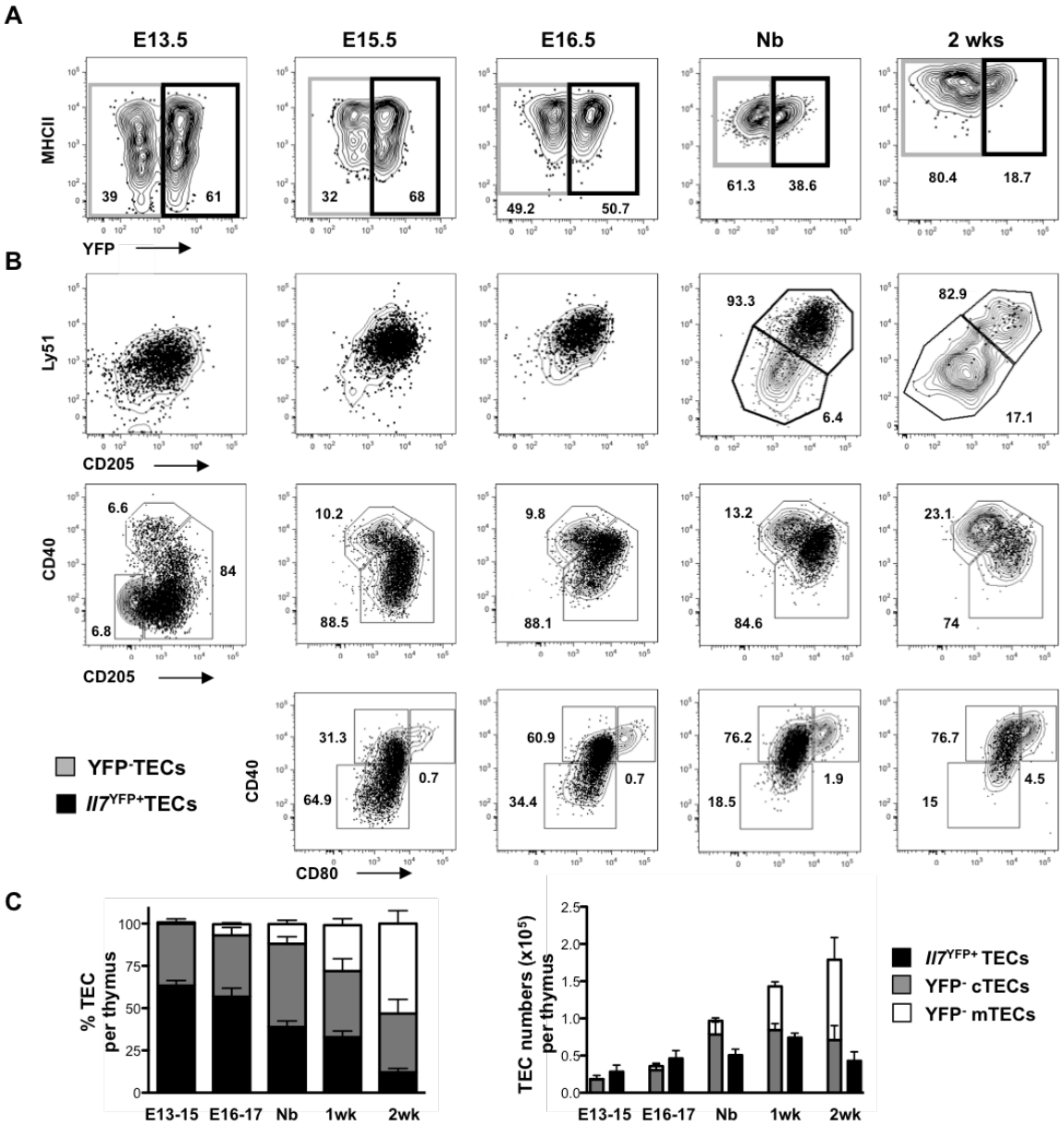

Figure 1. *Il7*$^{YFP+}$ TECs define a cortical epithelial subset that segregates from mTECs throughout thymic development. Thymi from IL-7 reporter mice were isolated at the indicated time points, and total TECs (defined hereafter as CD45$^-$EpCAM$^+$) were analyzed for the expression of **(A)** MHCII and YFP and **(B)** CD205, Ly51, CD40, and CD80. **(A)** The frequency of *Il7*$^{YFP+}$ TECs declines throughout organogenesis. Percentages in gated cells are shown. **(B)** Phenotypic comparison of YFP$^-$ (gray contour) and *Il7*$^{YFP+}$ TECs (black dot plot). The percentage of *Il7*$^{YFP+}$ TECs TECs within each gate is shown. Data are representative of at least three experiments per time point. **(C)** Bar graphs display the percentage and number of TEC subsets as mean 6 SD: YFP$^-$ cTECs (Ly51$^+$CD205$^+$) (gray bars), YFP$^-$ mature mTECs (Ly51$^-$CD205$^-$CD80$^+$) (white bars), and *Il7*$^{YFP+}$ TECs (black bars). *The number of *Il7*$^{YFP+}$ TECs at 2 wk is significantly lower than at 1 wk, $p < 0.05$.

We next analyzed how the phenotypic traits of *Il7*$^{YFP+}$ TECs related to the genetic profile of cTEC and mTEC lineages. The expression of genes associated with either cTEC [*Ccl25*, *Dll4*, *Il7*, *Ccrl1*, *Ctsl* (Cathepsin L), *Prss16* (TSSP), and *Psmb11* (β5t)] [7, 9, 38, 60, 105] or mTEC [*Tnfrs11a* (RANK), *Ctss* (Cathepsin S), and *Aire*] [7, 96] functions was compared in purified *Il7*$^{YFP+}$ and YFP^{-} TECs at successive stages of thymic development. Both subsets expressed similar levels of cTEC-associated genes at E14.5. However, as TEC differentiation ensued, the differences in gene expression progressively diverged between subsets, with *Il7*$^{YFP+}$ TECs retaining *Ccl25*, *Dll4*, *Il7*, *Ccrl1*, *Ctsl*, *Prss16*, and *Psmb11* expression (Fig. 2). *Il7*$^{YFP+}$ TECs were virtually devoid of the medullary-associated genes *Tnfrsf11a*, *Ctts*, and *Aire* at all analyzed stages. Of interest, these transcripts were detected in YFP^{-} TECs as early as E14.5 and steadily increased throughout development in this fraction (Fig. 2, *bottom*), reinforcing the idea that some direct precursors of mTECs may exist within YFP^{-} TECs.

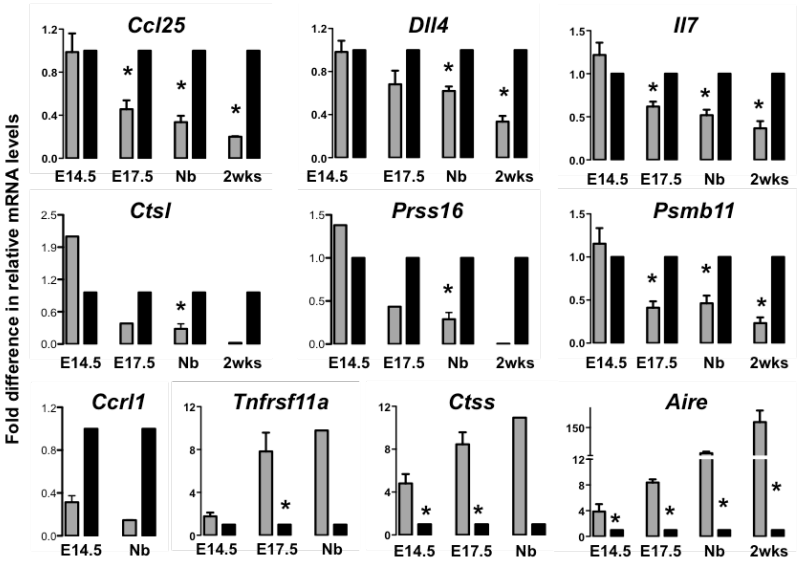

Figure 2. *Il7*$^{YFP+}$ TECs display a gene expression profile throughout development associated with cTECs. YFP^{-} (gray bars) and *Il7*$^{YFP+}$ TECs (black bars) were purified at the indicated time points and compared for the expression of *Ccl25*, *Dll4*, *Il7*, *Ctsl* (Cathepsin L), *Prss16* (TSSP), *Psmb11* (β5t), *Ccrl1*, *Tnfrsf11a* (RANK), *Ctss* (Cathepsin S), and *Aire*. Values were normalized to *18s*, *Hprt*, or *Actb*. *Il7*$^{YFP+}$ TECs were set as 1, at each time point, and the fold difference in the relative mRNA expression was compared with that of YFP^{-} TECs. Data are representative of two to four experiments per time point. *p<0.05.

To corroborate that *Il7*$^{YFP+}$ cells define a cTEC subset, we generated dual IL-7^{YFP}-CCRL1^{GFP} reporter mice by crossing IL-7 reporter mice with CCRL1-reporter mice, in which GFP expression identifies exclusively cTECs within thymic stromal cells [105]. Analysis of IL-7^{YFP}-CCRL1^{GFP} mice revealed four distinct epithelial subtypes in the postnatal thymus: YFP^{+}GFP^{+}, YFP^{-}GFP^{+}, YFP^{-}GFP^{low}, and YFP^{-}GFP^{-} (Fig. 3). *Il7*$^{YFP+}$ cells resided within *Ccrl1*$^{GFP+}$ cTECs, but a fraction

of *Ccrl1*$^{GFP+}$ cTECs lacked the expression of YFP. Conversely, the YFP^{-}GFP^{low} subset contained a mixture of CD80^{-} and CD80^{+} mTECs, and the YFP^{-}GFP^{-} fraction was majorly enriched in CD80^{+} mTECs (Fig. 3). Collectively, our phenotypic and genotypic characterization during thymic ontogeny provides evidence that *Il7*$^{YFP+}$ cells define a specialized cortical epithelial lineage.

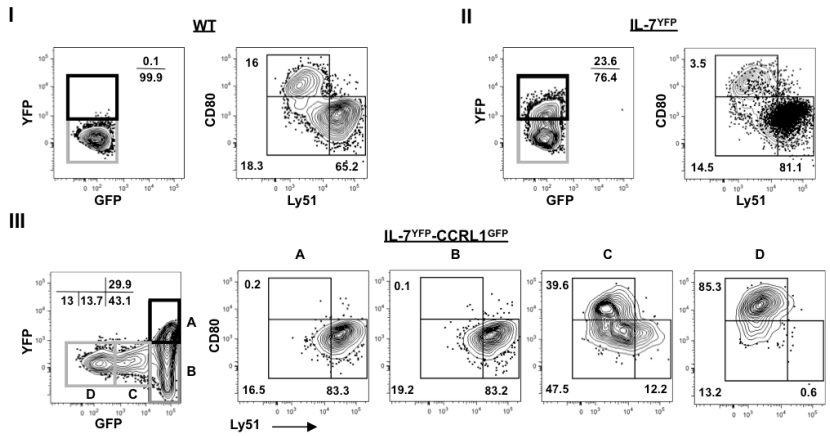

Figure 3. *Il7*$^{YFP+}$ cells are Ccrl1^{GFP+}- expressing cTECs. TECs from WT **(A)**, IL-7 reporter mice **(B)**, and IL-7^{YFP}-CCRL1^{GFP} dual reporter **(C)** neonatal littermates were analyzed for the expression of YFP and GFP. Subsets defined on the basis of YFP and GFP expression were compared for the expression of Ly51 and CD80. The percentages of total TECs **(A)**, *Il7*$^{YFP+}$ TECs **(B)**, and subtypes (a), (b), (c), and (d) **(C)** within each gate are shown. Data are representative of three independent experiments.

Thymocyte-induced loss of Il7^{YFP+} TECs dissociates from the RANK-mediated differentiation of CD80^{+} mTECs

We previously described a thymocyte-induced decay of *Il7*$^{YFP+}$ TECs that correlated inversely with the development of mTECs (Fig. 1) [62]. Using FTOCs, we first assessed whether *Il7*$^{YFP+}$ TECs share a direct precursor-product lineage relationship with mTECs. The differentiation of CD80^{+}Aire^{+} mTECs depends on signal transduction pathways induced by the TNFR superfamily members LTβR, RANK, and CD40, whose ligands are provided by hematopoietic cells [20, 77, 91, 92, 94, 108]. E14.5 FTOCs were maintained in medium for 8 d, which allowed a normal program of T cell differentiation (FTOCs), or were treated with dGuo (dGuo-FTOCs), which selectively eliminated thymocytes (data not shown). Because RANK signaling has a dominant effect in the generation of CD80^{+}Aire^{+} mTECs [77, 91, 92], in dGuo-FTOCs an agonistic anti-RANK mAb (αRANK) was used to “rescue” mTEC development (24). In dGuo-FTOC, *Il7*$^{YFP+}$ TECs were maintained and the formation of mTECs was impaired. Conversely, in FTOCs, *Il7*$^{YFP+}$ TECs markedly decreased the intensity of YFP reporter activity and

sustained a cTEC phenotype, with mTECs developing within the YFP$^-$ subset (Fig. 4A, 4B), partially recapitulating the perinatal in vivo phenotype. Treatment of dGuo-FTOCs with αRANK stimulated the development of CD80$^+$ mTECs within the YFP$^-$ fraction, as observed in FTOCs (Fig. 4A, 4C; the total patterns of TECs for WT and IL-7 reporter FTOCs are shown in Supplemental Fig. 2A and B, respectively). In contrast to FTOC, RANK activation did not induce a substantial decay in the intensity of YFP expression in *Il7*$^{YFP+}$ TECs (Fig. 4A–C).

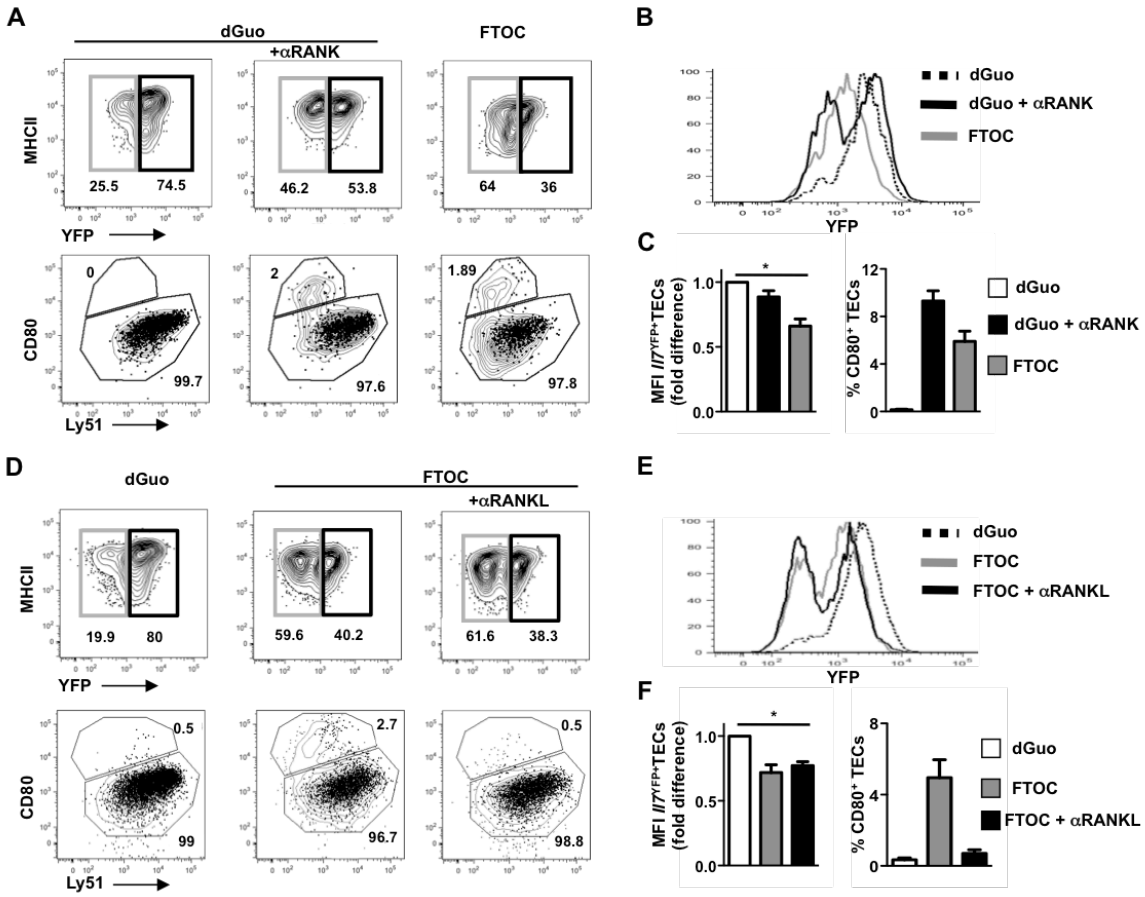

Figure 4. Thymocyte-mediated decrease in *Il7*$^{YFP+}$ TECs is independent of RANK-induced mTEC differentiation. (A–C) E14.5 FTOCs and dGuo- treated FTOCs (dGuo-FTOC) from IL-7 reporter mice were cultured in medium or, for dGuo-FTOC, in the presence of anti-RANK (αRANK). **(D–F)** E14.5 FTOCs were supplemented with the blocking Ab for RANK ligand (αRANKL). **(A and D)** Top, Total TECs were analyzed for the expression of YFP and MHCII. Percentages in gated cells are shown. Bottom, *Il7*$^{YFP+}$ (black dot plot) and YFP$^-$ (gray contour) TECs were compared for the expression of Ly51 and CD80. The percentage of *Il7*$^{YFP+}$ TECs within each gate is shown. Data are representative of four to six independent experiments. **(B and E)** The YFP expression on total TECs is compared for the conditions represented in **(A)** and **(D)**, respectively. **(C)** and **(F)** represent the fold difference in the recorded mean fluorescence intensity (MFI) of YFP expression in *Il7*$^{YFP+}$ TECs (left) and percentage of CD80$^+$ cells in the total TEC gate (right). *p<0.05.

As LTβR signals augment the RANK-driven development of mTECs [108],

we further treated dGuo-FTOCs with an agonistic anti-LTβR (αLTβR) mAb [108] alone or in combination with αRANK. Combined αRANK and αLTβR stimulation increased the frequency of $CD80^{+}YFP^{-}$ mTECs, whereas the YFP reporter activity was not substantially affected in $Il7^{YFP+}$ TECs (Supplemental Fig. 2D–F). No changes were observed upon single LTβR activation (data not shown). In a complementary approach, we examined the effects of blocking hematopoietic-derived RANKL on TEC differentiation in FTOCs, using anti-RANKL (αRANKL) Ab. Blocking of RANKL abrogated mTEC generation without affecting thymocyte-induced decay in the YFP reporter intensity of $Il7^{YFP+}$ TECs (Fig. 4D–F; the total patterns of TECs are shown in Supplemental Fig. 2C). These results underscore that the maintenance of $Il7^{YFP+}$ TECs is regulated by thymocyte-dependent interactions that are independent of the RANK- and LTβR-mediated maturation of mTECs.

$Il7^{YFP+}$ TECs can give rise to $CD80^{+}$ mTECs via a $YFP^{-}CD80^{low}Ly51^{low}$ intermediate stage

To directly determine the lineage potential of $Il7^{YFP+}$ TECs, we established RTOCs using isolated $Il7^{YFP+}$ and YFP^{-} TECs from E14.5 embryos (Fig 5A) mixed with mature DP and SP4 thymocytes to induce mTEC differentiation [91, 92, 94]. Whereas YFP^{-} TECs showed prominent mTEC progenitor activity, $Il7^{YFP+}$ TECs were also able to generate $CD80^{+}$ mTECs, following a stepwise downregulation of YFP expression and differentiation through a $YFP^{-}CD80^{low}Ly51^{low}$ intermediate stage (Fig. 5B–D). Collectively, the results suggest that although $Il7^{YFP+}$ TECs can give rise to mTECs, they are not the immediate precursor of mTECs, and instead indicate that mTECs arise from precursors residing within the YFP^{-} fraction.

$Il7^{YFP+}$ TECs persist in $Rag2^{-/-}$ thymus

Our previous observations showed that $Il7^{YFP+}$ TECs are sustained in mice with severe and premature arrest in thymopoiesis caused by the combined deficiency in *Rag2* and *Il2rg* genes [62]. Because lympho-epithelial interactions

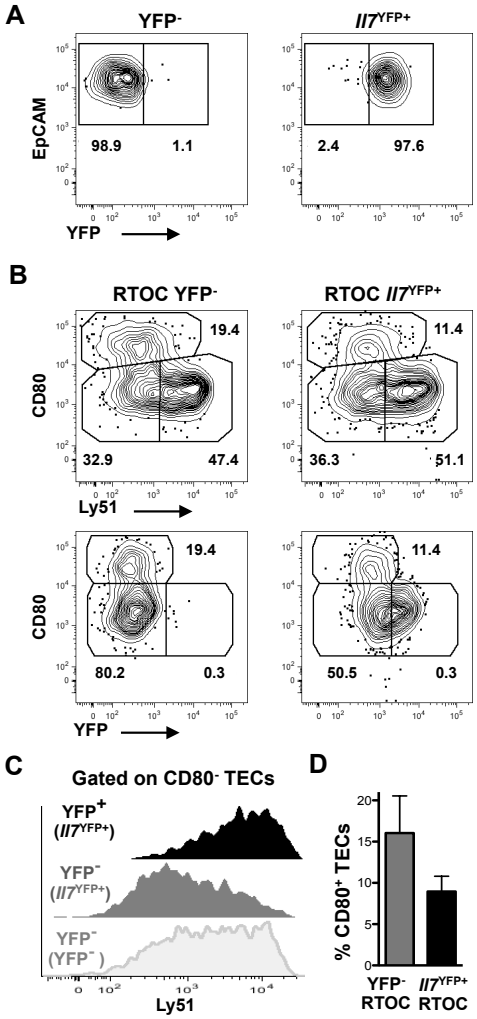

Figure 5. *Il7*$^{YFP+}$ TECs can give rise to mTECs. (A) YFP$^-$ and *Il7*$^{YFP+}$ TECs were purified from E14.5 embryos. RTOCs were established with sorted TEC fractions (average, 1–1.5x10^5) and thymocytes (DP and SP4) mixed in 1:1:1 ratio. (B) RTOCs were analyzed for the expression of YFP, Ly51, and CD80. (C) Ly51 expression levels within CD80$^-$ TECs: YFP$^+$ (black) and YFP$^-$ (gray) TECs derived from *Il7*$^{YFP+}$ RTOC and YFP$^-$ (white) TECs from YFP$^-$ RTOCs. (D) Bar graphs show frequencies of CD80$^+$ mTECs. Data from three experiments, each with three paired RTOCs per condition.

are minimal in *Rag2*$^{-/-}$*Il2rg*$^{-/-}$ mice [62], we analyzed the thymic microenvironment of *Rag2*$^{-/-}$ mice in which T cell development is blocked at the double negative (DN) 3 stage [103].As early stages of thymic cortical epithelium development are apparently normal in *Rag2*$^{-/-}$ mice [38], we examined whether the homeostasis of *Il7*$^{YFP+}$ TECs was regulated by lympho-epithelial interactions between immature thymocytes (DN1 to DN3) and TECs. During early stages of embryogenesis, *Il7*$^{YFP+}$ TECs follow developmental kinetics similar to those observed in mice with a normal T cell differentiation program (see Fig. 1). However, the proportion of *Il7*$^{YFP+}$ TECs was markedly maintained in *Rag2*$^{-/-}$ mice, displaying a cortical phenotype (Fig. 6A, 6B). An overall drop in the cellularity of both subsets in adult *Rag2*$^{-/-}$ mice was observed (Fig. 6C). The differentiation of mTECs was partially impaired, although few CD80$^+$ mTECs were detected within the YFP$^-$ fraction (Fig. 6B). These data suggest that the homeostasis of *Il7*$^{YFP+}$ TECs is regulated by

thymocyte-derived signals generated beyond β-selection.

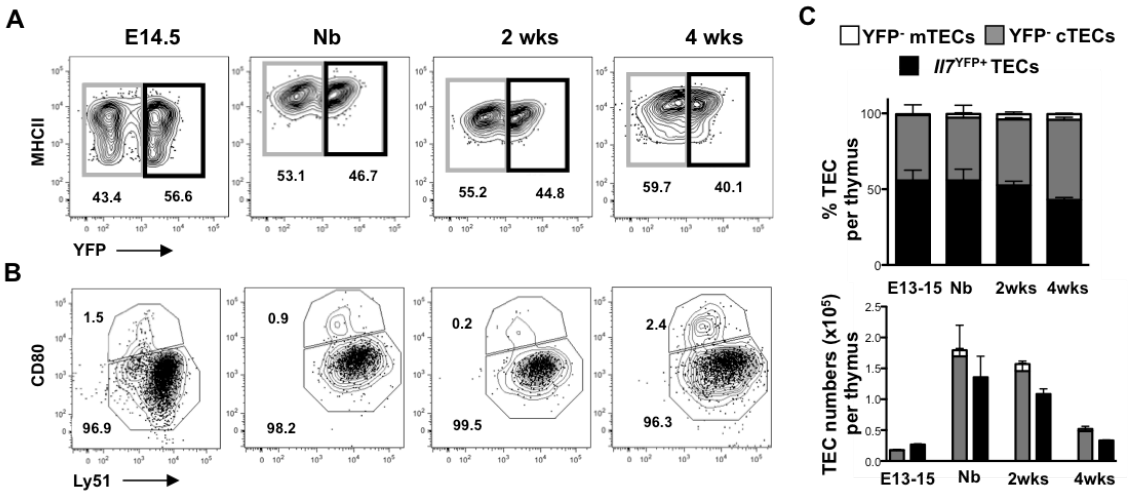

Figure 6. *Il7*$^{YFP+}$ TECs develop normally but are sustained in *Rag2*$^{-/-}$ mice. Thymi from IL-7 reporter *Rag2*$^{-/-}$ mice were isolated at the indicated time points. (A) Total TECs were analyzed for the expression of MHCII and YFP. Percentages in gated cells are shown. (B) The expression of Ly51 and CD80 was compared between YFP^{-} (gray contour) and *Il7*$^{YFP+}$ TECs (black dot plot). The percentage of *Il7*$^{YFP+}$ TECs within each gate is shown. Data are representative of two to three experiments per time point. (C) Bar graphs display the percentage and number of TEC subsets as mean 6 SD: YFP^{-} cTECs (Ly51^{+}CD205^{+}) (gray bars), YFP^{-} mature mTECs (Ly51^{-}CD205^{-}CD80^{+}) (white bars), and *Il7*$^{YFP+}$ TECs (black bars).

The homeostasis of Il7^{YFP+} *TECs is not altered by thymic crosstalk with TCR-deficient DP thymocytes*

Progression through the β-selection checkpoint involves the expression of a functional pre-TCR complex, composed of rearranged TCR β-chain together with pre-Tα and CD3 chains [9, 109]. To analyze whether thymic crosstalk during β-selection regulated the maintenance of *Il7*$^{YFP+}$ TECs, we used an *in vivo* experimental model of pre-TCR activation in which neonatal IL-7 reporter *Rag2*$^{-/-}$ mice were treated with anti-CD3ε mAb. Analysis 12 d after anti-CD3ε treatment showed a conspicuous increase in thymic size and total cellularity, reaching numbers similar to those in age-matched immunocompetent counterparts (Supplemental Fig. 3A, 3B). Cross-linking of CD3ε at the surface of *Rag2*$^{-/-}$ DN3 thymocytes mimics the pre-TCR signaling during β-selection [107], generating TCR-deficient DP thymocytes (Supplemental Fig. 3C) that cannot be positively selected and die by neglect. In treated IL-7 reporter *Rag2*$^{-/-}$ mice, despite the vast increase in thymocyte cellularity, the decrease in the frequency and intensity of the

YFP reporter activity of *Il7*$^{YFP+}$ TECs was significantly attenuated relative to age-matched immunocompetent thymus, and only moderately affected when compared with control *Rag2*$^{-/-}$ mice (Fig. 7A–C). Interestingly, *Il7*$^{YFP+}$ TEC numbers were also found to be augmented in this condition, indicating that the loss of this subset observed in immunocompetent mice is not regulated by thymic crosstalk with TCR-deficient DP thymocytes (Fig. 7D). This treatment increases the development of CD80^{+} mTECs within the YFP^{-} subset. Yet, the representation of mTECs did not reach the levels of the immunocompetent thymus (Fig. 7A–C; the total pattern of TECs is shown in Supplemental Fig. 3D). In E14 dGuo-FTOCs treated with anti-CD3ε mAb, mTECs were not generated (data not shown). This finding indicates that the *in vivo* observations were not due to a direct effect of the Ab on TECs, but resulted from the TCR-deficient DP thymocyte-TEC crosstalk.

To represent spatial organization in thymic microenvironments, thymic sections of control and treated IL-7 reporter *Rag2*$^{-/-}$ mice were analyzed by immunofluorescence. In control *Rag2*$^{-/-}$ thymus, the CD205^{+} cortical epithelium predominated, with few MTS10^{+} mTECs and scattered distribution of *Il7*$^{YFP+}$ TECs. In IL-7 reporter *Rag2*$^{-/-}$-treated mice, the formation of small medullary MHCII^{high}MTS10^{+} islets [22] was detected, yet smaller relative to immunocompetent mice. Immature single positive-DP thymocytes, marked by CD8 immunostaining, were compartmentalized within cortical areas and excluded from the medulla of *Rag2*$^{-/-}$-treated thymus. *Il7*$^{YFP+}$ TECs were clearly detected and scattered across the cortex of treated mice, with some cells found within the MTS10^{+} medullary pouches (Fig. 7E). Together, signals derived from TCR-deficient thymocytes progressing across DN to DP stages partially restored mTEC differentiation without substantially curtailing *Il7*$^{YFP+}$ TECs. In addition, these data point to the involvement of TCR-peptide/MHC interactions in regulating their maintenance.

The strength of thymocyte selection influences Il7^{YFP+} TEC homeostasis

To study the role of positive and negative selection events in the regulation

of *Il7*$^{YFP+}$ TEC homeostasis, we crossed IL-7 reporter *Rag2*$^{-/-}$ mice onto the Marilyn-*Rag2*$^{-/-}$ TCR transgenic background [104]. Marilyn- *Rag2*$^{-/-}$ mice express I-A-restricted TCR recognizing the male-specific HY Ag. Thymocyte development in IL-7 reporter Marilyn- *Rag2*$^{-/-}$ TCR double transgenic mice (Supplemental Fig. 4A, 4B) reproduced that observed in WT Marilyn- *Rag2*$^{-/-}$ TCR transgenic mice (data not shown), with positive selection in female mice and negative selection in male mice. Analysis of TEC differentiation showed that in IL-7 reporter Marilyn-*Rag2*$^{-/-}$

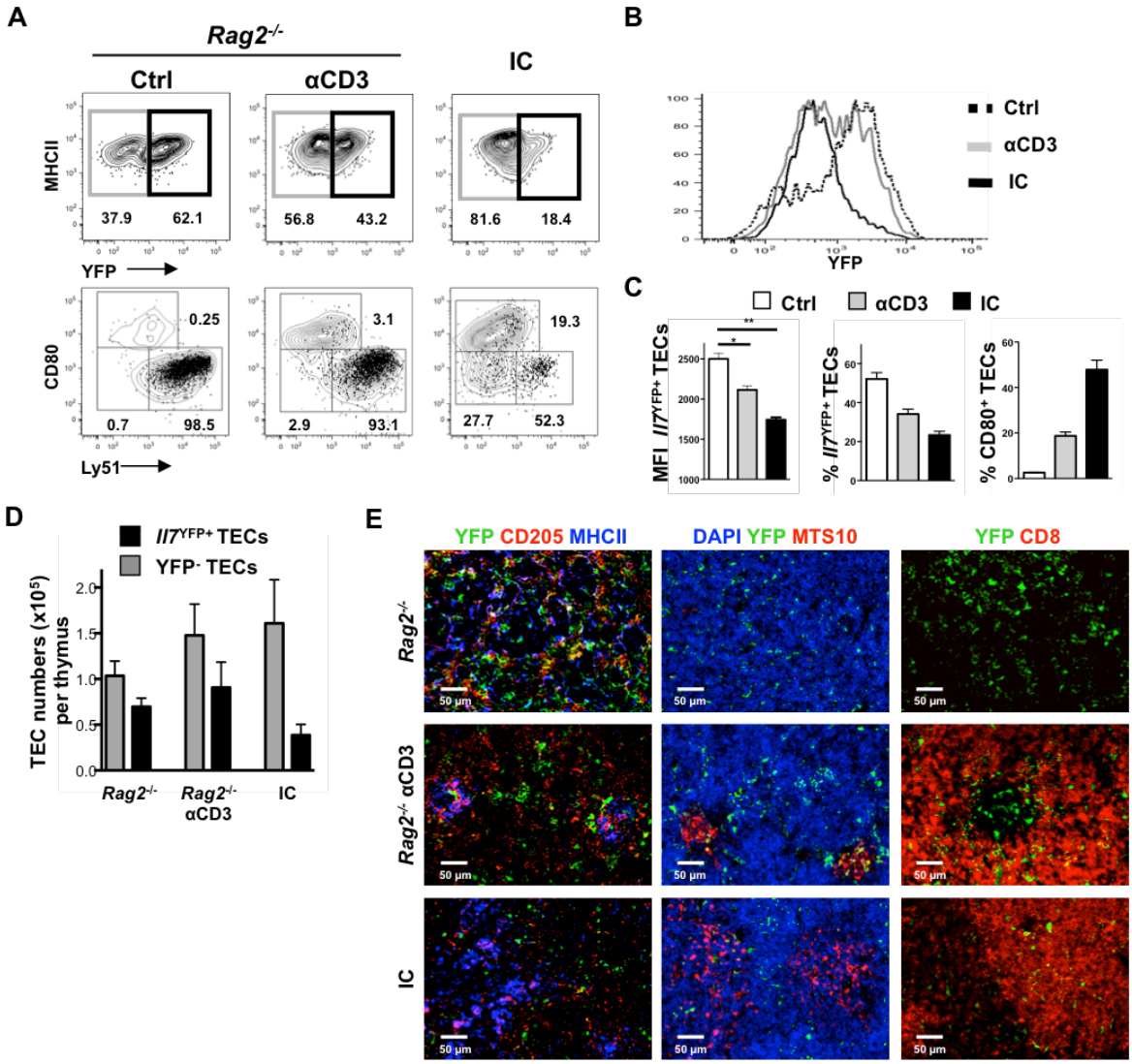

Figure 7. Bypassing β-selection by TCR-deficient thymocytes partially restores mTEC differentiation without significantly curtailing *Il7*$^{YFP+}$ TECs. (A) IL-7 reporter *Rag2*$^{-/-}$ neonatal mice were analyzed 12 d after anti-CD3ε treatment (αCD3), together with age-matched (12–14 d old) IL-7 reporter *Rag2*$^{-/-}$ control (Ctrl) and IL-7 reporter immunocompetent (IC) mice. Top, Total TECs were analyzed for the expression of YFP and MHCII. Percentages in gated cells are shown. Bottom, YFP^{-} (gray contour) and *Il7*$^{YFP+}$ TECs (black dot plot) were compared for the expression of Ly51 and CD80. Numbers represent the percentages of *Il7*$^{YFP+}$ TECs within each gate. (B) The YFP expression on total TECs is compared for the different conditions in (A). Data are representative of four experiments. (C) Mean fluorescence intensity (MFI) of YFP expression in *Il7*$^{YFP+}$ TECs (left), percentage of *Il7*$^{YFP+}$(middle), and CD80^{+} (right) cells within total TECs. *p<0.05, **p<0.0001. (D) Bar graphs display the percentage and number of YFP^{-} (gray) and *Il7*$^{YFP+}$(black) TECs as mean 6 SD. (E)

Immunohistochemical analysis of untreated *Rag2*$^{-/-}$, αCD3-treated *Rag2*$^{-/-}$ (αCD3), and age-matched IC IL-7 reporter mice thymic sections stained with the indicated Abs (CD205 red and MHCII blue; DAPI blue and MTS10 red; YFP green and CD8 red).

female, and comparatively so with IL-7 reporter *Rag2*$^{-/-}$ littermates, positive selection of CD4 thymocytes was sufficient to reduce the frequency and abundance of *Il7*$^{YFP+}$ TECs and promoted the development of YFP^{-} mTECs (Fig. 8A–C), phenocopying the epithelial differentiation observed in the age-matched immunocompetent thymus (Fig. 7). Strikingly, negative selection induced a conspicuous loss in the proportion and intensity of YFP reporter activity of *Il7*$^{YFP+}$ TECs, with a concomitant increase in the number of YFP^{-} TECs and the emergence of Ly51^{-}CD80^{low} TECs (Fig. 8A–C). These sex differences in the representation of TEC subsets were not manifested in IL-7 reporter *Rag2*$^{-/-}$ mice (data not shown). The total pattern of TECs for IL-7 reporter-*Rag2*$^{-/-}$ and IL-7 reporter-Marilyn- *Rag2*$^{-/-}$ and for C57BL/6 *Rag2*$^{-/-}$ and Marilyn- *Rag2*$^{-/-}$ are shown in Supplemental Fig. 4C and 4D. Thus, our findings indicate that the strength of TCR–peptide/MHC interactions occurring during thymocyte selection dynamically controls the proportion of the IL-7-expressing cortical epithelial niche.

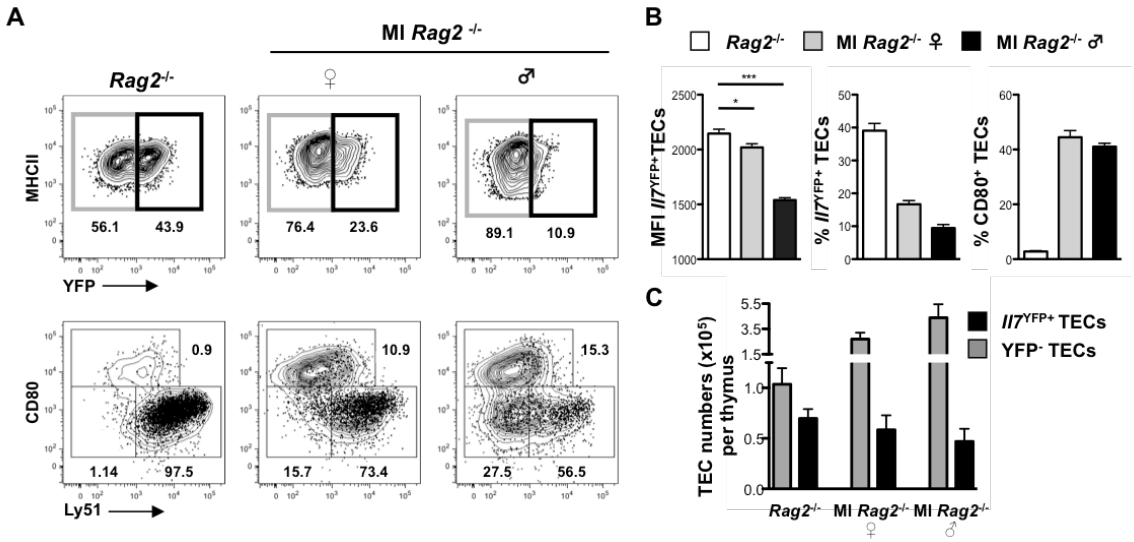

Figure 8. The strength of TCR–MHC interactions during thymocyte selection controls the homeostasis of *Il7*$^{YFP+}$ TECs. Thymi from female (♀) and male (♂) IL-7 reporter Marilyn-*Rag2*$^{-/-}$ mice (MI *Rag2*$^{-/-}$) were analyzed together with IL-7 reporter *Rag2*$^{-/-}$ (*Rag2*$^{-/-}$) littermates at 12–14 d of age. (A) Top, Total TECs from *Rag2*$^{-/-}$ and from female and male MI *Rag2*$^{-/-}$ mice were examined for the expression of YFP and MHCII. Percentages in gated cells are shown. Bottom, YFP^{-} (gray contour) and *Il7*$^{YFP+}$ (black dot plot) TECs were compared for the expression of Ly51 and CD80. The percentage of *Il7*$^{YFP+}$ TECs within each gate is shown (B)

Mean fluorescence intensity (MFI) of YFP expression in *Il7*$^{YFP+}$ TECs and percentages of *Il7*$^{YFP+}$ and CD80^{+} TECs are shown. Data are representative of two to three experiments per time point. *Statistical significance, $p<0.05$. (C) Bar graphs display the percentage and number of YFP^{-} (gray) and *Il7*$^{YFP+}$ (black) TECs as mean 6 SD.

Discussion

The establishment and maintenance of cTECs determine the thymopoietic capacity of the thymus, given their chief function in supporting early stages of T cell development [7, 9]. However, our understanding of fundamental aspects of thymic cortical epithelial homeostasis remains limited [38]. The representation of cTECs gradually decreases in postnatal life [22], possibly elicited by extrinsic and/or intrinsic mechanisms. The cTECs share with mTECs a common bipotent progenitor [30, 36]. One can consider that the potential of progenitor cells to self-renew or differentiate into mature cells is progressively lost with age. Concurrently, continual thymocyte-TEC interactions throughout life may also control the epithelial progenitor activity and/or other TEC functional properties, while promoting the maturation of TECs [102]. In this view, thymocyte development up to the DP stage seems sufficient to restrain the expression of IL-7 [62] and Dll4 [61] by TECs, although identification of the molecular liaisons remains undisclosed. In this article, we report that previously identified *Il7*$^{YFP+}$ TECs [50, 102] define a subset of *Ccrl1*-expressing cortical epithelial cells and examine the mechanisms that regulate the homeostasis of these IL-7-expressing cTECs.

The developmental stages as well as the molecular signals that regulate cTEC differentiation from bipotent precursors are just beginning to be identified. A heterogeneity within the cortical microenvironment is suggested to exist on the basis of the differential expression of CD205, Ly51, IL-7, Dll4, β5t, and CCRL1 [22, 37, 38, 61, 62, 105]. Our kinetic analysis during thymic ontogeny revealed that *Il7*$^{YFP+}$ TECs sustained phenotypic and molecular traits associated with cTECs [38]. Of interest, although YFP^{-} TECs steadily accumulate more medullary characteristics as TEC maturation proceeds, they share cortical- and medullary-associated features at an early phase of thymic development. These findings indicate that mTEC precursors may reside at early stages within a subset that shares some cTEC features. Still, the degree of heterogeneity within cTECs

remains to be determined. The frequency of *Il7*$^{YFP+}$ TECs gradually declines as mTEC development advances. One can envisage that *Il7*$^{YFP+}$ TECs represent a lineage that participates in the differentiation of mTECs as a result of lympho-stromal interactions. Alternatively, one can consider that YFP^{-} TECs detected at the E13–14 stage include direct mTEC precursors poised to differentiate, which expands and replaces (or dilutes) *Il7*$^{YFP+}$ TECs. The establishment of medullary microenvironments involves the hierarchical, but concerted, participation of TNFRSF RANK, LTβR, and CD40 molecules [10]. Our *in vitro* findings corroborate that RANK signaling has a dominant function in the development of mTECs [91, 92, 94], whereas signaling through LTβR seems to amplify the RANK-mediated effects [108]. These signals delivered upon interactions with hematopoietic cells did not, however, substantially affect the homeostasis of *Il7*$^{YFP+}$ TECs. Instead, they seem to drive mTEC development from a precursor within the YFP^{-} fraction, indicating that *Il7*$^{YFP+}$ TECs do not have an immediate precursor–product relationship with mature mTECs. Our analysis of the lineage potential of purified subsets revealed that although YFP^{-} TECs appeared to be more competent in differentiating mTECs, *Il7*$^{YFP+}$ TECs can still give rise to medullary epithelia in a suggested stepwise fashion, terminating YFP expression as they progress through an intermediate immature stage of mTEC differentiation. Further studies are needed to address whether mTECs derived from both subsets represent functional distinct medullary subtypes and to study their physiological relevance in regulating T cell development. In agreement with our results, it has been recently shown that mTECs can arise from CD205^{+}CD40^{-} TEC progenitors [110], which are generally associated with the cTEC lineage [38]. Collectively, these findings suggest that mTEC differentiation may be more complex than previously appreciated, following a linear stepwise differentiation pathway from progenitors that simultaneously express cTEC and mTEC traits, rather than a simple dichotomist model from compartment-specific progenitors. Still, the degree of heterogeneity within cTECs remains to be determined, and further studies on the stepwise generation of the cTEC and mTEC lineages are warranted.

In mice with early blocks in thymopoiesis, including *Rag2*$^{-/-}$*Il2rg*$^{-/-}$ [62] and CD3εTg26 mice [40, 111], the thymic epithelium is devoid of distinct cortical and

medullary areas [40]. In these models, TEC differentiation is severely compromised [40, 62, 111], which limits the study of cTEC development downstream of a bipotent progenitor. We previously reported that *Il7*$^{YFP+}$ TECs are markedly maintained in *Rag2*$^{-/-}$*Il2rg*$^{-/-}$ mice. Restoration of normal thymopoiesis following WT stem cell transplantation reduces their frequency [62], suggesting that thymic crosstalk regulates their homeostasis. *Rag2*$^{-/-}$ mice offer an intermediate version because the development of cTECs is overtly normal [38, 39, 112]. Yet, it has been suggested that DNs facilitate the establishment of the three-dimensional reticular cTEC structure [113], implying the existence of a DN stage–specific requirement for differentiation of cTECs. It has been documented that cTECs retain a Ly51^{high} phenotype in *Rag2*$^{-/-}$ mice [22], suggesting that further cortical maturation stages dependent on post–b-selected thymocytes may be absent in this setting. Our results showed that *Il7*$^{YFP+}$ cTECs developed normally and were sustained in *Rag2*$^{-/-}$ mice, corroborating that thymocyte-derived signals generated beyond β-selection regulate the maintenance of this cTEC immature lineage [62]. In line with previous studies [22, 113], we observed an insufficient differentiation of mTECs in *Rag2*$^{-/-}$ mice. Still, vestigial mTECs could be detected within the YFP^{-} TEC fraction, indicating that the hematopoietic fraction (e.g., DN2–3 thymocytes, lymphoid tissue inducer cells, NK cells) elicits a certain degree of mTEC maturation.

The β-selection defines a chief checkpoint during the progression from DN to DP thymocytes [109]. Using a pre-TCR activation model in *Rag2*$^{-/-}$ mice [107], we bypassed the β-selection. In this *in vivo* model, progression through DN-immature single positive-DP stages allows physiological lympho-stromal interactions, but in the absence of TCR-derived signals. DP thymocytes from anti-CD3-treated *Rag2*$^{-/-}$ mice lack TCR complexes, are not positively selected, and die by apoptosis, similarly to the majority of WT DP thymocytes that do not receive survival signals for lack of TCR–MHC/peptide interactions. Our results showed that *Il7*$^{YFP+}$ cTECs were not substantially affected in this condition, indicating that thymocyte TCR-dependent signals generated during thymic selection might control their homeostasis. We observed a concomitant moderate improvement in mTEC development in anti-CD3ε-treated *Rag2*$^{-/-}$ mice. An amelioration of medullary niches upon anti-CD3ε treatment has been recently reported in a mouse model of

Omenn syndrome, which is associated with a hypomorphic R229Q mutation in the RAG2 enzyme [114]. In contrast to our model, TCR-expressing cells are found in the thymus of R229Q RAG2 mice [114], which may also contribute to the improvement of the medullary epithelium. In both cases, insufficient mTEC differentiation might reflect a lack of instructive signals from mature thymocytes [10].

It is an accepted idea that positive selection and negative selection occur in the cortex and medulla, respectively. Whereas intermediate signals from low-affinity interactions between TCR and peptide/MHC ligands result in positive selection, strong signals from recognition of high-affinity peptide/MHC ligands lead to negative selection [9, 10]. Still, whether positive and negative selection can be sequential or independent events remains unanswered. Some evidence does exist that negative selection also occurs in the cortex [115-117], although the medulla provides a larger repertoire of self-antigens for the elimination of autoreactive T cells [7, 96]. Using a TCR transgenic model, we examined the consequences of positive and negative selection in the thymic microenvironment [104]. Our findings indicate that positive selection of thymocytes in Marilyn TCR transgenic cortex suffices to induce the proportional loss of *Il7*$^{YFP+}$ cTECs and the expansion of medullary TECs. During negative selection, the premature expression of transgenic MI TCR may accelerate the deletion of autoreactive thymocytes in the cortical microenvironment [104]. Indeed, deletion of DP thymocytes expressing self-reactive TCR is observed in the cortex [116, 117]. Our findings indicated that the IL-7-expressing cTEC niche might be limited by strong TCR– peptide/MHC interactions within the cortical thymic microenvironment. It is worth mentioning that the modulation of the IL-7 cTEC niche detected in *Rag2*$^{-/-}$ TCR transgenic mice is also seen in WT immunocompetent mice. In a normal thymus, strong TCR signals are probably less frequent at the DP stage. Because positive selection occurs within the cortex [9, 10], continual positive selection may locally feed back to cTECs and induce the loss of *Il7*$^{YFP+}$ cTECs in WT thymus. One can hypothesize that bidirectional crosstalk directly transmits outside-in signaling through MHC molecules on TECs. Alternatively, the high-avidity TCR-MHC/peptide recognition may elicit a downstream molecular interaction that restrains the IL-7-expressing

cortical epithelial niche. Further studies are required to elucidate the specific signals generated during thymic selection that can regulate the cTEC microenvironment.

To our knowledge this is the first study indicating that the strength of MHC/peptide-TCR interactions between TECs and thymocytes during selection constitutes a rheostat regulating the maintenance of IL-7-expressing cTECs. These findings have implications for understanding the molecular basis of cTEC differentiation and should inspire further studies aimed at uncovering the physiological consequences linked to the functional capacity of the thymus, an ongoing topic of investigation.

Acknowledgments

We thank Drs. Catarina Leitão, Alexandre Carmo, and Rui Appelberg (Instituto de Biologia Molecular e Celular, Porto, Portugal) for critical reading of the manuscript; Dr. Catarina Leitão (Advanced Flow Cytometry Unit, Instituto de Biologia Molecular e Celular) for technical assistance during cell sorting; personnel from the Instituto de Biologia Molecular e Celular animal facility—in particular, Dr. Sofia Lamas, Isabel Duarte, and Liliana Silva for technical assistance with animal experimentation; Dr. Benedita Rocha (Hôpital Necker, Paris, France) for the anti-CD3ε mAb; Dr. Jeff Browning (Biogen Idec, Weston, MA) for anti-LTβR mAb; and Drs. Jocelyne Demengeot (Instituto Gulbenkian de Ciência, Oeiras, Portugal) and Thomas Boehm (Max Planck Institute of Immunobiology and Epigenetics, Freiburg, Germany) for providing Ml TCR Tg and Ccx-Ckr1:eGFP reporter mice, respectively. We thank Drs. Graham Anderson and Andrea White (Birmingham, U.K.) for the introduction to RTOCs.

Supplementary Information

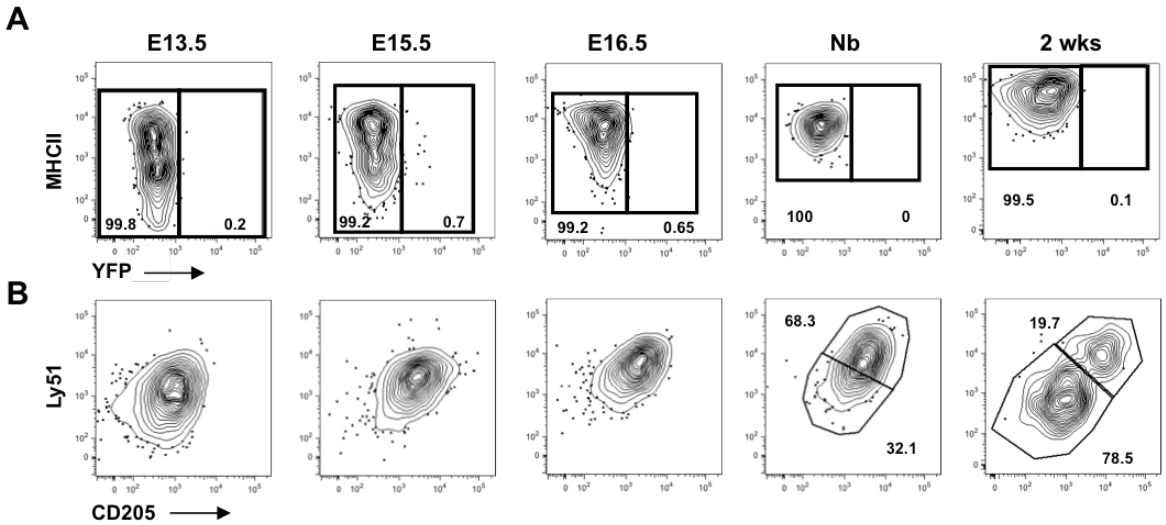

Figure S1. Thymic epithelium development in WT mice. WT thymi were isolated at the indicated time points and total TECs (gated on $CD45^{-}EpCAM^{+}$) were analyzed for the expression of **(A)** MHCII and YFP **(B)** Ly51 and CD205. Percentages of gated cells are shown. Data are representative of 2-3 experiments per time point.

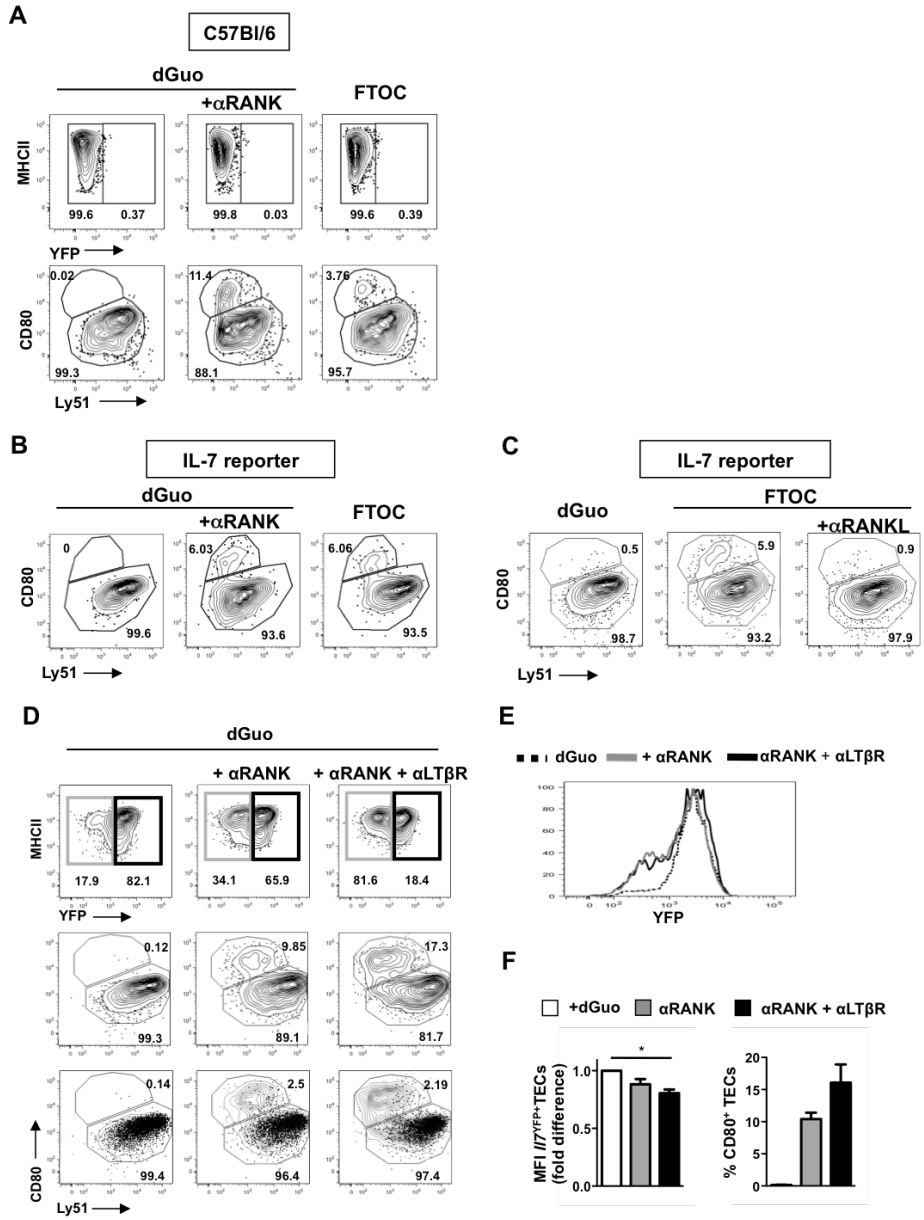

Figure S2. E14.5 FTOCs and dGuo-treated FTOCs (dGuo) were cultured in medium. **(A)** C57Bl/6 WT and **(B)** IL-7 reporter E14.5 FTOCs and dGuo-FTOCs were cultured in medium, or for dGuo-FTOCs with anti-RANK (αRANK). **(C)** IL-7 reporter E14.5 FTOCs were supplemented with the blocking Ab against RANK ligand (αRANKL). Total TECs represented in Figure 4 were analyzed for the expression of MHCII and YFP **(A)** and for the expression of Ly51 and CD80 **(A-C)**. Percentages in gated cells are shown **(A-C)**. **(D-F)** The cooperative RANK and LTβR signals do not affect the homeostasis of *Il7*$^{YFP+}$ TECs. dGuo-treated E14.5 FTOCs from IL-7 reporter mice were cultured in the absence or presence of anti-RANK (αRANK) and anti-LTβR (αLTβR). **D)** Total TECs were analyzed for the expression of MHCII and YFP (top row) and for the expression of Ly51 and CD80 (middle row). Percentages of the cells in the indicated areas are included. YFP^{-} (gray contour) and *Il7*$^{YFP+}$ TECs (back dot plot) were compared for the expression of Ly51 and CD80 (bottom row). The percentage of *Il7*$^{YFP+}$ TECs within each gate is shown. **E)** The YFP expression on total TECs is compared for the different conditions represented in D. **F)** Fold difference in the Mean Fluorescence Intensity (MFI) of YFP expression on *Il7*$^{YFP+}$ TECs (left graph) and percentage of CD80^{+} TECs (right). * p<0.05. Data are representative of 4 independent experiments.

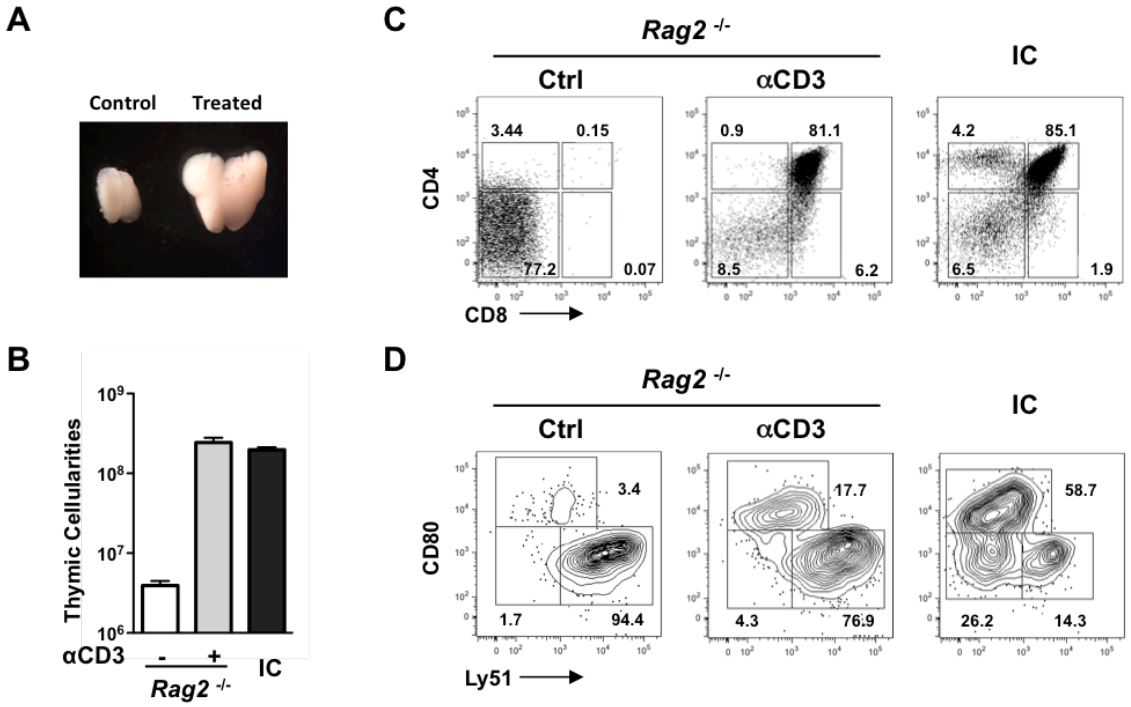

Figure S3. Anti-CD3ε treatment in IL-7 reporter *Rag2*$^{-/-}$ mice. *Rag2*$^{-/-}$ neonatal mice were analyzed 12 days after anti-CD3ε treatment (αCD3) together with age-matched (12-14 days old) IL-7 reporter *Rag2*$^{-/-}$ control (Ctrl) and immuno-competent mice (IC). **A)** Macroscopic image of control and αCD3-treated thymi. **B)** Total thymic cellularity and (**C)** CD4/CD8 expression profile of the thymocytes for control and αCD3- treated *Rag2*$^{-/-}$, and IC mice. **D)** Partial restoration of mTEC compartment. Total TECs were analyzed for the expression of Ly51 and CD80. Numbers represent the percentages of gated cells.

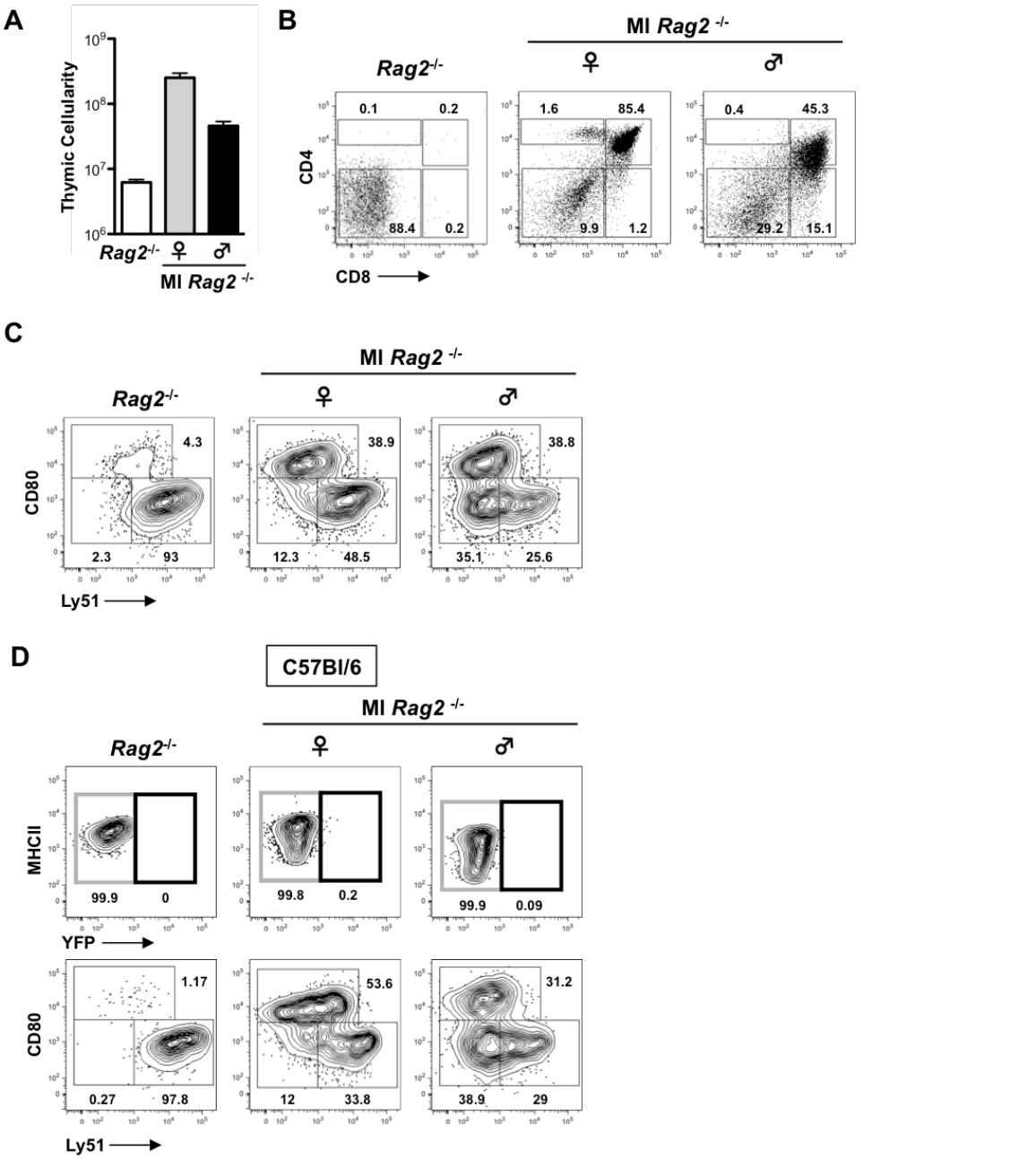

Figure S4. Thymocyte selection in Marilyn *Rag2*$^{-/-}$ mice depends on the sex. Thymi from female (♀) and male (♂) IL-7 reporter Marilyn TCR Tg *Rag2*$^{-/-}$ (MI *Rag2*$^{-/-}$) mice were analyzed together with IL-7 reporter *Rag2*$^{-/-}$ (*Rag2*$^{-/-}$) littermates at 12-14 days of age. **A)** Total thymic cellularity and **B)** CD4/CD8 expression profile of thymocytes is represented. **C)** Total TECs were analyzed for the expression of Ly51 and CD80. Numbers represent the percentages of gated cells. **D)** Total TECs from C57Bl/6 *Rag2*$^{-/-}$ and Marilyn TCR Tg *Rag2*$^{-/-}$ mice were analyzed for the expression of MHCII and YFP; Ly51 and CD80. Percentages in gated cells are shown. Data are representative of 2-3 experiments per time point.

Results Chapter II

The intermediate expression of CCRL1 reveals novel subpopulations of medullary thymic epithelial cells that emerge in the postnatal thymus

Ana R. Ribeiro, Catarina Meireles, Pedro M. Rodrigues and Nuno L. Alves

European Journal of Immunology, 44(10):2918-2924 (2014)

Summary

Cortical and medullary thymic epithelial cells (cTECs and mTECs, respectively) provide inductive microenvironments for T-cell development and selection. The differentiation pathway of cTEC/mTEC lineages downstream of common bipotent progenitors at discrete stages of development remains unresolved. Using IL-7/CCRL1 dual reporter mice that identify specialized TEC subsets, we show that the stepwise acquisition of CCRL1 is a late determinant of cTEC differentiation. Although cTECs expressing high CCRL1 levels ($CCRL1^{hi}$) develop normally in immunocompetent and *Rag2*$^{-/-}$ thymi, their differentiation is partially blocked in *Rag2*$^{-/-}$*Il2rg*$^{-/-}$ counterparts. These results unravel a novel checkpoint in cTEC maturation that is regulated by the crosstalk between TECs and immature thymocytes. Additionally, we identify new Ulex europaeus agglutinin 1 $(UEA1)^{+}$ mTEC subtypes expressing intermediate CCRL1 levels ($CCRL1^{int}$) that conspicuously emerge in the postnatal thymus and differentially express *Tnfrsf11a*, *Ccl21* and *Aire*. While rare in the fetal and in *Rag2*$^{-/-}$ thymi, $CCRL1^{int}$ mTECs are restored in *Rag2*$^{-/-}$-Marilyn TCR-Tg mice, indicating that the appearance of postnatal-restricted mTECs is closely linked with T-cell selection. Our findings suggest that alternative temporally restricted routes of new mTEC differentiation contribute to the establishment of the medullary niche in the postnatal thymus.

Introduction

Within the thymus, it is well established the role of distinct thymic epithelial cell (TEC) microenvironments in supporting the generation of functionally diverse and self-tolerant T cells [9]. While cortical TECs (cTECs) promote T-cell lineage commitment and positive selection, medullary TECs (mTECs) participate in the elimination of autoreactive T cells and the differentiation of Treg cells [10]. In particular, Autoimmune regulator $(Aire)^{+}$ mTECs have an established role in tolerance induction [69]. Cortical and medullary TECs are derived from common bipotent progenitors present within the fetal and postnatal thymus [30, 36]. Importantly, the cTEC/mTEC maturation pathways downstream of bipotent

progenitors, as well as the requirements for the establishment of these specialized compartments at discrete stages of development are still unresolved.

The cTEC/mTEC lineage specification branches early in embryonic development [118]. During initial stages of gestation, the thymic epithelium predominately comprises $Ly51^{+}CD205^{+}\beta5t^{+}$ cTECs [37, 38, 62], and mature mTECs, including $Aire^{+}$ mTECs, first appear around embryonic day 16 (E16) [64, 83]. The emergence of embryonic mTECs depends on cellular interactions with lymphoid tissue inducer cells and invariant γδ T cells [77, 93], and involves signalling through TNFR superfamily receptor activator of NF-κB (RANK) and lymphotoxin beta receptor (LTβR) expressed on TEC precursors [77, 108]. However, and despite the elucidation of distinct maturation stages in mTECs [10], there are still gaps in the understanding of cTEC differentiation. We, and others, have recently demonstrated that fetal TEC progenitors expressing cortical properties are able to generate mTECs [110, 119, 120]. These reports support the idea that embryonic TEC precursors progress transitionally through the cortical lineage prior to commitment to the medullary pathway, emphasising that TEC differentiation is more complex then previously recognized [121].

The size of the medullary epithelial microenvironment continues to expand after birth, fostered by additional interactions between TECs and mature thymocytes, namely positively selected and CD4 single positive (SP4) thymocytes [10]. The concerted activation of RANK-, LTβR- and CD40-mediated signalling on mTECs and their precursors completes the formation of the adult medullary niche [10]. It has been previously demonstrated a clonal nature for discrete embryonic mTEC islets, which progressively coalesce into larger medullary areas in the adult thymus [63, 64]. Hence, one can argue that the adult mTEC niche exclusively results from the expansion of embryonic-derived mTECs and their precursors. Still, it remains possible that alternative developmental stage-specific pathways participate in the organization of the adult mTEC niche.

Here, we report a novel checkpoint in cTEC differentiation, which is defined by the sequential acquisition of CCRL1 expression and is compromised in mice with profound blocks in early T-cell development. Additionally, we define original

subsets of mTECs, characterized by the intermediate CCRL1 expression, that emerge in the postnatal thymus in tight association with thymocytes that develop beyond the TCRβ selection. Our findings provide evidence for the existence of several waves of mTEC development in the embryonic and postnatal thymus.

Results and Discussion

The acquisition of CCRL1 expression is a late cTEC determinant

The expression of CCRL1, an atypical chemokine receptor that controls the bioavailability of key chemoattractants CCL19, CCL21 and CCL25, identifies cTECs in the postnatal thymus [105]. Given the incomplete knowledge on the differentiation of CCRL1^{+}cTECs, we assessed their generation using previously generated IL7^{YFP}-CCRL1^{GFP} dual reporter mice[119]. While in IL7^{YFP} reporter mice, YFP expression is a surrogate of a subtype of cTECs expressing abundant levels of the crucial thymopoietin IL-7 (*Il7*$^{YFP+}$)[62, 119], in CCRL1^{GFP} reporter mice, GFP expression labels cTECs in the postnatal thymus [105]. We previously showed that postnatal *Il7*$^{YFP+}$ TECs locate within cTECs that express high CCRL1 levels (referred as CCRL1^{hi}) [119]. Here, analysis during early stages of thymic development showed that the emergence of *Il7*$^{YFP+}$, CD205^{+} and Ly51^{+} TECs around E12.5-13.5 [37, 38, 62] preceded the appearance of CCRL1-expressing cells (Figure 1A and Supporting information Fig. 1B; non-reporter thymi in Supporting information Fig. 1A). During the E12.5-15.5 period, both *Il7*$^{YFP+}$ and remaining YFP^{-} cTECs progressively acquired the expression of CCRL1. At E18.5, and similarly to the postnatal thymus [119], *Il7*$^{YFP+}$ TECs reside within CCRL1^{hi} cells (Figure 1A). The number of CCRL1^{hi} cTECs gradually increased throughout development, contributing to the expansion of TEC cellularity during perinatal life. TECs lacking CCRL1 and expressing intermediate CCRL1 levels (referred as CCRL1^{-} and CCRL1^{int}, respectively) followed steadier numbers during this period (Figure 1B). To address whether the acquisition of CCRL1 defined a late cTEC maturation stage dependent on signals provided by developing thymocytes, we crossed double reporter mice onto a *Rag2*$^{-/-}$ or *Rag2*$^{-/-}$*Il2rg*$^{-/-}$ background. While the majority of TECs were CCRL1^{hi} in the postnatal *Rag2*$^{-/-}$ thymus, we detected an

accumulation of CCRL1^{int} TECs in the *Rag2*$^{-/-}$*Il2rg*$^{-/-}$ thymus (Figure 1 C-D, non-reporter thymi in Supporting information Fig. 1C), akin to the CCRL1 pattern observed at E15.5 (Figure 1A). Contrarily to CCRL1, the expression of Ly51, CD205, *Psmb11* (β5t) and *Ctsl* was not impaired in TECs from *Rag2*$^{-/-}$*Il2rg*$^{-/-}$ thymi (Supporting information Fig. 1D-E) [62, 119]. CCRL1^{-} and CCRL1^{int} TECs in the *Rag2*$^{-/-}$*Il2rg*$^{-/-}$ thymus were distinct from immunocompetent counterparts, as in the later these subsets comprised mostly mTECs (bellow in Figure 2) that are virtually absent in the *Rag2*$^{-/-}$*Il2rg*$^{-/-}$ thymus [62].

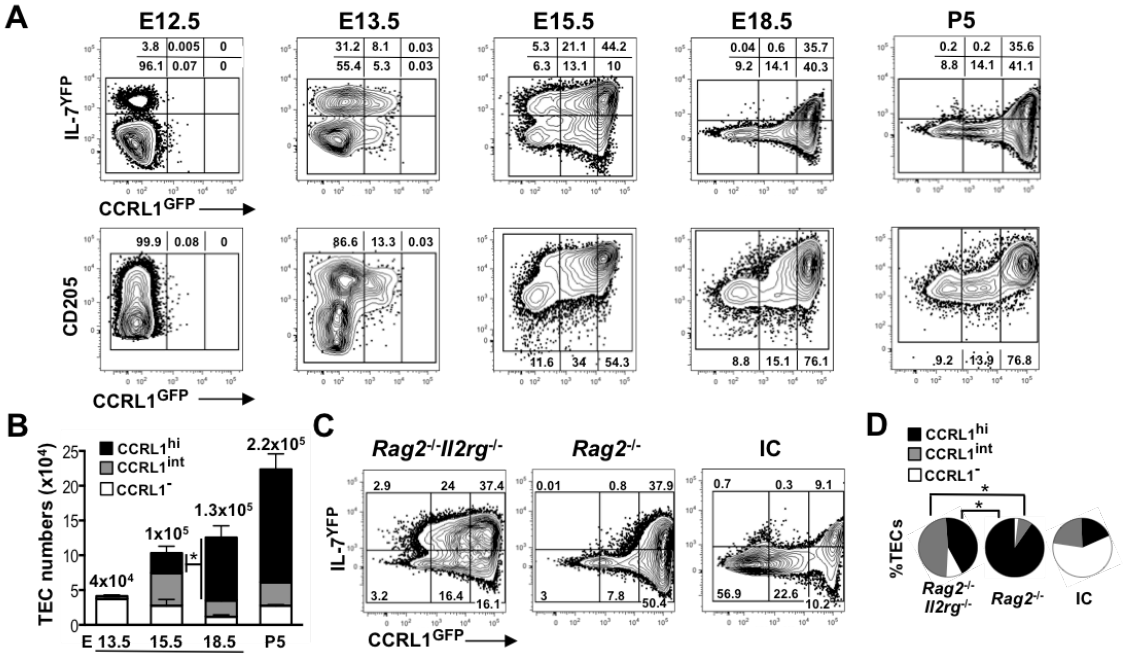

Figure 1. CCRL1 is a late cTEC determinant. (A) Total TECs (gated as CD45^{-}EpCAM^{+}) from IL-7^{YFP}CCRL1^{GFP} mice were analyzed for IL-7^{YFP} and CCRL1^{GFP} or CD205 and CCRL1^{GFP} expression by flow cytometry (FC) at the indicated time points. Numbers in plots indicate the frequency of cells found within each gate. Plots are representative of three to five independent experiments per time point. *E* represents embryonic day and *P5* represents postnatal day 5. (B) Cellularity of TECs expressing high (CCRL1^{hi}), intermediate (CCRL1^{int}), and no CCRL1 (CCRL1^{-}) was determined by the absolute thymic cell numbers and the respective frequencies of each subset obtained by FC. Numbers on top of bars indicate average TEC cellularity for each time point. Data are shown as mean + SD of 3–5 samples pooled from three to five independent experiments. * $p < 0.05$ (unpaired *t* test). (C) TECs from 2-week-old *Rag2*$^{-/-}$, *Rag2*$^{-/-}$ *Il2rg*$^{-/-}$, and immunocompetent (IC) thymi were analyzed by FC for IL-7^{YFP} and CCRL1^{GFP} expression. Numbers in plots indicate the frequency of each gate. Plots are representative of three independent experiments. (D) The mean proportion (%) of CCRL1 subsets in 2-week-old *Rag2*$^{-/-}$, *Rag2*$^{-/-}$ *Il2rg*$^{-/-}$, and IC mice, determined by FC, is depicted. *$p < 0.001$ (unpaired *t* test). Data represent means of three to five experiments (n = 5–6 mice/group).

The partial blockade in CCRL1, CD40 and MHCII expression in *Rag2*$^{-/-}$*Il2rg*$^{-/-}$ mice (Supporting information Fig. 1D) was similar to blocks in the expression of CD40 and MHCII also reported in CD3εTg26 mice [38]. Although the signals

remain unidentified, our results indicate that lympho-epithelial interactions with DN1-DN3 thymocytes provide differentiation cues that control late stages in the cTEC differentiation program.

Intermediate CCRL1 levels define distinct mTEC subtypes in the postnatal thymus

We reciprocally examined the generation of mTECs relatively to the differentiation of CCRL1-expressing TECs. The primordial $CD80^+$ mTECs were found within $CCRL1^-$ cells ($CCRL1^-CD80^+$) at E15.5 (Figure 2A), preceding the complete differentiation of $CCRL1^{hi}$ cTECs around E18.5-postnatal (Figure 1A). The proportion and number of $CCRL1^-CD80^+$ mTECs augmented throughout time (Figure 2A and D). Notably, a subset of $CD80^+$ TECs, expressing intermediate levels of CCRL1 ($CCRL1^{int}CD80^+$), emerged distinctly after birth (Figure 2A; non-reporter $CD80^+$ mTECs and *Ccrl1* expression are shown in Supporting information Fig. 2A and B, respectively). As this subtype was virtually absent at E15.5, we compared $CCRL1^{int}$ TECs for the expression of additional cTEC (Ly51) and mTEC (UEA binding) markers [119, 120] in E18.5 and neonatal thymus. At both periods, $CCRL1^{hi}$ and $CCRL1^-CD80^+$ TECs majorly identified either $Ly51^+$ cTECs or UEA^+ mTECs, respectively (Figure 2A-B). The $CCRL1^-CD80^-$ TECs, which represent a minor subset in the neonatal thymus, were predominantly composed of $Ly51^{int}UEA^+$ TECs at this stage. $CCRL1^{int}$ TECs at E18.5 comprised mostly $Ly51^+UEA^-CD80^-$, although few UEA^+CD80^- and scarce UEA^+CD80^+ were detected (Figure 2B-C). Interestingly, three discrete sizeable subpopulations accumulated within neonatal $CCRL1^{int}$ TECs, including UEA^-CD80^-, UEA^+CD80^- and UEA^+CD80^+ (Figures 2C). Both $CD80^-$ and $CD80^+$ $CCRL1^{int}UEA^+$ mTEC subsets, while scarce at E18.5 (Figure 2B-C), totally represented approximately half and one quarter of the mTEC compartment in neonatal and young thymi, respectively (Figure 2D). To examine whether $CD80^+CCRL1^{int}$ mTECs differentiate by the reiteration of the same pathways defined for postnatal mTECs [10, 92], we set E18.5 fetal thymic organ cultures (FTOCs). While rare in intact FTOCs, RANK and/or CD40 stimulation induced the differentiation of $CD80^+CCRL1^{int}$ mTECs

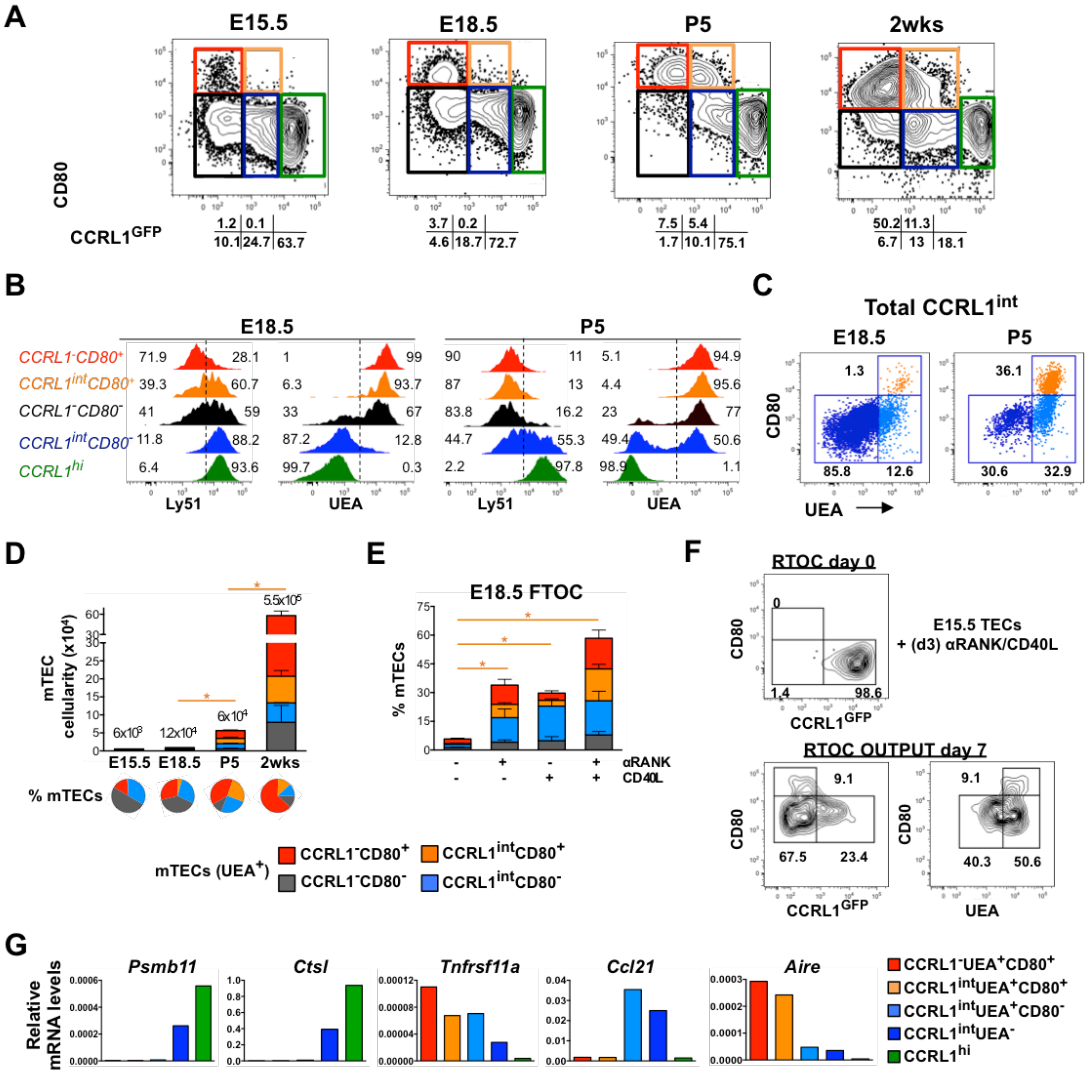

Figure 2. Intermediate CCRL1 expression reveals novel postnatal mTECs. (A) TECs (gated as CD45$^-$ EpCAM$^+$) from IL-7^{YFP}CCRL1^{GFP} mice were analyzed for CCRL1^{GFP} and CD80 expression by FC at the indicated time points. Colored gates define different subsets and grids indicate the frequencies of each respective one. (B) TEC subsets defined by the colored gates in (A) from E18.5 and postnatal day 5 (P5) thymi were analyzed for Ly51 and UEA expression by FC. Numbers in histograms indicate the frequency within each gate. Histograms are representative of three to five independent experiments. (C) Expression of UEA and CD80 within gated E18.5 and postnatal day 5 (P5) total CCRL1^{int} TECs was determined by FC. Numbers in plots indicate the frequency of cells found within each gate. (A–C) Plots are representative of three to five independent experiments. (D) Cellularity of UEA$^+$ mTEC subsets from IL-7^{YFP}CCRL1^{GFP} mice was assessed as in Figure 1. Average total mTEC cellularity is detailed above bars. Pie graphs represent the mean proportion of color-coded subsets within total UEA$^+$ mTECs. *p < 0.05 (unpaired t test) (data are shown as mean + SD of 4–6 mice/group, pooled from three to five independent experiments (E) E18.5 FTOCs were cultured for 4 days with the indicated stimuli and then assessed for mTEC induction (UEA$^+$CD80$^{-/+}$) by FC. The proportion of subsets within UEA$^+$ mTECs is color-coded. Data are shown as mean + SD of 8–10 thymic lobes/group, pooled from three independent experiments. *p < 0.05 (unpaired t test). (F) RTOCs established with E15.5-derived CCRL1$^+$UEA$^-$CD80$^-$ TECs were stimulated with αRANK and/or CD40L and gated TECs were analyzed for the expression of the indicated markers by FC. Plots are representative of three independent experiments. (G) Expression of *Psmb11*, *Ctsl*, *Tnfrsf11a*, *Ccl21*, and *Aire* was assessed by qPCR in purified TEC subsets (colored columns) from postnatal day 5 (P5) IL-7^{YFP}CCRL1^{GFP} mice. Values were normalized to *18s*. Data are shown as representative of three independent experiments.

(Figure 2E and Supporting information Fig. 2C and D). Additionally, reaggregate thymic organ cultures (RTOCs) established with E15.5 CCRL1^{+}UEA^{-}CD80^{-} TECs, and RANK- and CD40-activated to induce mTEC differentiation, showed that a fraction of fetal CCRL1^{+} cTECs displayed CD80^{+} mTEC progenitor activity (Figure 2F). Next, we analyzed how the phenotypic traits of the emergent neonatal CCRL1^{int} TECs related to the expression of genes linked to cTECs (*Psmb11* and *Cstl*) and mTECs (*Tnfrsf11a* (RANK), *Ccl21* and *Aire*) [10, 69]. Increasing *Psmb11* and *Cstl* expression was exclusively detected within CCRL1^{int}UEA^{-} and CCRL1^{hi} cells. Interestingly, a gradual increase in *Tnfrsf11a* expression was observed in CCRL1^{int}UEA^{-}, CCRL1^{int}UEA^{+}CD80^{-}, CCRL1^{int}UEA^{+}CD80^{+} and CCRL1^{-} CD80^{+} TECs. *Ccl21*, which is expressed by postnatal immature mTECs [122], was specifically found within the CCRL1^{int}UEA^{-}CD80^{-} and CCRL1^{int}UEA^{+}CD80^{-} subsets. Lastly, *Aire* expression was equally enriched in CCRL1^{-} and CCRL1^{int}CD80^{+} mTECs (Figure 2G). Although fetal CCRL1^{+}UEA^{-} TECs have the potential to generate mTECs (Figure 2F), and the gradual increase in the expression of RANK and CCL21 within CCRL1^{int} cells might suggest a continual stepwise differentiation: CCRL1^{int}UEA^{-} - CCRL1^{int}UEA^{+} - CCRL1^{int}UEA^{+}CD80^{+}, our attempts to evaluate a direct lineage relationship between neonatal CCRL1^{int} TEC subsets have been unsuccessful, given the difficulty of establishing RTOC with perinatal TECs [34]. Thus, we can only speculate that the postnatal cTEC niche harbours progenitors that are able to differentiate into mTECs, as shown in the fetal thymus [110, 119, 120]. Alternatively, one cannot exclude that postnatal CCRL1^{int} mTECs might differentiate from a lineage unrelated to cTECs. Collectively, our data indicates that while CCRL1^{int}UEA^{-} TECs co-express molecular traits of cTECs and mTECs, CCRL1^{int}UEA^{+}CD80^{-} and CCRL1^{int}UEA^{+}CD80^{+} cells define novel subtypes of immature and mature mTECs, respectively, that emerge postnatally.

Thymic selection promotes the generation of CCRL1^{int} mTECs

The differentiation of the CCRL1^{int}CD80^{+} mTECs correlates timely with the intensification of positive thymic selection around the perinatal period [118]. Given that activation of RANK and CD40 fostered CCRL1^{int}CD80^{+} mTECs (Figure 2C)

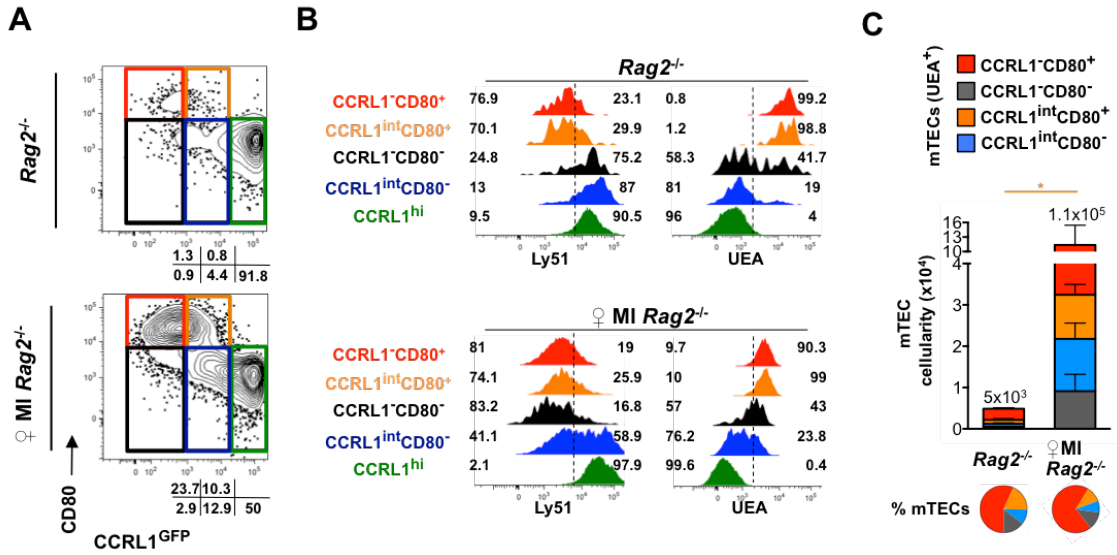

Figure 3. Thymic selection drives the emergence of the postnatal-specific CCRL1^{int}CD80^{+} TECs. (A) TECs (gated as CD45^{-}EpCAM^{+}) from postnatal day 5 (P5) *Rag2*$^{-/-}$ and female Marilyn- *Rag2*$^{-/-}$ mice were analyzed for CCRL1^{GFP} and CD80 expression by FC. Colored boxes define different TEC subsets and grids indicate the frequencies of each one. Plots are representative of two to three independent experiments. (B) Subsets defined by the colored gates in (A) from *Rag2*$^{-/-}$ and Marilyn- *Rag2*$^{-/-}$ mice were analyzed for Ly51 and UEA expression by FC. Numbers in histograms indicate the frequency within each gate. Histograms are representative of three independent experiments. (C) Frequency of subsets within total mTECs (pie graphs) and numbers of mTEC subsets was determined by FC. Data are shown as mean + SD of three to five samples, pooled from two independent experiments. *$p < 0.05$ (unpaired *t* test).

and the ligands for those mTEC-inductive signals are expressed by SP4 thymocytes [10], we investigated whether the appearance of CCRL1^{int}CD80^{+} mTECs depends on TEC-SP4 interactions during selection. To this end we crossed CCRL1-reporter mice onto a Marilyn- *Rag2*$^{-/-}$ TCR transgenic background, in which T cells express an I-A^{b}-restricted TCR that recognizes the male H-Y antigen [119]. As control, we co-analyzed *Rag2*$^{-/-}$ littermates, wherein mTEC differentiation is compromised due to the lack of mature thymocytes [119]. Few CD80^{+} mTECs were present in the neonatal *Rag2*$^{-/-}$ thymus, and those were majorly CCRL1^{-} (Figure 3A-C), resembling mTECs found in the E18.5 thymus (Figure 2). Contrarily to the normal postnatal thymus, the scarce CCRL1^{-} and CCRL1^{int}CD80^{+} subsets found in *Rag2*$^{-/-}$ mice were predominantly composed of Ly51^{+}UEA^{-} cells (Figure 3 A, B). Strikingly, we detected a marked expansion of both CCRL1^{-}CD80^{+} and CCRL1^{int}CD80^{+} mTECs in neonatal Marilyn-*Rag2*$^{-/-}$ females (Figure 3A-C, non-reporter *Rag2*$^{-/-}$ and Marilyn-*Rag2*$^{-/-}$ are shown in S2E), recapitulating the mTEC composition of the young thymus (Figure 2A). Akin to the WT thymus, CCRL1^{hi} and CCRL1^{-}CD80^{+} TECs specifically identified cTECs and

mTECS, respectively, and the emergent CCRL1^{int}CD80^{+} TECs were Ly51^{lo}UEA^{+} (Figure 3B). One can envision that temporally restricted mTEC differentiation pathways are engaged by interactions between mTEC precursors and distinct hematopoietic cells. As shown previously [64, 83], the generation of the first embryonic mature CD80^{+} mTECs (CCRL1^{-}) precedes the development of SP4s and depends on LTβR- and RANK-mediated signalling engaged upon lympho-epithelial interaction with lymphoid tissue inducer cells and γδ T cells [77, 93, 108]. Our findings indicate that the differentiation of the postnatal-restricted CCRL1^{int}CD80^{+} mTECs results from MHC-TCR, CD40-CD40L and RANK-RANKL interactions [10, 92] between TEC precursors and TCRβ-selected thymocytes.

Concluding Remarks

The neonatal life marks a period characterized by a drop in cTECs and an expansion in mTECs [105]. The identification of novel postnatal mTEC subsets supports the concept that the foundation of the adult medullary microenvironment results from alternative waves of mTEC differentiation. In this regard, recent evidence suggests that the expansion of the medulla after birth involves de novo formation of mTECs [123]. This notion implicates that fetal mTEC precursors might have limited self-renewal potential, as shown for bipotent TEC progenitors [35], and in turn the formation of the adult mTEC niche relies on additional inputs arising after birth. Still, further studies are needed to elucidate to what extent bipotent progenitors might progress through the cortical differentiation program in the adult thymus. Also, the functional relevance of the mTEC heterogeneity reported herein should be further dissected. As mTECs have a crucial role in T-cell maturation and tolerance induction, our findings have implications in therapeutics aimed at modulating TEC niches in the adult thymus.

Material and Methods

Mice

Dual IL-7^{YFP}CCRL1^{GFP} reporter mice were backcrossed onto *Rag2*$^{-/-}$, *Rag2*$^{-/-}$ *Il2rg*$^{-/-}$ and Marilyn-*Rag2*$^{-/-}$ C57BL/6 background [62, 119]. E0.5 was the day of vaginal plug detection. Animal experiments were performed in accordance with European guidelines.

TEC isolation and flow cytometry

TECs were isolated as described [119]. Cells were stained with anti-I-A/I-E (Alexa 780); anti-CD45.2 (PerCP-Cy5.5); anti-EpCAM (A647); anti-CD80 (A660); anti-Ly51, anti- CD205, UEA-1 (biotin), anti-EpCAM (eFluor 450) Abs, and streptavidin (PE-Cy7) (eBioscience). Flow cytometry (FC) was performed on a FACSCanto II, with data analyzed on FlowJo software (BD). Cell sorting was performed using the FACSAria I (BD Biosciences), with purities >95%. A 510/10-nm band pass (502LP dichroic mirror) and a 542/27-nm band pass (525LP dichroic mirror) filters were used to discriminate the GFP/YFP signals.

Gene expression

mRNA (RNAeasy MicroKit, Quiagen) isolation and cDNA synthesis (Superscript First- Strand Synthesis System, Invitrogen) were performed as described [15]. Real-time PCR (iCycler iQ5) was performed using either TaqMan Universal PCR Master Mix and primers for *18s*, *Ctsl*, *Aire*, *Ccl21*, *Tnfrsf11a*, and *Psmb11* (Applied Biosystems); or iQ SYBR Green Supermix (Bio-Rad) and primers for *Actb* and *Ccrl1* as detailed [119]; Triplicated samples were analyzed and the ΔΔCt method was used to calculate relative levels of targets compared with *18s*/*Actb* as described [119].

FTOCs and RTOCs

FTOCs and RTOCs were established with E18.5 and E15.5 embryos, respectively, as described [119]. For FTOCs, TECs were analyzed after 4 days culturing with 1 mg/ml anti- RANK and/or with 5 mg/ml recombinant CD40L (R&D Systems). For RTOCs, 10^5 E15.5 CCRL1$^+$UEA$^-$CD80$^-$ TECs were sorted and mixed with

$CD4^+CD8^+$ and $CD4^+$ thymocytes at 1:1:1 ratio. After 3 days, 0.3 mg/ml anti-RANK and 1.3 mg/ml recombinant CD40L were added to the cultures. RTOC were analyzed after 7 days.

Statistical Analysis

The unpaired t test was used to perform statistical analysis. $P < 0.05$ was considered significant.

Acknowledgments

We thank James Di Santo, Jocelyne Demengeot and Thomas Boehm for *Rag2*$^{-/-}$ *Il2rg*$^{-/-}$, Marilyn-*Rag2*$^{-/-}$ and CCRL1-reporter mice, respectively. We thank Dr. Catarina Leitão for critical reading of the manuscript and technical assistance. We thank FEDER funds through the Operational Competitiveness Programme – COMPETE and by National Funds through Fundação para a Ciência e a Tecnologia (FCT) under the project PTDC/SAU- IMU/117057/2010 funded this work. N.L.A., A.R.R., C.M. and P.M.R. are supported by FCT Investigator program and PhD fellowships.

Supplementary Information

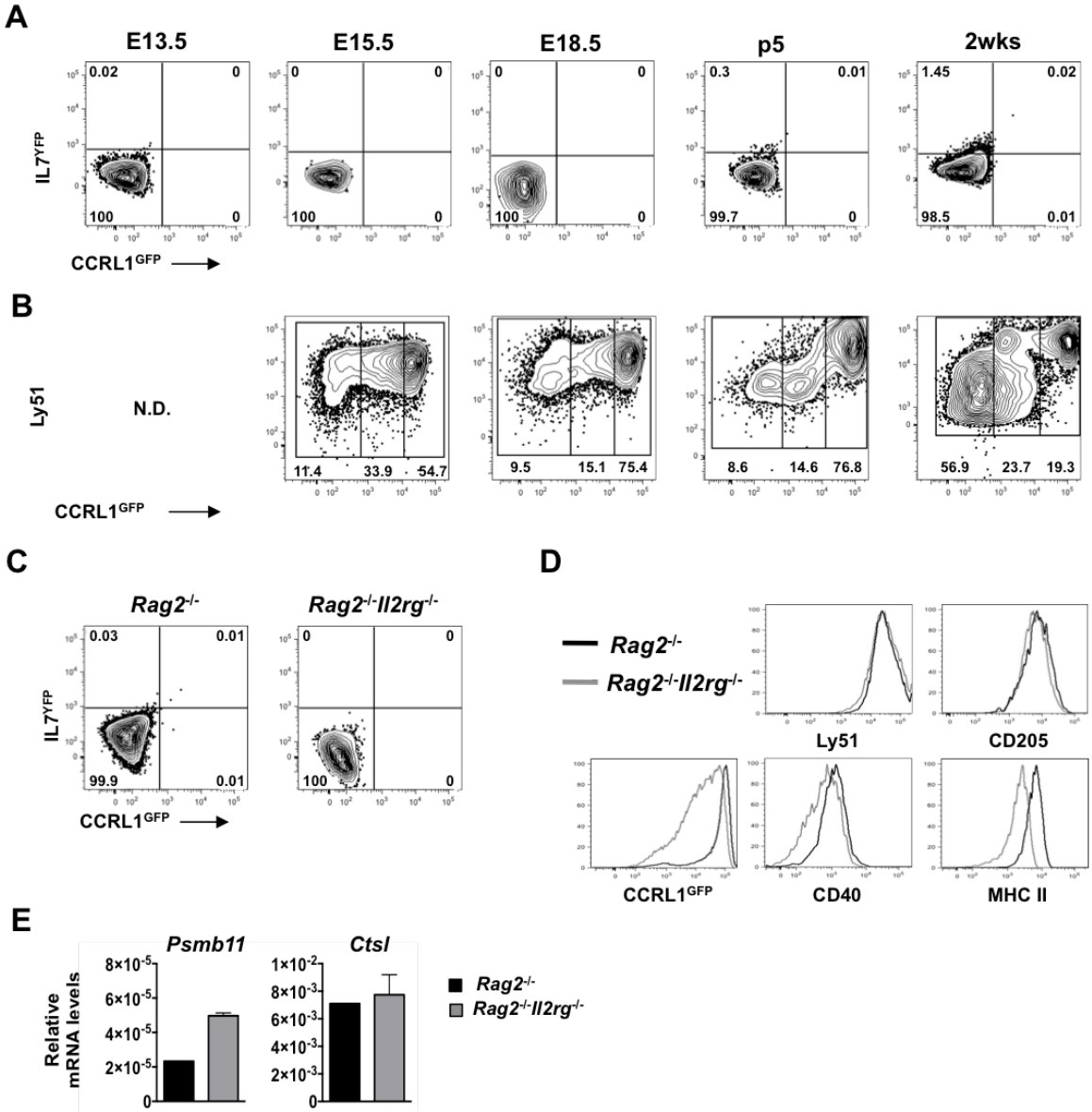

Figure S1. Total TECs (gated as $CD45^{-}EPCAM^{+}$) from non-reporter littermates isolated at the indicated time points were analysed for $IL7^{YFP}$ and $CCRL1^{GFP}$ expression by flow cytometry. (B) Total TECs from $IL-7^{YFP}CCRL1^{GFP}$ dual reporter mice were analyzed for the expression of Ly51 and $CCRL1^{GFP}$. N.D. not determined. Ly51 expression in E13.5 has been shown previously in [8]. (A–B) Numbers in plots indicate the frequency of cells found within each gate. Plots are representative of three to five independent experiments. E numbers represent embryonic day and P5 represents postnatal day 5. (C) Total TECs from *Rag2*$^{-/-}$ and *Rag2*$^{-/-}$*Il2rg*$^{-/-}$ non-reporter littermates were analyzed for $IL7^{YFP}$ and $CCRL1^{GFP}$ expression by flow cytometry. Numbers in plots indicate the frequency of cells found within each quadrant. (D) Histograms for Ly51, CD205, CCRL1GFP, CD40 and MHC II expression in total TECs from 2 weeks old *Rag2*$^{-/-}$ and *Rag2*$^{-/-}$*Il2rg*$^{-/-}$ $IL7^{YFP}CCRL1^{GFP}$ dual reporter mice. (E) Expression of *Psmb11* and *Ctsl* in TECs purified from 2 weeks old *Rag2*$^{-/-}$ and *Rag2*$^{-/-}$*Il2rg*$^{-/-}$ mice was accessed by qPCR. Values were normalized to *18s*.

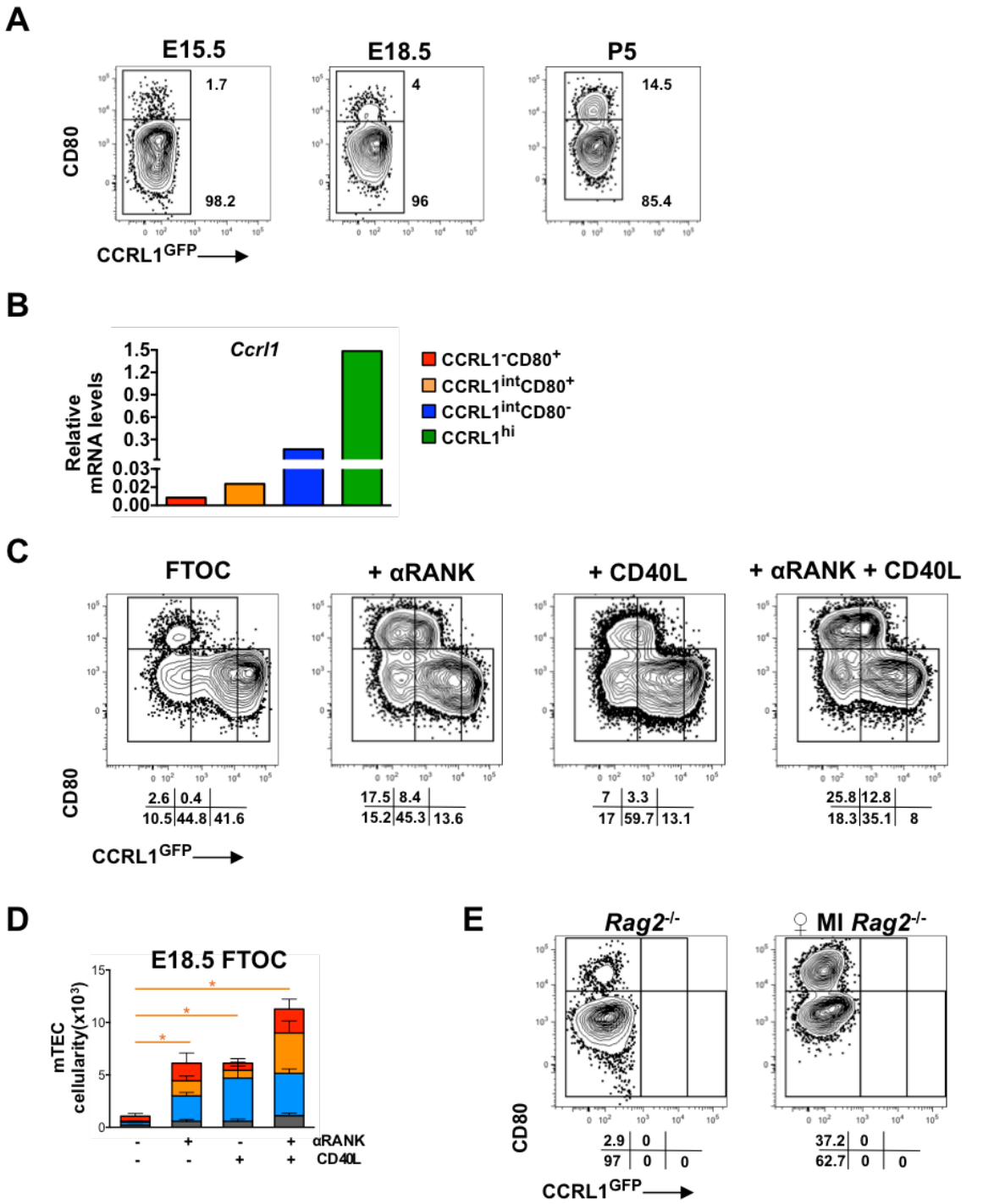

Figure S2. Total TECs (gated as CD45$^-$EPCAM$^+$) from non-reporter littermates isolated at the indicated time points were analysed for CD80 and CCRL1^{GFP} expression by flow cytometry. Numbers in plots indicate the frequency of cells found within each gate. Plots are representative of three independent experiments. (B) The expression of *Ccrl1* in TEC subsets purified from postnatal day 5 (P5) thymus was analyzed by qPCR . Values were normalized to *Actb*. (C-D) E18.5-FTOCs were left intact or stimulated with anti-RANK (αRANK) and/or CD40L. (C) CCRL1^{GFP} and CD80 expression in total TECs analyzed by flow cytometry. Grids indicate the frequencies of each respective one. (D) numbers UEA$^+$mTECs recovered after FTOC analyzed by flow cytometry. * The number of CCRL1^{int}CD80$^+$TECs (orange) in treated FTOCs is significantly higher than in controls, $p<0.05$ (unpaired t test). (E) Total TECs from non-reporter P5 *Rag2*$^{-/-}$ and female Marilyn-*Rag2*$^{-/-}$ littermates were analyzed for CD80 and CCRL1^{GFP} expression by flow cytometry.

Results Chapter III

(Adapted from)

Lympho-epithelial interactions restrain the pool of thymic epithelial progenitors residing within the postnatal cortex.

Catarina Meireles*, Ana R. Ribeiro*, Pedro M. Rodrigues, Catarina Leitão and Nuno L. Alves

*Co-first authors

To be Submitted

Abstract

Cortical (cTEC) and medullary (mTEC) thymic epithelial cells establish key microenvironments for T-cell differentiation, which arise from thymic epithelial cell progenitors (TEP). However, the nature of TEPs and the mechanism controlling their stemness in the postnatal thymus remain poorly defined. Here, we found that a fraction of cTECs generates specialized clonal-derived colonies (*Clono*TECs). We show that *Clono*TECs are EpCAM^{+}MHCII^{-}Foxn1^{lo} cells, which lack cTEC or mTEC traits but co-express stem-cell markers. Supporting their progenitor identity, *Clono*TECs are able to integrate within native thymic microenvironment and a fraction of them generate cTECs or mTECs. Furthermore, *Clono*TECs improve thymopoiesis in IL7-deficient mice. Additionally, we show that the abundance of cTECs able to generate *Clono*TECs gradually wanes with age in immunocompetent thymus. Our findings provide evidence that the postnatal cortex harbors a reservoir of TEPs, which are depleted across lifespan.

Introduction

The development and selection of highly diverse T cells, which are responsive against pathogens while tolerant to one's own organs, takes place in dedicated niches of the thymus. Central to this instructive process are thymic epithelial cells (TECs) that segregate into specialized cortical (cTEC) and medullary (mTEC) thymic epithelial microenvironments [10]. While cTECs instruct the commitment of hematopoietic precursors into the T cell lineage and positively select thymocytes expressing MHC-restricted TCR, mTECs contribute to the elimination of thymocytes expressing autoreactive TCR and the development of regulatory T cells [102]. Consequently, genetic alterations that affect the differentiation of TECs lead to pathologies that range from immunodeficiency to autoimmunity [10]. Since TECs are sensitive to aging and conditioning regiments linked to bone marrow transplantation or cancer therapy [124], the functionalization of thymic epithelial niches emerges as a direct approach to improve thymopoiesis in disorders associated with ineffective T cell responses.

The two prototypical cTEC and mTEC subsets differentiate from common bipotent TEC progenitors (TEP) that exist in the embryonic [32, 33, 36] and postnatal [30] thymus. Deciphering how bipotent TEPs self-renew and transmogrify into cTECs and mTECs has been under intense investigation. The discovery of mTEC-restricted precursors [63, 64, 78] led to the concept that TEP give rise to cortical and medullary lineages through unrelated differentiation pathways. Yet, evidence that embryonic cTEC-like progenitors have the potential to generate cTECs and mTECs [110, 119, 120] suggests the existence of TEPs that progress through the cortical lineage prior to commitment to mTECs [125]. These findings equally implicate that TEPs nestle within the embryonic cortex. Recent studies identify distinct subsets of TECs in the postnatal thymus that are purportedly enriched in TEPs [126-128]. Whether TEC differentiation in the postnatal thymus follows the same precursor-product relationships is not airtight. Moreover, the singular identity and anatomical location of TEPs are still elusive.

Thymic epithelial cell microenvironments turnover more rapidly than previously recognized, with an estimated replacement rate of one-two weeks to mTECs of the young adult thymus [22, 129]. These results suggest a requirement for regular differentiation of new mature TECs by their upstream progenitors. Two, not necessarily mutually exclusive, scenarios can be considered. On one hand, long-lasting TEPs must continually produce lineage-committed precursors without self-renewing capacity. Alternatively, the abundance of functional TEPs might drop with age, being the replenishment of cortical and medullary epithelial niches assured by downstream compartment-restricted precursors. Fate-mapping studies show that the majority of adult mTEC network arise from fetal- and newborn-derived TEPs expressing beta5t (β5t), a prototypical cTEC marker [130, 131]. Furthermore, mTEC-restricted SSEA-1^{+} progenitors [132, 133] and specialized podoplanin^{+} (PDPN) mTEPs residing at the cortico-medullary junction [134] have been identified, both contributing to the maintenance of mTEC compartment. Together these findings infer that the bipotency capacity of TEPs is preserved beyond birth, but might be progressively lost with age. Consequently, the maintenance of adult medullary epithelial network seems to be secured by unipotent mTEP(s).

How changes in the bioavailability of TEPs across life impact on the maintenance of TEC microenvironment, and ultimately on thymic output, is not understood. Another unexplored area pertains to the physiological causes underlying the presumed age-dependent senescence of TEPs. Since the amount of embryonic TEP dictates the size of functional TEC microenvironments [35], it is conceivable that the loss of TEC with age might be coupled to the deterioration of TEP stemness. Nevertheless, we lack experimental evidence that argues in favor, or against, this possibility. Herein, combining the usage of reporter, clonogenic assays and thymic transplantations, we identify a subset of cTECs capable of forming colonies, which contain cells with the potential to generate cTECs and mTECs. These results indicate that TEP-like cells nestle in the postnatal cTEC compartment. Temporal analysis reveals an age-dependent loss in epithelial stem cell activity during the first weeks of life.

Material and methods

Mice

Transgenic Actin reporter C57BL/6J mice in which the chicken β-actin promoter respectively drives enhanced Green Fluorescent Protein (eGFP) ($Actin^{GFP}$) or Red Fluorescent Protein (RFP) ($Actin^{RFP}$) expression were purchased from Jackson Laboratory. Ccrl1:eGFP ($CCRL1^{GFP}$) reporter mice were kindly provided by Dr. Thomas Boehm (Germany) [105] and were used as such or were backcrossed onto *Rag2*$^{-/-}$ *Il2rg*$^{-/-}$ [62] C57BL/6J background. *Il7*$^{-/-}$ were purchased from Instituto Gulbenkian de Ciência (Portugal). For thymic transplantation, 6-8 weeks C57BL/6J mice were used as recipients. Mice were housed under specific pathogen–free conditions and experiments were performed in accordance with institutional guidelines. For fetal studies, the day of vaginal plug detection was designated embryonic day (E) 0.5.

TEC Clonogenic Assay

Purified TECs were cultured onto a feeder layer of irradiated mouse embryonic NIH/3T3 (3T3) fibroblast cell line as described [135, 136]. 3T3 cells were regularly maintained in culture using Dulbecco-Vogt modification of Eagle's Medium

(DMEM, Gibco–Invitrogen) supplemented with 10% fetal bovine serum (FBS) and penicillin/streptomycin. For the preparation of feeder layer, 3T3 cells were irradiated (60 Gy) one day before the experiment, seeded onto 6-well culture plates coated with 0,05mg/mL of fibronectin (Sigma-Aldrich), at a density of 12.5 x 10^4 cells cm^{-2}. TEC purified by cell sorting were directly cultured onto feeder layer in a specialized medium consisting of a 3:1 mixture of DMEM and Ham's F-12 medium (Gibco–Invitrogen), supplemented with 10% FBS, hydrocortisone 0.4 µg ml^{-1}, 10^{-6} M cholera toxin, 5 µg ml^{-1} insulin, 2 x 10^{-9} M 3,3',5-triiodo-L-thyronin (T3), 10 ng ml^{-1} recombinant human epidermal growth factor rhEGF, and penicillin/streptomycin. (Peprotech). All cultures were performed at 37 ºC in a 5% CO_2 atmosphere for 12 days.

TEC and ClonoTEC isolation and flow cytometry analysis

TECs were isolated as described [119]. *Clono*TEC were recovered from Clonogenic assays using 0,05% trypsin-EDTA (Gibco-Invitrogen) and cold PBS supplemented with 10% FBS to stop the reaction. Single-cell suspensions were stained with anti-Ly51 (PE) (BD Biosciences); anti-Sca-1 (BV785); CD24 (BV510) and anti-EpCAM (BV421) (BioLegend); anti–I-A/I-E (Alexa 780); anti-CD45.2 (PerCP-Cy5.5); UEA-1 (biotin); anti-CD80 (APC) and streptavidin (PE-Cy7) (eBioscience); anti-FOXN1 (Alexa 647) [137] was kindly provided by Dr. Hans-Reimer Rodewald (Germany). For intracellular staining, cells were fixed and permeabilised with the Transcription Factor Staining Buffer Set (eBioscience) according to the manufacture's instructions. Flow cytometry analysis was performed with the LSRFortessa instrument (BD Biosciences) and FlowJo software. Cell sorting was performed using the FACSAria II (BD Biosciences), with sort purities >95%.

Immunofluorescence analysis

Immunofluorescence staining was performed directly either on clonogenic assays or on 8-mm sections of reaggregate thymic organ cultures (RTOCs) samples. Cultures or tissues were fixed in 4% paraformaldehyde (Electron Microscopy Sciences) and stained with rabbit anti-GFP (Thermo Fisher Scientific), rabbit anti-keratin 5 (Covance), rat Troma-I (from Brulet/Kemler lab), rat anti–I-A/I-E, rat anti-

Aire, UEA1- or Ly51-biotinilated (eBioscience); and revealed with secondary Alexa Fluor 488 anti-rabbit, Alexa Fluor 647 anti-rat, or streptavidin Alexa 555 (Invitrogen). Nuclei were stained with DAPI (Invitrogen). Vectashield mounting medium (Vector Laboratories) was used to prepare the slides. Analysis was performed with IN Cell Analyzer 2000 (GE lifesciences) and collected images were processed with Fiji Software.

Gene expression

For quantitative PCR, mRNA from sorted cells was purified using the RNeasy Micro Kit (QIAGEN). RNA was reverse transcribed to cDNA, using the SuperScript III First-Strand Synthesis System for RT-PCR (Invitrogen) and Random Hexamers (Fermentas), and then subjected to real-time PCR using TaqMan Universal PCR Master Mix (Applied Biosystems) and primers for *18s*, *Foxn1*, *Il7*, *Psmb11*, *Tnfrsf11a*, *Aire, Kitl, Dll4, Cxcl12, Ccl25, Ccl19, Ccl21* (Applied Biosystems). All samples were analyzed as triplicates, and the DDCt method was used to calculate relative levels of target mRNA compared with *18s*. Procedures were done according to the manufacturer's protocols. Real-time PCR was performed in an iCycler iQ5 Real-Time PCR thermocycler (Bio- Rad). Data were analyzed using iQ5 Optical System software (Bio-Rad).

RTOC

Freshly isolated E14.5 thymic lobes were used to establish RTOCs, as described [119]. Previous to aggregation, embryonic lobes were cultured for 3 days in DMEM supplemented with 10% FCS and 360mg/l 2-deoxyguanosine (dGuo) (Sigma-Aldrich). *Clono*TEC^{GFP+} were sorted to high purity (>95%). RTOCs were established from mixtures of 100,000–150,000 *Clono*TEC^{GFP+} with E14.5 thymic cells at 1:5 ratio, and transplanted under the kidney capsule of WT mice. Ectopic thymus were recovered after 4 weeks of transplantation and analyzed by flow cytometry or immunohistochemistry.

Intrathymic Injections

*Clono*TEC^{GFP+} were intrathymically injected into *Il7*$^{-/-}$ mice [49] as previously described in [138]. Briefly, 150,000 to 200,000 FACS sorted *Clono*TEC^{GFP+} were

injected per mouse, using a 10ml Hamilton syringe with 33g needle, and thymus were recovered and analyzed 2 weeks after the procedure.

Results

The postnatal cortical thymic epithelium contains cells with clonogenic capacity.

The postnatal thymus represents a period of intense growth of the TEC network, which plateaus during young adulthood prior their progressive reduction with age [22, 139]. We conceived that these dynamic changes in TEC niches might be coupled to a temporal exhaustion of TEPs. To seek for stemness within the postnatal thymus, we established clonogenic assays that were reported to support the growth of stem cells from other stratified epithelial cells and purported TEPs from the rat thymus [135, 136]. In clonogenic assays, purified bulk postnatal-TECs are cultivated onto a monolayer of feeder cells in specialized cultured medium (as reported in [135, 136]). The growth of a large amount of colonies with tightly packed cells was visualized by immunofluorescence, using the antibodies against the pan-epithelial markers cytokeratin 8 (K8) and K5 (Figure 1 A) [39]. Colony-forming units became microscopically visible around day 6 in culture and grew in size up to day 12, suggestive of serial rounds of cellular division (data not shown). A limitation of experiments with “bulk” TECs is that they might hinder a possible heterogeneity at the single cell level. Thus, we determined if this was a property of all, or only a fraction of postnatal-TECs. For that, we performed co-cultures experiments using equal amounts of postnatal TECs isolated from mice that constitutively express Green Fluorescent Protein (GFP) or Red Fluorescent Protein (RFP) under the control of β-actin promoter. The development of single GFP^+ or RFP^+ colonies suggested their possible clonal origin (Figure 1 B). Given their clonal nature, these cells will be referred hereafter as *Clono*TECs.

The observations that *Clono*TECs were generated from a fraction of postnatal TECs (Figure 1 B) led us to investigate whether the clonogenic capacity was restricted to a subpopulation of cTECs and/or mTECs. To do so, we used

CCRL1^{GFP} reporter mice, in which the combined analysis of the expression of CCRL1^{GFP} and CD80 defines discrete subsets of cTECs and mTECs in the postnatal thymus [139] (Figure 1 C). While high levels of CCRL1^{GFP} cells (CCRL1^{hi}) identifies Ly51^{+}cTECs, intermediate levels of CCRL1^{GFP} define novel subsets of mTECs that arise in the postnatal thymus (Figure 1 C) [139]. Analysis of the discrete TEC subsets showed that the capacity to generate *Clono*TECs was markedly restricted and enriched to CCRL1^{hi} cTECs. Yet, we also found residual clonogenic activity in CCRL1^{int}CD80$^{+/-}$ and CCRL1^{-}CD80^{+} expressing subsets. Furthermore, analysis of broadly defined cTECs (Ly51^{+}) and mTECs (UEA^{+}) from actin-reporter mice yielded similar results (Figure 1 D). Together, these findings indicate that the postnatal thymus harbors a subset of cTECs that display clonogenic and self-renewal capacity *in vitro*.

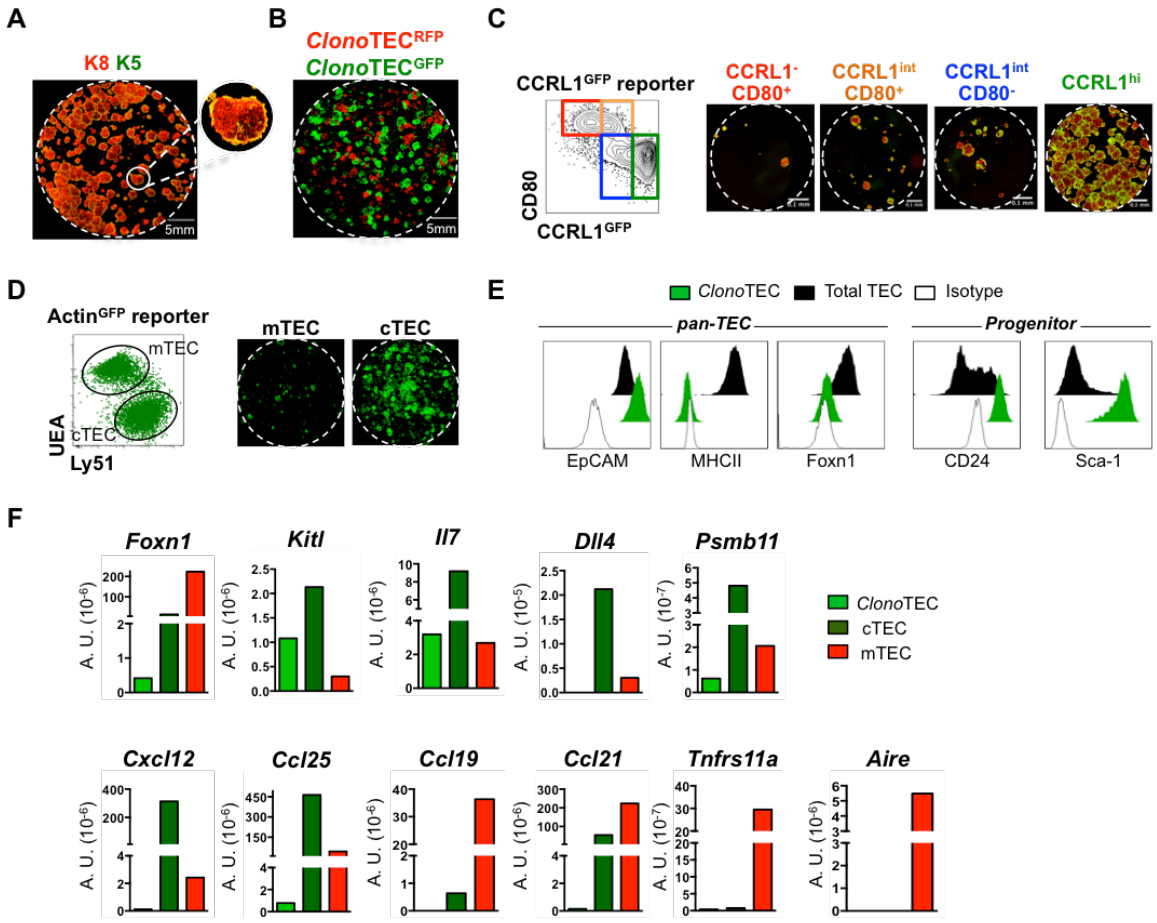

Figure 1. *Clono*TECs typify TEP-like cells and are markedly restricted to the cortical thymic epithelium of the postnatal thymus. (A) Total TECs (defined as CD45^{-}EpCAM^{+} cells) from 5 days old (P5) thymus were purified and cultured in midscale clonogenic assays (6-well plate). After 12 days, cultures were analyzed by microscopy for the expression of cytokeratin 8 (K8) and cytokeratin 5 (K5). **(B)** Total TECs purified from P5 actin-GFP and actin-RFP mice were co-culture at 1:1 ratio and analyzed for the expression of GFP and RFP. **(C)** Depicted TEC subsets from P5 CCRL1^{GFP} reporter mice were purified based on CCRL1^{GFP} and CD80

expression, cultured and analyzed as in (A). (**D**) cTECs and mTECs from P5 actin-GFP thymus were purified, cultured and analyzed as in (B). Images represent complete individual wells from clonogenic assays and are illustrative of at least three experiments. **(E)** *Clono*TECs were analyzed by flow cytometry for the expression of the indicated markers, which were compared to total TECs isolated from postnatal day 5 thymus. Isotype antibody controls for each marker is also represented **(F)** *Clono*TECs, cTECs and mTECs were purified by FACS cell sorting and analyzed by RT-qPCR for the expression of the indicated genes. Relative mRNA expression for represented target genes was normalized to *18s* and values are represented in arbitrary units (A.U.). Data are representative of two to three experiments.

ClonoTECs present phenotypic and molecular traits of TEP-like cells.

To gain further knowledge on the lineage identity and role of *Clono*TECs, we next characterized them at phenotypic and molecular levels for pan-TEC, stem cell, cTEC- and mTEC-restricted markers. As comparison, we co-analyzed freshly isolated cTECs and mTECs. Flow cytometry analysis showed that *Clono*TECs were EpCAM^{+}, but contrarily to mature TEC, lacked MHCII and expressed minute amounts of Foxn1 both at protein and transcription level (Figure 1 E and F). Interestingly, *Clono*TECs expressed CD24 and Sca-1, which have been reported to identify epithelial stem cells in other anatomical sites, including breast and lung [140, 141]. Additionally, we analyzed the molecular profile of purified *Clono*TECs for a restricted set of genes associated to cTECs (*Kitl*, *Dll4*, *Il7*, *Psmb11* (β5t), *Cxcl12* and *Ccl25*) or mTECs (*Ccl19*, *Ccl21*, *Tnfrs11a* (RANK) and *Aire*). Relatively to *ex vivo* isolated cTECs and mTECs, *Clono*TECs expressed lower to undetectable levels of cortical- and medullary-associated genes. Together, these findings infer that *Clono*TECs segregate from a typical mature epithelial identity, and instead they might typify a TEP-like subset.

ClonoTECs display bipotent and regenerative properties in vivo.

The results presented above raise the possibility that bipotent TEPs nestle after birth within the cortical thymic niche. To define the lineage potential of *Clono*TECs *in vivo,* we combined the usage of reaggregate thymic organ cultures (RTOC) with thymic transplantation under the kidney capsule. *Clono*TECs generated from CCRL1^{GFP} TECs lost GFP expression in culture (data not shown) and thus were not appropriate for fate mapping experiments. Since Ly51^{+}cTEC

from actin-GFP reporter mice exhibited similar enriched clonogenic capacity (Figure 1), we employed *Clono*TECs generated from Actin^{GFP} cTECs, in which constitutive active GFP expression provides an intrinsic label for subsequent lineage tracing. To reconstruct thymic epithelial microenvironments, we mixed *Clono*TEC^{GFP+} with dGUO-treated E14.5 thymic cells and the resulting hybrid RTOC was engrafted under the kidney capsule of WT mice to allow the ectopic formation of a thymus (Figure 2 A). As control, dGUO-treated E14.5 thymus without *Clono*TEC^{GFP} were reaggregated and subjected to similar procedure. From 6 control and 11 hybrid RTOCs, 4 and 8 ectopic thymi were respectively recovered 4 weeks post-thymic transplantation. A fraction of ectopic thymi were dissociated and analyzed by flow cytometry for the detection of *Clono*TEC^{GFP+} cells (CD45^{-} EpCAM^{+}GFP^{+}). *Clono*TECs were distinctly present in all RTOCs and expressed MHCII (3/3), indicating that this subset contained cells competent to engage into the TEC differentiation pathway (Figure 2 B).

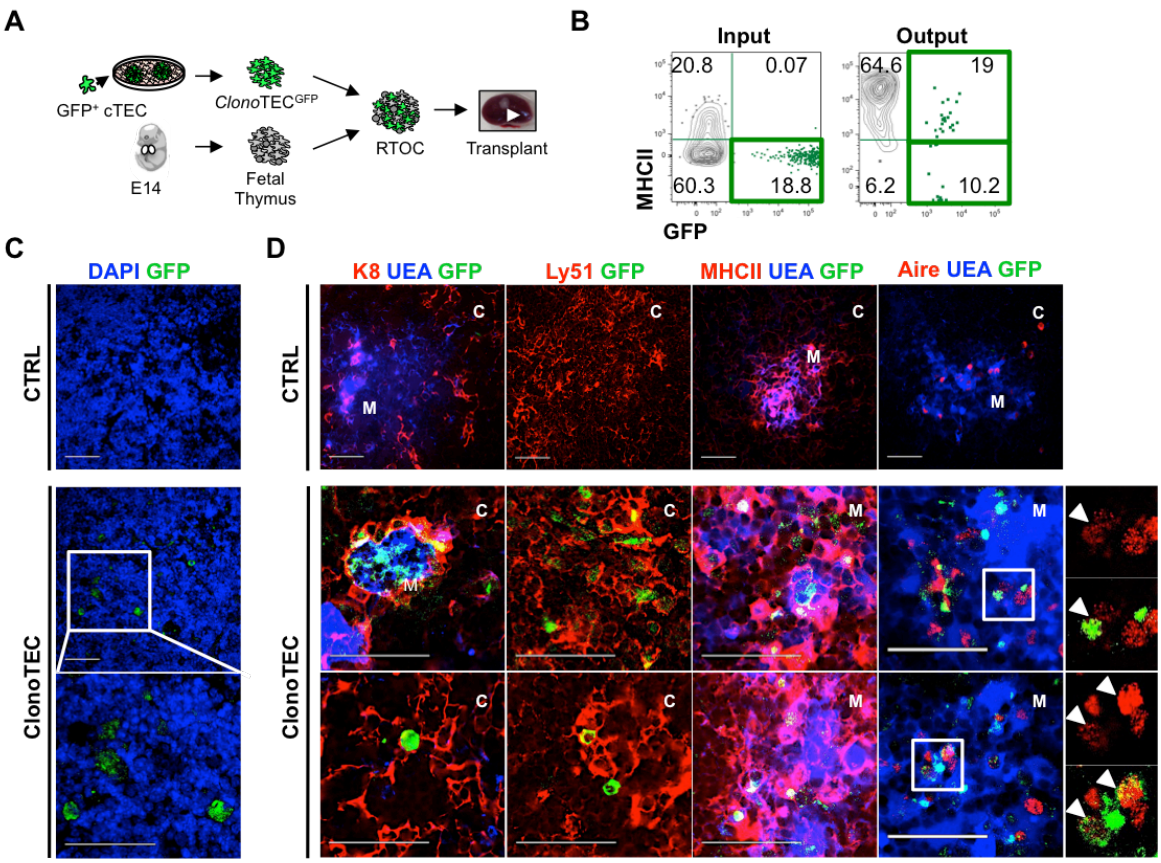

Figure 2. *Clono*TECs are able to generate cTECs and mTECs *in vivo*. (A) Scheme of the lineage tracing experiment. Briefly, *Clono*TECs^{GFP} were isolated and aggregated with dGuo-treated E14.5 thymic lobes. RTOCs were transplanted into the kidney capsule of WT mice, ectopic thymi were recovered 4 weeks post-transplantation and analyzed by flow cytometry **(B)** or fluorescent microscopy **(C and D)**. **(B)** Cells were

analyzed for the expression of MHCII and GFP before reaggregation (input) and after transplantation (output). FACS plots are representative of 3 experiments/ectopic thymus. **(C and D)** Immunofluorescence analysis of ectopic thymus. **(C)** Control and *Clono*TECs RTOCs were screened for GFP cells (anti-GFP Ab) and **(D)** analyzed for the expression of K8, UEA, Ly51, MHCII and Aire, as depicted. Cortical (C) and medullary (M) zones are indicated. Squares (in C) designate the zoomed areas and triangles (in D) indicate $Aire^{+}GFP^{+}$ TECs. 50μm scale is shown. Images are representative of 5 ectopic thymus containing *Clono*TEC^{GFP}.

Nevertheless, we systematically recovered few TECs (either from embryonic or *Clono*TEC origin) from individual RTOCs for cytometer analysis. Thus, to gain insights in the phenotypic properties and spatial distribution of *Clono*$TECs^{GFP+}$ within native thymic niches, another set of transplanted RTOC experiments was analyzed by immunofluorescence microscopy. We observed that *Clono*$TECs^{GFP+}$ engrafted within thymic microenvironments and were detected in all recovered RTOC (5/5) (Figure 2 C). Notably, *Clono*TECs spanned within discrete cortical or medullary areas, with a fraction of these cells expressing cTEC traits, such as K8 and Ly51, and other fraction expressing mTEC features, including UEA, $MHCII^{hi}$, and Aire specific markers (Figure 2 C and D). Furthermore, we tested the regenerative contribution of *Clono*TECs under defective thymic settings provoked by the absence of Interleukin 7 (IL-7). Since IL-7 is mainly produced by TECs *in vivo* [50, 142], we assessed whether intrathymic transplantation of *Clono*$TECs^{GFP+}$ improved the defective thymopoiesis of $Il7^{-/-}$ mice. Immunofluorescence analysis showed that *Clono*TEC were majorly found within the cTECs areas, but only in a half of intrathymically injected mice (Figure 3 A). Noteworthy, mTEC areas are sparse in $Il7^{-/-}$ thymus, presumably due to the insufficient TEC-thymocyte crosstalk. Still, we observed that *Clono*TEC transplantation augmented the thymopoietic activity of IL-7-deficient mice (Figure 3 B), partly ameliorating defective thymopoietic stages coupled to the lack of IL-7 signals, such as the accumulation of double-negative (DN) thymocytes and the prototypical DN2-DN3 ($CD44^{+}CD25^{+}$-$CD44^{-}CD25^{-}$) blockage (Figure 3 C). Collectively, these results indicate that *in vitro* generated *Clono*TECs contain TEPs with multilineage potential capable of generating cTECs and mTECs and possess intrinsic regenerative function upon integration in native thymic microenvironments.

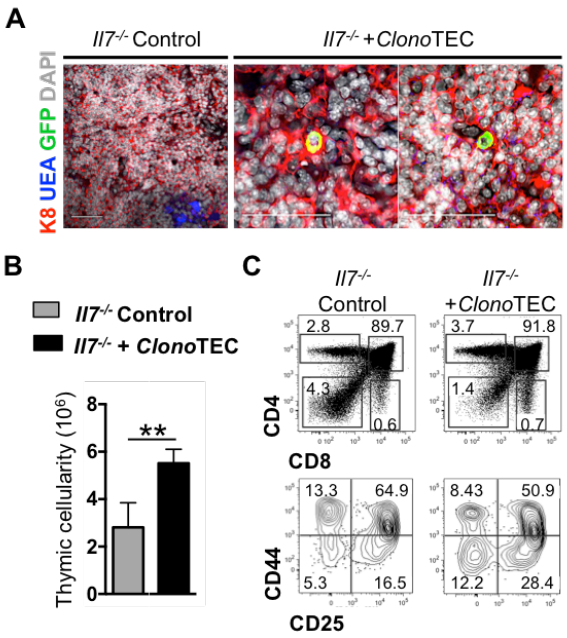

Figure 3. Intrathymic transplantation of *Clono*TECs partially restores thymopoiesis in IL-7 deficient mice. Purified *Clono*TEC^{GFP} were intrathymically injected into *Il7*$^{-/-}$ mice and thymus were harvested 2 weeks after procedure. **(A)** PBS injected (Control) and *Clono*TEC transplanted (+*Clono*TEC) thymi were screened for the presence of GFP cells (Anti-GFP Ab) and analyzed for the co-expression of K8, UEA and DAPI. 50μm scale is shown. **(B)** Thymic cellularity and **(C)** indicated thymocyte subsets were examined based on the expression of CD4 and CD8, and CD44 and CD25 within DN compartment. Data are representative of two experiments.

The pool of postnatal cTECs displaying clonogenic potential decreases with age.

Given their progenitor features, we used *Clono*TECs as a proxy to survey alterations in TEP dynamics across life. To do so, we have established competitive clonogenic assays with age-matched or age-mismatched TECs isolated from GFP and RFP actin-report mice. Since we have shown that clonogenic activity is mostly restricted to cTECs, we have focused our analysis to the postnatal cortical compartment and we have observed a conspicuous loss in the capacity of cTECs to generate *Clono*TEC with age. While co-culture experiments with cTEC^{GFP} and cTEC^{RFP} purified from postnatal day 5 mice yielded a similar proportion of *Clono*TECs of both origins, cTECs purified from postnatal day 5 revealed a marked clonogenic advantage over their older counterparts (around four fold) (Figure 4). Together, our findings indicate that cTECs autonomously lose the capacity to generate *Clono*TECs with age, suggesting that this potential decreased concomitantly with the loss of cTECs and the expansion of the mTEC network that occurs during the first weeks of life.

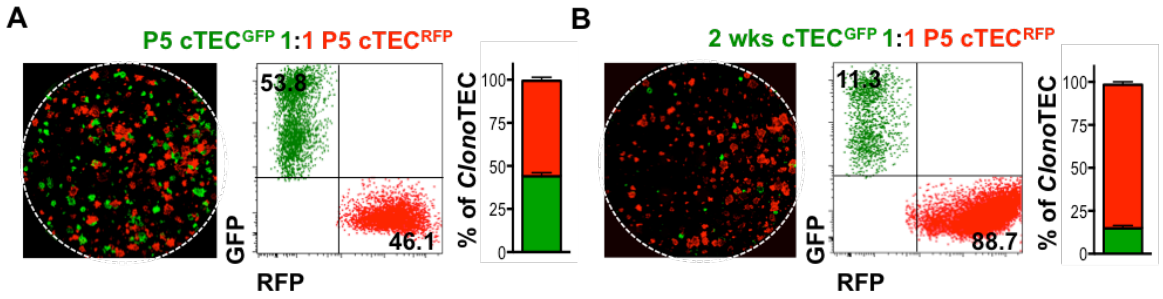

Figure 4. The pool of postnatal cTECs that generate *Clono*TECs decreases with age. (A) Age-matched postnatal day 5 (P5) or **(B)** mismatched P5 and 2-weeks old cTECs from Actin^{GFP} and Actin^{RFP} reporter mice were co-cultured in clonogenic assays for 12 days. *Clono*TEC^{GFP} and *Clono*TEC^{RFP} were analyzed by fluorescence microscopy and flow cytometry. The percentages of recovered cells analyzed by flow cytometry are represented in the graphs. Images represent complete individual wells and are illustrative of three experiments.

Discussion

Comprehending the principles that underlie the maintenance of cortical and medullary thymic epithelial compartments is chief to harness thymopoiesis in the elderly and in patients with immunodeficiency disorders or autoimmunity. Therefore, the prospective isolation of TEPs within the adult thymus emerge as a central objective in thymic biology, as it would provide means for reconstructing functionalized thymic epithelial microenvironments in therapies targeting thymus disorders. An aspect of equal importance that has been overlooked pertains to the principles that control the bioavailability and functionality of TEPs in the adulthood. Our findings reveal that the postnatal life defines a period of intense TEP stem cell activity within the thymic cortex, which gradually diminished thereafter into the adulthood. The deterioration of the pool of TEPs and/or defect in their replenishment rate might explain the incapacity to sustain functional epithelial niches in the aged thymus.

Given that the TEC network expands vigorously during the period between birth and early adulthood, we centered our initial attention in this temporal window with the hypothesis that it might reveal new insights on how TEP homeostasis is balanced *in vivo*. We identified and characterized a subset of postnatal cTECs that is able to form colony-forming units under specialized clonogenic culture assays

(*Clono*TECs). Interestingly, detailed phenotypic and molecular analyses show that *Clono*TECs lacked traits that are typically associated with cortical or medullary lineages, but instead expressed markers linked to stem cells. These observations correlate with their reduced levels of Foxn1, which is central for the initiation and maintenance of the TEC program but appears dispensable for the maintenance of the thymic epithelial stem cell pool [30, 31, 126]. One possibility is that *Clono*TECs arise directly from progenitors that settle within the cTECs and express low levels of Foxn1. Alternatively, *Clono*TECs might gradually lose Foxn1 expression *in vitro*, indicating that its levels are tightly controlled by thymic microenvironmental factors. Further experiments are required to understand how this master regulator of TEC identity is balanced *in vivo*. Importantly, the findings that *Clono*TECs self-renew *in vitro* and diversify into cTECs and mTECs *in vivo* reinforce their TEP-like signature. Worth mentioning, the recovered *Clono*TECs that reintegrated within thymic microenvironment was reduced. Whether the low engraftment of *Clono*TECs is due to experimental impediments related to the establishment of organotypic cultures and/or a competitive disadvantage relatively to embryonic TEC within RTOCs is unclear. This technical limitation seems to be transversal to other studies using hybrid RTOC, which are composed of predominant embryonic thymic stromal cells mixed with adult TEC subsets purportedly enriched with TEPs [126-128]. Furthermore, due to high cell density requirements, *Clono*TECs used in RTOC experiments derived from a pool of multiple colony-forming units. Despite phenotypic similarities, possible intra and inter-clonal heterogeneity within *Clono*TECs might also influence their engraftment. Future refined experimental setups are required to address these possibilities. Additionally, the observations that *Clono*TECs integrate within the defective thymic microenvironment of IL-7-deficient mice and ameliorate their defective thymopoeisis, in a condition in which they constitute the only source of IL-7, provide functional evidence for their regenerative properties *in vivo.* Most of the current studies have so far addressed the lineage potential of purported TEP. Improved experimental methods are however necessary to analyze the autonomous contribution of isolated TEPs to distinct aspects of thymopoiesis, including lineage commitment, migration positive and negative selection and T regulatory cell differentiation.

Using distinct TEC cellular fractionating approaches, three recent reports have revealed the existence of TEC stem cell activity within the adult thymus. First, Ucar *et al*. reported the presence of EpCAM^{-} Foxn1^{-} cells within the thymic stromal cells that form spheroids, named thymosphere, under specialized *in vitro* culture system and have the capacity to generate cTECs and mTECs [126]. We reason that cTECs with clonogenic potential represent a distinct TEP subset from thymospheres. First, although the location of thymospheres remains undetermined, *Clono*TECs arise from cells belonging to the prototypical cTEC lineage (EpCAM^{+}Ly51^{+}CCRL1^{+}). Secondly, CD45^{-}EpCAM^{-} thymic stromal cells failed to form colonies in our experimental condition (data not shown). More recently, Wong *et al*. documented that bipotent TEPs exist within the UEA-1^{-}MHII^{lo} cTEC-like cells of the adult thymus [127] and Ulyanchenko *et al*. further mapped them to a fraction of Ly51^{+}MHCII^{hi}Plet1^{+} cTECs[128], inferring that TEPs share to some extent a cortical-associated signature. Along this line, genetic inducible cell-fate mapping studies by Ohigashi *et al.* and Mayer *et al.* found that a large fraction of adult cTECs and mTECs develop from fetal- and newborn-derived TEPs expressing β5t [130, 131]. Concordantly to our findings, these results suggest that TEC differentiation in the postnatal period follows a similar process to the one defined in the embryonic life [121], in which the cortex represents a reservoir of TEPs wherefrom they can potentially differentiate into cortical and epithelial lineages. Yet, it remains to be elucidated whether cTEC-derived *Clono*TECs, and all the recently identified subsets enriched in TEP-like cells, contain truly bipotent progenitors or unipotent progenitors for each lineage. Albeit it is conceptually possible that several pools of TEP-like cells exist within the thymus, further studies are required to determine the lineage and temporal relationship between the distinct types of reported TEPs that are being revealed within the adult thymus. It is important to underline that even with the most refined subsets and distinct assays, TEC precursors are still being described at the population level, but are not yet recognized as single cells.

It remains unclear how TEC stem cell activity is controlled in the adult thymus. The incapacity of TEC progenitors to undergo compensatory proliferation to maintain the number of mature TECs [35] indicates a direct deficit in their

stemness. Based on their progenitor activity, we used the clonogenic capacity of cTECs as a surrogate to survey the detailed dynamics of TEP during early postnatal life and adulthood. Our findings suggest that TEP activity is predominantly enriched with the CCRL1^{hi} cTECs during the first week of life. Previous observations showed that cTECs regenerate after the specific ablation of CCRL1^{hi} cTECs [105]. Nevertheless, the complete cTEC depletion was not achieved in this study and therefore resistant TEP within CCRL1-expressing subset might explain the observed regenerative capacity of cortical epithelium. The loss in the capacity of CCRL1^{hi} cTECs to generate *Clono*TECs in the ensuing weeks indicates that the bioavailable pool of TEPs is reduced with the entry into the adulthood. Supportive of this view are the findings that the contribution of β5t^{+} progenitors to cTEC and mTEC lineages declines postnatally [130, 131] and TEPs isolated from the adult thymus are extremely rare cells [126, 127, 130]. Our results suggest that the epithelial progenitor capacity decreases concomitantly with the loss of cTECs and the expansion of the mTEC network, driven by continual interaction with developing thymocytes [102]. Albeit lympho-epithelial interactions are often considered stimulatory to TEC differentiation, we conjectured that signals provided by developing thymocytes might restrain functional properties coupled to immature TECs [102]. Further worker from our lab has shown that the clonogenic activity in TEC is maintained in adult alymphoid thymus, suggesting that aging is, not *per se*, a defining factor in this process (data not shown). In particular, we observed that clonogenic activity was to a certain extent enriched within CCRL1^{hi} cTEC-like subset of adult mice, indicating that TEPs progress through, and settle within, the cortical lineage in a thymocyte-independent manner (data not shown). These observations provide evidence for a negative feedback mechanism in which continual thymocyte-TEC crosstalk fine-tunes the stem cell activity of TEPs. Similar observations were recently suggested to Cld3,4^{+}SSEA1^{+} mTEC-restricted cells, which are rare in the adult thymus and enriched in *Rag2*$^{-/-}$ mice [133]. Thymocyte-derived signals are often considered stimulatory for TEC differentiation [10]. Nonetheless, previous studies, including from our group, have shown that thymocyte-TEC crosstalk negatively regulates functional attributes coupled to cTECs, including the expression of DLL4 and IL-7 [61, 119]. Now, our findings implicate that continuous lympho-epithelial interactions impact upstream on the TEC differentiation branch, deteriorating the pool of TEPs and possibly limiting

their replenishment rate. This notion provides a possible explanation to the failure in maintaining TEC microenvironments in the aged thymus [22], and the success in inducing cortical and medullary epithelial compartments in adult mice that lack functional thymocytes-crosstalk [62, 111]. Together, our data question whether the mere prospective isolation of bipotent progenitors from the adult and aged thymus represents the more desirable strategy for cellular replacement therapies in thymic disorders. Alternative approaches might focus in unraveling active mediators of stem cell activity, which will permit a more effective functionalization of TEPs isolated the adult thymus.

Acknowledgments

We thank Drs. James Di Santo (Pasteur Institute, Paris, France) and Thomas Boehm (Max Planck Institute of Immunology and Epigenetics, Freiburg, Germany) for *Rag2*$^{-/-}$*Il2rg*$^{-/-}$ and and CCRL1-reporter, respectively. We thank Dr. Hans-Reimer Rodewald (German Cancer Research Center, Heidelberg, Germany) for the anti-Foxn1 antibody. We thank Drs. Chiara Perrod and Gema Romera-Cardenas for critical reading the manuscript. We also thank Dr. Sofia Lamas and the caretakers from the animal facility for the assistance with animal experimentation. This study was supported by a starting grant to N.L.A from the European Research Council (ERC) under the project 637843. N.L.A., P.M.R., A.R.R. and C.M. are supported by the Investigator program and PhD fellowships from FCT (Portugal).

General Discussion and Future directions

The thymic epithelium defines a specialized microenvironment for T cell generation, which rely on the proper diversification of uncommitted epithelial progenitors into functionally different cortical and medullary subsets [10]. In this thesis, we have deciphered novel TEC differentiation pathways that advance our current knowledge on thymus development. We showed that the cortical compartment of the embryonic and postnatal thymus harbors a pool of cells with bipotent capacity to generate cTECs and mTECs. Interestingly, we also demonstrated that the bioavailability of cortical-related progenitors is reduced across life, possibly as a result of continual lympho-epithelial interactions. Although the role of TEC-thymocyte crosstalk in promoting mTEC differentiation has been intensively studied, its function on the cortical compartment is not yet understood. Herein, we have additionally shown that MHC-peptide/TCR interactions control the homeostasis of cTECs, limiting the size of their niche.

In this section, I discuss the major findings obtained in this thesis and integrate them with several key studies that have contributed to our current understanding of the processes underlying thymic microenvironment ontogeny and maintenance.

Uncovering embryonic thymic development: establishment and patterning of the epithelial microenvironment

TEC ontogeny is initiated early in embryonic development with the formation endodermal-derived thymic anlagen [27, 28]. Thymus development is then followed by a presumed expansion of thymic epithelial progenitor cells and their differentiation into cortical and medullary epithelium, in a dynamic process that continues in the postnatal life [22]. Yet, the true TEP identity and their requirements for maintenance and/or differentiation are still poorly defined.

Several studies have examined the development of the downstream progeny of bipotent TEPs. The description of compartment-restricted progenitors led to the idea that cTEC and mTEC developmental pathways diverge early in their developmental pathways and therefore the establishment of both compartments would rely on lineage committed intermediate progenitors [121]

(Introduction – figure V). Supportive of this, the nature of the medullary epithelium was shown to be clonal, deriving from a single cell progenitor [63] and the expression of the tight junction proteins Cld3,4 marks a minor subset of $Aire^{+}$-mTEC progenitors at E13 thymus [64]. More recently, the emergence of $RANK^{+}$ mTEC-restricted cells within the $Cld3,4^{hi}$ population of the E14 thymus was described as a purported downstream progeny of $Cld3,4^{hi}SSEA1^{+}$ early TEC medullary precursors [132]. Further maturation can be analyzed by following the acquisition of MHCII and CD80 maturation markers, confirming the direct precursor-product relationship within mTEC lineage [22]. On the other side, less is known about discrete developmental stages of cTECs, being their specific progenitors identified by CD205 and β5t expression in thymus ontogeny [38]. Specifically, segregation between β5t and Claudins expression pattern in the outer and inner layer of early thymic anlage, respectively, provided evidence for this hypothesis of bimodal and unrelated TEC differentiation pathways [37]. Nevertheless, these studies do not unveil how transitional compartment-specific progenitors relate with the other epithelial lineage or the common bipotent precursor.

Here, we took advantage of a previously described IL-7 reporter mouse model, in which a homogenous population of cTECs expressing high levels of *Il7* transcripts is present in the embryonic and young postnatal thymus [50, 62], to follow cortical epithelium dynamics throughout development. Employing RTOC, we have shown that $Il7^{hi/YFP}$ cortical TEC population contains cells with the ability to differentiate into both cTECs and mTECs **(Results Chapter I, Figure 5)**. These results suggest the existence of cells within the cortex with the capacity to divert into the medullary lineage. In agreement, two complementary studies reported similar findings. While Baik *et al* demonstrated that $CD205^{+}CD40^{-}$ cTECs are able to generate both β5t/CD205 cortical and Aire-expressing medullary TECs in RTOC grafts [110]; Ohigashi *et al* used β5t-Cre-mediated reporter expression to demonstrate that the great majority of mTECs derive from cells with a cTEC-associated β5t expression history [120].

These findings imply that the early segregation model, in which cTEC and mTEC differentiate through individual unrelated pathways downstream of bipotent

TEPs, might be more complex than previously recognized. Instead, embryonic epithelial progenitors seem to transiently progress through the cortical lineage, prior to the commitment into mTEC, a process that we described as a serial progression model for TEC differentiation [121] **(Figure I)**. This notion would implicate that the cortical compartment acts as a niche for cells with bipotent capacity. Nevertheless, several questions remain unanswered: (1) what are the molecular mechanisms regulating the dynamics of lineage conversion?; (2) how many cells within the cortex retain the capacity to divert into both cTECs and mTECs? One can speculate that only a small fraction of cells displaying cortical features preserve their bipotency. Nonetheless, since none of these studies was performed at the single cell level, one cannot exclude the existence of unipotent cTEC and mTEC progenitors residing within the cortical compartment; (3) Do these cells represent immature or mature cTECs? The complete segregation between the timing of expression of the putative later cTEC marker CCRL1 and the first mTECs emerging in the embryonic thymus **(Results Chapter II, Figure 2)** suggests that these transitional precursors do not progress further within the cTEC lineage. Still, further studies are warranted to address these queries. The definition of more refined subsets of epithelial progenitors and their genome-wide analysis might be of great interest to better understand their single cell nature and, consequently, their specific molecular signature.

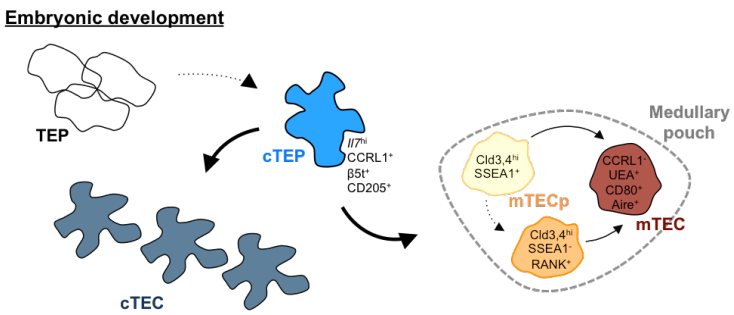

Figure I – Serial progression model for TEC differentiation. In this model, TEPs transverse through a transitional stage in which they express phenotypic and molecular traits associated with cTECs prior to the commitment into a cTEC or mTEC fate. Within the medullary lineage, the relation between the distinct mTEPs described is still not understood.

Although thymus development and compartmentalization into cortical and medullary areas starts during embryonic development, thymic epithelium

establishment and expansion continues throughout life [22]. The maintenance of the thymic microenvironment throughout postnatal life will be discussed in the following section.

Expanding and maintaining thymic microenvironments: from the embryonic to the adult thymus

The maintenance of the thymic epithelium throughout life requires a continuous replenishment of mature TECs. Nevertheless, the adult thymus undergoes an age-related atrophy that results in the loss of normal cortical and medullary architecture. Yet, the fact that thymic involution and consequent decreased T-cell output can be partially reverted under specific conditions, such as sex steroid ablation [21, 22], suggests that the TEC compartment is able to maintain some plasticity and regenerative capacity, which can be associated to the presence of TEC progenitors in the adult thymus. It has been shown that TEPs persist beyond the embryonic period [30]. Whether postnatal TEPs contribute to the maintenance of the adult thymic epithelial compartment across life, is still not completely understood.

The evidence that embryonic TEPs progress through the cortical lineage prior to the commitment into mTECs led to the idea that the cortex functions as a niche for bipotent precursors. Multi-color flow cytometry analysis of CCRL1-reporter mice throughout thymic development enabled us to unravel novel mTEC subsets that share cTEC and mTEC traits, which suggests a possible continual contribution of the cortex to the medullary compartment. These subsets are particularly prominent during the first week of age and point to the cortical compartment as a possible niche for postnatal bipotent precursors **(Results Chapter II, Figure 2)**.

To test this, we employed specialized *in vitro* clonogenic assays [135, 136] to selectively grow TEC progenitors and study their dynamics in the early postnatal life. Our results suggest that epithelial cells with self-renewal and bipotent capacity can be generated from cells nestling within the postnatal cTEC compartment **(Results Chapter III, Figures 1-3)**. Moreover, these cells appear to retain their

functional capacity to boost T cell development upon reintegration in IL-7 deficient thymus, indicative of their *in vivo* regenerative capacity **(Results Chapter III, Figure 4)**. Still, further investigation using more refined experimental systems are required to access their capacity to support distinct crucial checkpoints during T cell development, such as lineage commitment, and selection. In this regard, the reconstruction of thymic environments exploiting cells with distinct MHC deficiencies and TCR transgenic models may be of great value to access the selection capacity of defined TEP-derived cells.

The amount of available TEPs appears to determine the size of the thymus and its output [35]. Nevertheless, how the age-associated thymic involution is related to a deterioration of the epithelial progenitor pool and consequent imbalance in TEC maintenance is still poorly understood. Our findings suggest that TEP activity is predominantly enriched in cTECs during the first week of life **(Results Chapter III, Figure 5)**, being timely correlated with the great expansion of the TEC microenvironment in the young thymus. Further studies from our lab, using microscaled assays to follow the dynamics of TECs with clonogenic potential, revealed that the frequency of cTECs able to generate colonies is prominently reduced between the first and the second week of age and becomes almost negligible in the four weeks old thymus, at the peak of thymic activity (Meireles & Ribeiro, unpublished). By taking advantage of mouse models displaying severe blocks in thymocyte development, we established a correlation between the loss of cTECs with clonogenic potential and continual lympho-epithelial interactions across life (Meireles & Ribeiro, unpublished). These results provide evidence for a possible negative feedback mechanism in which TEC-thymocyte crosstalk acts as regulator of TEP stem cell activity. Therefore, these findings also implicate that these continual interactions take place early in the TEC differentiation pathway and might contribute the incapacity of the aged thymus to maintain and replenish its TEC microenvironment [22]. Further studies using mice with distinct blocks in T cell development are warranted to decipherer the cellular and molecular partners of these interactions.

Our results are in line with two collaborative studies that have addressed the contribution of cortical-associated precursors to the mTEC compartment in the

postnatal thymus. By applying inducible models of lineage tracing based on β5t expression [130, 131], the authors could follow the progeny of β5t$^+$ TEPs during postnatal life. Their reports showed that the contribution of cTEC-associated progenitors to the adult mTEC niche decreases with age. In fact, cTEC-derived *de novo* mTEC differentiation seems to be restricted to the first week of age and almost negligible in the adult thymus. Instead, the growth and maintenance of the mTEC compartment appears to be guaranteed by medullary-restricted precursors [130] **(Figure II)**. The existence of precursors committed to the medullary lineage (mTEPs) in the adult thymus has been scrutinized by several studies. Within these, Cld3,4$^+$SSEA1$^+$ cells were shown to be a rare population containing mTEC-restricted progenitors in the adult thymus, suggesting that the pool of mTEPs is exhausted throughout life [133]. Additionally, podoplanin$^+$ (PDPN) TECs residing at the cortical-medullary junction (jTECs) were described to be able to generate nearly half of the adult mTECs [134]. Although Cld3,4$^+$SSEA1$^+$ mTEPs were shown to derive from β5t$^+$ cortical precursors, their link to PDPN$^+$ jTECs is not yet clear. One can speculate that the latter PDPN$^+$ subset might represent a downstream progeny of Cld3,4$^+$SSEA1$^+$ adult mTEPs, which contribute to the maintenance of the medullary network, acting as transient amplifying subsets [143] **(Figure II)**.

These findings point to a scenario in which the maintenance of the epithelium is guaranteed by the turnover of compartment-restricted cells. Indeed, it has been previously shown that mature TEC populations proliferate in the adult thymus [22]. Nevertheless, the contribution of bipotent TEPs throughout life is not excluded in none of the above-discussed studies, and the cooperative action of bipotent progenitors and turnover of committed cells throughout life might also be considered. Several studies have focused their attention on the identification of TEP throughout development. Adult TEPs with the capacity to generate cTECs and mTECs were shown to be present either within the EpCAM$^-$Foxn1$^-$ fraction of stromal cells [126] and EpCAM$^+$Foxn1$^+$ epithelial lineages [127, 128]. Among these latest, Wong *et al* reported that bipotent TEPs exist within the UEA-1$^-$ MHCII^{lo} cTEC compartment [127], while Ulyanchenko *et al* further mapped them to a fraction of Ly51$^+$MHCII^{hi}Plet1$^+$ cells [128], suggesting that TEPs maintain their cortical associated features in the adult life. Yet, it is important to emphasize that

the described epithelial subsets may be enriched for such progenitors, which are described at the population level rather than as single cells. Still, one can speculate that these identified subsets comprise different, yet some how developmental-related, precursors.

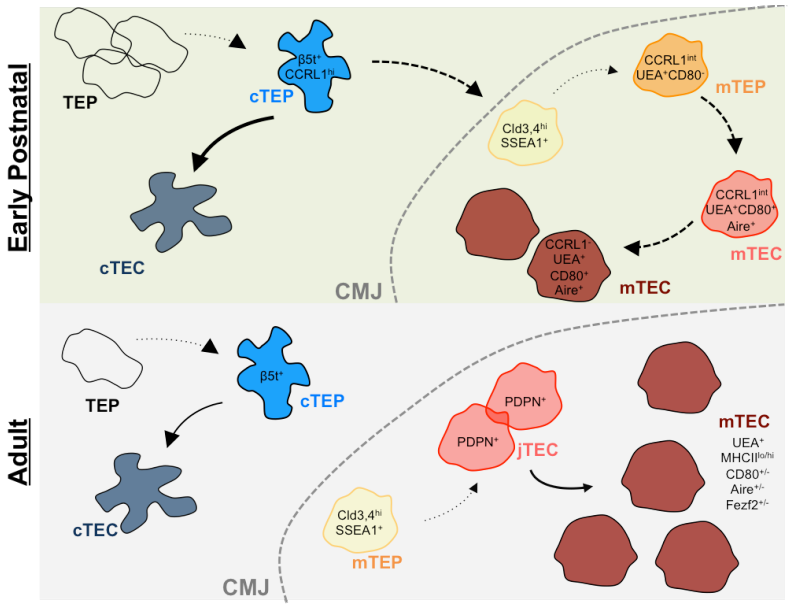

Figure II – Establishment and maintenance of the epithelial compartments in the early postnatal and adult thymus. While in the first week of life bipotent progenitors within cTECs contribute for the establishment and growth of the medullary compartment, the adult niches are maintained by the expansion of lineage-restricted precursors. How the distinct progenitors relate to each other is not completely addressed.

All together, these findings demonstrate that functional TEPs are present in the postnatal thymic cortical compartment and they preserve their bipotent capacity. Nevertheless, their bioavailability diminishes across life, possibly as a result of continual lympho-epithelial interactions. Therefore, the adult TEC compartment seems to be expanded and maintained by lineage-restricted intermediate precursors [133, 134, 143], rather than by the pool of bipotent progenitors, which have undergone age-dependent exhaustion.

As TEPs seem to settle within the cTEC lineage and their bioavailability appears to parallel the dynamics of their harboring cortical niche, it is of great interest to gain a better understanding of the development of the thymic cortical epithelium.

Deciphering the cortical epithelial niche

Epithelial cells from the thymic cortex form the unique microenvironment that provides crucial factors for thymocyte survival and T-cell commitment, and that is able to process and present a myriad of self-derived peptides, responsible for the selection of a great TCR diversity [10, 102]. Nonetheless, the discrimination of distinct developmental stages within the cortical lineage is still not clear. In fact, most of the cTEC-restricted markers are acquired early in ontogeny and are widely expressed through the thymic cortex. For instance, both CD205 and β5t are detected as early as the E12 thymus and their expression is progressively upregulated throughout early development, concomitantly with MCHII levels [37, 38].

It is well established that continual interaction with developing thymocytes elicit an increase of the mTEC compartment in the postnatal life with a concomitant decrease in cTEC areas [22, 102]. Although mTEC developmental stages and thymocyte-derived signals have been extensively studied, our understanding on fundamental aspects of the cortical thymic epithelium development and homeostasis remains limited. It was previously recognized that cTEC development is not a cell autonomous process, in which mesenchymal cells and developing thymocytes seem to cooperate to regulate cTEC homeostasis and maturation [38-41]. Still, we lack information on the nature of the thymocyte-derived signals that control the thymic cortex.

As the dynamics of *Il7*$^{hi/YFP}$ TECs in IL-7 reporter mice mimics the one observed for cTECs during embryonic and postnatal development [50, 62], we followed this population as a surrogate cTEC subset to better understand the homeostasis of this compartment. Thymocytes beyond DP subset were shown to restrain the size of the cortical *Il7*$^{hi/YFP}$ compartment [62]. Here, we demonstrated that this restraining lympho-stromal association is mediated by TCR/MHC-peptide interactions during selection events **(Results Chapter I, Figure 7 and 8)**. Nevertheless, it is still not clear how these interactions affect cTEC homeostasis. One can speculate that upon TCR-MHCII interaction, novel signaling pathways are engaged in the thymocytes that culminate on the delivery of still unidentified important signals for cTECs. Yet, little is known about cTEC-specific pathways

controlling their differentiation and homeostasis. In this regard, a recent report had suggested that Notch signaling is particularly evident in cTECs, and that its action in mTECs leads to impaired medullary maturation [144], possibly indicating a putative specific role for Notch pathway on the maintenance of the cortical identity. However, further functional assays are required to clarify its role on cTEC homeostasis, as well as the cellular source of Notch ligands within the thymic microenvironment.

In order to further dissect the heterogeneity of the cortical compartment, we have combined specific cTEC-associated *Il7*^{YFP} with CCRL1^{GFP} reporter mouse models. Analysis of the double-reporter thymus throughout ontogeny has revealed that initiation of CCRL1^{GFP} expression typifies a later cTEC maturation marker that is progressively acquired through embryogenesis and early postnatal life. **(Results Chapter II, Figure 1, S1)**. Additionally, CCRL1 and MHCII acquisition is partially blocked in mice displaying combined *Rag2* and *Il2rg* deficiencies, suggesting that cTEC maturation is partially impaired **(Results Chapter II, Figure 1)** [38]. These findings support the key role of interaction with DN2-DN3 thymocytes in cTEC maturation. Nevertheless, one cannot exclude a possible additional and complementary role of γc cytokine-dependent cells on cTEC differentiation. The role of IL-7R-expressing Lti cells in tissue formation and organization is well known for secondary lymphoid organs [145-147]. In the thymus, these cells belonging to the group 3 of Innate Lymphoid Cells (ILC) express high levels of RANKL and were shown to drive mTEC differentiation in the embryonic thymus [77]. Additionally, IL-22 produced by Lti cells was demonstrated as a crucial cue in thymic regeneration upon acute damage, by acting mostly in cTECs and immature mTECs [148]. Whether Ltis and IL-22 play a major role in cTEC differentiation and homeostasis is still uncovered. The analysis of thymus with combined deficiency in the *Rag* and *Rorgc* genes should further elucidate these questions.

The above-described possible heterogeneity within the TEP harboring cortical compartment has raised the idea that developmental distinct progenitors preserve the capacity to divert into the mTEC lineage. Whether these distinct waves of mTEC differentiation result in a functional heterogeneity within the medulla is not yet addressed.

Unveiling mTEC development and heterogeneity

The neonatal life represents a very challenging developmental window for the immune system and for its adaptation to the external environment. During the first weeks of age, the peripheral T cell pool is greatly augmented and it is known that specific Treg subsets that assure central tolerance throughout life are generated during this developmental window [149, 150]. It is, then, a demanding period for mTEC expansion and function in T cell selection and Treg development. Accordingly, although the first mature mTECs are observed around embryonic day 16 in mice, major expansion of the medullary compartment occurs mainly in the postnatal life, concomitantly with the emergence of positively selected SP thymocytes [83].

Analysis of the cTEC-restricted CCRL1 reporter mouse model throughout development has revealed novel mTEC subsets that emerge specifically in the postnatal thymus and still co-express cortical features **(Results Chapter II, Figure 2)**, suggesting the existence of distinct waves of mTEC differentiation in the embryonic and postnatal thymus**.** Whether these temporally distinct waves generate functionally distinct mTEC subsets is currently unclear. A recent report has shown that embryonic and neonatally β5t-derived mTECs display subtle differences in their expression pattern of TNF receptor-associated factor 3 (TRAF3) and some TRAs [130]. One can speculate that these differences may arise from mTEC of possible distinct developmental origin.

Whether the two described postnatal subsets of mature medullary ($CCRL1^-$ and $CCRL1^+$) TECs differ in their antigen presentation capacity or in their ability to support thymocyte maturation upon selection it is currently unaddressed. Our gene expression analysis showed similar Aire expression patterns in both subsets **(Results Chapter II, Figure 2)**, suggesting that they are likely equally functional on Aire-dependent antigens presentation. Nevertheless, we still do not know whether this is also the case for Aire-independent TRAs. Recently, a novel regulator of mTEC-mediated antigen presentation was described. However, in contrast to Aire, Fezf2 is expressed in both immature and mature mTECs [74], suggesting a broader presentation of Fezf2-dependent antigens. Further studies

on the expression pattern of TRAs and their specific regulators are needed to further dissect the distinct mTEC subsets.

Another degree of heterogeneity in early steps of mTEC differentiation has been recently added, when Baik et al employed their RANK-reporter mouse model to show that the emergence of the first $RANK^+$ mTEPs occurs within the $Cld3,4^{hi}$ population at E14 embryonic thymus. These mTEC-restricted cells seem to represent a developmental stage distinct from the $Cld3,4^{hi}SSEA1^+$ TECs, based on their levels of MHCII and CD205 expression [132]. However, although $RANK^+$ mTEPs emerge temporally downstream of $SSEA1^+$ mTEPs, the direct lineage relationship between these two subsets remains undetermined. Additionally, future experiments are required to access the expression of additional cTEC and mTEC markers in both subsets. One can speculate that the segregation of $Cld3,4^{hi}SSEA1^+$ and $Cld3,4^{hi}RANK^+$ cells may indicate the initiation of alternative routes of embryonic mTEC differentiation. The functional relevance of the described mTEC heterogeneity at embryonic and postnatal stages and the possible correlation with their distinct ontogeny requires further dissection.

Additionally, Baik *et al* have shown that although $Cld3,4^{hi}SSEA1^+$ mTEC-restricted progenitors are reduced in nude mice, their progression into the medullary lineage as a $RANK^+$ population is only dependent on Relb-signaling, suggesting that the non-canonical NF-κB pathway [132] as an important checkpoint in the regulation of RANK expression in mTEPs. This evidence also infers that mTEC commitment and maturation are independently regulated. Further experiments are required to define the identity of upstream receptors controlling the expression of RANK *in vivo*. One can speculate that these signals might dictate the divergence between epithelial lineages.

Final remarks and future directions

All together, the recent developments in the thymus field provide an important part on our current understanding of TEC biology. Nevertheless, we still lack evidence on how transcriptional and epigenetic changes contribute to TEP maintenance or TEC lineage specification. The recent experimental advances on

genome-wide data mining should be further exploited to solve this fundamental question. I believe that deciphering the transcriptional master regulators for cortical and medullary genetic program would represent the next big advance in the field. Although we might have uncovered some of the signals related to lineage specification, we still known very little about their induction and regulation at the gene level and how its expression influence downstream differentiation processes.

Additionally, further functional studies involving more refined TEP populations are required to address the factors involved in TEP nature and regulation. In this regard, the advances in multi-parametric flow cytometry analysis have been proven extremely useful on the definition of novel developmental subsets within the thymic epithelium. Still, we should always take in consideration that the studies at the population level are not powerful enough to address the real bipotent capacity. As already discussed, single-cell functional assays are in demand.

In this thesis, we have focused our attention on the embryonic and neonatal developmental periods of the thymic epithelial microenvironment to unveil some of the aspects related to cTEC and mTEC diversification. We have further dissected the cortical compartment and its previously overseen heterogeneity, being able to show that it harbors a pool of bipotent epithelial progenitors and cTEC-like phenotype in both embryonic and postnatal thymus. Having this in mind, I believe that it is of great value to unveil the cellular and molecular mechanisms that control the homeostasis of the cortical harboring TEP niche, in order to better understand TEP dynamics and function. In fact, we have shown that continual lympho-stromal interactions curtain both niches of cTECs and cortical-associated TEPs, suggesting that thymocyte-derived signals negatively regulate cTEC- and TEP-homeostasis and functional properties. Whether cTECs and TEPs are governed by the same thymocyte-derived signals and by the same molecular functional regulators, it is still unclear, however, given their similar phenotype, a certain degree of overlap may be considered.

Collectively, the recent advances in TEC biology have demonstrated that distinct progenitors might regulate initial establishment of the epithelium and its later growth or maintenance. While bipotent epithelial progenitors control TEC

homeostasis in the embryonic and early postnatal thymus, the expansion of the adult niches seems to be guaranteed by compartment-restricted progenitors. Comprehending how thymic function is tightly regulated throughout life is of great interest, as alterations in the thymic epithelium are closely related to age-associated decrease in thymic output and consequent impaired T cell responses, as well as disrupted self-tolerance. Therefore, uncovering the cellular and molecular pathways involved in the maintenance and function of the thymic epithelium and its progenitors represents a great challenge for designing strategies to therapeutically intervene to treat and revert the deterioration of the immune system.

References

1. Singhrao, S.K., et al., *Spontaneous classical pathway activation and deficiency of membrane regulators render human neurons susceptible to complement lysis.* Am J Pathol, 2000. **157**(3): p. 905-18.
2. Boyington, J.C. and P.D. Sun, *A structural perspective on MHC class I recognition by killer cell immunoglobulin-like receptors.* Mol Immunol, 2002. **38**(14): p. 1007-21.
3. Mosmann, T.R., et al., *Differentiation and functions of T cell subsets.* Ciba Found Symp, 1997. **204**: p. 148-54; discussion 154-8.
4. Miller, J.F., *Immunological function of the thymus.* Lancet, 1961. **2**(7205): p. 748-9.
5. Miller, J.F., *The golden anniversary of the thymus.* Nat Rev Immunol, 2011. **11**(7): p. 489-95.
6. Swann, J.B., et al., *Conversion of the thymus into a bipotent lymphoid organ by replacement of FOXN1 with its paralog, FOXN4.* Cell Rep, 2014. **8**(4): p. 1184-97.
7. Anderson, G., P.J. Lane, and E.J. Jenkinson, *Generating intrathymic microenvironments to establish T-cell tolerance.* Nat Rev Immunol, 2007. **7**(12): p. 954-63.
8. Anderson, G., et al., *MHC class II-positive epithelium and mesenchyme cells are both required for T-cell development in the thymus.* Nature, 1993. **362**(6415): p. 70-3.
9. Takahama, Y., *Journey through the thymus: stromal guides for T-cell development and selection.* Nat Rev Immunol, 2006. **6**(2): p. 127-35.
10. Anderson, G. and Y. Takahama, *Thymic epithelial cells: working class heroes for T cell development and repertoire selection.* Trends in immunology, 2012. **33**(6): p. 256-63.
11. Nehls, M., et al., *New member of the winged-helix protein family disrupted in mouse and rat nude mutations.* Nature, 1994. **372**(6501): p. 103-7.
12. Nehls, M., et al., *Two genetically separable steps in the differentiation of thymic epithelium.* Science, 1996. **272**(5263): p. 886-9.
13. Blackburn, C.C., et al., *The nu gene acts cell-autonomously and is required for differentiation of thymic epithelial progenitors.* Proc Natl Acad Sci U S A, 1996. **93**(12): p. 5742-6.
14. Nitta, T., et al., *Thymoproteasome shapes immunocompetent repertoire of CD8+ T cells.* Immunity, 2010. **32**(1): p. 29-40.
15. Gommeaux, J., et al., *Thymus-specific serine protease regulates positive selection of a subset of CD4+ thymocytes.* Eur J Immunol, 2009. **39**(4): p. 956-64.
16. Hsieh, C.S., et al., *A role for cathepsin L and cathepsin S in peptide generation for MHC class II presentation.* J Immunol, 2002. **168**(6): p. 2618-25.
17. Murata, S., et al., *Regulation of CD8+ T cell development by thymus-specific proteasomes.* Science, 2007. **316**(5829): p. 1349-53.
18. Naquet, P., M. Naspetti, and R. Boyd, *Development, organization and function of the thymic medulla in normal, immunodeficient or autoimmune mice.* Seminars in immunology, 1999. **11**(1): p. 47-55.
19. Lomada, D., et al., *Thymus medulla formation and central tolerance are restored in IKKalpha-/- mice that express an IKKalpha transgene in keratin 5+ thymic epithelial cells.* J Immunol, 2007. **178**(2): p. 829-37.
20. Boehm, T., et al., *Thymic medullary epithelial cell differentiation, thymocyte emigration, and the control of autoimmunity require lympho-epithelial cross talk via LTbetaR.* The Journal of experimental medicine, 2003. **198**(5): p. 757-69.
21. Lynch, H.E., et al., *Thymic involution and immune reconstitution.* Trends Immunol, 2009. **30**(7): p. 366-73.
22. Gray, D.H., et al., *Developmental kinetics, turnover, and stimulatory capacity of thymic epithelial cells.* Blood, 2006. **108**(12): p. 3777-85.

23. Gui, J., et al., *The aged thymus shows normal recruitment of lymphohematopoietic progenitors but has defects in thymic epithelial cells.* Int Immunol, 2007. **19**(10): p. 1201-11.
24. Mackall, C.L., et al., *Thymic function in young/old chimeras: substantial thymic T cell regenerative capacity despite irreversible age-associated thymic involution.* Eur J Immunol, 1998. **28**(6): p. 1886-93.
25. Heng, T.S., A.P. Chidgey, and R.L. Boyd, *Getting back at nature: understanding thymic development and overcoming its atrophy.* Curr Opin Pharmacol, 2010. **10**(4): p. 425-33.
26. Gordon, J., et al., *Gcm2 and Foxn1 mark early parathyroid- and thymus-specific domains in the developing third pharyngeal pouch.* Mech Dev, 2001. **103**(1-2): p. 141-3.
27. Gordon, J., et al., *Functional evidence for a single endodermal origin for the thymic epithelium.* Nat Immunol, 2004. **5**(5): p. 546-53.
28. Rodewald, H.R., *Thymus organogenesis.* Annual review of immunology, 2008. **26**: p. 355-88.
29. Jenkinson, W.E., E.J. Jenkinson, and G. Anderson, *Differential requirement for mesenchyme in the proliferation and maturation of thymic epithelial progenitors.* J Exp Med, 2003. **198**(2): p. 325-32.
30. Bleul, C.C., et al., *Formation of a functional thymus initiated by a postnatal epithelial progenitor cell.* Nature, 2006. **441**(7096): p. 992-6.
31. Nowell, C.S., et al., *Foxn1 regulates lineage progression in cortical and medullary thymic epithelial cells but is dispensable for medullary sublineage divergence.* PLoS Genet, 2011. **7**(11): p. e1002348.
32. Gill, J., et al., *Generation of a complete thymic microenvironment by MTS24(+) thymic epithelial cells.* Nat Immunol, 2002. **3**(7): p. 635-42.
33. Bennett, A.R., et al., *Identification and characterization of thymic epithelial progenitor cells.* Immunity, 2002. **16**(6): p. 803-14.
34. Rossi, S.W., et al., *Redefining epithelial progenitor potential in the developing thymus.* Eur J Immunol, 2007. **37**(9): p. 2411-8.
35. Jenkinson, W.E., et al., *An epithelial progenitor pool regulates thymus growth.* J Immunol, 2008. **181**(9): p. 6101-8.
36. Rossi, S.W., et al., *Clonal analysis reveals a common progenitor for thymic cortical and medullary epithelium.* Nature, 2006. **441**(7096): p. 988-91.
37. Ripen, A.M., et al., *Ontogeny of thymic cortical epithelial cells expressing the thymoproteasome subunit beta5t.* European journal of immunology, 2011. **41**(5): p. 1278-87.
38. Shakib, S., et al., *Checkpoints in the development of thymic cortical epithelial cells.* Journal of immunology, 2009. **182**(1): p. 130-7.
39. Klug, D.B., et al., *Interdependence of cortical thymic epithelial cell differentiation and T-lineage commitment.* Proceedings of the National Academy of Sciences of the United States of America, 1998. **95**(20): p. 11822-7.
40. Klug, D.B., et al., *Cutting edge: thymocyte-independent and thymocyte-dependent phases of epithelial patterning in the fetal thymus.* Journal of immunology, 2002. **169**(6): p. 2842-5.
41. Sitnik, K.M., et al., *Mesenchymal cells regulate retinoic acid receptor-dependent cortical thymic epithelial cell homeostasis.* J Immunol, 2012. **188**(10): p. 4801-9.
42. Calderon, L. and T. Boehm, *Three chemokine receptors cooperatively regulate homing of hematopoietic progenitors to the embryonic mouse thymus.* Proc Natl Acad Sci U S A, 2011. **108**(18): p. 7517-22.
43. Krueger, A., et al., *CC chemokine receptor 7 and 9 double-deficient hematopoietic progenitors are severely impaired in seeding the adult thymus.* Blood, 2010. **115**(10): p. 1906-12.
44. Liu, C., et al., *Coordination between CCR7- and CCR9-mediated chemokine signals in prevascular fetal thymus colonization.* Blood, 2006. **108**(8): p. 2531-9.

45. Zlotoff, D.A., et al., *CCR7 and CCR9 together recruit hematopoietic progenitors to the adult thymus.* Blood, 2010. **115**(10): p. 1897-905.
46. Bleul, C.C. and T. Boehm, *Chemokines define distinct microenvironments in the developing thymus.* Eur J Immunol, 2000. **30**(12): p. 3371-9.
47. Liu, C., et al., *The role of CCL21 in recruitment of T-precursor cells to fetal thymi.* Blood, 2005. **105**(1): p. 31-9.
48. Peschon, J.J., et al., *Early lymphocyte expansion is severely impaired in interleukin 7 receptor-deficient mice.* J Exp Med, 1994. **180**(5): p. 1955-60.
49. von Freeden-Jeffry, U., et al., *Lymphopenia in interleukin (IL)-7 gene-deleted mice identifies IL-7 as a nonredundant cytokine.* J Exp Med, 1995. **181**(4): p. 1519-26.
50. Alves, N.L., et al., *Characterization of the thymic IL-7 niche in vivo.* Proc Natl Acad Sci U S A, 2009. **106**(5): p. 1512-7.
51. Radtke, F., et al., *Deficient T cell fate specification in mice with an induced inactivation of Notch1.* Immunity, 1999. **10**(5): p. 547-58.
52. Hozumi, K., et al., *Delta-like 4 is indispensable in thymic environment specific for T cell development.* J Exp Med, 2008. **205**(11): p. 2507-13.
53. Feyerabend, T.B., et al., *Deletion of Notch1 converts pro-T cells to dendritic cells and promotes thymic B cells by cell-extrinsic and cell-intrinsic mechanisms.* Immunity, 2009. **30**(1): p. 67-79.
54. Koch, U., et al., *Delta-like 4 is the essential, nonredundant ligand for Notch1 during thymic T cell lineage commitment.* J Exp Med, 2008. **205**(11): p. 2515-23.
55. Ciofani, M., et al., *Stage-specific and differential notch dependency at the alphabeta and gammadelta T lineage bifurcation.* Immunity, 2006. **25**(1): p. 105-16.
56. Klein, L., et al., *Antigen presentation in the thymus for positive selection and central tolerance induction.* Nat Rev Immunol, 2009. **9**(12): p. 833-44.
57. Starr, T.K., S.C. Jameson, and K.A. Hogquist, *Positive and negative selection of T cells.* Annu Rev Immunol, 2003. **21**: p. 139-76.
58. Bynoe, M.S., P. Bonorino, and C. Viret, *Control of experimental autoimmune encephalomyelitis by CD4+ suppressor T cells: peripheral versus in situ immunoregulation.* J Neuroimmunol, 2007. **191**(1-2): p. 61-9.
59. Nakagawa, T., et al., *Cathepsin L: critical role in Ii degradation and CD4 T cell selection in the thymus.* Science, 1998. **280**(5362): p. 450-3.
60. Honey, K., et al., *Cathepsin L regulates CD4+ T cell selection independently of its effect on invariant chain: a role in the generation of positively selecting peptide ligands.* J Exp Med, 2002. **195**(10): p. 1349-58.
61. Fiorini, E., et al., *Cutting edge: thymic crosstalk regulates delta-like 4 expression on cortical epithelial cells.* J Immunol, 2008. **181**(12): p. 8199-203.
62. Alves, N.L., et al., *Cutting Edge: a thymocyte-thymic epithelial cell cross-talk dynamically regulates intrathymic IL-7 expression in vivo.* J Immunol, 2010. **184**(11): p. 5949-53.
63. Rodewald, H.R., et al., *Thymus medulla consisting of epithelial islets each derived from a single progenitor.* Nature, 2001. **414**(6865): p. 763-8.
64. Hamazaki, Y., et al., *Medullary thymic epithelial cells expressing Aire represent a unique lineage derived from cells expressing claudin.* Nature immunology, 2007. **8**(3): p. 304-11.
65. Kim, C.H., et al., *Differential chemotactic behavior of developing T cells in response to thymic chemokines.* Blood, 1998. **91**(12): p. 4434-43.
66. Ueno, T., et al., *CCR7 signals are essential for cortex-medulla migration of developing thymocytes.* J Exp Med, 2004. **200**(4): p. 493-505.
67. Choi, Y.I., et al., *PlexinD1 glycoprotein controls migration of positively selected thymocytes into the medulla.* Immunity, 2008. **29**(6): p. 888-98.
68. Derbinski, J., et al., *Promiscuous gene expression in medullary thymic epithelial cells mirrors the peripheral self.* Nature immunology, 2001. **2**(11): p. 1032-9.
69. Mathis, D. and C. Benoist, *Aire.* Annu Rev Immunol, 2009. **27**: p. 287-312.

70. Hubert, F.X., et al., *Aire regulates the transfer of antigen from mTECs to dendritic cells for induction of thymic tolerance.* Blood, 2011. **118**(9): p. 2462-72.
71. Sansom, S.N., et al., *Population and single-cell genomics reveal the Aire dependency, relief from Polycomb silencing, and distribution of self-antigen expression in thymic epithelia.* Genome Res, 2014. **24**(12): p. 1918-31.
72. Meredith, M., et al., *Aire controls gene expression in the thymic epithelium with ordered stochasticity.* Nat Immunol, 2015. **16**(9): p. 942-9.
73. Anderson, M.S., et al., *Projection of an immunological self shadow within the thymus by the aire protein.* Science, 2002. **298**(5597): p. 1395-401.
74. Takaba, H., et al., *Fezf2 Orchestrates a Thymic Program of Self-Antigen Expression for Immune Tolerance.* Cell, 2015. **163**(4): p. 975-87.
75. Klein, L. and K. Jovanovic, *Regulatory T cell lineage commitment in the thymus.* Semin Immunol, 2011. **23**(6): p. 401-9.
76. McCaughtry, T.M., M.S. Wilken, and K.A. Hogquist, *Thymic emigration revisited.* J Exp Med, 2007. **204**(11): p. 2513-20.
77. Rossi, S.W., et al., *RANK signals from CD4(+)3(-) inducer cells regulate development of Aire-expressing epithelial cells in the thymic medulla.* The Journal of experimental medicine, 2007. **204**(6): p. 1267-72.
78. Gabler, J., J. Arnold, and B. Kyewski, *Promiscuous gene expression and the developmental dynamics of medullary thymic epithelial cells.* Eur J Immunol, 2007. **37**(12): p. 3363-72.
79. Nishikawa, Y., et al., *Biphasic Aire expression in early embryos and in medullary thymic epithelial cells before end-stage terminal differentiation.* The Journal of experimental medicine, 2010. **207**(5): p. 963-71.
80. Wang, X., et al., *Post-Aire maturation of thymic medullary epithelial cells involves selective expression of keratinocyte-specific autoantigens.* Frontiers in immunology, 2012. **3**(March): p. 19.
81. Metzger, T.C., et al., *Lineage tracing and cell ablation identify a post-Aire-expressing thymic epithelial cell population.* Cell Rep, 2013. **5**(1): p. 166-79.
82. White, A.J., et al., *Lymphotoxin signals from positively selected thymocytes regulate the terminal differentiation of medullary thymic epithelial cells.* J Immunol, 2010. **185**(8): p. 4769-76.
83. White, A.J., et al., *Sequential phases in the development of Aire-expressing medullary thymic epithelial cells involve distinct cellular input.* European journal of immunology, 2008. **38**(4): p. 942-7.
84. Shores, E.W., W. Van Ewijk, and A. Singer, *Disorganization and restoration of thymic medullary epithelial cells in T cell receptor-negative scid mice: evidence that receptor-bearing lymphocytes influence maturation of the thymic microenvironment.* European journal of immunology, 1991. **21**(7): p. 1657-61.
85. Shores, E.W., W. Van Ewijk, and A. Singer, *Maturation of medullary thymic epithelium requires thymocytes expressing fully assembled CD3-TCR complexes.* Int Immunol, 1994. **6**(9): p. 1393-402.
86. Surh, C.D., B. Ernst, and J. Sprent, *Growth of epithelial cells in the thymic medulla is under the control of mature T cells.* J Exp Med, 1992. **176**(2): p. 611-6.
87. Derbinski, J., et al., *Promiscuous gene expression in thymic epithelial cells is regulated at multiple levels.* J Exp Med, 2005. **202**(1): p. 33-45.
88. Derbinski, J. and B. Kyewski, *Linking signalling pathways, thymic stroma integrity and autoimmunity.* Trends Immunol, 2005. **26**(10): p. 503-6.
89. Zhu, M., et al., *NF-kappaB2 is required for the establishment of central tolerance through an Aire-dependent pathway.* J Clin Invest, 2006. **116**(11): p. 2964-71.
90. Akiyama, T., et al., *Dependence of self-tolerance on TRAF6-directed development of thymic stroma.* Science, 2005. **308**(5719): p. 248-51.
91. Hikosaka, Y., et al., *The cytokine RANKL produced by positively selected thymocytes fosters medullary thymic epithelial cells that express autoimmune regulator.* Immunity, 2008. **29**(3): p. 438-50.

92. Akiyama, T., et al., *The tumor necrosis factor family receptors RANK and CD40 cooperatively establish the thymic medullary microenvironment and self-tolerance.* Immunity, 2008. **29**(3): p. 423-37.
93. Roberts, N.A., et al., *Rank signaling links the development of invariant gammadelta T cell progenitors and Aire(+) medullary epithelium.* Immunity, 2012. **36**(3): p. 427-37.
94. Irla, M., et al., *Autoantigen-specific interactions with CD4+ thymocytes control mature medullary thymic epithelial cell cellularity.* Immunity, 2008. **29**(3): p. 451-63.
95. Irla, M., G. Hollander, and W. Reith, *Control of central self-tolerance induction by autoreactive CD4+ thymocytes.* Trends Immunol, 2010. **31**(2): p. 71-9.
96. Kyewski, B. and L. Klein, *A central role for central tolerance.* Annu Rev Immunol, 2006. **24**: p. 571-606.
97. Giliani, S., et al., *Interleukin-7 receptor alpha (IL-7Ralpha) deficiency: cellular and molecular bases. Analysis of clinical, immunological, and molecular features in 16 novel patients.* Immunol Rev, 2005. **203**: p. 110-26.
98. Iwanami, N., et al., *Genetic evidence for an evolutionarily conserved role of IL-7 signaling in T cell development of zebrafish.* J Immunol, 2011. **186**(12): p. 7060-6.
99. Mazzucchelli, R.I., et al., *Visualization and identification of IL-7 producing cells in reporter mice.* PLoS One, 2009. **4**(11): p. e7637.
100. Repass, J.F., et al., *IL7-hCD25 and IL7-Cre BAC transgenic mouse lines: new tools for analysis of IL-7 expressing cells.* Genesis, 2009. **47**(4): p. 281-7.
101. Hara, T., et al., *Identification of IL-7-producing cells in primary and secondary lymphoid organs using IL-7-GFP knock-in mice.* J Immunol, 2012. **189**(4): p. 1577-84.
102. Alves, N.L., et al., *Thymic epithelial cells: the multi-tasking framework of the T cell "cradle".* Trends Immunol, 2009. **30**(10): p. 468-74.
103. Shinkai, Y., et al., *RAG-2-deficient mice lack mature lymphocytes owing to inability to initiate V(D)J rearrangement.* Cell, 1992. **68**(5): p. 855-67.
104. Lantz, O., et al., *Gamma chain required for naive CD4+ T cell survival but not for antigen proliferation.* Nature immunology, 2000. **1**(1): p. 54-8.
105. Rode, I. and T. Boehm, *Regenerative capacity of adult cortical thymic epithelial cells.* Proceedings of the National Academy of Sciences of the United States of America, 2012. **109**(9): p. 3463-8.
106. Gray, D.H., A.P. Chidgey, and R.L. Boyd, *Analysis of thymic stromal cell populations using flow cytometry.* J Immunol Methods, 2002. **260**(1-2): p. 15-28.
107. Levelt, C.N., et al., *Restoration of early thymocyte differentiation in T-cell receptor beta-chain-deficient mutant mice by transmembrane signaling through CD3 epsilon.* Proc Natl Acad Sci U S A, 1993. **90**(23): p. 11401-5.
108. Mouri, Y., et al., *Lymphotoxin signal promotes thymic organogenesis by eliciting RANK expression in the embryonic thymic stroma.* J Immunol, 2011. **186**(9): p. 5047-57.
109. von Boehmer, H., *Unique features of the pre-T-cell receptor alpha-chain: not just a surrogate.* Nat Rev Immunol, 2005. **5**(7): p. 571-7.
110. Baik, S., et al., *Generation of both cortical and Aire(+) medullary thymic epithelial compartments from CD205(+) progenitors.* European journal of immunology, 2013. **43**(3): p. 589-94.
111. Roberts, N.A., et al., *Absence of thymus crosstalk in the fetus does not preclude hematopoietic induction of a functional thymus in the adult.* Eur J Immunol, 2009. **39**(9): p. 2395-402.
112. Zuklys, S., et al., *Normal thymic architecture and negative selection are associated with Aire expression, the gene defective in the autoimmune-polyendocrinopathy-candidiasis-ectodermal dystrophy (APECED).* Journal of immunology, 2000. **165**(4): p. 1976-83.

113. van Ewijk, W., et al., *Stepwise development of thymic microenvironments in vivo is regulated by thymocyte subsets.* Development, 2000. **127**(8): p. 1583-91.
114. Marrella, V., et al., *Anti-CD3epsilon mAb improves thymic architecture and prevents autoimmune manifestations in a mouse model of Omenn syndrome: therapeutic implications.* Blood, 2012. **120**(5): p. 1005-14.
115. Goldman, K.P., et al., *Thymic cortical epithelium induces self tolerance.* Eur J Immunol, 2005. **35**(3): p. 709-17.
116. McCaughtry, T.M. and K.A. Hogquist, *Central tolerance: what have we learned from mice?* Semin Immunopathol, 2008. **30**(4): p. 399-409.
117. Stritesky, G.L., et al., *Murine thymic selection quantified using a unique method to capture deleted T cells.* Proc Natl Acad Sci U S A, 2013. **110**(12): p. 4679-84.
118. Anderson, G., E.J. Jenkinson, and H.R. Rodewald, *A roadmap for thymic epithelial cell development.* Eur J Immunol, 2009. **39**(7): p. 1694-9.
119. Ribeiro, A.R., et al., *Thymocyte selection regulates the homeostasis of IL-7-expressing thymic cortical epithelial cells in vivo.* Journal of immunology, 2013. **191**(3): p. 1200-9.
120. Ohigashi, I., et al., *Aire-expressing thymic medullary epithelial cells originate from beta5t-expressing progenitor cells.* Proceedings of the National Academy of Sciences of the United States of America, 2013. **110**(24): p. 9885-90.
121. Alves, N.L., et al., *Serial progression of cortical and medullary thymic epithelial microenvironments.* European journal of immunology, 2013.
122. Lkhagvasuren, E., et al., *Lymphotoxin beta receptor regulates the development of CCL21-expressing subset of postnatal medullary thymic epithelial cells.* J Immunol, 2013. **190**(10): p. 5110-7.
123. Dumont-Lagace, M., et al., *Adult thymic epithelium contains nonsenescent label-retaining cells.* J Immunol, 2014. **192**(5): p. 2219-26.
124. Boehm, T. and J.B. Swann, *Thymus involution and regeneration: two sides of the same coin?* Nat Rev Immunol, 2013. **13**(11): p. 831-8.
125. Alves, N.L., et al., *Serial progression of cortical and medullary thymic epithelial microenvironments.* Eur J Immunol, 2014. **44**(1): p. 16-22.
126. Ucar, A., et al., *Adult thymus contains FoxN1(-) epithelial stem cells that are bipotent for medullary and cortical thymic epithelial lineages.* Immunity, 2014. **41**(2): p. 257-69.
127. Wong, K., et al., *Multilineage potential and self-renewal define an epithelial progenitor cell population in the adult thymus.* Cell Rep, 2014. **8**(4): p. 1198-209.
128. Ulyanchenko, S., et al., *Identification of a Bipotent Epithelial Progenitor Population in the Adult Thymus.* Cell Rep, 2016. **14**(12): p. 2819-32.
129. Nishikawa, Y., et al., *Temporal lineage tracing of Aire-expressing cells reveals a requirement for Aire in their maturation program.* J Immunol, 2014. **192**(6): p. 2585-92.
130. Ohigashi, I., et al., *Adult Thymic Medullary Epithelium Is Maintained and Regenerated by Lineage-Restricted Cells Rather Than Bipotent Progenitors.* Cell Rep, 2015. **13**(7): p. 1432-43.
131. Mayer, C.E., et al., *Dynamic spatio-temporal contribution of single beta5t+ cortical epithelial precursors to the thymus medulla.* Eur J Immunol, 2015.
132. Baik, S., et al., *Relb acts downstream of medullary thymic epithelial stem cells and is essential for the emergence of RANK(+) medullary epithelial progenitors.* Eur J Immunol, 2016. **46**(4): p. 857-62.
133. Sekai, M., Y. Hamazaki, and N. Minato, *Medullary thymic epithelial stem cells maintain a functional thymus to ensure lifelong central T cell tolerance.* Immunity, 2014. **41**(5): p. 753-61.
134. Onder, L., et al., *Alternative NF-kappaB signaling regulates mTEC differentiation from podoplanin-expressing presursors in the cortico-medullary junction.* Eur J Immunol, 2015. **45**(8): p. 2218-31.

135. Senoo, M., et al., *p63 Is essential for the proliferative potential of stem cells in stratified epithelia.* Cell, 2007. **129**(3): p. 523-36.
136. Bonfanti, P., et al., *Microenvironmental reprogramming of thymic epithelial cells to skin multipotent stem cells.* Nature, 2010. **466**(7309): p. 978-82.
137. Rode, I., et al., *Foxn1 Protein Expression in the Developing, Aging, and Regenerating Thymus.* J Immunol, 2015. **195**(12): p. 5678-87.
138. Liu, L.L., et al., *A simplified intrathymic injection technique for mice.* Biotech Histochem, 2012. **87**(2): p. 140-7.
139. Ribeiro, A.R., et al., *Intermediate expression of CCRL1 reveals novel subpopulations of medullary thymic epithelial cells that emerge in the postnatal thymus.* Eur J Immunol, 2014. **44**(10): p. 2918-24.
140. Shackleton, M., et al., *Generation of a functional mammary gland from a single stem cell.* Nature, 2006. **439**(7072): p. 84-8.
141. McQualter, J.L., et al., *Evidence of an epithelial stem/progenitor cell hierarchy in the adult mouse lung.* Proc Natl Acad Sci U S A, 2010. **107**(4): p. 1414-9.
142. Shitara, S., et al., *IL-7 produced by thymic epithelial cells plays a major role in the development of thymocytes and TCRgammadelta+ intraepithelial lymphocytes.* J Immunol, 2013. **190**(12): p. 6173-9.
143. Alves, N.L. and A.R. Ribeiro, *Thymus medulla under construction: Time and space oddities.* Eur J Immunol, 2016. **46**(4): p. 829-33.
144. Goldfarb, Y., et al., *HDAC3 Is a Master Regulator of mTEC Development.* Cell Rep, 2016. **15**(3): p. 651-65.
145. Mebius, R.E., *Organogenesis of lymphoid tissues.* Nat Rev Immunol, 2003. **3**(4): p. 292-303.
146. Eberl, G., *Inducible lymphoid tissues in the adult gut: recapitulation of a fetal developmental pathway?* Nat Rev Immunol, 2005. **5**(5): p. 413-20.
147. Lane, P.J., et al., *Lymphoid tissue inducer cells: pivotal cells in the evolution of CD4 immunity and tolerance?* Front Immunol, 2012. **3**: p. 24.
148. Dudakov, J.A., et al., *Interleukin-22 drives endogenous thymic regeneration in mice.* Science, 2012. **336**(6077): p. 91-5.
149. Guerau-de-Arellano, M., et al., *Neonatal tolerance revisited: a perinatal window for Aire control of autoimmunity.* The Journal of experimental medicine, 2009. **206**(6): p. 1245-52.
150. Yang, S., et al., *Immune tolerance. Regulatory T cells generated early in life play a distinct role in maintaining self-tolerance.* Science, 2015. **348**(6234): p. 589-94.

Annex

Thymocyte Selection Regulates the Homeostasis of IL-7–Expressing Thymic Cortical Epithelial Cells In Vivo

Ana R. Ribeiro,*,† Pedro M. Rodrigues,*,† Catarina Meireles,* James P. Di Santo,‡ and Nuno L. Alves*

Thymic epithelial cells (TECs) help orchestrate thymopoiesis, and TEC differentiation relies on bidirectional interactions with thymocytes. Although the molecular mediators that stimulate medullary thymic epithelial cell (mTEC) maturation are partially elucidated, the signals that regulate cortical thymic epithelial cell (cTEC) homeostasis remain elusive. Using IL-7 reporter mice, we show that TECs coexpressing high levels of IL-7 (*Il7*$^{YFP+}$ TECs) reside within a subset of CD205^{+}Ly51^{+}CD40^{low} cTECs that coexpresses *Dll4*, *Ccl25*, *Ccrl1*, *Ctsl*, *Psmb11*, and *Prss16* and segregates from CD80^{+}CD40^{high} mTECs expressing *Tnfrsf11a*, *Ctss*, and *Aire*. As the frequency of *Il7*$^{YFP+}$ TECs gradually declines as mTEC development unfolds, we explored the relationship between *Il7*$^{YFP+}$ TECs and mTECs. In thymic organotypic cultures, the thymocyte-induced reduction in *Il7*$^{YFP+}$ TECs dissociates from the receptor activator of NF-κB–mediated differentiation of CD80^{+} mTECs. Still, *Il7*$^{YFP+}$ TECs can generate some CD80^{+} mTECs in a stepwise differentiation process via YFP^{-}Ly51^{low}CD80^{low} intermediates. *Il7*$^{YFP+}$ TECs are sustained in *Rag2*$^{-/-}$ mice, even following in vivo anti-CD3ε treatment that mimics the process of pre-TCR β-selection of thymocytes to the double positive (DP) stage. Using Marilyn-*Rag2*$^{-/-}$ TCR transgenic, we find that positive selection into the CD4 lineage moderately reduces the frequency of *Il7*$^{YFP+}$ TECs, whereas negative selection provokes a striking loss of *Il7*$^{YFP+}$ TECs. These results imply that the strength of MHC/peptide–TCR interactions between TECs and thymocytes during selection constitutes a novel rheostat that controls the maintenance of IL-7–expressing cTECs. ***The Journal of Immunology*****, 2013, 191: 1200–1209.**

Thymic epithelial cells (TECs) provide essential instructive signals for the differentiation of T lymphocytes bearing a diverse TCR repertoire restricted to self-MHCs and tolerant to self-antigens. Cortical thymic epithelial cells (cTECs) and medullary thymic epithelial cells (mTECs) constitute two functionally distinct microenvironments for T cell differentiation (1, 2). Whereas cTECs mediate early stages of T cell development, including lineage commitment, proliferation, and positive selection, mTECs are largely responsible for negative selection (2, 3). These two prototypical TEC subsets derive from a common bipotent precursor (4, 5), although the definition of compartment-specific progenitors remains incomplete.

The complete partitioning into cTECs and mTECs requires reciprocal instructive signals from developing thymocytes, a bidirectional interaction known as "thymic crosstalk" (6–8). It has been recently elucidated that the establishment of the medullary epithelial niche relies on the cooperative contribution of members of the TNFR superfamily, including receptor activator of NF-κB (RANK), lymphotoxin β receptor (LTβR), and CD40, whose ligands are differentially expressed by several thymic hematopoietic cell types, namely, lymphoid tissue inducer cells, positively selected double positive (DP) thymocytes, αβ CD4^{+} single positive thymocytes (SP4), and γδ T cells (9). Still, our understanding of the molecular nature, as well as the impact, of thymic crosstalk for the homeostasis of cTECs is largely unresolved, owing in part to the paucity of appropriate markers to define checkpoints in their differentiation.

IL-7 is an essential cytokine for T cell development in humans, mice, and jawed fish (10–12), indicating a high functional conservation of the IL-7 signaling pathway in thymopoiesis. Several reports, including our own, have shown that IL-7 is predominantly produced by TECs within the thymus (13–16). Using IL-7 reporter transgenic mice, in which YFP expression identifies a subset of TECs that coexpress high levels of *Il7* (referred to as *Il7*$^{YFP+}$ TECs), we documented that *Il7*$^{YFP+}$ TECs gradually decay with age in a thymocyte-dependent manner that correlated inversely with the emergence of CD80-expressing mTECs, suggesting that these cells may define a particular cortical epithelial subset. Of interest, *Il7*$^{YFP+}$ TECs are, conversely, sustained when T cell development is profoundly blocked in *Rag2*$^{-/-}$*Il2rg*$^{-/-}$ mice (13, 17), indicating that the regulation of their homeostasis is coupled to thymocyte–TEC interactions. These findings have raised the hypothesis that lympho–epithelial interactions affect the size and function of cortical epithelial microenvironments while promoting mTEC diversification (17–19). Still, identification of the thymocyte-derived signals that modulate the size of the thymic IL-7 epithelial niche remains elusive.

*Infection and Immunity Unit, CAGE Laboratory, Institute for Molecular and Cellular Biology, University of Porto, 4150-180 Porto, Portugal; †Doctoral Program in Biomedical Sciences, Institute for Biomedical Sciences Abel Salazar, University of Porto, 4050-313 Porto, Portugal; and ‡Innate Immunity Unit, INSERM Unit 668, Institut Pasteur, 75724 Paris, France

Received for publication November 2, 2012. Accepted for publication May 23, 2013.

This work was supported by funds from the European Regional Development Fund (FEDER) through the Operational Competitiveness Program (COMPETE), by National Funds through the Foundation for Science and Technology (FCT, Portugal) under Project FCOMP-01-0124-FEDER-015803 (PTDC/SAU-IMU/110116/2009), and a University of Porto grant (Pluridisciplinary project 10-2010). N.L.A. is supported by program Ciência2008 from FCT. A.R.R. and P.M.R. are supported by Ph.D. fellowships from FCT (SFRH/BD/78380/2011 and SFRH/BD/86605/2012, respectively).

Address correspondence and reprint requests to Dr. Nuno L. Alves, Institute for Molecular and Cellular Biology, Rua do Campo Alegre, 823, 4150-180 Porto, Portugal. E-mail address: nalves@ibmc.up.pt

The online version of this article contains supplemental material.

Abbreviations used in this article: cTEC, cortical thymic epithelial cell; dGuo, 2-deoxyguanosine; DN, double negative (CD4^{-}CD8^{-} thymocyte); DP, double positive (CD4^{+}CD8^{+} thymocyte); E, embryonic day; FTOC, fetal thymic organ culture; LtβR, lymphotoxin β receptor; mTEC, medullary thymic epithelial cell; RANK, receptor activator of NF-κB; RTOC, reaggregate thymic organ culture; SP4, CD4^{+} single positive thymocyte; TEC, thymic epithelial cell; WT, wild-type.

In this article, we study the lineage relationship between *Il7*$^{YFP+}$ TECs and other well-defined TEC subsets. In addition, we examine the regulation of *Il7*$^{YFP+}$ TEC homeostasis in models of absent, positive, and negative thymocyte selection. We find that *Il7*$^{YFP+}$ TECs represent a cortical epithelial subset that is able to give rise to mTECs in reaggregate thymic organ cultures (RTOCs), although less efficiently when compared with YFP$^-$ counterparts. *Il7*$^{YFP+}$ TECs are maintained in *Rag2*$^{-/-}$ mice, and their homeostasis is not substantially affected by in vivo anti-CD3ε treatment, which generates functionally incompetent DP thymocytes to undergo selection. Using TCR transgenic models, we show that thymocyte–TEC interactions during positive selection reduce *Il7*$^{YFP+}$ TECs. Of note, negative selection induces a severe depletion of this subset. Our findings indicate that TCR-mediated signals delivered by thymocytes during thymic selection regulate IL-7–expressing TECs.

Materials and Methods

Mice

IL-7 reporter mice [B6.Cg-Tg (Il7-EYFP)5Pas] were backcrossed onto *Rag2*$^{-/-}$ (20) and Marilyn-*Rag2*$^{-/-}$ (21) C57BL/6 background. Dual reporter mice were generated by crossing IL-7 reporter mice with *Ccrl1:eGFP* reporter mice (CCRL1-reporter) (22). Marilyn-*Rag2*$^{-/-}$ and CCRL1-reporter mice were kindly provided by Jocelyne Demengeot (Instituto Gulbenkian de Ciência, Oeiras, Portugal) and by Thomas Boehm (Max Planck Institute of Immunobiology and Epigenetics, Freiburg, Germany), respectively. Mice were housed under specific pathogen–free conditions, and experiments were performed in accordance with institutional guidelines. For fetal studies, the day of vaginal plug detection was designated embryonic day (E) 0.5.

Isolation and flow cytometry analysis of TECs

TECs were isolated as described (23). Single-cell suspensions were stained with anti-CD4, anti-CD80, and anti-Ly51 (PE) Abs (BD Biosciences); anti–I-A/I-E (Alexa 780); anti-CD40 (PE); anti-CD45.2 (PerCP-Cy5.5); anti-EpCAM, anti-CD8 (APC); anti-CD205 (biotin), anti-EpCAM (eFluor 450) Abs, and streptavidin (PE-Cy7) (eBioscience). Analysis was made with the FACSCanto II (BD Biosciences) and FlowJo software. Cell sorting was performed using the FACSAria I (BD Biosciences), with sort purities > 95%. A 510/10-nm band pass filter (502LP dichroic mirror) and 542/27-nm band pass filter (525LP dichroic mirror) were used to discriminate the GFP from the YFP signal.

Gene expression

For quantitative PCR, mRNA from sorted cells was purified using the RNeasy Micro Kit (QIAGEN). RNA was reverse transcribed to cDNA, using the SuperScript III First-Strand Synthesis System for RT-PCR (Invitrogen) and Random Hexamers (Fermentas), and then subjected to real-time PCR using either TaqMan Universal PCR Master Mix (Applied Biosystems) and primers for *Hprt*, *18s*, *Il7*, *Prss16, Ctsl, Aire*, *Dll4*, *Ccl25, Tnfrsf11a*, and *Psmb11* (also from Applied Biosystems); or iQ SYBR Green Supermix (Bio-Rad), using primers specific for *Actb* (forward: 5′-CGTGAAAAGATGACCCAGATACA-3′; reverse: 5′-TGGTACCAGCAGAGGCATACAG-3′), *Ctss* (forward: 5′-CCATTGGGATCTCTGGAAGAAAA-3′; reverse: 5′-TCATGCCCACTTGGTAGGTAT-3′), and *Ccrl1* (forward: 5′-AGGTCCTCTGATTTCCTCTGC-3′; reverse: 5′-GCAGGAAGACTTTTGCGAAC-3′). All samples were analyzed as triplicates, and the ΔΔCt method was used to calculate relative levels of target mRNA compared with *Hprt*, *18s*, or *Actb*. Procedures were done according to the manufacturer's protocols. Real-time PCR was performed in an iCycler iQ5 Real-Time PCR thermocycler (Bio-Rad). Data were analyzed using iQ5 Optical System software (Bio-Rad).

Fetal thymic organ culture

Freshly isolated E14.5 thymic lobes were used to establish fetal thymic organ cultures (FTOCs), as described (24). Three to four lobes were used per condition to normalize intrathymic variations. FTOCs were cultured for 4 d in DMEM (Life Technologies), supplemented with 10% FCS, 2 mM L-glutamine (Life Technologies), and 360 mg/l 2-deoxyguanosine (dGuo) (Sigma-Aldrich). The dGuo-treated FTOCs were cultured with 5 μg/ml anti-RANK (αRANK) (R&D Systems) and/or with 10 μg/ml anti-LTβR mAb AC.H6 (kindly provided by Jeff Browning, Biogen Idec, Weston, MA). For blocking experiments, anti-RANKL Ab (PeproTech) was added on days 0 and 4 of FTOC at a final concentration of 10 μg/ml. After 8 d in culture, stromal cells were isolated and analyzed by flow cytometry.

RTOC

Freshly isolated E14.5 thymic lobes were used to establish RTOCs, as described (24). *Il7*$^{YFP+}$ and YFP$^-$ TECs (CD45$^-$EpCAM1$^+$) were sorted to high purity (>95%) using a FACSAria. RTOCs were established from mixtures of 100,000–150,000 TECs, with CD4$^+$CD8$^+$ and CD4$^+$ thymocytes at 1:1:1 ratio. After 8 d in culture, RTOCs were dissociated, and single-cell suspensions were analyzed by flow cytometry.

In vivo anti-CD3ε treatment

Neonatal 3- to 4-d-old *Rag2*$^{-/-}$ mice were injected i.p. with 10 μg/g (body weight) of purified anti-CD3ε mAb (25) (clone 1452C11; kindly provided by Dr. Benedita Rocha, Hôpital Necker, Paris, France). Mice thymi were collected and analyzed 12 d after treatment.

Immunohistological analysis

Thymic lobes were prepared as described (13). Briefly, samples were fixed in 4% paraformaldehyde (Electron Microscopy Sciences), and 8-μm sections were stained with rabbit anti-GFP, biotinylated anti-CD205, anti-CD8, anti-MTS10, and rat anti-MHCII Alexa Fluor 647 as primary Abs, with Alexa Fluor 488 anti-rabbit, Alexa Fluor 647 anti-rat, and streptavidin Alexa 555 as secondary Abs (Invitrogen). MTS10 was kindly provided by Dr. R. Boyd (Monash Immunology and Stem Cell Laboratories, Monash University, Melbourne, Australia). Vectashield mounting medium with DAPI (Vector Laboratories) was used to prepare the slides. Analysis was performed in an AxioImager.Z1 (Zeiss). Images were processed with AxioVision (Zeiss) and Fiji Software.

Statistical analysis

Statistical analysis of the results was made using GraphPad Prism Software. The two-tailed Mann–Whitney *U* test was used for analysis between groups. A 95% confidence interval was applied in the calculations, and samples with p values < 0.05 were considered significant (marked with *).

Results

Il7^{YFP+} *TECs identify a subset of cortical epithelial cells throughout development*

In IL-7 reporter mice, the expression of YFP identifies TECs (*Il7*$^{YFP+}$ TECs) that arise early in embryonic development, gradually declining in proportion postnatally (Fig. 1A, 1C) in a thymocyte-dependent manner (13, 17). We first examined how the development of *Il7*$^{YFP+}$ TECs correlated with the differentiation of distinct thymic epithelial subsets. Both *Il7*$^{YFP+}$ and YFP$^-$ TECs were phenotypically indistinguishable at E13.5–14.5, having the Ly51^{low} CD205^{low} phenotype. However, from E15.5 onward, although the majority of *Il7*$^{YFP+}$ TECs retained a cortical Ly51^{high}CD205^{high} phenotype, a fraction of Ly51^{low}CD205^{low} cells emerged exclusively within the YFP$^-$ fraction [Fig. 1B, *top*; age-matched wild-type (WT) thymi are shown in Supplemental Fig. 1]. It has been previously shown that the differential expression of CD205, CD40, and MHCII define distinct stages during cTEC development (26). We found that *Il7*$^{YFP+}$ and YFP$^-$ subsets gradually expressed CD205 and CD40 between E13.5 and 16.5. Noticeably, and in contrast to some YFP$^-$ cells that progressively acquired higher levels of CD40 and decreased the expression of CD205, the majority of *Il7*$^{YFP+}$ TECs continually expressed CD205 and intermediate levels of CD40 (Fig. 1B, *middle*). The emergence of CD80$^+$ mature mTECs occurred exclusively within the YFP$^-$CD40^{high} TEC subset and continually segregated from *Il7*$^{YFP+}$ TECs (Fig. 1B, *bottom*). Proportionally, *Il7*$^{YFP+}$ TECs made up 60% of the cortical-enriched TEC compartment about E13–15, identifying a cTEC subset that gradually declined as mTEC differentiation unfolded from E16 onward (Fig. 1C). Quantitatively, the initial rise in mature mTECs (E16-Nb) preceded the conspicuous drop in *Il7*$^{YFP+}$ TEC numbers observed from 1–2 postnatal wk onward (Fig. 1C and as shown

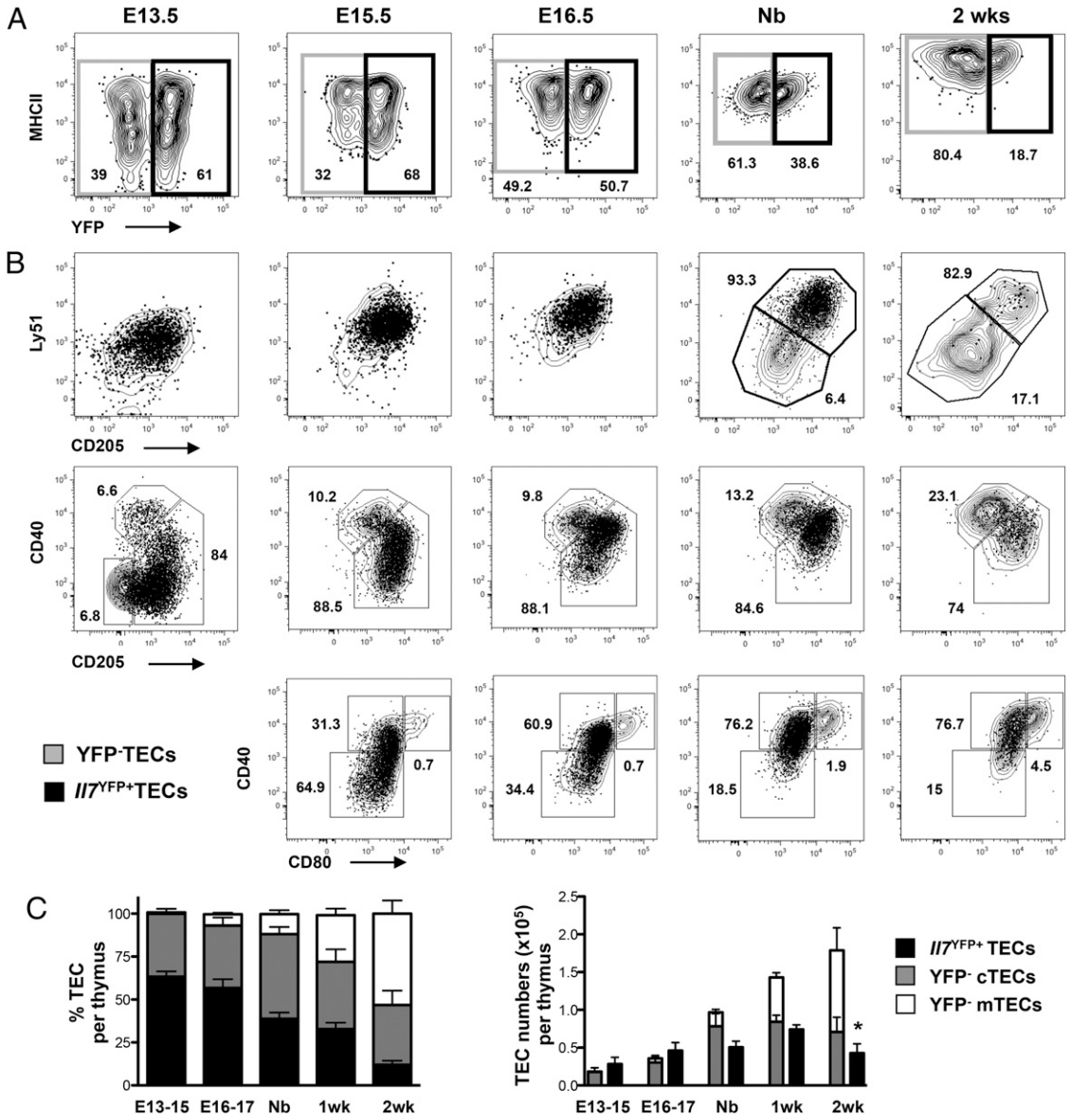

FIGURE 1. *Il7*$^{YFP+}$ TECs define a cortical epithelial subset that segregates from mTECs throughout thymic development. Thymi from IL-7 reporter mice were isolated at the indicated time points, and total TECs (defined hereafter as CD45$^-$EpCAM$^+$) were analyzed for the expression of (**A**) MHCII and YFP and (**B**) CD205, Ly51, CD40, and CD80. (A) The frequency of *Il7*$^{YFP+}$ TECs declines throughout organogenesis. Percentages in gated cells are shown. (B) Phenotypic comparison of YFP$^-$ (gray contour) and *Il7*$^{YFP+}$ TECs (black dot plot). The percentage of *Il7*$^{YFP+}$ TECs within each gate is shown. Data are representative of at least three experiments per time point. (**C**) Bar graphs display the percentage and number of TEC subsets as mean ± SD: YFP$^-$ cTECs (Ly51$^+$CD205$^+$) (gray bars), YFP$^-$ mature mTECs (Ly51$^-$CD205$^-$CD80$^+$) (white bars), and *Il7*$^{YFP+}$ TECs (black bars). *The number of *Il7*$^{YFP+}$ TECs at 2 wk is significantly lower than at 1 wk, $p < 0.05$.

previously in Ref. 13), implying that YFP$^-$TECs may be enriched in direct precursors of mTECs. As such, we further investigate the mechanisms underlying the decay in *Il7*$^{YFP+}$ TECs and its relationship to the developing mTEC compartment.

We next analyzed how the phenotypic traits of *Il7*$^{YFP+}$ TECs related to the genetic profile of cTEC and mTEC lineages. The expression of genes associated with either cTEC [*Ccl25*, *Dll4*, *Il7*, *Ccrl1*, *Ctsl* (Cathepsin L), *Prss16* (TSSP), and *Psmb11* (β5t)] (1, 2, 22, 26, 27) or mTEC [*Tnfrs11a* (RANK), *Ctss* (Cathepsin S), and *Aire*] (1, 3) functions was compared in purified *Il7*$^{YFP+}$ and YFP$^-$ TECs at successive stages of thymic development. Both subsets expressed similar levels of cTEC-associated genes at E14.5. However, as TEC differentiation ensued, the differences in gene expression progressively diverged between subsets, with *Il7*$^{YFP+}$ TECs retaining *Ccl25*, *Dll4*, *Il7*, *Ccrl1*, *Ctsl, Prss16*, and *Psmb11* expression (Fig. 2). *Il7*$^{YFP+}$ TECs were virtually devoid of the medullary-associated genes *Tnfrsf11a, Ctts*, and *Aire* at all analyzed stages. Of interest, these transcripts were detected in YFP$^-$ TECs as early as E14.5 and steadily increased throughout development in this fraction (Fig. 2, *bottom*), reinforcing the idea that some direct precursors of mTECs may exist within YFP$^-$ TECs.

To corroborate that *Il7*$^{YFP+}$ cells define a cTEC subset, we generated dual IL-7^{YFP}–CCRL1^{GFP} reporter mice by crossing IL-7 reporter mice with CCRL1-reporter mice, in which GFP expression identifies exclusively cTECs within thymic stromal cells (22). Analysis of IL-7^{YFP}–CCRL1^{GFP} mice revealed four distinct epithelial subtypes in the postnatal thymus: YFP$^+$GFP$^+$, YFP$^-$GFP$^+$, YFP$^-$GFP^{low}, and YFP$^-$GFP$^-$ (Fig. 3). *Il7*$^{YFP+}$ cells resided within *Ccrl1*$^{GFP+}$ cTECs, but a fraction of *Ccrl1*$^{GFP+}$ cTECs lacked the expression of YFP. Conversely, the YFP$^-$GFP^{low} subset contained a

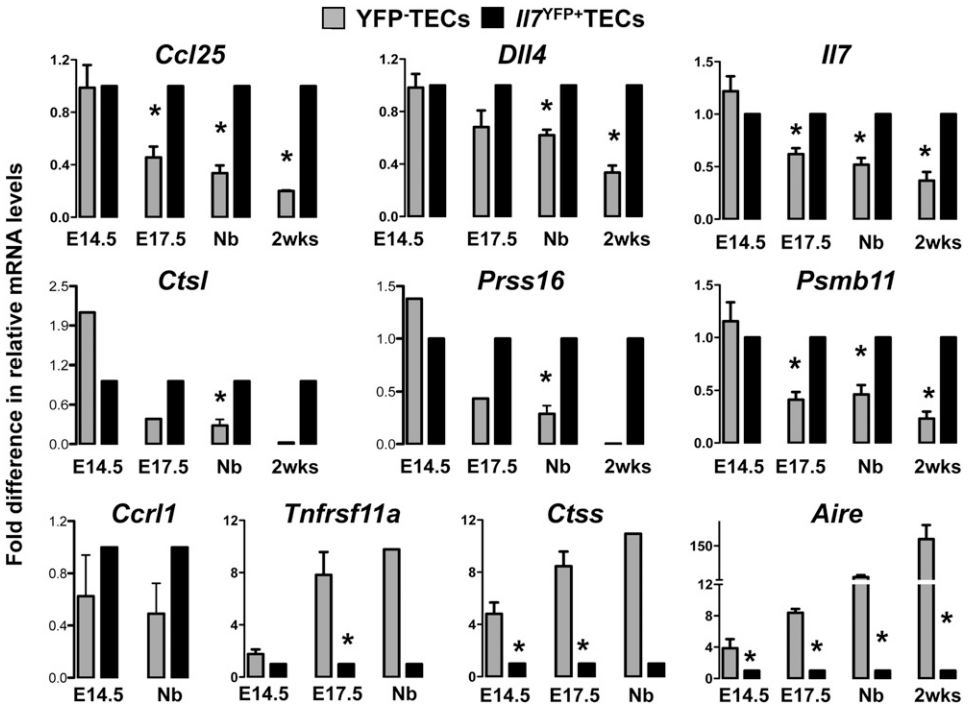

FIGURE 2. *Il7*$^{YFP+}$ TECs display a gene expression profile throughout development associated with cTECs. YFP$^-$ (gray bars) and *Il7*$^{YFP+}$ TECs (black bars) were purified at the indicated time points and compared for the expression of *Ccl25*, *Dll4, Il7*, *Ctsl* (Cathepsin L), *Prss16* (TSSP), *Psmb11* (β5t), *Ccrl1*, *Tnfrsf11a* (RANK), *Ctss* (Cathepsin S), and *Aire*. Values were normalized to *18s, Hprt*, or *Actb*. *Il7*$^{YFP+}$ TECs were set as 1, at each time point, and the fold difference in the relative mRNA expression was compared with that of YFP$^-$ TECs. Data are representative of two to four experiments per time point. $*p < 0.05$.

mixture of CD80$^-$ and CD80$^+$ mTECs, and the YFP$^-$GFP$^-$ fraction was majorly enriched in CD80$^+$ mTECs (Fig. 3). Collectively, our phenotypic and genotypic characterization during thymic ontogeny provides evidence that *Il7*$^{YFP+}$ cells define a specialized cortical epithelial lineage.

Thymocyte-induced loss of Il7^{YFP+} TECs dissociates from the RANK-mediated differentiation of CD80$^+$ mTECs

We previously described a thymocyte-induced decay of *Il7*$^{YFP+}$ TECs that correlated inversely with the development of mTECs (Fig. 1) (17). Using FTOCs, we first assessed whether *Il7*$^{YFP+}$ TECs share a direct precursor-product lineage relationship with mTECs. The differentiation of CD80$^+$Aire$^+$ mTECs depends on signal transduction pathways induced by the TNFR superfamily members LTβR, RANK, and CD40, whose ligands are provided by hematopoietic cells (24, 28–32). E14.5 FTOCs were maintained in medium for 8 d, which allowed a normal program of T cell differentiation (FTOCs), or were treated with dGuo (dGuo-FTOCs), which selectively eliminated thymocytes (data not shown). Because RANK signaling has a dominant effect in the generation of CD80$^+$Aire$^+$ mTECs (24, 28, 32), in dGuo-FTOCs an agonistic anti-RANK mAb (αRANK) was used to "rescue" mTEC development (24). In dGuo-FTOC, *Il7*$^{YFP+}$ TECs were maintained and the formation of mTECs was impaired. Conversely, in FTOCs, *Il7*$^{YFP+}$ TECs markedly decreased the intensity of YFP reporter activity and sustained a cTEC phenotype, with mTECs developing within the YFP$^-$ subset (Fig. 4A, 4B), partially recapitulating the perinatal in vivo phenotype. Treatment of dGuo-FTOCs with αRANK stimulated the development of CD80$^+$ mTECs within the YFP$^-$ fraction, as observed in FTOCs (Fig. 4A, 4C; the total patterns of TECs for WT and IL-7 reporter FTOCs are shown in Supplemental Fig. 2A and B, respectively). In contrast to FTOC, RANK activation did not induce a substantial decay in the intensity of YFP expression in *Il7*$^{YFP+}$ TECs (Fig. 4A–C).

As LTβR signals augment the RANK-driven development of mTECs (29), we further treated dGuo-FTOCs with an agonistic anti-LTβR (αLTβR) mAb (29) alone or in combination with αRANK. Combined αRANK and αLTβR stimulation increased the fre-

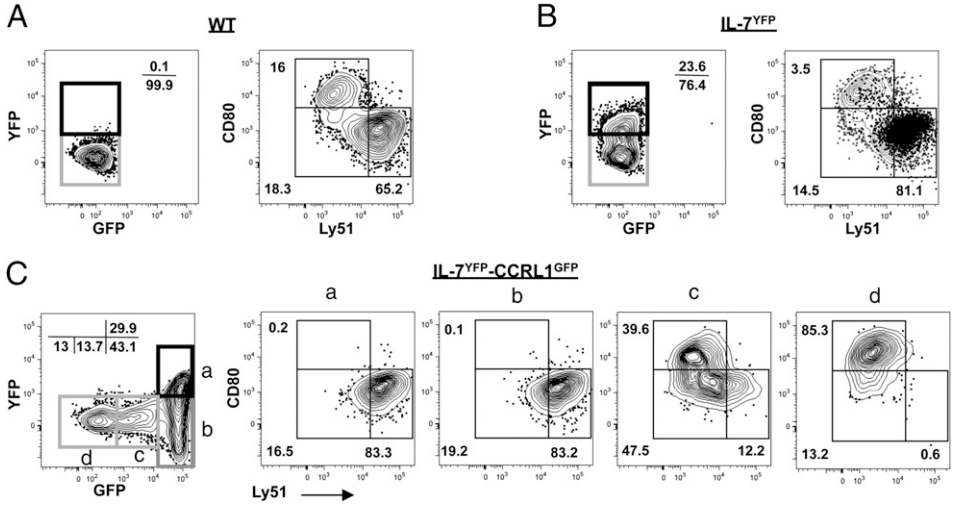

FIGURE 3. *Il7*$^{YFP+}$ cells are *Ccrl1*$^{GFP+}$-expressing cTECs. TECs from WT (**A**), IL-7 reporter mice (**B**), and IL-7^{YFP}-CCRL1^{GFP} dual reporter (**C**) neonatal littermates were analyzed for the expression of YFP and GFP. Subsets defined on the basis of YFP and GFP expression were compared for the expression of Ly51 and CD80. The percentages of total TECs (A), *Il7*$^{YFP+}$ TECs (B), and subtypes (a), (b), (c), and (d) (C) within each gate are shown. Data are representative of three independent experiments.

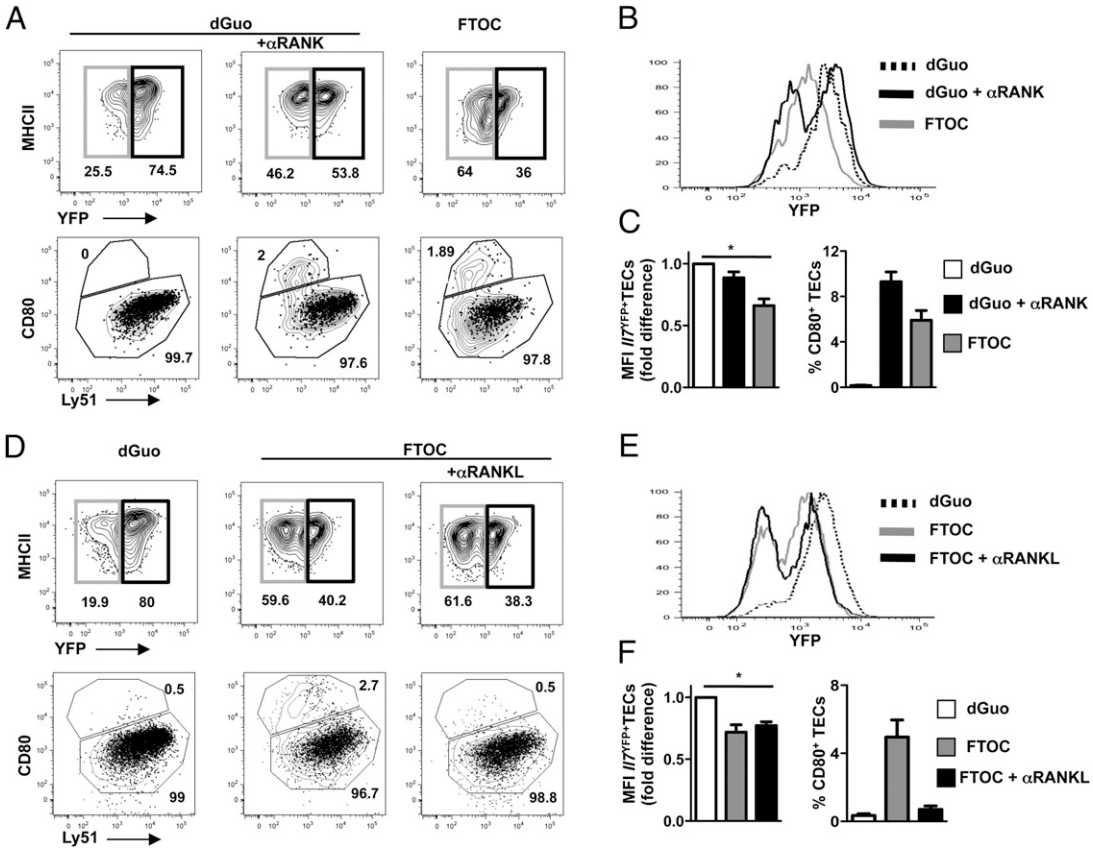

FIGURE 4. Thymocyte-mediated decrease in *Il7*$^{YFP+}$ TECs is independent of RANK-induced mTEC differentiation. (**A**–**C**) E14.5 FTOCs and dGuo-treated FTOCs (dGuo-FTOC) from IL-7 reporter mice were cultured in medium or, for dGuo-FTOC, in the presence of anti-RANK (αRANK). (**D**–**F**) E14.5 FTOCs were supplemented with the blocking Ab for RANK ligand (αRANKL). (A and D) *Top*, Total TECs were analyzed for the expression of YFP and MHCII. Percentages in gated cells are shown. *Bottom*, *Il7*$^{YFP+}$ (black dot plot) and YFP$^-$ (gray contour) TECs were compared for the expression of Ly51 and CD80. The percentage of *Il7*$^{YFP+}$ TECs within each gate is shown. Data are representative of four to six independent experiments. (B and E) The YFP expression on total TECs is compared for the conditions represented in (A) and (D), respectively. (C) and (F) represent the fold difference in the recorded mean fluorescence intensity (MFI) of YFP expression in *Il7*$^{YFP+}$ TECs (*left*) and percentage of CD80$^+$ cells in the total TEC gate (*right*). *$p < 0.05$.

quency of CD80$^+$YFP$^-$ mTECs, whereas the YFP reporter activity was not substantially affected in *Il7*$^{YFP+}$ TECs (Supplemental Fig. 2D–F). No changes were observed upon single LTβR activation (data not shown). In a complementary approach, we examined the effects of blocking hematopoietic-derived RANKL on TEC differentiation in FTOCs, using anti-RANKL (αRANKL) Ab. Blocking of RANKL abrogated mTEC generation without affecting thymocyte-induced decay in the YFP reporter intensity of *Il7*$^{YFP+}$ TECs (Fig. 4D–F; the total patterns of TECs are shown in Supplemental Fig. 2C). These results underscore that the maintenance of *Il7*$^{YFP+}$ TECs is regulated by thymocyte-dependent interactions that are independent of the RANK- and LTβR-mediated maturation of mTECs.

Il7^{YFP+} *TECs can give rise to CD80*$^+$ *mTECs via a YFP*$^-$ *CD80*^{low}*Ly51*^{low} *intermediate stage*

To directly determine the lineage potential of *Il7*$^{YFP+}$ TECs, we established RTOCs using isolated *Il7*$^{YFP+}$ and YFP$^-$ TECs from E14.5 embryos (Fig 5A) mixed with mature DP and SP4 thymocytes to induce mTEC differentiation (28, 31, 32). Whereas YFP$^-$ TECs showed prominent mTEC progenitor activity, *Il7*$^{YFP+}$ TECs were also able to generate CD80$^+$ mTECs, following a stepwise downregulation of YFP expression and differentiation through a YFP$^-$CD80^{low}Ly51^{low} intermediate stage (Fig. 5B–D). Collectively, the results suggest that although *Il7*$^{YFP+}$ TECs can give rise to mTECs, they are not the immediate precursor of mTECs, and instead indicate that mTECs arise from precursors residing within the YFP$^-$ fraction.

Il7^{YFP+} *TECs persist in Rag2*$^{-/-}$ *thymus*

Our previous observations showed that *Il7*$^{YFP+}$ TECs are sustained in mice with severe and premature arrest in thymopoiesis caused by the combined deficiency in *Rag2* and *Il2rg* genes (17). Because lympho–epithelial interactions are minimal in *Rag2*$^{-/-}$*Il2rg*$^{-/-}$ mice (17), we analyzed the thymic microenvironment of *Rag2*$^{-/-}$ mice in which T cell development is blocked at the double negative (DN) 3 stage (20). As early stages of thymic cortical epithelium development are apparently normal in *Rag2*$^{-/-}$ mice (26), we examined whether the homeostasis of *Il7*$^{YFP+}$ TECs was regulated by lympho–epithelial interactions between immature thymocytes (DN1 to DN3) and TECs. During early stages of embryogenesis, *Il7*$^{YFP+}$ TECs follow developmental kinetics similar to those observed in mice with a normal T cell differentiation program (see Fig. 1). However, the proportion of *Il7*$^{YFP+}$ TECs was markedly maintained in *Rag2*$^{-/-}$ mice, displaying a cortical phenotype (Fig. 6A, 6B). An overall drop in the cellularity of both subsets in adult *Rag2*$^{-/-}$ mice was observed (Fig. 6C). The differentiation of mTECs was partially impaired, although few CD80$^+$ mTECs were detected within the YFP$^-$ fraction (Fig. 6B). These data suggest that the homeostasis of *Il7*$^{YFP+}$ TECs is regulated by thymocyte-derived signals generated beyond β-selection.

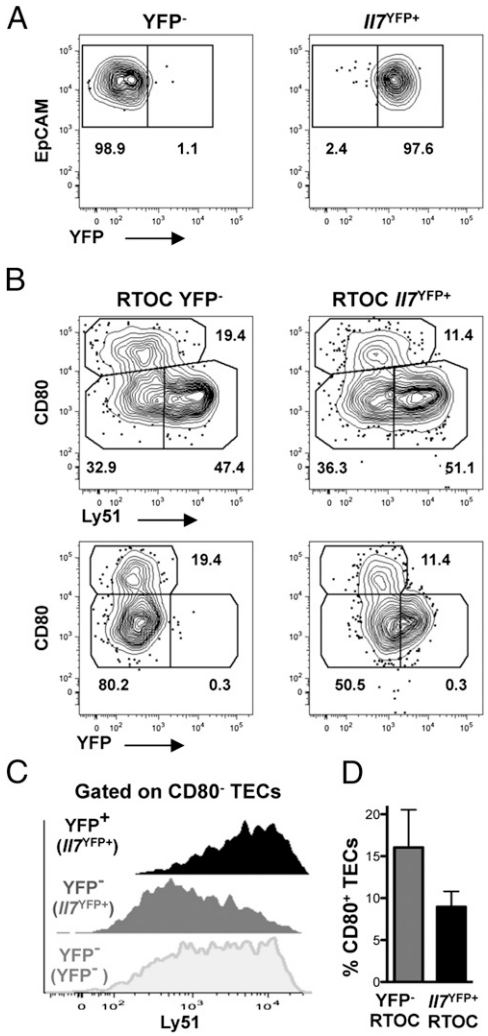

FIGURE 5. *Il7*$^{YFP+}$ TECs can give rise to mTECs. (**A**) YFP$^-$ and *Il7*$^{YFP+}$ TECs were purified from E14.5 embryos. RTOCs were established with sorted TEC fractions (average, 1–1.5 × 10^5) and thymocytes (DP and SP4) mixed in 1:1:1 ratio. (**B**) RTOCs were analyzed for the expression of YFP, Ly51, and CD80. (**C**) Ly51 expression levels within CD80$^-$ TECs: YFP$^+$ (black) and YFP$^-$ (gray) TECs derived from *Il7*$^{YFP+}$ RTOC and YFP$^-$ (white) TECs from YFP$^-$ RTOCs. (**D**) Bar graphs show frequencies of CD80$^+$ mTECs. Data from three experiments, each with three paired RTOCs per condition.

The homeostasis of Il7^{YFP+} TECs is not altered by thymic crosstalk with TCR-deficient DP thymocytes

Progression through the β-selection checkpoint involves the expression of a functional pre-TCR complex, composed of rearranged TCR β-chain together with pre-Tα and CD3 chains (2, 33). To analyze whether thymic crosstalk during β-selection regulated the maintenance of *Il7*$^{YFP+}$ TECs, we used an in vivo experimental model of pre-TCR activation in which neonatal IL-7 reporter *Rag2*$^{-/-}$ mice were treated with anti-CD3ε mAb. Analysis 12 d after anti-CD3ε treatment showed a conspicuous increase in thymic size and total cellularity, reaching numbers similar to those in age-matched immunocompetent counterparts (Supplemental Fig. 3A, 3B). Cross-linking of CD3ε at the surface of *Rag2*$^{-/-}$ DN3 thymocytes mimics the pre-TCR signaling during β-selection (25), generating TCR-deficient DP thymocytes (Supplemental Fig. 3C) that cannot be positively selected and die by neglect. In treated IL-7 reporter *Rag2*$^{-/-}$ mice, despite the vast increase in thymocyte cellularity, the decrease in the frequency and intensity of the YFP reporter activity of *Il7*$^{YFP+}$ TECs was significantly attenuated relative to age-matched immunocompetent thymus, and only moderately affected when compared with control *Rag2*$^{-/-}$ mice (Fig. 7A–C). Interestingly, *Il7*$^{YFP+}$ TEC numbers were also found to be augmented in this condition, indicating that the loss of this subset observed in immunocompetent mice is not regulated by thymic crosstalk with TCR-deficient DP thymocytes (Fig. 7D). This treatment increases the development of CD80$^+$ mTECs within the YFP$^-$ subset. Yet, the representation of mTECs did not reach the levels of the immunocompetent thymus (Fig. 7A–C; the total pattern of TECs is shown in Supplemental Fig. 3D). In E14 dGuo-FTOCs treated with anti-CD3ε mAb, mTECs were not generated (data not shown). This finding indicates that the in vivo observations were not due to a direct effect of the Ab on TECs, but resulted from the TCR-deficient DP thymocyte–TEC crosstalk.

To represent spatial organization in thymic microenvironments, thymic sections of control and treated IL-7 reporter *Rag2*$^{-/-}$ mice were analyzed by immunofluorescence. In control *Rag2*$^{-/-}$ thymus, the CD205$^+$ cortical epithelium predominated, with few MTS10$^+$ mTECs and scattered distribution of *Il7*$^{YFP+}$ TECs. In IL-7 reporter *Rag2*$^{-/-}$–treated mice, the formation of small medullary MHCII^{high}MTS10$^+$ islets (34) was detected, yet smaller relative to immunocompetent mice. Immature single positive–DP thymocytes, marked by CD8 immunostaining, were compartmentalized within cortical areas and excluded from the medulla of *Rag2*$^{-/-}$-treated thymus. *Il7*$^{YFP+}$ TECs were clearly detected and scattered across the cortex of treated mice, with some cells found within the MTS10$^+$ medullary pouches (Fig. 7E). Together, signals derived from TCR-deficient thymocytes progressing across DN to DP stages partially restored mTEC differentiation without substantially curtailing *Il7*$^{YFP+}$ TECs. In addition, these data point to the involvement of TCR–peptide/MHC interactions in regulating their maintenance.

The strength of thymocyte selection influences Il7^{YFP+} TEC homeostasis

To study the role of positive and negative selection events in the regulation of *Il7*$^{YFP+}$ TEC homeostasis, we crossed IL-7 reporter *Rag2*$^{-/-}$ mice onto the Marilyn-*Rag2*$^{-/-}$ TCR transgenic background (21). Marilyn-*Rag2*$^{-/-}$ mice express I-A^b–restricted TCR recognizing the male-specific HY Ag. Thymocyte development in IL-7 reporter Marilyn-*Rag2*$^{-/-}$ TCR double transgenic mice (Supplemental Fig. 4A, 4B) reproduced that observed in WT Marilyn-*Rag2*$^{-/-}$ TCR transgenic mice (data not shown), with positive selection in female mice and negative selection in male mice. Analysis of TEC differentiation showed that in IL-7 reporter Marilyn-*Rag2*$^{-/-}$ female, and comparatively so with IL-7 reporter *Rag2*$^{-/-}$ littermates, positive selection of CD4 thymocytes was sufficient to reduce the frequency and abundance of *Il7*$^{YFP+}$ TECs and promoted the development of YFP$^-$ mTECs (Fig. 8A–C), phenocopying the epithelial differentiation observed in the age-matched immunocompetent thymus (Fig. 7). Strikingly, negative selection induced a conspicuous loss in the proportion and intensity of YFP reporter activity of *Il7*$^{YFP+}$ TECs, with a concomitant increase in the number of YFP$^-$ TECs and the emergence of Ly51$^-$ CD80^{low} TECs (Fig. 8A–C). These sex differences in the representation of TEC subsets were not manifested in IL-7 reporter *Rag2*$^{-/-}$ mice (data not shown). The total pattern of TECs for IL-7 reporter–*Rag2*$^{-/-}$ and IL-7 reporter–Marilyn-*Rag2*$^{-/-}$ and for C57BL/6 *Rag2*$^{-/-}$ and Marilyn-*Rag2*$^{-/-}$ are shown in Supplemental Fig. 4C and 4D. Thus, our findings indicate that the strength of TCR–peptide/MHC interactions occurring during thymocyte selection dynamically controls the proportion of the IL-7–expressing cortical epithelial niche.

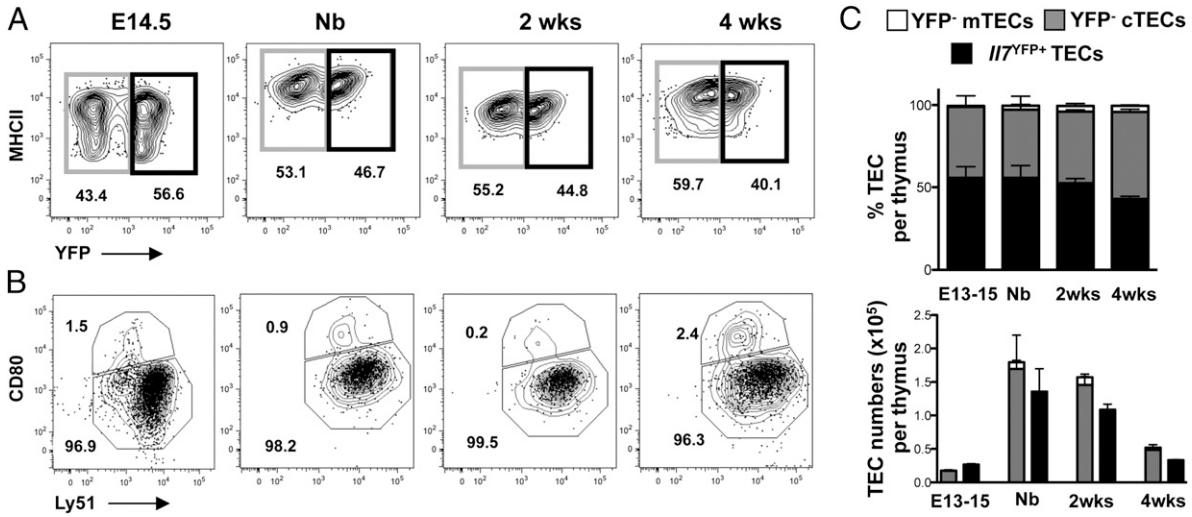

FIGURE 6. *Il7*$^{YFP+}$ TECs develop normally but are sustained in *Rag2*$^{-/-}$ mice. Thymi from IL-7 reporter *Rag2*$^{-/-}$ mice were isolated at the indicated time points. (**A**) Total TECs were analyzed for the expression of MHCII and YFP. Percentages in gated cells are shown. (**B**) The expression of Ly51 and CD80 was compared between YFP$^-$ (gray contour) and *Il7*$^{YFP+}$ TECs (black dot plot). The percentage of *Il7*$^{YFP+}$ TECs within each gate is shown. Data are representative of two to three experiments per time point. (**C**) Bar graphs display the percentage and number of TEC subsets as mean ± SD: YFP$^-$ cTECs (Ly51$^+$CD205$^+$) (gray bars), YFP$^-$ mature mTECs (Ly51$^-$CD205$^-$CD80$^+$) (white bars), and *Il7*$^{YFP+}$ TECs (black bars).

Discussion

The establishment and maintenance of cTECs determine the thymopoietic capacity of the thymus, given their chief function in supporting early stages of T cell development (1, 2). However, our understanding of fundamental aspects of thymic cortical epithelial homeostasis remains limited (26). The representation of cTECs gradually decreases in postnatal life (34), possibly elicited by extrinsic and/or intrinsic mechanisms. The cTECs share with mTECs a common bipotent progenitor (4, 5). One can consider that the potential of progenitor cells to self-renew or differentiate into mature cells is progressively lost with age. Concurrently, continual thymocyte–TEC interactions throughout life may also control the epithelial progenitor activity and/or other TEC functional properties, while promoting the maturation of TECs (19). In this view, thymocyte development up to the DP stage seems sufficient to restrain the expression of IL-7 (17) and Dll4 (18) by TECs, although identification of the molecular liaisons remains undisclosed. In this article, we report that previously identified *Il7*$^{YFP+}$ TECs (13, 19) define a subset of *Ccrl1*-expressing cortical epithelial cells and examine the mechanisms that regulate the homeostasis of these IL-7–expressing cTECs.

The developmental stages as well as the molecular signals that regulate cTEC differentiation from bipotent precursors are just beginning to be identified. A heterogeneity within the cortical microenvironment is suggested to exist on the basis of the differential expression of CD205, Ly51, IL-7, Dll4, β5t, and CCRL1 (17, 18, 22, 26, 34, 35). Our kinetic analysis during thymic ontogeny revealed that *Il7*$^{YFP+}$ TECs sustained phenotypic and molecular traits associated with cTECs (26). Of interest, although YFP$^-$ TECs steadily accumulate more medullary characteristics as TEC maturation proceeds, they share cortical- and medullary-associated features at an early phase of thymic development. These findings indicate that mTEC precursors may reside at early stages within a subset that shares some cTEC features. Still, the degree of heterogeneity within cTECs remains to be determined. The frequency of *Il7*$^{YFP+}$ TECs gradually declines as mTEC development advances. One can envisage that *Il7*$^{YFP+}$ TECs represent a lineage that participates in the differentiation of mTECs as a result of lympho–stromal interactions. Alternatively, one can consider that YFP$^-$ TECs detected at the E13–14 stage include direct mTEC precursors poised to differentiate, which expands and replaces (or dilutes) *Il7*$^{YFP+}$ TECs. The establishment of medullary microenvironments involves the hierarchical, but concerted, participation of TNFRSF RANK, LTβR, and CD40 molecules (9). Our in vitro findings corroborate that RANK signaling has a dominant function in the development of mTECs (28, 31, 32), whereas signaling through LTβR seems to amplify the RANK-mediated effects (29). These signals delivered upon interactions with hematopoietic cells did not, however, substantially affect the homeostasis of *Il7*$^{YFP+}$ TECs. Instead, they seem to drive mTEC development from a precursor within the YFP$^-$ fraction, indicating that *Il7*$^{YFP+}$ TECs do not have an immediate precursor–product relationship with mature mTECs. Our analysis of the lineage potential of purified subsets revealed that although YFP$^-$ TECs appeared to be more competent in differentiating mTECs, *Il7*$^{YFP+}$ TECs can still give rise to medullary epithelia in a suggested stepwise fashion, terminating YFP expression as they progress through an intermediate immature stage of mTEC differentiation. Further studies are needed to address whether mTECs derived from both subsets represent functional distinct medullary subtypes and to study their physiological relevance in regulating T cell development. In agreement with our results, it has been recently shown that mTECs can arise from CD205$^+$CD40$^-$ TEC progenitors (36), which are generally associated with the cTEC lineage (26). Collectively, these findings suggest that mTEC differentiation may be more complex than previously appreciated, following a linear stepwise differentiation pathway from progenitors that simultaneously express cTEC and mTEC traits, rather than a simple dichotomist model from compartment-specific progenitors. Still, the degree of heterogeneity within cTECs remains to be determined, and further studies on the stepwise generation of the cTEC and mTEC lineages are warranted.

In mice with early blocks in thymopoiesis, including *Rag2*$^{-/-}$*Il2rg*$^{-/-}$ (17) and CD3εTg26 mice (7, 37), the thymic epithelium is devoid of distinct cortical and medullary areas (7). In these models, TEC differentiation is severely compromised (7, 17, 37), which limits the study of cTEC development downstream of a bipotent progenitor. We previously reported that *Il7*$^{YFP+}$ TECs are markedly maintained in *Rag2*$^{-/-}$*Il2rg*$^{/-}$ mice. Restoration of normal thymopoiesis following WT stem cell transplantation reduces their frequency (17), suggesting that thymic crosstalk regulates their

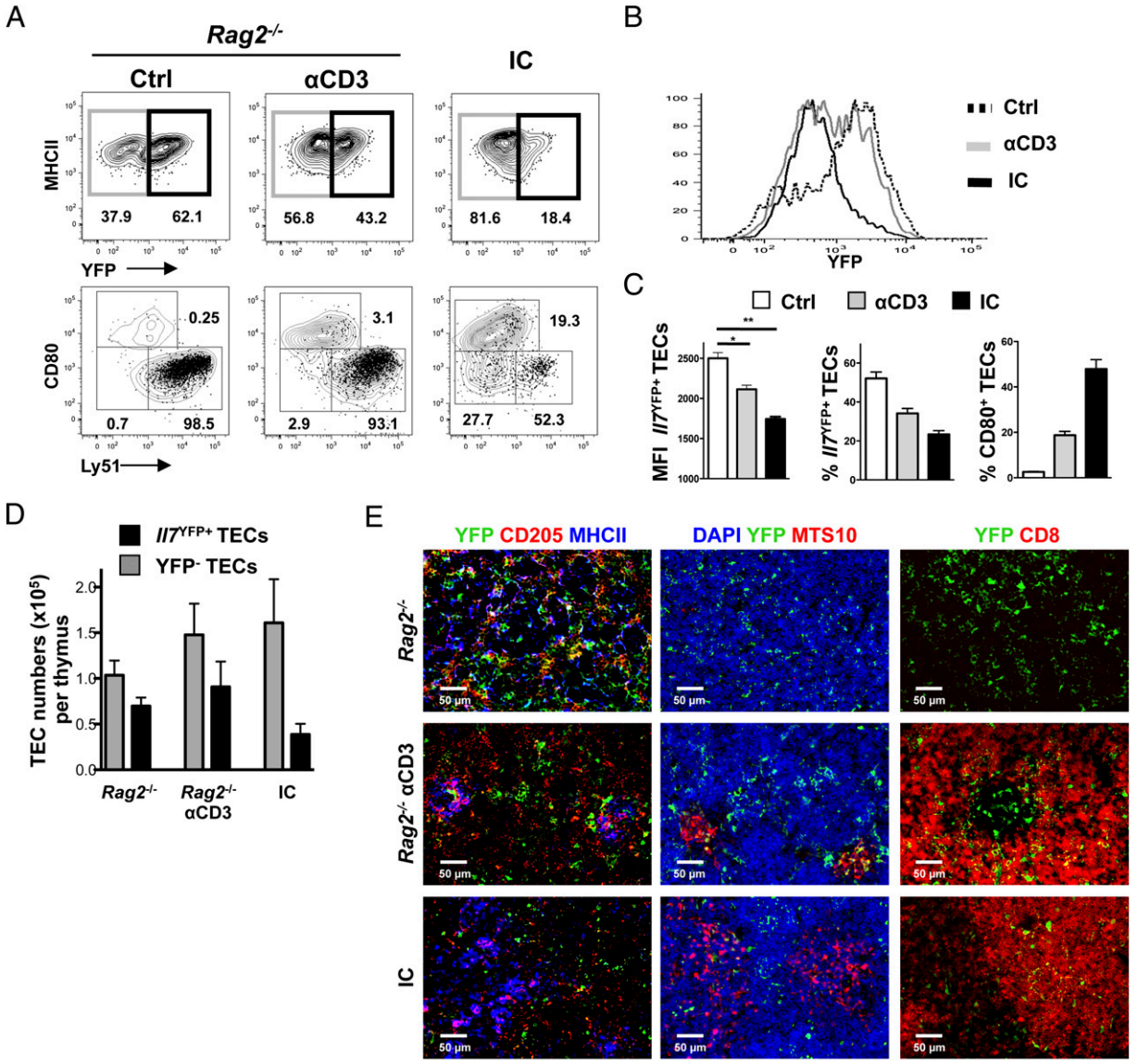

FIGURE 7. Bypassing β-selection by TCR-deficient thymocytes partially restores mTEC differentiation without significantly curtailing $Il7^{YFP+}$ TECs. (**A**) IL-7 reporter $Rag2^{-/-}$ neonatal mice were analyzed 12 d after anti-CD3ε treatment (αCD3), together with age-matched (12–14 d old) IL-7 reporter $Rag2^{-/-}$ control (Ctrl) and IL-7 reporter immunocompetent (IC) mice. *Top*, Total TECs were analyzed for the expression of YFP and MHCII. Percentages in gated cells are shown. *Bottom*, YFP^{-} (gray contour) and $Il7^{YFP+}$ TECs (black dot plot) were compared for the expression of Ly51 and CD80. Numbers represent the percentages of $Il7^{YFP+}$ TECs within each gate. (**B**) The YFP expression on total TECs is compared for the different conditions in (A). Data are representative of four experiments. (**C**) Mean fluorescence intensity (MFI) of YFP expression in $Il7^{YFP+}$ TECs (*left*), percentage of $Il7^{YFP+}$ (*middle*), and $CD80^{+}$ (*right*) cells within total TECs. $*p < 0.05$, $**p < 0.0001$. (**D**) Bar graphs display the percentage and number of YFP^{-} (gray) and $Il7^{YFP+}$ (black) TECs as mean ± SD. (**E**) Immunohistochemical analysis of untreated $Rag2^{-/-}$, αCD3-treated $Rag2^{-/-}$ (αCD3), and age-matched IC IL-7 reporter mice thymic sections stained with the indicated Abs (CD205 *red* and MHCII *blue*; DAPI *blue* and MTS10 *red*; YFP *green* and CD8 *red*).

homeostasis. $Rag2^{-/-}$ mice offer an intermediate version because the development of cTECs is overtly normal (8, 26, 38). Yet, it has been suggested that DNs facilitate the establishment of the three-dimensional reticular cTEC structure (39), implying the existence of a DN stage–specific requirement for differentiation of cTECs. It has been documented that cTECs retain a $Ly51^{high}$ phenotype in $Rag2^{-/-}$ mice (34), suggesting that further cortical maturation stages dependent on post–β-selected thymocytes may be absent in this setting. Our results showed that $Il7^{YFP+}$ cTECs developed normally and were sustained in $Rag2^{-/-}$ mice, corroborating that thymocyte-derived signals generated beyond β-selection regulate the maintenance of this cTEC immature lineage (17). In line with previous studies (34, 39), we observed an insufficient differentiation of mTECs in $Rag2^{-/-}$ mice. Still, vestigial mTECs could be detected within the YFP^{-} TEC fraction, indicating that the hematopoietic fraction (e.g., DN2–3 thymocytes, lymphoid tissue inducer cells, NK cells) elicits a certain degree of mTEC maturation.

The β-selection defines a chief checkpoint during the progression from DN to DP thymocytes (33). Using a pre-TCR activation model in $Rag2^{-/-}$ mice (25), we bypassed the β-selection. In this in vivo model, progression through DN–immature single positive–DP stages allows physiological lympho–stromal interactions, but in the absence of TCR-derived signals. DP thymocytes from anti-CD3–treated $Rag2^{-/-}$ mice lack TCR complexes, are not positively selected, and die by apoptosis, similarly to the majority of WT DP thymocytes that do not receive survival signals for lack of TCR–MHC/peptide interactions. Our results showed that $Il7^{YFP+}$ cTECs were not substantially affected in this condition, indicating that thymocyte TCR-dependent signals generated during thymic selection might control their homeostasis. We observed a con-

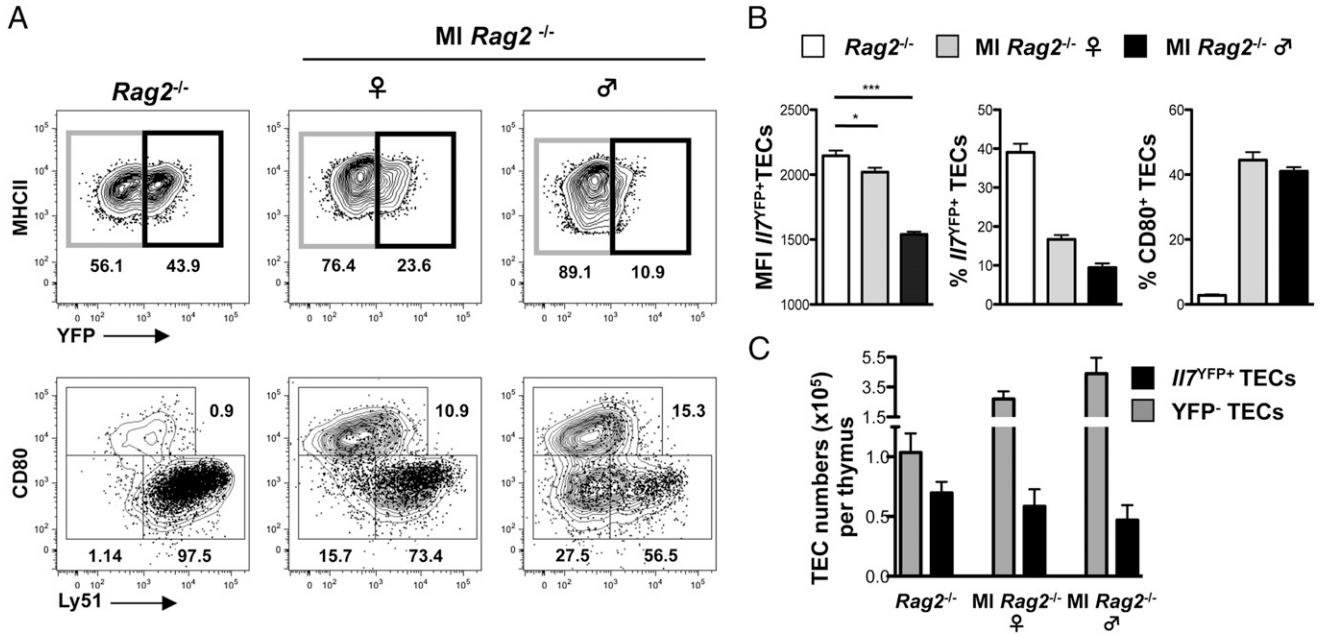

FIGURE 8. The strength of TCR–MHC interactions during thymocyte selection controls the homeostasis of $Il7^{YFP+}$ TECs. Thymi from female (♀) and male (♂) IL-7 reporter Marilyn-$Rag2^{-/-}$ mice (MI $Rag2^{-/-}$) were analyzed together with IL-7 reporter $Rag2^{-/-}$ ($Rag2^{-/-}$) littermates at 12–14 d of age. (**A**) *Top*, Total TECs from $Rag2^{-/-}$ and from female and male MI $Rag2^{-/-}$ mice were examined for the expression of YFP and MHCII. Percentages in gated cells are shown. *Bottom*, YFP^- (gray contour) and $Il7^{YFP+}$ (black dot plot) TECs were compared for the expression of Ly51 and CD80. The percentage of $Il7^{YFP+}$ TECs within each gate is shown (**B**) Mean fluorescence intensity (MFI) of YFP expression in $Il7^{YFP+}$ TECs and percentages of $Il7^{YFP+}$ and $CD80^+$ TECs are shown. Data are representative of two to three experiments per time point. *Statistical significance, $p < 0.05$. (**C**) Bar graphs display the percentage and number of YFP^- (gray) and $Il7^{YFP+}$ (black) TECs as mean ± SD.

comitant moderate improvement in mTEC development in anti-CD3ε–treated $Rag2^{-/-}$ mice. An amelioration of medullary niches upon anti-CD3ε treatment has been recently reported in a mouse model of Omenn syndrome, which is associated with a hypomorphic *R229Q* mutation in the RAG2 enzyme (40). In contrast to our model, TCR-expressing cells are found in the thymus of *R229Q* RAG2 mice (40), which may also contribute to the improvement of the medullary epithelium. In both cases, insufficient mTEC differentiation might reflect a lack of instructive signals from mature thymocytes (9).

It is an accepted idea that positive selection and negative selection occur in the cortex and medulla, respectively. Whereas intermediate signals from low-affinity interactions between TCR and peptide/MHC ligands result in positive selection, strong signals from recognition of high-affinity peptide/MHC ligands lead to negative selection (2, 9). Still, whether positive and negative selection can be sequential or independent events remains unanswered. Some evidence does exist that negative selection also occurs in the cortex (41–43), although the medulla provides a larger repertoire of self-antigens for the elimination of autoreactive T cells (1, 3). Using a TCR transgenic model, we examined the consequences of positive and negative selection in the thymic microenvironment (21). Our findings indicate that positive selection of thymocytes in Marilyn TCR transgenic cortex suffices to induce the proportional loss of $Il7^{YFP+}$ cTECs and the expansion of medullary TECs. During negative selection, the premature expression of transgenic MI TCR may accelerate the deletion of autoreactive thymocytes in the cortical microenvironment (21). Indeed, deletion of DP thymocytes expressing self-reactive TCR is observed in the cortex (42, 43). Our findings indicated that the IL-7–expressing cTEC niche might be limited by strong TCR–peptide/MHC interactions within the cortical thymic microenvironment. It is worth mentioning that the modulation of the IL-7 cTEC niche detected in $Rag2^{-/-}$ TCR transgenic mice is also seen in WT immunocompetent mice. In a normal thymus, strong TCR signals are probably less frequent at the DP stage. Because positive selection occurs within the cortex (2, 9), continual positive selection may locally feed back to cTECs and induce the loss of $Il7^{YFP+}$ cTECs in WT thymus. One can hypothesize that bidirectional crosstalk directly transmits outside-in signaling through MHC molecules on TECs. Alternatively, the high-avidity TCR–MHC/peptide recognition may elicit a downstream molecular interaction that restrains the IL-7–expressing cortical epithelial niche. Further studies are required to elucidate the specific signals generated during thymic selection that can regulate the cTEC microenvironment.

To our knowledge this is the first study indicating that the strength of MHC/peptide–TCR interactions between TECs and thymocytes during selection constitutes a rheostat regulating the maintenance of IL-7–expressing cTECs. These findings have implications for understanding the molecular basis of cTEC differentiation and should inspire further studies aimed at uncovering the physiological consequences linked to the functional capacity of the thymus, an ongoing topic of investigation.

Acknowledgments

We thank Drs. Catarina Leitão, Alexandre Carmo, and Rui Appelberg (Instituto de Biologia Molecular e Celular, Porto, Portugal) for critical reading of the manuscript; Dr. Catarina Leitão (Advanced Flow Cytometry Unit, Instituto de Biologia Molecular e Celular) for technical assistance during cell sorting; personnel from the Instituto de Biologia Molecular e Celular animal facility—in particular, Dr. Sofia Lamas, Isabel Duarte, and Liliana Silva for technical assistance with animal experimentation; Dr. Benedita Rocha (Hôpital Necker, Paris, France) for the anti-CD3ε mAb; Dr. Jeff Browning (Biogen Idec, Weston, MA) for anti-LTβR mAb; and Drs. Jocelyne Demengeot (Instituto Gulbenkian de Ciência, Oeiras, Portugal) and Thomas Boehm (Max Planck Institute of Immunobiology and Epigenetics, Freiburg, Germany) for providing MI TCR Tg and *Ccx-Ckr1:eGFP* reporter mice, respectively. We thank Drs. Graham Anderson and Andrea White (Birmingham, U.K.) for the introduction to RTOCs.

Disclosures

The authors have no financial conflicts of interest.

References

1. Anderson, G., P. J. Lane, and E. J. Jenkinson. 2007. Generating intrathymic microenvironments to establish T-cell tolerance. *Nat. Rev. Immunol.* 7: 954–963.
2. Takahama, Y. 2006. Journey through the thymus: stromal guides for T-cell development and selection. *Nat. Rev. Immunol.* 6: 127–135.
3. Kyewski, B., and L. Klein. 2006. A central role for central tolerance. *Annu. Rev. Immunol.* 24: 571–606.
4. Bleul, C. C., T. Corbeaux, A. Reuter, P. Fisch, J. S. Mönting, and T. Boehm. 2006. Formation of a functional thymus initiated by a postnatal epithelial progenitor cell. *Nature* 441: 992–996.
5. Rossi, S. W., W. E. Jenkinson, G. Anderson, and E. J. Jenkinson. 2006. Clonal analysis reveals a common progenitor for thymic cortical and medullary epithelium. *Nature* 441: 988–991.
6. Shores, E. W., W. Van Ewijk, and A. Singer. 1991. Disorganization and restoration of thymic medullary epithelial cells in T cell receptor-negative scid mice: evidence that receptor-bearing lymphocytes influence maturation of the thymic microenvironment. *Eur. J. Immunol.* 21: 1657–1661.
7. Klug, D. B., C. Carter, I. B. Gimenez-Conti, and E. R. Richie. 2002. Cutting edge: thymocyte-independent and thymocyte-dependent phases of epithelial patterning in the fetal thymus. *J. Immunol.* 169: 2842–2845.
8. Klug, D. B., C. Carter, E. Crouch, D. Roop, C. J. Conti, and E. R. Richie. 1998. Interdependence of cortical thymic epithelial cell differentiation and T-lineage commitment. *Proc. Natl. Acad. Sci. USA* 95: 11822–11827.
9. Anderson, G., and Y. Takahama. 2012. Thymic epithelial cells: working class heroes for T cell development and repertoire selection. *Trends Immunol.* 33: 256–263.
10. von Freeden-Jeffry, U., P. Vieira, L. A. Lucian, T. McNeil, S. E. Burdach, and R. Murray. 1995. Lymphopenia in interleukin (IL)-7 gene-deleted mice identifies IL-7 as a nonredundant cytokine. *J. Exp. Med.* 181: 1519–1526.
11. Giliani, S., L. Mori, G. de Saint Basile, F. Le Deist, C. Rodriguez-Perez, C. Forino, E. Mazzolari, S. Dupuis, R. Elhasid, A. Kessel, et al. 2005. Interleukin-7 receptor alpha (IL-7Ralpha) deficiency: cellular and molecular bases. Analysis of clinical, immunological, and molecular features in 16 novel patients. *Immunol. Rev.* 203: 110–126.
12. Iwanami, N., F. Mateos, I. Hess, N. Riffel, C. Soza-Ried, M. Schorpp, and T. Boehm. 2011. Genetic evidence for an evolutionarily conserved role of IL-7 signaling in T cell development of zebrafish. *J. Immunol.* 186: 7060–7066.
13. Alves, N. L., O. Richard-Le Goff, N. D. Huntington, A. P. Sousa, V. S. Ribeiro, A. Bordack, F. L. Vives, L. Peduto, A. Chidgey, A. Cumano, et al. 2009. Characterization of the thymic IL-7 niche in vivo. *Proc. Natl. Acad. Sci. USA* 106: 1512–1517.
14. Mazzucchelli, R. I., S. Warming, S. M. Lawrence, M. Ishii, M. Abshari, A. V. Washington, L. Feigenbaum, A. C. Warner, D. J. Sims, W. Q. Li, et al. 2009. Visualization and identification of IL-7 producing cells in reporter mice. *PLoS ONE* 4: e7637.
15. Repass, J. F., M. N. Laurent, C. Carter, B. Reizis, M. T. Bedford, K. Cardenas, P. Narang, M. Coles, and E. R. Richie. 2009. IL7-hCD25 and IL7-Cre BAC transgenic mouse lines: new tools for analysis of IL-7 expressing cells. *Genesis* 47: 281–287.
16. Hara, T., S. Shitara, K. Imai, H. Miyachi, S. Kitano, H. Yao, S. Tani-ichi, and K. Ikuta. 2012. Identification of IL-7-producing cells in primary and secondary lymphoid organs using IL-7-GFP knock-in mice. *J. Immunol.* 189: 1577–1584.
17. Alves, N. L., N. D. Huntington, J. J. Mention, O. Richard-Le Goff, and J. P. Di Santo. 2010. Cutting edge: a thymocyte-thymic epithelial cell cross-talk dynamically regulates intrathymic IL-7 expression in vivo. *J. Immunol.* 184: 5949–5953.
18. Fiorini, E., I. Ferrero, E. Merck, S. Favre, M. Pierres, S. A. Luther, and H. R. MacDonald. 2008. Cutting edge: thymic crosstalk regulates delta-like 4 expression on cortical epithelial cells. *J. Immunol.* 181: 8199–8203.
19. Alves, N. L., N. D. Huntington, H. R. Rodewald, and J. P. Di Santo. 2009. Thymic epithelial cells: the multi-tasking framework of the T cell "cradle." *Trends Immunol.* 30: 468–474.
20. Shinkai, Y., G. Rathbun, K. P. Lam, E. M. Oltz, V. Stewart, M. Mendelsohn, J. Charron, M. Datta, F. Young, A. M. Stall, and F. W. Alt. 1992. RAG-2-deficient mice lack mature lymphocytes owing to inability to initiate V(D)J rearrangement. *Cell* 68: 855–867.
21. Lantz, O., I. Grandjean, P. Matzinger, and J. P. Di Santo. 2000. Gamma chain required for naïve CD4+ T cell survival but not for antigen proliferation. *Nat. Immunol.* 1: 54–58.
22. Rode, I., and T. Boehm. 2012. Regenerative capacity of adult cortical thymic epithelial cells. *Proc. Natl. Acad. Sci. USA* 109: 3463–3468.
23. Gray, D. H., A. P. Chidgey, and R. L. Boyd. 2002. Analysis of thymic stromal cell populations using flow cytometry. *J. Immunol. Methods* 260: 15–28.
24. Rossi, S. W., M. Y. Kim, A. Leibbrandt, S. M. Parnell, W. E. Jenkinson, S. H. Glanville, F. M. McConnell, H. S. Scott, J. M. Penninger, E. J. Jenkinson, et al. 2007. RANK signals from CD4(+)3(-) inducer cells regulate development of Aire-expressing epithelial cells in the thymic medulla. *J. Exp. Med.* 204: 1267–1272.
25. Levelt, C. N., P. Mombaerts, A. Iglesias, S. Tonegawa, and K. Eichmann. 1993. Restoration of early thymocyte differentiation in T-cell receptor beta-chain-deficient mutant mice by transmembrane signaling through CD3 epsilon. *Proc. Natl. Acad. Sci. USA* 90: 11401–11405.
26. Shakib, S., G. E. Desanti, W. E. Jenkinson, S. M. Parnell, E. J. Jenkinson, and G. Anderson. 2009. Checkpoints in the development of thymic cortical epithelial cells. *J. Immunol.* 182: 130–137.
27. Honey, K., T. Nakagawa, C. Peters, and A. Rudensky. 2002. Cathepsin L regulates CD4+ T cell selection independently of its effect on invariant chain: a role in the generation of positively selecting peptide ligands. *J. Exp. Med.* 195: 1349–1358.
28. Hikosaka, Y., T. Nitta, I. Ohigashi, K. Yano, N. Ishimaru, Y. Hayashi, M. Matsumoto, K. Matsuo, J. M. Penninger, H. Takayanagi, et al. 2008. The cytokine RANKL produced by positively selected thymocytes fosters medullary thymic epithelial cells that express autoimmune regulator. *Immunity* 29: 438–450.
29. Mouri, Y., M. Yano, M. Shinzawa, Y. Shimo, F. Hirota, Y. Nishikawa, T. Nii, H. Kiyonari, T. Abe, H. Uehara, et al. 2011. Lymphotoxin signal promotes thymic organogenesis by eliciting RANK expression in the embryonic thymic stroma. *J. Immunol.* 186: 5047–5057.
30. Boehm, T., S. Scheu, K. Pfeffer, and C. C. Bleul. 2003. Thymic medullary epithelial cell differentiation, thymocyte emigration, and the control of autoimmunity require lympho-epithelial cross talk via LTbetaR. *J. Exp. Med.* 198: 757–769.
31. Irla, M., S. Hugues, J. Gill, T. Nitta, Y. Hikosaka, I. R. Williams, F. X. Hubert, H. S. Scott, Y. Takahama, G. A. Holländer, and W. Reith. 2008. Autoantigen-specific interactions with CD4+ thymocytes control mature medullary thymic epithelial cell cellularity. *Immunity* 29: 451–463.
32. Akiyama, T., Y. Shimo, H. Yanai, J. Qin, D. Ohshima, Y. Maruyama, Y. Asaumi, J. Kitazawa, H. Takayanagi, J. M. Penninger, et al. 2008. The tumor necrosis factor family receptors RANK and CD40 cooperatively establish the thymic medullary microenvironment and self-tolerance. *Immunity* 29: 423–437.
33. von Boehmer, H. 2005. Unique features of the pre-T-cell receptor alpha-chain: not just a surrogate. *Nat. Rev. Immunol.* 5: 571–577.
34. Gray, D. H., N. Seach, T. Ueno, M. K. Milton, A. Liston, A. M. Lew, C. C. Goodnow, and R. L. Boyd. 2006. Developmental kinetics, turnover, and stimulatory capacity of thymic epithelial cells. *Blood* 108: 3777–3785.
35. Ripen, A. M., T. Nitta, S. Murata, K. Tanaka, and Y. Takahama. 2011. Ontogeny of thymic cortical epithelial cells expressing the thymoproteasome subunit β5t. *Eur. J. Immunol.* 41: 1278–1287.
36. Baik, S., E. J. Jenkinson, P. J. Lane, G. Anderson, and W. E. Jenkinson. 2013. Generation of both cortical and Aire(+) medullary thymic epithelial compartments from CD205(+) progenitors. *Eur. J. Immunol.* 43: 589–594.
37. Roberts, N. A., G. E. Desanti, D. R. Withers, H. R. Scott, W. E. Jenkinson, P. J. Lane, E. J. Jenkinson, and G. Anderson. 2009. Absence of thymus crosstalk in the fetus does not preclude hematopoietic induction of a functional thymus in the adult. *Eur. J. Immunol.* 39: 2395–2402.
38. Zuklys, S., G. Balciunaite, A. Agarwal, E. Fasler-Kan, E. Palmer, and G. A. Holländer. 2000. Normal thymic architecture and negative selection are associated with Aire expression, the gene defective in the autoimmune-polyendocrinopathy-candidiasis-ectodermal dystrophy (APECED). *J. Immunol.* 165: 1976–1983.
39. van Ewijk, W., G. Holländer, C. Terhorst, and B. Wang. 2000. Stepwise development of thymic microenvironments in vivo is regulated by thymocyte subsets. *Development* 127: 1583–1591.
40. Marrella, V., P. L. Poliani, E. Fontana, A. Casati, V. Maina, B. Cassani, F. Ficara, M. Cominelli, F. Schena, M. Paulis, et al. 2012. Anti-CD3ε mAb improves thymic architecture and prevents autoimmune manifestations in a mouse model of Omenn syndrome: therapeutic implications. *Blood* 120: 1005–1014.
41. Goldman, K. P., C. S. Park, M. Kim, P. Matzinger, and C. C. Anderson. 2005. Thymic cortical epithelium induces self tolerance. *Eur. J. Immunol.* 35: 709–717.
42. McCaughtry, T. M., and K. A. Hogquist. 2008. Central tolerance: what have we learned from mice? *Semin. Immunopathol.* 30: 399–409.
43. Stritesky, G. L., Y. Xing, J. R. Erickson, L. A. Kalekar, X. Wang, D. L. Mueller, S. C. Jameson, and K. A. Hogquist. 2013. Murine thymic selection quantified using a unique method to capture deleted T cells. *Proc. Natl. Acad. Sci. USA* 110: 4679–4684.

European Journal of Immunology

SHORT COMMUNICATION

Intermediate expression of CCRL1 reveals novel subpopulations of medullary thymic epithelial cells that emerge in the postnatal thymus

Ana R. Ribeiro[1,2], *Catarina Meireles*[1,2], *Pedro M. Rodrigues*[1,2] *and Nuno L. Alves*[1]

[1] Thymus Development and Function Laboratory, Institute for Molecular and Cellular Biology, Porto, Portugal
[2] Institute for Biomedical Sciences Abel Salazar, University of Porto, Porto, Portugal

Cortical and medullary thymic epithelial cells (cTECs and mTECs, respectively) provide inductive microenvironments for T-cell development and selection. The differentiation pathway of cTEC/mTEC lineages downstream of common bipotent progenitors at discrete stages of development remains unresolved. Using IL-7/CCRL1 dual reporter mice that identify specialized TEC subsets, we show that the stepwise acquisition of chemokine (C–C motif) receptor-like 1 (CCRL1) is a late determinant of cTEC differentiation. Although cTECs expressing high CCRL1 levels (CCRL1^{hi}) develop normally in immunocompetent and *Rag2*$^{-/-}$thymi, their differentiation is partially blocked in *Rag2*$^{-/-}$*Il2rg*$^{-/-}$ counterparts. These results unravel a novel checkpoint in cTEC maturation that is regulated by the cross-talk between TECs and immature thymocytes. Additionally, we identify new *Ulex europaeus* agglutinin 1 (UEA)$^{+}$ mTEC subtypes expressing intermediate CCRL1 levels (CCRL1^{int}) that conspicuously emerge in the postnatal thymus and differentially express *Tnfrsf11a*, *Ccl21*, and *Aire*. While rare in fetal and in *Rag2*$^{-/-}$ thymi, CCRL1^{int} mTECs are restored in *Rag2*$^{-/-}$Marilyn TCR-Tg mice, indicating that the appearance of postnatal-restricted mTECs is closely linked with T-cell selection. Our findings suggest that alternative temporally restricted routes of new mTEC differentiation contribute to the establishment of the medullary niche in the postnatal thymus.

Keywords: Cortex · Medulla · Thymic epithelial cells · Thymus

Additional supporting information may be found in the online version of this article at the publisher's web-site

Introduction

Within the thymus, it is well established the role of distinct thymic epithelial cell (TEC) microenvironments in supporting the generation of functionally diverse and self-tolerant T cells [1]. While cortical TECs (cTECs) promote T-cell lineage commitment and positive selection, medullary TECs (mTECs) participate in the elimination of autoreactive T cells and the differentiation of Treg cells [2]. In particular, auto-immune regulator (Aire)$^{+}$ mTECs have an established role in tolerance induction [3]. Cortical and medullary TECs are derived from common bipotent progenitors present within the fetal and postnatal thymus [4, 5]. Importantly, the cTEC/mTEC maturation pathways downstream of bipotent progenitors, as well as the requirements for the establishment of these specialized compartments at discrete stages of development are still unresolved.

Correspondence: Ms. Ana R. Ribeiro
e-mail: ana.ribeiro@ibmc.up.pt

The cTEC/mTEC lineage specification branches early in embryonic development [6]. During initial stages of gestation, the thymic epithelium predominately comprises Ly51$^+$CD205$^+$β5t$^+$ cTECs [7–9], and mature mTECs, including Aire$^+$ mTECs, first appear around embryonic day 16 (E16) [10, 11]. The emergence of embryonic mTECs depends on cellular interactions with lymphoid tissue inducer cells and invariant γδ T cells [12, 13], and involves signaling through TNFR superfamily receptor activator of NF-κB (RANK) and lymphotoxin beta receptor (LTβR) expressed on TEC precursors [12, 14]. However, and despite the elucidation of distinct maturation stages in mTECs [2], there are still gaps in the understanding of cTEC differentiation. We, and others, have recently demonstrated that fetal TEC progenitors expressing cortical properties are able to generate mTECs [15–17]. These reports support the idea that embryonic TEC precursors progress transitionally through the cortical lineage prior to commitment to the medullary pathway, emphasising that TEC differentiation is more complex then previously recognized [18].

The size of the medullary epithelial microenvironment continues to expand after birth, fostered by additional interactions between TECs and mature thymocytes, namely positively selected and CD4 single positive (SP4) thymocytes [2]. The concerted activation of RANK-, LTβR-, and CD40-mediated signaling on mTECs and their precursors completes the formation of the adult medullary niche [2]. It has been previously demonstrated a clonal nature for discrete embryonic mTEC islets, which progressively coalesce into larger medullary areas in the adult thymus [10, 19]. Hence, one can argue that the adult mTEC niche exclusively results from the expansion of embryonic-derived mTECs and their precursors. Still, it remains possible that alternative developmental stage-specific pathways participate in the organization of the adult mTEC niche.

Here, we report a novel checkpoint in cTEC differentiation, which is defined by the sequential acquisition of chemokine (C–C motif) receptor-like 1 (CCRL1) expression and is compromised in mice with profound blocks in early T-cell development. Additionally, we define original subsets of mTECs, characterized by the intermediate CCRL1 expression, that emerge in the postnatal thymus in tight association with thymocytes that develop beyond the TCRβ selection. Our findings provide evidence for the existence of several waves of mTEC development in the embryonic and postnatal thymus.

Results and discussion

Acquisition of CCRL1 expression is a late cTEC determinant

The expression of CCRL1, an atypical chemokine receptor that controls the bioavailability of key chemoattractants CCL19, CCL21, and CCL25, identifies cTECs in the postnatal thymus [20]. Given the incomplete knowledge on the differentiation of CCRL1$^+$cTECs, we assessed their generation using previously generated IL7^{YFP}-CCRL1^{GFP} dual reporter mice [15]. While in IL7^{YFP} reporter mice, YFP expression is a surrogate of a subtype of cTECs expressing abundant levels of the crucial thymopoietin IL-7 (*Il7*$^{YFP+}$) [8, 15], in CCRL1^{GFP} reporter mice, GFP expression labels cTECs in the postnatal thymus [20]. We previously showed that postnatal *Il7*$^{YFP+}$ TECs locate within cTECs that express high CCRL1 levels (referred as CCRL1^{hi}) [15]. Here, analysis during early stages of thymic development showed that the emergence of *Il7*$^{YFP+}$, CD205$^+$, and Ly51$^+$ TECs around E12.5–13.5 [7–9] preceded the appearance of CCRL1-expressing cells (Fig. 1A and Supporting information Fig. 1B; nonreporter thymi in Supporting Information Fig. 1A). During the E12.5–15.5 period, both *Il7*$^{YFP+}$ and remaining YFP$^-$ cTECs progressively acquired the expression of CCRL1. At E18.5, and similarly to the postnatal thymus [15], *Il7*$^{YFP+}$ TECs reside within CCRL1^{hi} cells (Fig. 1A). The number of CCRL1^{hi} cTECs gradually increased throughout development, contributing to the expansion of TEC cellularity during perinatal life. TECs lacking CCRL1 and expressing intermediate CCRL1 levels (referred as CCRL1$^-$ and CCRL1^{int}, respectively) followed steadier numbers during this period (Fig. 1B). To address whether the acquisition of CCRL1 defined a late cTEC maturation stage dependent on signals provided by developing thymocytes, we crossed double reporter mice onto a *Rag2*$^{-/-}$ or *Rag*$^{-/-}$*Il2r*$^{-/-}$ background. While the majority of TECs were CCRL1^{hi} in the postnatal *Rag*$^{-/-}$ thymus, we detected an accumulation of CCRL1^{int} TECs in the *Rag2*$^{-/-}$*Il2rg*$^{-/-}$ thymus (Fig. 1C and D, nonreporter thymi in Supporting Information Fig. 1C), akin to the CCRL1 pattern observed at E15.5 (Fig. 1A). Contrarily to CCRL1, the expression of Ly51, CD205, *Psmb11* (β5t), and *Ctsl* was not impaired in TECs from *Rag2*$^{-/-}$*Il2rg*$^{-/-}$ thymi (Supporting Information Fig. 1D and E) [8, 15]. CCRL1$^-$ and CCRL1^{int} TECs in the *Rag2*$^{-/-}$*Il2rg*$^{-/-}$ thymus were distinct from immunocompetent counterparts, as in the later these subsets comprised mostly mTECs (below in Fig. 2) that are virtually absent in the *Rag2*$^{-/-}$*Il2rg*$^{-/-}$ thymus [8]. The partial blockade in CCRL1, CD40, and MHCII expression in *Rag2*$^{-/-}$*Il2rg*$^{-/-}$ mice (Supporting Information Fig. 1D) was similar to blocks in the expression of CD40 and MHCII also reported in CD3εTg26 mice [7]. Although the signals remain unidentified, our results indicate that lymphoepithelial interactions with DN1–DN3 thymocytes provide differentiation cues that control late stages in the cTEC differentiation program.

Intermediate CCRL1 levels define distinct mTEC subtypes in the postnatal thymus

We reciprocally examined the generation of mTECs relatively to the differentiation of CCRL1-expressing TECs. The primordial CD80$^+$ mTECs were found within CCRL1$^-$ cells (CCRL1$^-$CD80$^+$) at E15.5 (Fig. 2A), preceding the complete differentiation of CCRL1^{hi} cTECs around E18.5-postnatal (Fig. 1A). The proportion and number of CCRL1$^-$CD80$^+$ mTECs augmented throughout time (Fig. 2A and D). Notably, a subset of CD80$^+$ TECs, expressing intermediate levels of CCRL1 (CCRL1^{int}CD80$^+$), emerged distinctly after birth (Fig. 2A; nonreporter CD80$^+$mTECs and

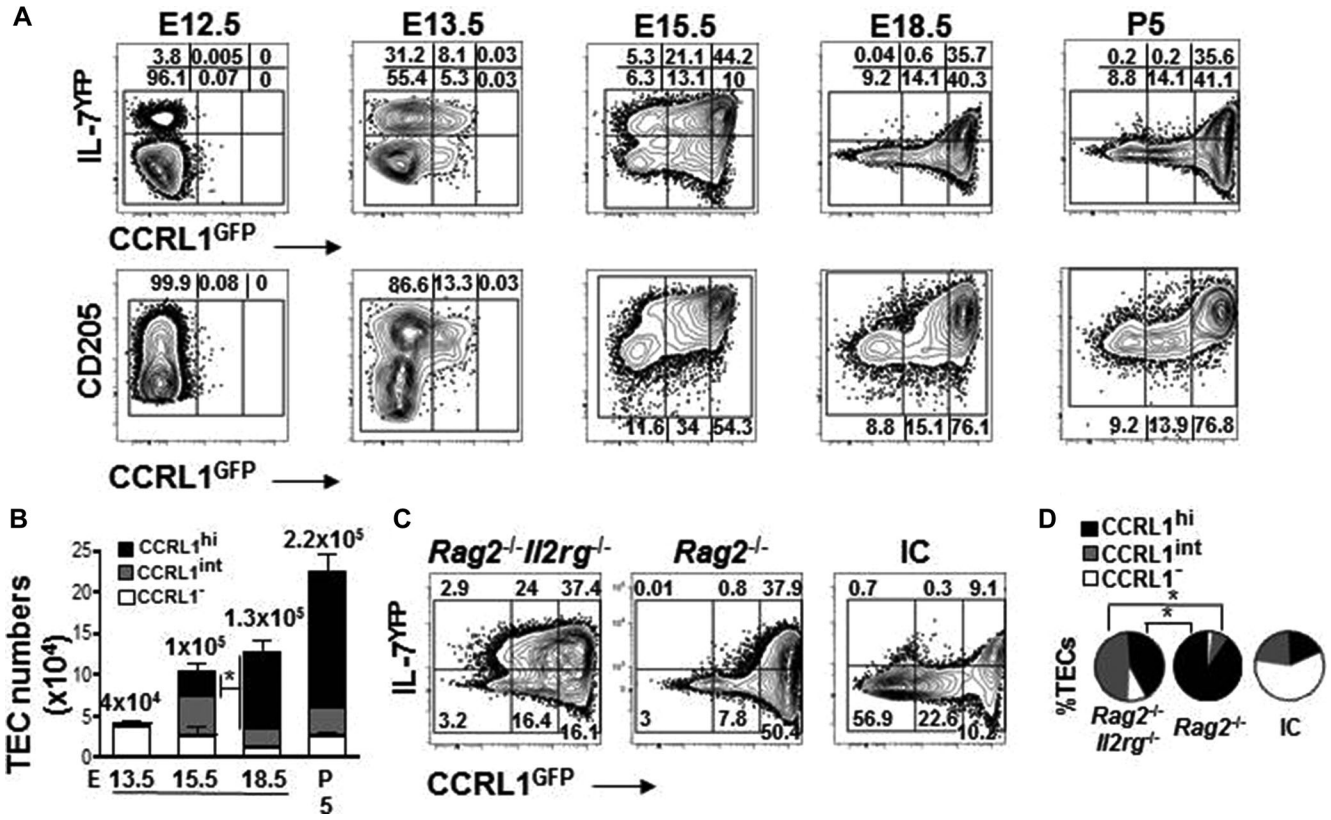

Figure 1. CCRL1 is a late cTEC determinant. (A) Total TECs (gated as CD45$^-$EpCAM$^+$) from IL-7^{YFP}CCRL1^{GFP} mice were analyzed for IL-7^{YFP} and CCRL1^{GFP} or CD205 and CCRL1^{GFP} expression by flow cytometry (FC) at the indicated time points. Numbers in plots indicate the frequency of cells found within each gate. Plots are representative of three to five independent experiments per time point. *E* represents embryonic day and *P5* represents postnatal day 5. (B) Cellularity of TECs expressing high (CCRL1^{hi}), intermediate (CCRL1^{int}), and no CCRL1 (CCRL1$^-$) was determined by the absolute thymic cell numbers and the respective frequencies of each subset obtained by FC. Numbers on top of bars indicate average TEC cellularity for each time point. Data are shown as mean + SD of 3–5 samples pooled from three to five independent experiments. $^*p < 0.05$ (unpaired *t* test). (C) TECs from 2-week-old *Rag2*$^{-/-}$, *Rag2*$^{-/-}$*Il2rg*$^{-/-}$, and immunocompetent (IC) thymi were analyzed by FC for IL-7^{YFP} and CCRL1^{GFP} expression. Numbers in plots indicate the frequency of each gate. Plots are representative of three independent experiments. (D) The mean proportion (%) of CCRL1 subsets in 2-week-old *Rag2*$^{-/-}$, *Rag2*$^{-/-}$*Il2rg*$^{-/-}$, and IC mice, determined by FC, is depicted. $^*p < 0.001$ (unpaired *t* test). Data represent means of three to five experiments ($n = 5$–6 mice/group).

Ccrl1 expression are shown in Supporting Information Fig. 2A and B, respectively). As this subtype was virtually absent at E15.5, we compared CCRL1^{int} TECs for the expression of additional cTEC (Ly51) and mTEC (UEA binding) markers [15, 17] in E18.5 and neonatal thymus. At both periods, CCRL1^{hi} and CCRL1$^-$CD80$^+$ TECs majorly identified either Ly51$^+$ cTECs or *Ulex Europaeus* Agglutinin 1 (UEA$^+$) mTECs, respectively (Fig. 2A and B). The CCRL1$^-$CD80$^-$ TECs, which represent a minor subset in the neonatal thymus, were predominantly composed of Ly51^{int}UEA$^+$ TECs at this stage. CCRL1^{int} TECs at E18.5 comprised mostly Ly51$^+$UEA$^-$CD80$^-$, although few UEA$^+$CD80$^-$ and scarce UEA$^+$CD80$^+$ were detected (Fig. 2B and C). Interestingly, three discrete sizeable subpopulations accumulated within neonatal CCRL1^{int} TECs, including UEA$^-$CD80$^-$, UEA$^+$CD80$^-$, and UEA$^+$CD80$^+$ (Fig. 2C). Both CD80$^-$ and CD80$^+$ CCRL1^{int}UEA$^+$ mTEC subsets, while scarce at E18.5 (Fig. 2B and C), totally represented approximately half and one quarter of the mTEC compartment in neonatal and young thymi, respectively (Fig. 2D). To examine whether CD80$^+$CCRL1^{int} mTECs differentiate by the reiteration of the same pathways defined for postnatal mTECs [2, 21], we set E18.5 fetal thymic organ cultures (FTOCs). While rare in intact FTOCs, RANK, and/or CD40 stimulation induced the differentiation of CD80$^+$CCRL1^{int} mTECs (Fig. 2E and Supporting Information Fig. 2C and D). Additionally, reaggregate thymic organ cultures (RTOCs) established with E15.5 CCRL1$^+$UEA$^-$CD80$^-$ TECs, and RANK- and CD40-activated to induce mTEC differentiation, showed that a fraction of fetal CCRL1$^+$ cTECs displayed CD80$^+$ mTEC progenitor activity (Fig. 2F). Next, we analyzed how the phenotypic traits of the emergent neonatal CCRL1^{int} TECs related to the expression of genes linked to cTECs (*Psmb11* and *Cstl*) and mTECs (*Tnfrsf11a* (RANK), *Ccl21*, and *Aire*) [2, 3]. Increasing *Psmb11* and *Cstl* expression was exclusively detected within CCRL1^{int}UEA$^-$ and CCRL1^{hi} cells. Interestingly, a gradual increase in *Tnfrsf11a* expression was observed in CCRL1^{int}UEA$^-$, CCRL1^{int}UEA$^+$CD80$^-$, CCRL1^{int}UEA$^+$CD80$^+$, and CCRL1$^-$CD80$^+$ TECs. *Ccl21*, which is expressed by postnatal immature mTECs [22], was specifically found within the CCRL1^{int}UEA$^-$CD80$^-$ and

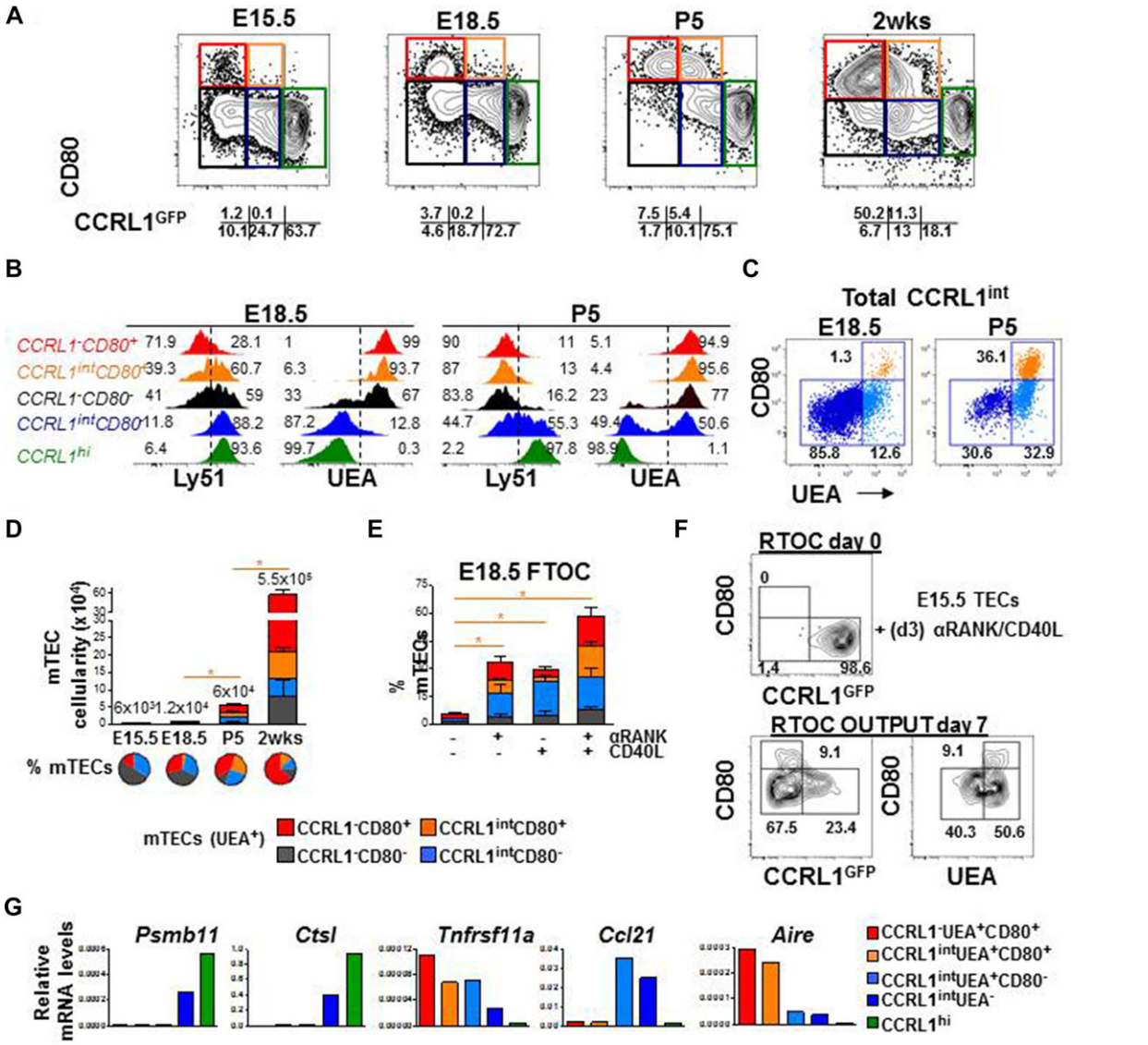

Figure 2. Intermediate CCRL1 expression reveals novel postnatal mTECs. (A) TECs (gated as CD45$^-$EpCAM$^+$) from IL-7^{YFP}CCRL1^{GFP} mice were analyzed for CCRL1^{GFP} and CD80 expression by FC at the indicated time points. Colored gates define different subsets and grids indicate the frequencies of each respective one. (B) TEC subsets defined by the colored gates in (A) from E18.5 and postnatal day 5 (P5) thymi were analyzed for Ly51 and UEA expression by FC. Numbers in histograms indicate the frequency within each gate. Histograms are representative of three to five independent experiments. (C) Expression of UEA and CD80 within gated E18.5 and postnatal day 5 (P5) total CCRL1^{int} TECs was determined by FC. Numbers in plots indicate the frequency of cells found within each gate. (A–C) Plots are representative of three to five independent experiments. (D) Cellularity of UEA$^+$ mTEC subsets from IL-7^{YFP}CCRL1^{GFP} mice was assessed as in Figure 1. Average total mTEC cellularity is detailed above bars. Pie graphs represent the mean proportion of color-coded subsets within total UEA$^+$ mTECs. *$p < 0.05$ (unpaired t test) (data are shown as mean + SD of 4–6 mice/group, pooled from three to five independent experiments (E) E18.5 FTOCs were cultured for 4 days with the indicated stimuli and then assessed for mTEC induction (UEA$^+$CD80$^{-/+}$) by FC. The proportion of subsets within UEA$^+$ mTECs is color-coded. Data are shown as mean + SD of 8–10 thymic lobes/group, pooled from three independent experiments. *$p < 0.05$ (unpaired t test). (F) RTOCs established with E15.5-derived CCRL1$^+$UEA$^-$CD80$^-$ TECs were stimulated with αRANK and/or CD40L and gated TECs were analyzed for the expression of the indicated markers by FC. Plots are representative of three independent experiments. (G) Expression of *Psmb11*, *Ctsl*, *Tnfrsf11a*, *Ccl21*, and *Aire* was assessed by qPCR in purified TEC subsets (colored columns) from postnatal day 5 (P5) IL-7^{YFP}CCRL1^{GFP} mice. Values were normalized to *18s*. Data are shown as representative of three independent experiments.

CCRL1^{int}UEA$^+$CD80$^-$ subsets. Lastly, *Aire* expression was equally enriched in CCRL1$^-$ and CCRL1^{int} CD80$^+$ mTECs (Fig. 2G). Although fetal CCRL1$^+$UEA$^-$ TECs have the potential to generate mTECs (Fig. 2F), and the gradual increase in the expression of RANK and CCL21 within CCRL1^{int} cells might suggest a continual stepwise differentiation: CCRL1^{int}UEA$^-$ – CCRL1^{int}UEA$^+$ – CCRL1^{int}UEA$^+$CD80$^+$, our attempts to evaluate a direct lineage relationship between neonatal CCRL1^{int} TEC subsets have been unsuccessful, given the difficulty of establishing RTOC with perinatal TECs [23]. Thus, we can only speculate that the postnatal cTEC niche harbors progenitors that are able to differentiate into mTECs, as shown in the fetal thymus [15–17]. Alternatively, one

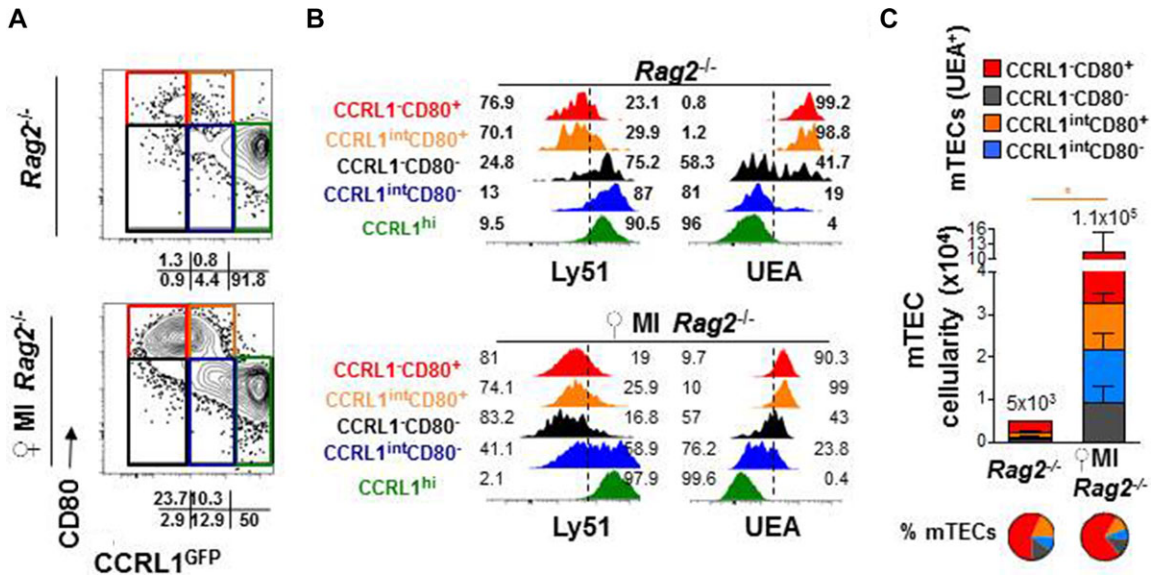

Figure 3. Thymic selection drives the emergence of the postnatal-specific CCRL1^{int}CD80^{+} TECs. (A) TECs (gated as CD45^{-}EpCAM^{+}) from postnatal day 5 (P5) *Rag2*$^{-/-}$ and female Marilyn-*Rag2*$^{-/-}$ mice were analyzed for CCRL1^{GFP} and CD80 expression by FC. Colored boxes define different TEC subsets and grids indicate the frequencies of each one. Plots are representative of two to three independent experiments. (B) Subsets defined by the colored gates in (A) from *Rag2*$^{-/-}$ and Marilyn-*Rag2*$^{-/-}$ mice were analyzed for Ly51 and UEA expression by FC. Numbers in histograms indicate the frequency within each gate. Histograms are representative of three independent experiments. (C) Frequency of subsets within total mTECs (pie graphs) and numbers of mTEC subsets was determined by FC. Data are shown as mean + SD of three to five samples, pooled from two independent experiments. $^{*}p < 0.05$ (unpaired *t* test).

cannot exclude that postnatal CCRL1^{int} mTECs might differentiate from a lineage unrelated to cTECs. Collectively, our data indicate that while CCRL1^{int}UEA^{-} TECs coexpress molecular traits of cTECs and mTECs, CCRL1^{int}UEA^{+}CD80^{-} and CCRL1^{int}UEA^{+}CD80^{+} cells define novel subtypes of immature and mature mTECs, respectively, that emerge postnatally.

Thymic selection promotes the generation of CCRL1^{int} mTECs

The differentiation of the CCRL1^{int}CD80^{+} mTECs correlates timely with the intensification of positive thymic selection around the perinatal period [6]. Given that activation of RANK and CD40 fostered CCRL1^{int}CD80^{+} mTECs (Fig. 2C) and the ligands for those mTEC-inductive signals are expressed by SP4 thymocytes [2], we investigated whether the appearance of CCRL1^{int}CD80^{+} mTECs depends on TEC-SP4 interactions during selection. To this end we crossed CCRL1-reporter mice onto a Marilyn-*Rag2*$^{-/-}$ TCR transgenic background, in which T cells express an I-A^{b}-restricted TCR that recognizes the male H-Y antigen [15]. As control, we coanalyzed *Rag2*$^{-/-}$ littermates, wherein mTEC differentiation is compromised due to the lack of mature thymocytes [15]. Few CD80^{+} mTECs were present in the neonatal *Rag2*$^{-/-}$ thymus, and those were majorly CCRL1^{-} (Fig. 3A–C), resembling mTECs found in the E18.5 thymus (Fig. 2). Contrarily to the normal postnatal thymus, the scarce CCRL1^{-} and CCRL1^{int} CD80^{-} subsets found in *Rag2*$^{-/-}$ mice were predominantly composed of Ly51^{+}UEA^{-} cells (Fig. 3A and B). Strikingly, we detected a marked expansion of both CCRL1^{-}CD80^{+} and CCRL1^{int}CD80^{+} mTECs in neonatal Marilyn-*Rag2*$^{-/-}$ females (Fig. 3A–C, nonreporter *Rag2*$^{-/-}$ and Marilyn-*Rag2*$^{-/-}$ are shown in S2E), recapitulating the mTEC composition of the young thymus (Fig. 2A). Akin to the WT thymus, CCRL1^{hi} and CCRL1^{-}CD80^{+} TECs specifically identified cTECs and mTECS, respectively, and the emergent CCRL1^{int}CD80^{+} TECs were Ly51^{lo}UEA^{+} (Fig. 3B). One can envision that temporally restricted mTEC differentiation pathways are engaged by interactions between mTEC precursors and distinct hematopoietic cells. As shown previously [10, 11], the generation of the first embryonic mature CD80^{+} mTECs (CCRL1^{-}) precedes the development of SP4s and depends on LTβR- and RANK-mediated signaling engaged upon lymphoepithelial interaction with lymphoid tissue inducer cells and γδ T cells [12–14]. Our findings indicate that the differentiation of the postnatal-restricted CCRL1^{int}CD80^{+} mTECs results from MHC-TCR, CD40-CD40L, and RANK-RANKL interactions [2, 21] between TEC precursors and TCRβ−selected thymocytes.

Concluding remarks

The neonatal life marks a period characterized by a drop in cTECs and an expansion in mTECs [20]. The identification of novel postnatal mTEC subsets supports the concept that the foundation of the adult medullary microenvironment results from alternative waves of mTEC differentiation. In this regard, recent evidence suggests that the expansion of the medulla after birth involves de novo formation of mTECs [24]. This notion implicates that fetal mTEC precursors might have limited self-renewal potential,

as shown for bipotent TEC progenitors [25], and in turn the formation of the adult mTEC niche relies on additional inputs arising after birth. Still, further studies are needed to elucidate to what extent bipotent progenitors might progress through the cortical differentiation program in the adult thymus. Also, the functional relevance of the mTEC heterogeneity reported herein should be further dissected. As mTECs have a crucial role in T-cell maturation and tolerance induction, our findings have implications in therapeutics aimed at modulating TEC niches in the adult thymus.

Materials and methods

Mice

Dual IL-7^{YFP}CCRL1^{GFP} reporter mice were backcrossed onto *Rag2*$^{-/-}$, *Rag2*$^{-/-}$*Il2rg*$^{-/-}$, and Marilyn-*Rag2*$^{-/-}$ C57BL/6 background [8, 15]. E0.5 was the day of vaginal plug detection. Animal experiments were performed in accordance with European guidelines.

TEC isolation and flow cytometry

TECs were isolated as described [15]. Cells were stained with anti– I-A/I-E (Alexa 780); anti-CD45.2 (PerCP-Cy5.5); anti-EpCAM (A647); anti-CD80 (A660); anti-Ly51, anti-CD205, UEA-1 (biotin), anti-EpCAM (eFluor 450) Abs, and streptavidin (PE-Cy7) (eBioscience). Flow cytometry was performed on a FACSCanto II, with data analyzed on FlowJo software (BD). Cell sorting was performed using the FACSAria I (BD Biosciences), with purities >95%. A 510/10-nm band pass (502LP dichroic mirror) and a 542/27-nm band pass (525LP dichroic mirror) filters were used to discriminate the GFP/YFP signals.

Gene expression

mRNA (RNAeasy MicroKit, Quiagen) isolation and cDNA synthesis (Superscript First-Strand Synthesis System, Invitrogen) were performed as described [15]. Real-time PCR (iCycler iQ5) was performed using either TaqMan Universal PCR Master Mix and primers for *18s, Ctsl, Aire, Ccl21, Tnfrsf11a*, and *Psmb11* (Applied Biosystems); or iQ SYBR Green Supermix (Bio-Rad) and primers for *Actb* and *Ccrl1* as detailed [15]; Triplicated samples were analyzed and the $\Delta\Delta$Ct method was used to calculate relative levels of targets compared with *18s/Actb* as described [15].

FTOCs and RTOCs

FTOCs and RTOCs were established with E18.5 and E15.5 embryos, respectively, as described [15]. For FTOCs, TECs were analyzed after 4 days culturing with 1 μg/mL anti-RANK and/or with 5 μg/mL recombinant CD40L (R&D Systems). For RTOCs, 10^5 E15.5 CCRL1^+UEA$^-$CD80^- TECs were sorted and mixed with CD4^+CD8^+ and CD4^+ thymocytes at 1:1:1 ratio. After 3 days, 0.3 μg/mL anti-RANK and 1.3 μg/mL recombinant CD40L were added to the cultures. RTOC were analyzed after 7 days.

Statistical analysis

The unpaired *t* test was used to perform statistical analysis. $p < 0.05$ was considered significant.

Acknowledgments: We thank James Di Santo, Jocelyne Demengeot, and Thomas Boehm for *Rag2*$^{-/-}$*Il2rg*$^{-/-}$, CCRL1-reporter, and Marilyn-*Rag2*$^{-/-}$ mice, respectively. We thank Dr. Catarina Leitão for critical reading of the manuscript and technical assistance. We thank FEDER funds through the Operational Competitiveness Programme – COMPETE and by National Funds through *Fundação para a Ciência e a Tecnologia* (FCT) under the project PTDC/SAU-IMU/117057/2010 funded this work. N.L.A., A.R.R., C.M., and P.M.R. are supported by FCT Investigator program and PhD fellowships.

Conflict of interest: The authors have no financial or commercial conflicts of interest.

References

1 **Takahama, Y.**, Journey through the thymus: stromal guides for T-cell development and selection. *Nat. Rev. Immunol.* 2006. **6**: 127–135.

2 **Anderson, G. and Takahama, Y.**, Thymic epithelial cells: working class heroes for T cell development and repertoire selection. *Trends Immunol.* 2012. **33**: 256–263.

3 **Mathis, D. and Benoist, C.**, Aire. *Annu. Rev. Immunol.* 2009. **27**: 287–312.

4 **Rossi, S. W., Jenkinson, W. E., Anderson, G. and Jenkinson, E. J.**, Clonal analysis reveals a common progenitor for thymic cortical and medullary epithelium. *Nature* 2006. **441**: 988–991.

5 **Bleul, C. C., Corbeaux, T., Reuter, A., Fisch, P., Monting, J. S. and Boehm, T.**, Formation of a functional thymus initiated by a postnatal epithelial progenitor cell. *Nature* 2006. **441**: 992–996.

6 **Anderson, G., Jenkinson, E. J. and Rodewald, H. R.**, A roadmap for thymic epithelial cell development. *Eur. J. Immunol.* 2009. **39**: 1694–1699.

7 **Shakib, S., Desanti, G. E., Jenkinson, W. E., Parnell, S. M., Jenkinson, E. J. and Anderson, G.**, Checkpoints in the development of thymic cortical epithelial cells. *J. Immunol.* 2009. **182**: 130–137.

8 **Alves, N. L., Huntington, N. D., Mention, J. J., Richard-Le Goff, O. and Di Santo, J. P.**, Cutting edge: a thymocyte-thymic epithelial cell cross-talk dynamically regulates intrathymic IL-7 expression in vivo. *J. Immunol.* 2010. **184**: 5949–5953.

9 **Ripen, A. M.**, **Nitta, T.**, **Murata, S.**, **Tanaka, K. and Takahama, Y.**, Ontogeny of thymic cortical epithelial cells expressing the thymoproteasome subunit beta5t. *Eur. J. Immunol.* 2011. **41**: 1278–1287.

10 **Hamazaki, Y.**, **Fujita, H.**, **Kobayashi, T.**, **Choi, Y.**, **Scott, H. S.**, **Matsumoto, M. and Minato, N.**, Medullary thymic epithelial cells expressing Aire represent a unique lineage derived from cells expressing claudin. *Nat. Immunol.* 2007. **8**: 304–311.

11 **White, A. J.**, **Withers, D. R.**, **Parnell, S. M.**, **Scott, H. S.**, **Finke, D.**, **Lane, P. J.**, **Jenkinson, E. J. et al.**, Sequential phases in the development of Aire-expressing medullary thymic epithelial cells involve distinct cellular input. *Eur. J. Immunol.* 2008. **38**: 942–947.

12 **Rossi, S. W.**, **Kim, M. Y.**, **Leibbrandt, A.**, **Parnell, S. M.**, **Jenkinson, W. E.**, **Glanville, S. H.**, **McConnell, F. M. et al.**, RANK signals from CD4(+)3(-) inducer cells regulate development of Aire-expressing epithelial cells in the thymic medulla. *J. Exp. Med.* 2007. **204**: 1267–1272.

13 **Roberts, N. A.**, **White, A. J.**, **Jenkinson, W. E.**, **Turchinovich, G.**, **Nakamura, K.**, **Withers, D. R.**, **McConnell, F. M. et al.**, Rank signaling links the development of invariant gammadelta T cell progenitors and Aire(+) medullary epithelium. *Immunity* 2012. **36**: 427–437.

14 **Mouri, Y.**, **Yano, M.**, **Shinzawa, M.**, **Shimo, Y.**, **Hirota, F.**, **Nishikawa, Y.**, **Nii, T. et al.**, Lymphotoxin signal promotes thymic organogenesis by eliciting RANK expression in the embryonic thymic stroma. *J. Immunol.* 2011. **186**: 5047–5057.

15 **Ribeiro, A. R.**, **Rodrigues, P. M.**, **Meireles, C.**, **Di Santo, J. P. and Alves, N. L.**, Thymocyte selection regulates the homeostasis of IL-7-expressing thymic cortical epithelial cells in vivo. *J. Immunol.* 2013. **191**: 1200–1209.

16 **Baik, S.**, **Jenkinson, E. J.**, **Lane, P. J.**, **Anderson, G. and Jenkinson, W. E.**, Generation of both cortical and Aire(+) medullary thymic epithelial compartments from CD205(+) progenitors. *Eur. J. Immunol.* 2013. **43**: 589–594.

17 **Ohigashi, I.**, **Zuklys, S.**, **Sakata, M.**, **Mayer, C. E.**, **Zhanybekova, S.**, **Murata, S.**, **Tanaka, S. et al.**, Aire-expressing thymic medullary epithelial cells originate from beta5t-expressing progenitor cells. *Proc. Natl. Acad. Sci. USA* 2013. **110**: 9885–9890.

18 **Alves, N. L.**, **Takahama, Y.**, **Ohigashi, I.**, **Ribeiro, A. R.**, **Baik, S.**, **Anderson, G. and Jenkinson, W. E.**, Serial progression of cortical and medullary thymic epithelial microenvironments. *Eur. J. Immunol.* 2014. **44**: 16–22.

19 **Rodewald, H. R.**, **Paul, S.**, **Haller, C.**, **Bluethmann, H. and Blum, C.**, Thymus medulla consisting of epithelial islets each derived from a single progenitor. *Nature* 2001. **414**: 763–768.

20 **Rode, I. and Boehm, T.**, Regenerative capacity of adult cortical thymic epithelial cells. *Proc. Natl. Acad. Sci. USA* 2012. **109**: 3463–3468.

21 **Akiyama, T.**, **Shimo, Y.**, **Yanai, H.**, **Qin, J.**, **Ohshima, D.**, **Maruyama, Y.**, **Asaumi, Y. et al.**, The tumor necrosis factor family receptors RANK and CD40 cooperatively establish the thymic medullary microenvironment and self-tolerance. *Immunity* 2008. **29**: 423–437.

22 **Lkhagvasuren, E.**, **Sakata, M.**, **Ohigashi, I. and Takahama, Y.**, Lymphotoxin beta receptor regulates the development of CCL21-expressing subset of postnatal medullary thymic epithelial cells. *J. Immunol.* 2013. **190**: 5110–5117.

23 **Rossi, S. W.**, **Chidgey, A. P.**, **Parnell, S. M.**, **Jenkinson, W. E.**, **Scott, H. S.**, **Boyd, R. L.**, **Jenkinson, E. J. et al.**, Redefining epithelial progenitor potential in the developing thymus. *Eur. J. Immunol.* 2007. **37**: 2411–2418.

24 **Dumont-Lagace, M.**, **Brochu, S.**, **St-Pierre, C. and Perreault, C.**, Adult thymic epithelium contains nonsenescent label-retaining cells. *J. Immunol.* 2014. **192**: 2219–2226.

25 **Jenkinson, W. E.**, **Bacon, A.**, **White, A. J.**, **Anderson, G. and Jenkinson, E. J.**, An epithelial progenitor pool regulates thymus growth. *J. Immunol.* 2008. **181**: 6101–6108.

Abbreviations: **Aire**: auto-immune regulator · **CCRL1**: chemokine (C–C motif) receptor-like 1 · **cTEC**: cortical TEC · **FC**: flow cytometry · **FTOC**: fetal thymic organ culture · **LTβR**: lymphotoxin beta receptor · **mTEC**: medullary TEC · **RANK**: receptor activator of NF-κB · **RTOC**: reaggregate thymic organ culture · **SP**: single positive · **TEC**: thymic epithelial cell · **UEA**: *Ulex Europaeus* Agglutinin 1

Full correspondence: Ana Rosalina Ribeiro, Institute for Molecular and Cellular Biology, Rua do Campo Alegre, 823, 4150-180 Porto, Portugal
Fax: +351-226-099-157
e-mail: ana.ribeiro@ibmc.up.pt

Additional correspondence: Dr. Nuno L. Alves, Institute for Molecular and Cellular Biology, Rua do Campo Alegre, 823, 4150–180 Porto, Portugal.
Fax: +351-226-099-157
e-mail nalves@ibmc.up.pt

Received: 20/2/2014
Revised: 6/6/2014
Accepted: 25/7/2014
Accepted article online: 28/7/2014

European Journal of Immunology

Review

Serial progression of cortical and medullary thymic epithelial microenvironments

Nuno L. Alves[1], Yousuke Takahama[2], Izumi Ohigashi[2], Ana R. Ribeiro[1], Song Baik[3], Graham Anderson[3] and William E. Jenkinson[3]

[1] Infection and Immunity Unit, Institute for Molecular and Cellular Biology, University of Porto, Porto, Portugal
[2] Division of Experimental Immunology, Institute for Genome Research, University of Tokushima, Tokushima, Japan
[3] Medical Research Council Centre for Immune Regulation, Institute for Biomedical Research, Medical School, University of Birmingham, Birmingham, UK

Thymic epithelial cells (TECs) provide key instructive signals for T-cell differentiation. Thymic cortical (cTECs) and medullary (mTECs) epithelial cells constitute two functionally distinct microenvironments for T-cell development, which derive from a common bipotent TEC progenitor. While seminal studies have partially elucidated events downstream of bipotent TECs in relation to the emergence of mTECs and their progenitors, the control and timing of the emergence of the cTEC lineage, particularly in relation to that of mTEC progenitors, has remained elusive. In this review, we describe distinct models that explain cTEC/mTEC lineage divergence from common bipotent progenitors. In particular, we summarize recent studies in mice providing evidence that mTECs, including the autoimmune regulator$^+$ subset, derive from progenitors initially endowed with phenotypic properties typically associated with the cTEC lineage. These observations support a novel "serial progression" model of TEC development, in which progenitors serially acquire cTEC lineage markers, prior to their commitment to the mTEC differentiation pathway. Gaining a better understanding of the phenotypic properties of early stages in TEC progenitor development should help in determining the mechanisms regulating cTEC/mTEC lineage development, and in strategies aimed at thymus reconstitution involving TEC therapy.

Keywords: Cortex · Medulla · Thymic epithelial cells · Thymus

Introduction

The thymus is dedicated to the generation of functional self-tolerant T lymphocytes, a chief effector arm of immune responses. Within thymic niches, hematopoietic progenitors, arriving from the fetal liver and bone marrow, differentiate primarily into T cells with diverse αβTCR specificities that are restricted to self-MHCs and tolerant to self-antigens (reviewed in [1, 2]).

The development of T cells is guided by thymic stromal cells, of which thymic epithelial cells (TECs) comprise a chief component. TECs constitute specialized structural and functional microenvironments that support critical steps of T-cell differentiation, by providing multiple cytokines, chemokines, lineage inductive ligands, and selective self-antigens that control T-cell commitment, migration, survival, proliferation, and selection (reviewed in [2, 3]).

Correspondence: Dr. Nuno L. Alves
e-mail: nalves@ibmc.up.pt

Cortical and medullary thymic epithelial niches define distinct functional microenvironments

The thymic epithelium is broadly organized into two main areas, the central medulla area in which thymic medullary epithelial cells (mTECs) reside, and the peripheral cortex area in which thymic cortical epithelial cells (cTECs) reside. These areas and the cells therein also define functionally distinct niches. cTECs have an important role during the early stages of T-cell development, driving the commitment and expansion of early T-cell progenitors via the expression of Notch ligand DLL4 [4] and IL-7 [5]. Subsequently, cTECs mediate the selection of DP thymocytes, by expressing an array of selective self-peptides presented by MHC class I and II molecules. To accomplish this chief function as antigen-presenting cells, cTECs express a unique set of proteolytic enzymes, including a cTEC-specific proteosomal subunit β5t, a serine protease TSSP, and a lysosomal protease cathepsin L [6–8]. On the other side of the "thymic yard," mTECs play decisive roles in later stages of T-cell development, notably acting in concert with DCs to mediate the negative selection of autoreactive T cells and the generation of regulatory T cells [1–3]. Crucial to the key role of mTECs in the screening of developing T cells with autoreactive TCRs is their capacity to express a myriad of tissue-restricted antigens, such as insulin 2, salivary protein 1, thyroglobulin [9]. The nuclear factor auto-immune regulator (Aire) has emerged as a chief effector in tolerance induction by regulating the expression of a large array of peripheral tissue antigens (e.g. insulin 2) in a specialized subset of mTECs (reviewed in [10]. Worth noting, there are other antigens associated with peripheral tissues (e.g. thyroglobulin) that are ectopically expressed in mTECs independently of Aire [11], implicating other factor(s) in the establishment of central tolerance. In addition to its key role in peripheral tissue antigen expression, Aire has recently been shown to control chemokine gene expression within the mTEC compartment [12, 13].

Despite being fundamentally different in their anatomical location and functions, cTECs and mTECs share some phenotypic markers; for example, both are routinely defined by the expression of epithelial cell adhesion molecule 1/CD326 and MHC class II (MHCII) within the nonhematopoietic ($CD45^-$) thymus fraction [14]. However, as different analytical tools are frequently employed across studies (flow cytometry and immunohistochemical analyses), some variation exists in how researchers discriminate TEC subsets. Whereas cTECs are commonly defined by the expression of cytokeratin-8/18, CDR1, Ly51 (CD249), and ER-TR4, mTECs are distinguished by the expression of cytokeratin-5/14, MTS10, ER-TR5, and reactivity with the lectin *Ulex europaeus* agglutinin 1 [14, 15]. The phenotypic discrimination of these cell types has considerably improved with the development of novel antibodies and the advent of newly generated reporter mice, which have allowed surveying the expression of molecules associated with cTEC- and mTEC-specific functions. Currently, cTECs are additionally identified on the basis of the expression of CD205 [16], Ccrl1 [17], β5t [18], and high levels of IL-7 [19] and DLL4 [20] expression. mTECs are usually further discriminated on the basis of the combined levels of expression of MHC class II, CD40, CD80, Aire, and most recently CCL21 [16,21–24]. Still, the relevance of cTEC/mTEC heterogeneity with respect to developmentally distinct stages within TEC lineages remains elusive.

In this review, we summarize recent studies in mice that have analyzed the lineage relationship between cTECs and mTECs, and we discuss possible models to explain the establishment of these two key thymic epithelial microenvironments.

cTECs and mTECs: Same origin, but unrelated divergent lineages?

The cells in the cortical and medullary thymic epithelial compartments differentiate from bipotent thymic epithelial progenitors (TEPs) present within the embryonic [25–28] and postnatal thymus [29]. The identification of TEPs, which lie at the base of the cTEC/mTEC branching point, has provided the cellular basis for a common origin of cTECs and mTECs. Despite this, the phenotypic properties and developmental requirements of bipotent TEPs are poorly understood. In mice, TEC ontogeny is initiated during early embryogenesis with the out-budding of the endoderm in the third pharyngeal pouch between day 9 and 10 of embryonic gestation (E9-E10) (reviewed in [30])[31]. At these early stages, the initiation of expression of the forkhead transcription factor Foxn1 represents a hallmark toward TEC specification [32, 33]. Although bipotent TEPs are maintained in Foxn1-deficient mice [29], Foxn1 is required for the initiation of a transcriptional program that engages the early differentiation of TEPs, and for the progression of cTECs and mTECs throughout distinct stages of differentiation [29, 34]. Recently, one study using mice with a reversible Foxn1 hypomorphic allele provided experimental evidence revealing differential requirements for Foxn1 levels in regulating these two events [34]. In line with an earlier study [35], low levels of Foxn1 were shown to be sufficient to initiate the TEC differentiation program, while higher Foxn1 expression levels are needed both to achieve fully functional mature TECs and to maintain TEC lineage identity postnatally [34, 35]. Presently, there is no experimental evidence demonstrating that the level of Foxn1 expression modulates the determination of TEPs into the cTEC or mTEC lineages.

The discrimination between cTECs and mTECs, although particularly evident in the postnatal adult thymus, is less conspicuous at early stages of thymic organogenesis. This perhaps results from their common ancestry and the dynamic nature of TEC patterning, which is initiated during fetal development and continues throughout postnatal life [30]. Yet, the precise developmental window at which cTECs and mTECs diverge, as well as the lineage relationship between TEPs and the emerging cortical and medullary progenies, remain poorly understood.

Building epithelial microenvironments through lineage-committed progenitors

Several studies in mice have examined the development of distinct lineages downstream of bipotent TEPs. While Rodewald et al. [36] initially provided functional evidence for the existence of mTEC progenitors, advances in understanding the identity of this cell-type and stages of mTEC development have been considerably extended in the past decade. For example, successive stages of mTEC maturation have been shown to exist in mice, defined as immature MHCII^{lo}CD80^{lo}Aire^{-} (mTEC^{lo}), mature MHCII^{hi}CD80^{hi}Aire^{hi} (mTEC^{hi}), and recently identified terminally differentiated MHCII^{lo}CD80^{lo}Aire^{lo}Involucrin^{+} (also residing within the originally defined mTEC^{lo}) [22,37,38]. Importantly, the cooperative contribution of members of the TNFR superfamily, including receptor activator of NF-κB (RANK), lymphotoxin β receptor by mTECs, is critical to the complete maturation of the Aire^{+} mTEC subset (reviewed in detail in [2, 3, 39]). These findings led to the idea that mTECs undergo a linear differentiation process, from mTEC progenitors down to terminally differentiated mTECs, recently defined by a final post-Aire stage of maturation that is controlled by expression of Aire itself [37, 40]. Interestingly, studies have shown a role for lymphotoxin β receptor signaling during late stages of mTEC development, which acts to control CCL21 within the mTEC^{lo} compartment [23, 41]. Thus, as well as containing progenitors for mTEC^{hi} cells [21, 22], mTEC^{lo} cells express molecules of known functional importance for αβ T-cell development. In addition, the expression of the tight junction proteins claudin-3 (Cld3) and Cld4 has been shown to mark a minor subset of TECs at E13 in mice, representing an mTEC progenitor subset at this developmental stage that is able to generate Aire-expressing mTECs [42]. Recently, it was reported that TECs expressing high levels of Cld4 are also detected within the Foxn1-deficient E13.5 thymic primordium [34]. Worth noting, while Cld3/4-expressing "mTEC progenitor-like" cells were also previously detected at E10.5 [42], it remains unclear how the Cld4^{hi} cells of the nude mouse relate to functionally identified mTEC progenitors [42]. In addition, a subset of CD205^{-} TECs expressing high levels of CD40 and a panel of mTEC-associated genes has been reported to arise at E14.5 [16]. Together, these studies provide evidence for the existence of a transitional mTEC progenitor and for direct precursor-product relationships within the mTEC lineage. However, it remains unclear whether the transitional mTEC progenitors exist immediately downstream of common bipotent TEPs, or whether such mTEC progenitors share a more intricate relationship with the nascent cTEC lineage.

In contrast to an emerging picture of discrete stages in the mTEC lineage, events occurring in the cTEC developmental pathway are less clear. However, recent studies in mice suggested the existence of cTEC-specific progenitors identified by the expression of CD205 and β5t, both hallmarks of the cTEC lineage, which appear as early as E12.5 and are absent in nude mouse embryos [16, 18]. While such cells were initially considered to mark a developmental stage that lies in between bipotent TEPs and mature cTECs [16], there is currently no functional evidence regarding the phenotypic identity of cTEC progenitors.

Based on current findings, a simple model of TEC lineage development from bipotent TEPs can be proposed (Fig. 1A), in which phenotypically and developmentally distinct cTEC progenitors and mTEC progenitors emerge in a synchronous and nonoverlapping fashion, that results in the generation of functionally distinct cTEC and mTEC compartments to control T-cell development and selection. While such a model fits well with several studies reporting the identification of lineage-restricted mTEC progenitors [16, 21, 42] initially identified at the clonal level [36], definitive support for this model is hampered by the lack of understanding of how and when the cTEC lineage emerges in relation to the mTEC population.

mTECs derive from progenitors expressing cTEC markers

The identification of bipotent TEPs and evidence for the existence of compartment-restricted progenitors has cemented the concept that cTECs and mTECs follow independent differentiation pathways. Interestingly, despite several studies demonstrating the presence of mTEC progenitors [16, 36, 42] at early stages of embryonic thymus development, the TEC compartment at these stages has also been reported to express markers typically associated with the cTEC lineage, including CD205, β5t, and high levels of IL-7 and DLL4 [16, 18–20, 43]. Importantly, the relationship between these "cTEC marker-expressing" TECs and the mTEC lineage itself has not been directly investigated. Recently, our laboratories independently generated experimental evidence in relation to our understanding of the timing and relationship between the establishment of the cortical and medullary microenvironments, particularly with respect to the emergence of mTEC progenitors relative to the cTEC lineage [44–46].

Using a cellular approach that combines reaggregate organ cultures and ectopic thymic transplantation of phenotypically defined embryonic putative TEC progenitor populations, Baik et al. demonstrated that purified CD205^{+}CD40^{-} TECs, displaying molecular traits associated with cTECs [16], comprise a source of progenitors in mice that generate both β5t/CD205-expressing cortical, and Aire-expressing medullary epithelial microenvironments in vivo [44]. Ontogenetic analysis showed that, at E12.5 of gestation, functional responsiveness to the mTEC regulator RANK is evident within both CD205^{+} and CD205^{-} compartments, demonstrating that mTEC progenitors exist within the TEC subset defined by expression of the cTEC marker CD205 [44]. Importantly, it remains unclear whether the RANK-responsive TECs contained within the CD205^{-} subset are derived from initial CD205^{+} progeny, or whether additional RANK^{+}CD205^{-} cells at early embryonic stages represent a separate stream of mTEC progenitors that do not pass through a CD205^{+} stage. Whatever the case, such observations demonstrate a "blurring" of cTEC/mTEC

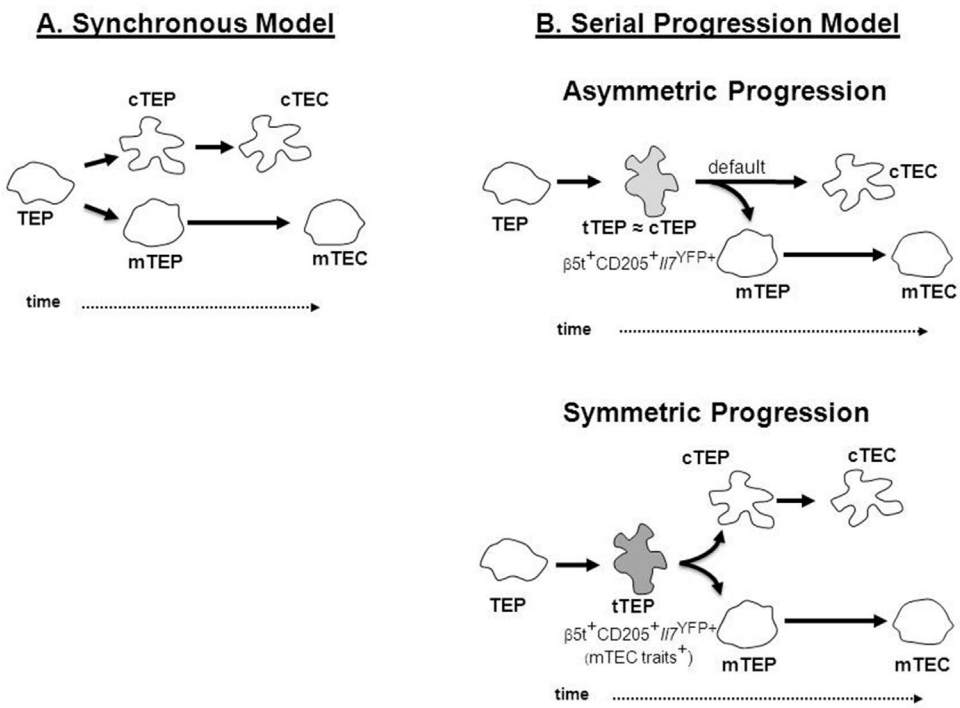

Figure 1. Models of thymic epithelial cell development. (A) In the "synchronous" model, uncommitted bipotent TEC progenitors (TEPs) diverge simultaneously to lineage-restricted cortical (cTEPs) and medullary (mTEPs) progenitors, which then progress into mature cTECs and mTECs. (B) In the "serial progression" model, TEPs transverse through a "transitional TEC progenitor" stage (tTEP) that expresses phenotypic and molecular traits associated with cTECs prior to the commitment into a cTEC or mTEC fate. In the asymmetric scenario (top), tTEPs are more closely linked, at the phenotypic and molecular levels, with cTEPs and have the potential to generate both mTEC progenitors and mature cTECs, with the cortical lineage being the "default" pathway. In the symmetric scenario (bottom), tTEPs express both cTEC and as-yet-unidentified mTEC traits prior to lineage specification.

properties at initial stages of development in TEC populations of the embryonic thymus, and argue against the synchronous emergence of cTEC progenitors and mTEC progenitors from a common TEP pool.

In a complementary study, Ribeiro et al. [46], exploring an IL-7 reporter mouse in which YFP marks a previously identified TEC subset expressing high levels of IL-7 (*Il7*$^{YFP+}$) [5, 19], demonstrated that *Il7*$^{YFP+}$ TECs represent a particular subset of CD205^{+}Ly51^{+} cTECs throughout fetal development and perinatal life. Of note, IL-7 expression is also detected in mTECs, albeit at significantly lower levels compared to *Il7*$^{YFP+}$ TECs [5]. *Il7*$^{YFP+}$ TECs emerge as early as E12.5 [19] and comprise the majority of TECs around E13–14 of gestation [46]. Employing reaggregate organ cultures (RTOCs), the authors show that E14.5 *Il7*$^{YFP+}$ TECs can give rise to both Ly51^{+}CD205^{+} cTECs and CD80^{+} mTECs [46]. Thus, *Il7*$^{YFP+}$ cells give rise to mTECs in a stepwise differentiation process via an intermediate CD80^{lo} immature mTEC stage. Still, *Il7*$^{YFP+}$ cells do not exclusively form the entire TEC compartment at E13–14, and a smaller fraction of YFP^{-} cells is detected at this period, which steadily accumulates medullary traits as TEC maturation proceeds, including responsiveness to RANK stimulation. Similarly to the E13 CD205^{-} progenitors detected by Baik et al. [44], it remains to be determined whether YFP^{-} TECs found within the E13 thymus have a direct lineage relationship with *Il7*$^{YFP+}$ cells or represent an alternative pathway of mTEC development. Although both studies indicate that embryonic TEC progenitors with cTEC features have the potential to generate mTECs, these studies do not determine to what degree such progenitors contribute to thymus medulla formation within the embryonic and adult thymus.

In this respect, using a knock-in mouse strategy and lineage tracing experiments, Ohigashi et al. [45] established a direct link between β5t-expressing TECs and mTECs. By crossing knock-in mice that express the recombinase Cre under the control of the endogenous β5t-encoding sequences with loxP-dependent EGFP or ZsGreen reporter mice, the authors showed that the reporter activity is not only detected in cTECs, but also in almost all mTECs, including the Aire^{+} subset, throughout ontogeny [45]. β5t-Cre-mediated reporter expression was detectable even in the majority of fetal mTECs and their progenitors visualized by the high expression of K5 [45] and Cld3/4 (Ohigashi and Takahama, unpublished data), indicating that all mTEC stages transverse through an early stage defined by β5t expression. As the expression of β5t is not detectable in the E11.5 thymus primordium [18, 45], one can consider that β5t expression is initiated at a differentiation stage downstream of common TEPs, but prior to the branching of mTEC progenitors. The analysis of β5t fate-reporter mice corroborate that fetal and adult mTECs are almost all derived from progenitors expressing bona-fide cTEC traits under normal physiological circumstances.

Collectively, these observations demonstrate that the medullary lineage is derived from progenitors defined by a cTEC "footprint," thereby arguing against a model of TEC development involving the synchronous emergence of distinct pools of cTEC progenitors and mTEC progenitors from bipotent TEPs. Based on these findings, we propose an alternative model of TEC development, referred to here as the "serial progression" model (Fig. 1B), to explain these findings in relation to the establishment of cortical and medullary microenvironments. This model points to the existence of a novel transitional progenitor stage in the TEC differentiation pathway currently defined by the expression of a set of cTEC-associated genes, including β5t, CD205, and high levels of IL-7. As the development of Aire-expressing mTECs is not affected in β5t- [6,47], CD205- [48], or IL-7-deficient mice (Rodrigues and Alves, unpublished data), these findings suggest that the expression of these cTEC traits solely identifies transitional TEC developmental stages, rather than being directly implicated in the divergence of the mTEC lineage. While such cortical attributes may be transiently transcribed at an early phase of both cTEC and mTEC lineages, and then either enhanced during the default cTEC development or progressively lost during differentiation into mature mTECs, this model supports a process in which cTEC and mTEC lineages follow asymmetrical differentiation pathways from bipotent TEPs. In this differentiation route, transitional and cortical TEC progenitors are more closely related at phenotypic, molecular, and functional levels (Fig. 1B). However, one cannot exclude that TEPs progress through the transitional TEP state prior to the commitment into the cTEC and mTEC lineages. In this variant "symmetric serial progression" model (Fig. 1B), one considers that transitional TEPs may begin coexpressing cTEC- in addition to, yet unresolved mTEC-associated genes. Once the lineage fate is programmed into cTEPs or mTEPs, the expression of lineage-specific molecules is permitted and the expression of molecules specific for another lineage is terminated. Further studies on the molecular mechanisms regulating the dynamics of the serial progression of the cTEC and mTEC lineages are warranted.

Conclusions

The recent developments discussed in this review provide an important change in the understanding of TEC lineage specification. The identification of transitional progenitors with cortical traits indicates that cTECs and mTECs might share a more intricate lineage relationship downstream of bipotent TEPs than previously recognized. This raises more general questions of how TEC differentiation is balanced to create functionally diverse epithelial microenvironments. Given the considerable plasticity in the lineage potential of transitional TEPs, it will be important to determine whether these cells exist in the adult thymus. Additionally, we still lack evidence on how transcriptional and epigenetic changes contribute to the specification of TEC lineages.

The "asymmetrical serial progression" model implies that the specification into the cortical lineage is the default pathway downstream of the TEC bipotent progenitors. From an evolutionary point of view, one can envisage that TECs from ancient vertebrates initially evolved with the functional capacity to commit thymic seeding precursors into the T-cell lineage and to restrict the immense diversity of generated TCR specificities to self-MHC molecules. In this scenario, the emergence of the mTEC lineage is a sophisticated event that evolved later to guarantee self-tolerance, either through the purging of autoreactive T cells or the generation of T regulatory cells [49]. It is interesting to note that distinct lymphopoietic microenvironments are also detected in the recently identified thymoids of jawless vertebrates [50]. Further studies on the TEC compartment of primitive vertebrates should elucidate whether these niches represent functional equivalents to the cortical and medullary lineages found in the thymus of jawed vertebrates. Knowledge in this area will enable us to gain a more complete appreciation of the fundamental rules that govern the complex diversification of TECs in mammals.

Interestingly, the concept presented here seems to extend to other cell types and tissues, in which the indistinctness between progenitors and lineage-specific phenotypes is observed. For example, during the development of the central nervous system, both glial and neuronal cell lineages emerge from a common progenitor that expresses proteolipid protein, a predominant myelin neuronal-restricted component [51].

Taken together, the recent studies discussed here provide a clearer definition of TEC progenitors capable of giving rise to both cTECs and mTECs. This could have important implications in relation to cellular immunotherapy approaches involving thymus regeneration/replacement [52], in which functional and self-tolerant T-cell production depends upon the presence of both thymic compartments.

Acknowledgments: N. L. A. is supported by program Ciência2008 from the Foundation for Science and Technology (FCT, Portugal). N. L. A. is supported by grants from FCT, funds from the European Regional Development Fund (FEDER) through the Operational Competitiveness Program (COMPETE), by National Funds through the Foundation for Science and Technology (FCT, Portugal) under Project FCOMP-01–0124-FEDER-015803 (PTDC/SAU-IMU/110116/2009). A. R. R. is supported by Ph.D. fellowships from FCT (SFRH/BD/78380/2011). Y. T. is supported by Grants-in-Aid for Scientific Research from MEXT and JSPS (23249025 and 24111004), Japan. G. A. and Y. T. are supported by An International Exchange Scheme from The Royal Society, UK. S. B. is supported by a PhD studentship from the European Union ITN "NINA." G. A. is supported by a Medical Research Council Programme Grant, W. E. J. is supported by a New Investigator Award from the Medical Research Council, UK (G1001055).

We thank members of our laboratories for their contribution to the manuscripts reviewed here. We apologize for not referring to all primary literature owing to space limitations.

Conflict of interest: The authors declare no financial or commercial conflict of interest.

References

1 **Takahama, Y.**, Journey through the thymus: stromal guides for T-cell development and selection. *Nat. Rev. Immunol.* 2006. **6**: 127–135.

2 **Anderson, G. and Takahama, Y.**, Thymic epithelial cells: working class heroes for T cell development and repertoire selection. *Trends Immunol.* 2012. **33**: 256–263.

3 **Alves, N. L., Huntington, N. D., Rodewald, H. R. and Di Santo, J. P.**, Thymic epithelial cells: the multi-tasking framework of the T cell "cradle." *Trends Immunol.* 2009. **30**: 468–474.

4 **Hozumi, K., Mailhos, C., Negishi, N., Hirano, K., Yahata, T., Ando, K., Zuklys, S. et al.**, Delta-like 4 is indispensable in thymic environment specific for T cell development. *J. Exp. Med.* 2008. **205**: 2507–2513.

5 **Alves, N. L., Goff, O. R., Huntington, N. D., Sousa, A. P., Ribeiro, V. S., Bordack, A., Vives, F. L. et al.**, Characterization of the thymic IL-7 niche in vivo. *Proc. Natl. Acad. Sci. USA* 2009. **106**: 1512–1517.

6 **Murata, S., Sasaki, K., Kishimoto, T., Niwa, S., Hayashi, H., Takahama, Y. and Tanaka, K.**, Regulation of CD8+ T cell development by thymus-specific proteasomes. *Science* 2007. **316**: 1349–1353.

7 **Gommeaux, J., Gregoire, C., Nguessan, P., Richelme, M., Malissen, M., Guerder, S., Malissen, B. and Carrier, A.**, Thymus-specific serine protease regulates positive selection of a subset of CD4(+) thymocytes. *Eur. J. Immunol.* 2009. **39**: 956–964.

8 **Nakagawa, T., Roth, W., Wong, P., Nelson, A., Farr, A., Deussing, J., Villadangos, J. A. et al.**, Cathepsin L: critical role in Ii degradation and CD4 T cell selection in the thymus. *Science* 1998. **280**: 450–453.

9 **Derbinski, J., Schulte, A., Kyewski, B. and Klein, L.**, Promiscuous gene expression in medullary thymic epithelial cells mirrors the peripheral self. *Nat. Immunol.* 2001. **2**: 1032–1039.

10 **Mathis, D. and Benoist, C.**, Aire. *Annu. Rev. Immunol.* 2009. **27**: 287–312.

11 **Anderson, M. S., Venanzi, E. S., Klein, L., Chen, Z., Berzins, S. P., Turley, S. J., von Boehmer, H. et al.**, Projection of an immunological self shadow within the thymus by the aire protein. *Science* 2002. **298**: 1395–1401.

12 **Lei, Y., Ripen, A. M., Ishimaru, N., Ohigashi, I., Nagasawa, T., Jeker, L. T., Bosl, M. R. et al.**, Aire-dependent production of XCL1 mediates medullary accumulation of thymic dendritic cells and contributes to regulatory T cell development. *J. Exp. Med.* 2011. **208**: 383–394.

13 **Laan, M., Kisand, K., Kont, V., Moll, K., Tserel, L., Scott, H. S. and Peterson, P.**, Autoimmune regulator deficiency results in decreased expression of CCR4 and CCR7 ligands and in delayed migration of CD4 +thymocytes. *J. Immunol.* 2009. **183**: 7682–7691.

14 **Gray, D. H., Chidgey, A. P. and Boyd, R. L.**, Analysis of thymic stromal cell populations using flow cytometry. *J. Immunol. Methods* 2002. **260**: 15–28.

15 **Klug, D. B., Carter, C., Crouch, E., Roop, D., Conti, C. J. and Richie, E. R.**, Interdependence of cortical thymic epithelial cell differentiation and T-lineage commitment. *Proc. Natl. Acad. Sci USA* 1998. **95**: 11822–11827.

16 **Shakib, S., Desanti, G. E., Jenkinson, W. E., Parnell, S. M., Jenkinson, E. J. and Anderson, G.**, Checkpoints in the development of thymic cortical epithelial cells. *J. Immunol.* 2009. **182**: 130–137.

17 **Rode, I. and Boehm, T.**, Regenerative capacity of adult cortical thymic epithelial cells. *Proc. Natl. Acad. Sci. USA* 2012. **109**: 3463–3468.

18 **Ripen, A. M., Nitta, T., Murata, S., Tanaka, K. and Takahama, Y.**, Ontogeny of thymic cortical epithelial cells expressing the thymoproteasome subunit beta5t. *Eur. J. Immunol.* 2011. **41**: 1278–1287.

19 **Alves, N. L., Huntington, N. D., Mention, J. J., Richard-Le Goff, O. and Di Santo, J. P.**, Cutting edge: a thymocyte-thymic epithelial cell cross-talk dynamically regulates intrathymic IL-7 expression in vivo. *J. Immunol.* 2010. **184**: 5949–5953.

20 **Fiorini, E., Ferrero, I., Merck, E., Favre, S., Pierres, M., Luther, S. A. and MacDonald, H. R.**, Cutting edge: thymic crosstalk regulates delta-like 4 expression on cortical epithelial cells. *J. Immunol.* 2008. **181**: 8199–8203.

21 **Gabler, J., Arnold, J. and Kyewski, B.**, Promiscuous gene expression and the developmental dynamics of medullary thymic epithelial cells. *Eur. J. Immunol.* 2007. **37**: 3363–3372.

22 **Rossi, S. W., Kim, M. Y., Leibbrandt, A., Parnell, S. M., Jenkinson, W. E., Glanville, S. H., McConnell, F. M. et al.**, RANK signals from CD4(+)3(–) inducer cells regulate development of Aire-expressing epithelial cells in the thymic medulla. *J. Exp. Med.* 2007. **204**: 1267–1272.

23 **Lkhagvasuren, E., Sakata, M., Ohigashi, I. and Takahama, Y.**, Lymphotoxin beta receptor regulates the development of CCL21-expressing subset of postnatal medullary thymic epithelial cells. *J. Immunol.* 2013. **190**: 5110–5117.

24 **Nelson, A. J., Hosier, S., Brady, W., Linsley, P. S. and Farr, A. G.**, Medullary thymic epithelium expresses a ligand for CTLA4 in situ and in vitro. *J. Immunol.* 1993. **151**: 2453–2461.

25 **Bennett, A. R., Farley, A., Blair, N. F., Gordon, J., Sharp, L. and Blackburn, C. C.**, Identification and characterization of thymic epithelial progenitor cells. *Immunity* 2002. **16**: 803–814.

26 **Gill, J., Malin, M., Hollander, G. A. and Boyd, R.**, Generation of a complete thymic microenvironment by MTS24(+) thymic epithelial cells. *Nat. Immunol.* 2002. **3**: 635–642.

27 **Rossi, S. W., Jenkinson, W. E., Anderson, G. and Jenkinson, E. J.**, Clonal analysis reveals a common progenitor for thymic cortical and medullary epithelium. *Nature* 2006. **441**: 988–991.

28 **Rossi, S. W., Chidgey, A. P., Parnell, S. M., Jenkinson, W. E., Scott, H. S., Boyd, R. L., Jenkinson, E. J. and Anderson, G.**, Redefining epithelial progenitor potential in the developing thymus. *Eur. J. Immunol.* 2007. **37**: 2411–2418.

29 **Bleul, C. C., Corbeaux, T., Reuter, A., Fisch, P., Monting, J. S. and Boehm, T.**, Formation of a functional thymus initiated by a postnatal epithelial progenitor cell. *Nature* 2006. **441**: 992–996.

30 **Rodewald, H. R.**, Thymus organogenesis. *Annu. Rev. Immunol.* 2008. **26**: 355–388.

31 **Gordon, J., Wilson, V. A., Blair, N. F., Sheridan, J., Farley, A., Wilson, L., Manley, N. R. and Blackburn, C. C.**, Functional evidence for a single endodermal origin for the thymic epithelium. *Nat. Immunol.* 2004. **5**: 546–553.

32 **Blackburn, C. C., Augustine, C. L., Li, R., Harvey, R. P., Malin, M. A., Boyd, R. L., Miller, J. F. and Morahan, G.**, The nu gene acts cell-autonomously and is required for differentiation of thymic epithelial progenitors. *Proc. Natl. Acad. Sci. USA* 1996. **93**: 5742–5746.

33 **Nehls, M., Kyewski, B., Messerle, M., Waldschutz, R., Schuddekopf, K., Smith, A. J., and Boehm, T.**, Two genetically separable steps in the differentiation of thymic epithelium. *Science* 1996. **272**: 886–889.

34 **Nowell, C. S., Bredenkamp, N., Tetelin, S., Jin, X., Tischner, C., Vaidya, H., Sheridan, J. M. et al.**, Foxn1 regulates lineage progression in cortical and medullary thymic epithelial cells but is dispensable for medullary sublineage divergence. *PLoS Genet.* 2011. **7**: e1002348.

35 **Chen, L., Xiao, S. and Manley, N. R.**, Foxn1 is required to maintain the postnatal thymic microenvironment in a dosage-sensitive manner. *Blood* 2009. **113**: 567–574.

36 **Rodewald, H. R.**, **Paul, S.**, **Haller, C.**, **Bluethmann, H. and Blum, C.**, Thymus medulla consisting of epithelial islets each derived from a single progenitor. *Nature* 2001. **414**: 763–768.

37 **Nishikawa, Y.**, **Hirota, F.**, **Yano, M.**, **Kitajima, H.**, **Miyazaki, J.**, **Kawamoto, H.**, **Mouri, Y. and Matsumoto, M.**, Biphasic Aire expression in early embryos and in medullary thymic epithelial cells before end-stage terminal differentiation. *J. Exp. Med.* 2010. **207**: 963–971.

38 **Wang, X.**, **Laan, M.**, **Bichele, R.**, **Kisand, K.**, **Scott, H. S. and Peterson, P.**, Post-Aire maturation of thymic medullary epithelial cells involves selective expression of keratinocyte-specific autoantigens. *Frontiers Immunol.* 2012. **3**: 19.

39 **Irla, M.**, **Hollander, G. and Reith, W.**, Control of central self-tolerance induction by autoreactive CD4+ thymocytes. *Trends Immunol.* 2010. **31**: 71–79.

40 **Metzger, T. C.**, **Khan, I. S.**, **Gardner, J. M.**, **Mouchess, M. L.**, **Johannes, K. P.**, **Krwawisz, A. K.**, **Skrzypczynska, K. M. and Anderson, M. S.**, Lineage tracing and cell ablation identify a post-Aire-expressing thymic epithelial cell population. *Cell Rep.* 2013. **5**: 166–179.

41 **White, A. J.**, **Nakamura, K.**, **Jenkinson, W. E.**, **Saini, M.**, **Sinclair, C.**, **Seddon, B.**, **Narendran, P. et al.**, Lymphotoxin signals from positively selected thymocytes regulate the terminal differentiation of medullary thymic epithelial cells. *J. Immunol.* 2010. **185**: 4769–4776.

42 **Hamazaki, Y.**, **Fujita, H.**, **Kobayashi, T.**, **Choi, Y.**, **Scott, H. S.**, **Matsumoto, M. and Minato, N.**, Medullary thymic epithelial cells expressing Aire represent a unique lineage derived from cells expressing claudin. *Nat. Immunol.* 2007. **8**: 304–311.

43 **Roberts, N. A.**, **Desanti, G. E.**, **Withers, D. R.**, **Scott, H. R.**, **Jenkinson, W. E.**, **Lane, P. J.**, **Jenkinson, E. J. and Anderson, G.**, Absence of thymus crosstalk in the fetus does not preclude hematopoietic induction of a functional thymus in the adult. *Eur. J. Immunol.* 2009. **39**: 2395–2402.

44 **Baik, S.**, **Jenkinson, E. J.**, **Lane, P. J.**, **Anderson, G. and Jenkinson, W. E.**, Generation of both cortical and Aire(+) medullary thymic epithelial compartments from CD205(+) progenitors. *Eur. J. Immunol.* 2013. **43**: 589–594.

45 **Ohigashi, I.**, **Zuklys, S.**, **Sakata, M.**, **Mayer, C. E.**, **Zhanybekova, S.**, **Murata, S.**, **Tanaka, K. et al.**, Aire-expressing thymic medullary epithelial cells originate from beta5t-expressing progenitor cells. *Proc. Natl. Acad. Sci. USA* 2013. **110**: 9885–9890.

46 **Ribeiro, A. R.**, **Rodrigues, P. M.**, **Meireles, C.**, **Di Santo, J. P. and Alves, N. L.**, Thymocyte selection regulates the homeostasis of IL-7-expressing thymic cortical epithelial cells in vivo. *J. Immunol.* 2013. **191**: 1200–1209.

47 **Nitta, T.**, **Murata, S.**, **Sasaki, K.**, **Fujii, H.**, **Ripen, A. M.**, **Ishimaru, N.**, **Koyasu, S. et al.**, Thymoproteasome shapes immunocompetent repertoire of CD8+ T cells. *Immunity* 2010. **32**: 29–40.

48 **Jenkinson, W. E.**, **Nakamura, K.**, **White, A. J.**, **Jenkinson, E. J. and Anderson, G.**, Normal T cell selection occurs in CD205-deficient thymic microenvironments. *PloS One* 2012. **7**: e53416.

49 **Cohn, M.**, Why Aire? Compensating for late bloomers. *Eur. J. Immunol.* 2009. **39**: 2969–2972.

50 **Boehm, T.**, **McCurley, N.**, **Sutoh, Y.**, **Schorpp, M.**, **Kasahara, M. and Cooper, M. D.**, VLR-based adaptive immunity. *Annu. Rev. Immunol.* 2012. **30**: 203–220.

51 **Delaunay, D.**, **Heydon, K.**, **Cumano, A.**, **Schwab, M. H.**, **Thomas, J. L.**, **Suter, U.**, **Nave, K. A. et al.**, Early neuronal and glial fate restriction of embryonic neural stem cells. *J. Neurosci.* 2008. **28**: 2551–2562.

52 **Boehm, T. and Swann, J. B.**, Thymus involution and regeneration: two sides of the same coin? *Nat. Rev. Immunol.* 2013. **13**: 831–838.

Abbreviations: **Aire**: auto-immune regulator · **Cld**: claudin · **cTEC**: cortical TEC · **mTEC**: medullary TEC · **RANK**: receptor activator of NF-κB · **TEC**: thymic epithelial cell · **TEP**: thymic epithelial progenitor

Full correspondence: Dr. Nuno L. Alves, Institute for Molecular and Cellular Biology, Rua do Campo Alegre, 823, 4150–180 Porto, Portugal
Fax: +351-226-099-157
e-mail: nalves@ibmc.up.pt

Additional correspondence: Prof. Yousuke Takahama, Division of Experimental Immunology, Institute for Genome Research, University of Tokushima, Tokushima 770–8503, Japan
e-mail: takahama@genome.tokushima-u.ac.jp

Additional correspondence: Prof. Graham Anderson and Dr. William E. Jenkinson, Medical Research Council Centre for Immune Regulation, Institute for Biomedical Research, University of Birmingham, Edgbaston, Birmingham, B15 2TT, UK
e-mail: G.Anderson@bham.ac.uk, w.e.jenkinson@bham.ac.uk

Received: 23/9/2013
Accepted: 5/11/2013
Accepted article online: 11/11/2013

European Journal of Immunology

Commentary

Thymus medulla under construction: Time and space oddities

Nuno L. Alves[1,2] *and Ana R. Ribeiro*[1,2]

[1] Instituto de Investigação e Inovação em Saúde (I3S), Universidade do Porto, Portugal
[2] Instituto de Biologia Molecular e Celular (IBMC), Universidade do Porto, Portugal

The development of effective T-cell-based immunotherapies to treat infection, cancer, and autoimmunity should incorporate the ground rules that control differentiation of T cells in the thymus. Within the thymus, thymic epithelial cells (TECs) provide microenvironments supportive of the generation and selection of T cells that are responsive to pathogen-derived antigens, and yet tolerant to self-determinants. Defects in TEC differentiation cause syndromes that range from immunodeficiency to autoimmunity, which makes the study of TECs of fundamental and clinical importance to comprehend how immunity and tolerance are balanced. Critical to tolerance induction are medullary thymic epithelial cells (mTECs), which purge autoreactive T cells, or redirect them to a regulatory T-cell lineage. In this issue of the *European Journal of Immunology*, studies by Baik et al. and Mayer et al. [Eur. J. Immunol. 2016. 46: 857-862 and 46: 846–856]) document novel spatial–temporal singularities in the lineage specification and maintenance of mTECs. While Baik et al. define a developmental checkpoint during mTEC specification in the embryo, Mayer et al. reveal that the generation and maintenance of the adult mTEC compartment is temporally controlled in vivo. The two reports described new developmentally related, but temporally distinct principles that underlie the homeostasis of the thymic medulla across life.

Keywords: Medullary thymic epithelial cells · Progenitor cells · Thymus · Tolerance induction

See accompanying articles by Mayer et al. and Baik et al.

Within the thymus, thymic epithelial cells (TECs) span along the outer cortex and inner medulla to form specialized niches capable of generating T cells, which are simultaneously reactive to pathogens and tolerant to one's own organs. To solve the conundrum imposed by the random assortment of αβ T-cell receptors (TCR), TECs select T cells with a broad range of reactivity against foreign antigens, while generally controlling the fate of self-reactive ones. Cortical TEC (cTEC) and medullary TEC (mTEC) sublineages constitute the two main stromal components of the preinvoluted thymus (reviewed in [1]). While cTECs promote T-cell lineage commitment and positive selection, mTECs regulate the elimination of autoreactive T cells and the differentiation of regulatory T cells (reviewed in [2]). The particular relevance of mTECs to tolerance induction is illustrated by studies in mice and humans showing a direct link between genetic defects in mTEC differentiation and the development of autoimmunity (reviewed in [1]). Intrinsic to the role of mTECs is their capacity to express tissue-restricted antigens (TRAs), a process that depends in part on autoimmune regulator (Aire) and the recently described Fezf2 [3, 4]. These two transcription factors control the expression of highly diverse and complementary TRAs in mTECs [3, 4], so that the coverage of virtually all self-antigens is organized in random patterns of gene expression in just a few hundred mTECs [3, 5, 6]. This seemingly stochastic process secures the repeated

Correspondence: Dr. Nuno L. Alves
e-mail: nalves@ibmc.up.pt

representation of the entire genome to developing T cells within the thymic medulla. In this regard, understanding the foundation of the mTEC microenvironment is important to comprehend how the thymus establishes the limits of tolerance to peripheral tissues.

The identification of bipotent TEC progenitors (TEPs) in both the embryonic [7] and postnatal [8] thymus provided evidence that mTECs and cTECs share a common origin. The initial descriptions of mTEC precursors (mTEPs) [9–11] led to the notion that mTECs undergo a diversification route unrelated from cTECs. Nonetheless, the blueprint of TEC development became more complex with the observations that embryonic TEPs expressing cortical markers can generate both cTECs and mTECs [12–14]. These findings support a refined model whereby progenitors transverse through the cortical lineage prior to commitment to mTEC differentiation in the embryonic thymus (reviewed in [15]). Still, we lack critical information on the nature of TEPs as well as on their functional contribution to the maintenance of thymic epithelial niches across life. Another area of uncertainty deals with the molecular networks that underlie the precursor–product relationship between TEPs, lineage-restricted precursors, and mature TEC subsets. Research in TEC progenitors has been under intense scrutiny in the past years, regularly providing new advances to our understanding of thymic biology. In this issue, reports by Baik et al. [16] and Mayer et al. [17] reveal novel spatial–temporal peculiarities in the generation of mTEC lineages that sprout in the fetal and postnatal life, respectively. These discoveries extend our knowledge on the program that regulates mTEC differentiation.

The establishment of the murine mTEC compartment starts during early embryogenesis [15]. Following the initial discovery of embryonic claudin-3$^+$ and claudin-4$^+$ (Cld3,4) mTEPs, which give rise to Aire$^+$ mTECs [11], subsequent studies show that these mTEPs are able to restore life-long tolerance induction in defective mTEC microenvironments caused by a dysfunctional mutation in NF-κB-inducing kinase [18]. Additionally, a further degree of heterogeneity has been resolved within Cld3,4$^+$ TECs with the description of long-lived mTEPs typified by SSEA-1 expression [18]. These findings support the notion that mTEPs sustain the breadth and function of the medullary epithelium for the duration of life [18]. Importantly, mTEC differentiation depends on crosstalk with developing thymocytes [2]. Past studies elucidated the chief role of members of TNF receptor superfamily receptor activator of NF-κB (RANK), lymphotoxin β receptor and CD40 in the establishment of mature mTECs [1]. Nonetheless, the determinants that control the responsiveness of mTECs and their precursors to these key inductors of the mTEC lineage program remain poorly understood.

Given the role of RANK in mTEC differentiation, it is important to understand the relationship between RANK expression and mTEC lineage specification. Using reporter mice in which the RANK promoter controls Venus fluorescent protein expression [19], Baik et al. describe the first temporal functional analysis of RANK^{Venus}-expressing (RANK$^+$) mTEPs in the embryonic thymus [16]. The authors start by surveying the ontogeny of RANK$^+$ TECs relative to Cld3,4^{hi}SSEA1$^+$ mTEPs in embryonic day (E) 13–15 thymus. While Cld3,4^{hi}SSEA1$^+$ TECs exist in the E13 thymus, RANK$^+$ TECs emerge one day later within the Cld3,4^{hi}SSEA1$^-$ subset and become prominently detected in the E15 thymus. Interestingly, RANK$^+$ TECs express higher levels of MHC class II (MHCII) and lower levels of CD205 than Cld3,4^{hi}SSEA1$^+$ mTEPs [16]. To address the lineage potential of RANK$^+$TECs, Baik et al. established reaggregate thymic organ cultures (RTOCs) in which MHCII-mismatched E15 Cld3,4^{hi}RANK$^+$ TECs were mixed with E15 WT thymus and their progeny was traced on the basis of distinct MHCII. The authors show that in chimeric RTOCs, E15 Cld3,4^{hi}RANK$^+$ cells preferentially generate MHCII^{hi}Ly51$^-$CD80$^{-/+}$TECs, indicating that RANK$^+$ TECs contain mTEC unipotent progenitors [16]. Although future experiments are required to map the expression of additional cTEC and mTEC markers in RANK$^+$ TECs, these results uncover a novel degree of heterogeneity in early steps of the mTEC differentiation program. Additionally, the study by Baik et al. provides genetic evidence for the role of chief regulators of TEC specification, such as Foxn1 and Relb [1], in the differentiation of RANK$^+$ mTEPs. The authors show that Foxn1 and Relb are differentially required for the development of Cld3,4^{hi}SSEA1$^+$ and Cld3,4^{hi}RANK$^+$ TEC subtypes [16]. While unaltered in Relb-deficient mice, the abundance of Cld3,4^{hi}SSEA1$^+$ cells was reduced in Nude mice. These observations indicate that the pool, but not the ontogeny, of primitive mTEPs is dependent on Foxn1. In this regard, Cld3,4$^+$ TECs have been previously reported in wild-type and Nude E11-12 thymic anlagen [11, 20]. Although these findings might indicate that mTEC commitment and maturation are independently regulated, it is challenging to demonstrate how Cld3,4^{hi}SSEA1$^+$ cells derived from Nude mice relate to their functionally identified Foxn1$^+$ counterparts [18]. On the other hand, the ontogeny of RANK$^+$ mTECs is dependent on Relb. These results implicate the non-canonical nuclear factor kappa B (NF-κB) pathway [1] as an important checkpoint in the regulation of RANK expression in mTEPs. Along these lines, previous studies demonstrate that RANK expression in embryonic TECs is controlled by activation of lymphotoxin beta receptor, a known inducer of NF-kB [21]. Further experiments are required to map the spatial location of RANK$^+$ and SSEA1$^+$ TECs in situ and define the identity of upstream receptors controlling the expression of RANK in vivo. Although RANK$^+$ mTEPs emerge temporally downstream of SSEA-1$^+$ mTEPs, the direct lineage relationship between these two subsets remains undetermined (Fig. 1). An alternative, and perhaps more speculative, scenario is that the segregation of Cld3,4^{hi}SSEA1$^+$ and Cld3,4^{hi}RANK$^+$ cells marks the initiation of alternative routes of embryonic mTEC differentiation.

The establishment of the medullary epithelial niche is a dynamic process that extends beyond embryonic life, so that the prototypical corticalmedullary compartmentalization is only achieved in the adult thymus. The observation that mTECs, in particular the Aire$^+$ subset, turn over at a rate of 7–10 days [22, 23] implicates a requirement for regular replacement by their (single or multiple) upstream progenitors. How mTEC niches are maintained across life has remained enigmatic until recently. One possibility is that the adult mTEC niche results from the expansion of embryonic-derived mTEPs. Cld3,4$^+$SSEA1$^+$ cells are

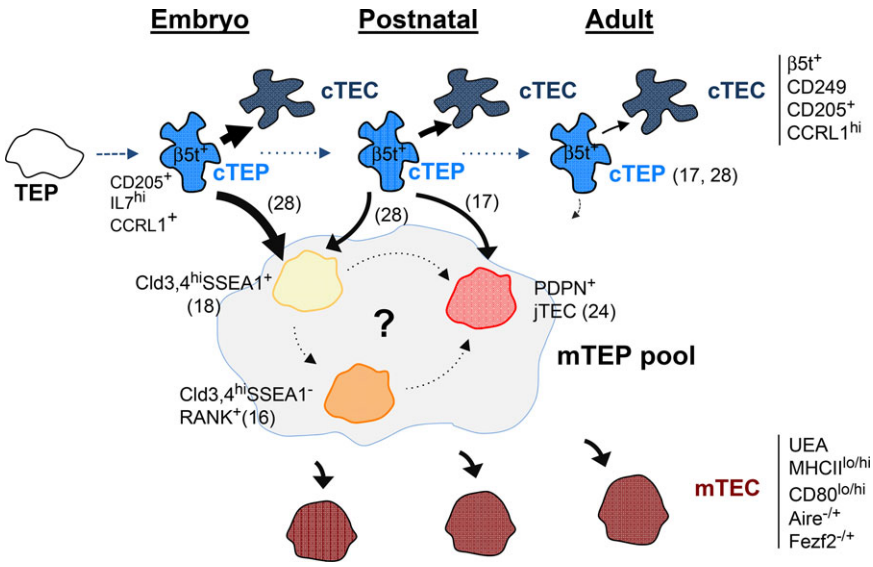

Figure 1. Spatial–temporal principles that underlie the development and maintenance of mTEC niches. This figure is based on the reports of Baik et al. [16], Mayer et al. [17], Ohigashi et al. [28], and other recent reports [18, 24]. Embryonic cTEC-like progenitors (cTEP) progress through cortical lineages and contribute to the development of cTECs and mTECs. The contribution of $\beta5t^+$ progenitors to the generation and maintenance of cTECs and mTECs is a developmental process that fades as life progresses (top). Three novel subsets of mTEC-restricted progenitors (mTEP) have been recently defined and represent the mTEP pool. Although $\beta5t^+$ progenitors are able to generate Cld3,4^{hi}SSEA1$^+$ [28] and PDPN$^+$jTECmTEPs [17], the direct precursors of Cld3,4^{hi}SSEA1$^-$RANK$^+$ cells remain unknown. Also, it is an open question whether the new mTEP subsets represent distinct mTEC lineages or various stages of a single differentiation program. Note: For simplicity other references used in the manuscript were excluded from the figure.

rare in the adult thymus, indicating that the pool of mTEPs is exhausted throughout life. In this respect, the recent identification of podoplanin$^+$ (PDPN) TECs, which reside at the corticomedullary junction (PDPN$^+$jTEC) and harbor the potential to generate nearly half of adult mTECs [24], has shed further light in the mTEC enigma. PDPN$^+$jTECs might represent one of the downstream, transiently amplifying subsets that contribute to maintain the adult medullary network (commented on [25]). Future studies on the ontogeny of PDPN$^+$jTECs as well as their spatial-lineage relationship to Cld3,4$^+$SSEA1$^+$ and Cld3,4$^+$RANK$^+$mTEPs are warranted (Fig. 1). A second possibility is that alternative temporal-restricted pathways might partake in the homeostasis of the adult medullary epithelial niche. This scenario implicates the new generation of mTEPs from bipotent progenitors. Recent reports have shown that distinct types of bipotent TEPs can be isolated from the adult murine thymus [26, 27], which in line with earlier reports [8], indicate that they persist in the postnatal life. Previous studies from Ohigashi et al. have demonstrated that the majority of adult mTECs descend from TEPs expressing beta5t ($\beta5t^+$), a cTEC-restricted marker [12]. As β5t is expressed in fetal TEPs [12], it is unclear whether the bipotent capacity is confined to embryonic progenitors, or a similar process is maintained in postnatal life. Nonetheless, the location and physiological contribution of TEPs to the maintenance and regeneration of the medulla remain unknown.

Now, Mayer et al. [17] and Ohigashi et al. [28] provide novel, and complementary, evidence that a large fraction of adult mTECs develop from fetal- and newborn-derived $\beta5t^+$ TEPs under physiological conditions. The groups of Holländer and Takahama engineered a new mouse line that expresses the reverse tetracycline transactivator (rtTA) under the control of Psmb11 (β5t) locus. β5t-rtTA knock-in mice were then crossed to transgenic mice which express the Cre recombinase under the control of doxycycline (Dox) and activate ZsGreen [17] or eGFP [28] reporter expression only after Cre-mediated recombination. Using this genetic inducible cell-fate mapping strategy, both studies follow the progeny of $\beta5t^+$ TEPs during adult life. The sensitivity of the new model was confirmed by performing prolonged Dox treatments, which span from early embryogenesis until birth or adulthood. In line with past observations [12], extended Dox treatment showed that $\beta5t^+$ progenitors generate the majorly of cTECs and mTECs in the young adult thymus. Interestingly, using a series of temporally restricted Dox regimens, both groups documented a differential involvement of $\beta5t^+$ TEPs of the embryonic, postnatal and adult thymus for the establishment of young adult mTECs. While Dox administration in the embryo labelled circa 70–80% of mTEC, the labelling efficiency declined to circa 20% when Dox was provided between birth and one week of age, and became marginal once Dox-treatment was administrated from 1 week onwards [17, 28]. These results indicate that the contribution of $\beta5t^+$ TEPs to the adult mTEC niche decreases with age. Worth noting, the labelling efficiency of cTECs also decreased, although to a lesser extent than mTECs, following Dox-treatment in young adult mice [17, 28]. A reduction in $\beta5t^+$ transcription in cTECs with age [28] might explain the discrepancy between the broad expression of β5t protein [12] and the limited labelling penetrance in adult cTECs. One cannot formally exclude the possibility that other (non-labelled) cell lineage(s) residing within the cortex contribute to the mTEC network. Nonetheless, both studies provide evidence that the majority of young adult mTECs arise from progenitors that express β5t during embryonic development, up to the first week of life (Fig. 1). Moreover, long-term analysis of embryonically and neonatally β5t-derived mTECs indicates that the maintenance of the adult medullary epithelium is likely assured by mTEPs which develop downstream of $\beta5t^+$ TEPs. In line with this view, Ohigashi and colleagues show that embryonic and postnatal $\beta5t^+$ progenitors give rise to Cld3,4^{hi}SSEA-1$^+$mTEPs [28]. On the other hand, not all mTECs of the aged thymus have a β5t-positive past. Despite the particularities of different reporter lines, several studies have described phenotypic heterogeneity within mTECs [4, 5, 19, 29]. Future studies are needed to address whether these examples point to the existence of alternative lineages of medullary

differentiation. Further experiments by Ohigashi et al. [28] indicate that embryonically/neonatally β5t-derived mTEPs are major participants in models of adult thymic medullary regeneration trigged by sub-lethal radiation or polyinosinic-polycytidylic acid (poly I:C) treatments. It is important to consider that complete mTEC depletion was, in this case, not achieved and thus intrathymic competition with resistant mTEPs might hinder the contribution of adult β5t progenitors in thymic regenerative responses [28]. Whatever the case may be, both studies imply the existence of distinct mechanisms controlling embryonic mTEC specification and postnatal mTEC maintenance. A second important finding is that $\beta5t^+$ progenitors preserved their bipotent capacity in the early postnatal period, indicating that TEPs might nestle in the cortical areas of the adult thymus. Using RTOC and a creative model which permits in vivo analysis of $\beta5t^+$ progeny at the clonal level, Mayer et al. present additional insights on the clonal progeny of $\beta5t^+$-derived mTEPs [17]. The authors show that $\beta5t^+$-derived TECs integrate in both the cortical and medullary region and form distinct clusters of clonal origin at the corticomedullary area, which presumably mark transit-amplifying mTEPs. Supportive of this view, postnatal $\beta5t^+$ progenitors are able to generate $PDPN^+$jTECs, inferring that the de novo formation of mTECs after birth contributes to the expansion of the medulla [24]. Given their particular spatial location, one can speculate that postnatal $\beta5t^+$-derived mTECs bridge discrete clonally derived medullary islets generated during embryonic period, providing the basis for the development of larger medullary areas of the adult thymus [9]. Although embryonically and neonatally β5t-derived mTECs express similar levels of genes coupled to the TNF receptor superfamily pathway, they differ in the expression of TNF receptor-associated factor 3 (TRAF3) and in some TRAs [28]. Future experiments must address whether postnatal-derived mTECs developed by the reiteration of the same differentiation pathways described to the fetal thymus [1]. Collectively, both reports highlight a critical, and yet restricted spatiotemporal contribution of $\beta5t^+$ progenitors to the mTEC differentiation (Fig. 1), supporting the notion that the adult mTEC compartment is (in part) maintained by unipotent mTEP(s).

Taken together with other recent discoveries [24, 26–29], the three new studies spark further avenues of investigation that need to be translated into experimental approaches to underpin, or argue against, current models of TEC differentiation [15, 30]. The plot thickens. One must consider that even with the most refined subsets, distinct TEC precursors are defined at the population level, but cannot be yet recognized as single cell. A major challenge is to define the nature and abundance of bipotent TEPs in the adult thymus. Furthermore, the physiologic contribution of all recently discovered mTEPs to the medullary compartment remains to be addressed. As a corollary, it will be of clinical relevance that researchers start applying the knowledge acquired in the last decade to potentially modulate TEC function to treat a broad range of thymic disorders, such as immunodeficiency and autoimmune disease.

Acknowledgments: Our studies are supported by a starting grant from European Research Council (StG_637843 to N.L.A) and FEDER funds through the Operational Competitiveness Programme COMPETE and by National Funds through *Fundação para a Ciência e Tecnologia* (FCT, Portugal) under the project PTDC/SAU-IMU/117057/2010 and N. L. A. and A.R.R. are respectively supported by the "Investigator FCT" and Ph.D. fellowship (SFRH/BD/78380/2011) programmes from FCT. We thank members of our laboratory for their contributions. We apologize for not referring to all primary literature owing to space limitations.

Conflict of interest: The authors declare no financial or commercial conflict of interest.

References

1 **Anderson, G. and Takahama, Y.**, Thymic epithelial cells: working class heroes for T cell development and repertoire selection. *Trends Immunol.* 2012. **33**: 256–263.

2 **Alves, N. L., Huntington, N. D., Rodewald, H. R. and DiSanto, J. P.**, Thymic epithelial cells: the multi-tasking framework of the T cell "cradle." *Trends Immunol.* 2009. **30**: 468–474.

3 **Sansom, S. N., Shikama-Dorn, N., Zhanybekova, S., Nusspaumer, G., Macaulay, I. C., Deadman, M. E., Heger, A. et al.**, Population and single-cell genomics reveal the Aire dependency, relief from polycomb silencing, and distribution of self-antigen expression in thymic epithelia. *Genome Res.* 2014. **24**: 1918–1931.

4 **Takaba, H., Morishita, Y., Tomofuji, Y., Danks, L., Nitta, T., Komatsu, N., Kodama, T. et al.**, Fezf2 orchestrates a thymic program of self-antigen expression for immune tolerance. *Cell* 2015. **163**: 975–987.

5 **Meredith, M., Zemmour, D., Mathis, D. and Benoist, C.**, Aire controls gene expression in the thymic epithelium with ordered stochasticity. *Nat. Immunol.* 2015. **16**: 942–949.

6 **Brennecke, P., Reyes, A., Pinto, S., Rattay, K., Nguyen, M., Kuchler, R., Huber, W. et al.**, Single-cell transcriptome analysis reveals coordinated ectopic gene-expression patterns in medullary thymic epithelial cells. *Nat. Immunol.* 2015. **16**: 933–941.

7 **Rossi, S. W., Jenkinson, W. E., Anderson, G. and Jenkinson, E. J.**, Clonal analysis reveals a common progenitor for thymic cortical and medullary epithelium. *Nature* 2006. **441**: 988–991.

8 **Bleul, C. C., Corbeaux, T., Reuter, A., Fisch, P., Monting, J. S. and Boehm, T.**, Formation of a functional thymus initiated by a postnatal epithelial progenitor cell. *Nature* 2006, **441**: 992–996.

9 **Rodewald, H. R., Paul, S., Haller, C., Bluethmann, H. and Blum, C.**, Thymus medulla consisting of epithelial islets each derived from a single progenitor. *Nature* 2001. **414**: 763–768.

10 **Gabler, J., Arnold, J. and Kyewski, B.**, Promiscuous gene expression and the developmental dynamics of medullary thymic epithelial cells. *Eur. J. Immunol.* 2007. **37**: 3363–3372.

11 **Hamazaki, Y., Fujita, H., Kobayashi, T., Choi, Y., Scott, H. S., Matsumoto, M. and Minato, N.**, Medullary thymic epithelial cells expressing Aire

represent a unique lineage derived from cells expressing claudin. *Nat. Immunol.* 2007. **8**: 304–311.

12 **Ohigashi, I., Zuklys, S., Sakata, M., Mayer, C. E., Zhanybekova, S., Murata, S., Tanaka, K. et al.**, Aire-expressing thymic medullary epithelial cells originate from beta5t-expressing progenitor cells. *Proc. Natl. Acad. Sci. U S A* 2013. **110**: 9885–9890.

13 **Baik, S., Jenkinson, E. J., Lane, P. J., Anderson, G. and Jenkinson, W. E.**, Generation of both cortical and Aire(+) medullary thymic epithelial compartments from CD205(+) progenitors. *Eur. J. Immunol.* 2013. **43**: 589–594.

14 **Ribeiro, A. R., Rodrigues, P. M., Meireles, C., Di Santo, J. P. and Alves, N. L.**, Thymocyte selection regulates the homeostasis of IL-7-expressing thymic cortical epithelial cells in vivo. *J. Immunol.* 2013. **191**: 1200–1209.

15 **Alves, N. L., Takahama, Y., Ohigashi, I., Ribeiro, A. R., Baik, S., Anderson, G. and Jenkinson, W. E.**, Serial progression of cortical and medullary thymic epithelial microenvironments. *Eur. J. Immunol.* 2014. **44**: 16–22.

16 **Baik, S., Sekai, M., Hamazaki, Y., Jenkinson, W. E. and Anderson, G.**, Relb acts downstream of medullary thymic epithelial stem cells and is essential for the emergence of RANK medullary epithelial progenitors. *Eur. J. Immunol.* 2016.

17 **Mayer, C. E., Zuklys, S., Zhanybekova, S., Ohigashi, I., Teh, H. Y., Sansom, S. N., Shikama-Dorn, N. et al.**, Dynamic spatio-temporal contribution of single beta5t+ cortical epithelial precursors to the thymus medulla. *Eur. J. Immunol.* 2016.

18 **Sekai, M., Hamazaki, Y. and Minato, N.**, Medullary thymic epithelial stem cells maintain a functional thymus to ensure lifelong central T cell tolerance. *Immunity* 2014. **41**: 753–761.

19 **McCarthy, N. I., Cowan, J. E., Nakamura, K., Bacon, A., Baik, S., White, A. J., Parnell, S. M. et al.**, Osteoprotegerin-mediated homeostasis of Rank+ thymic epithelial cells does not limit Foxp3+ regulatory T-cell development. *J. Immunol.* 2015. **195**: 2675–2682.

20 **Nowell, C. S., Bredenkamp, N., Tetelin, S., Jin, X., Tischner, C., Vaidya, H., Sheridan, J. M. et al.**, Foxn1 regulates lineage progression in cortical and medullary thymic epithelial cells but is dispensable for medullary sublineage divergence. *PLoS Genet.* 2011. **7**: e1002348.

21 **Mouri, Y., Yano, M., Shinzawa, M., Shimo, Y., Hirota, F., Nishikawa, Y., Nii, T. et al.**, Lymphotoxin signal promotes thymic organogenesis by eliciting RANK expression in the embryonic thymic stroma. *J. Immunol.* 2011. **186**: 5047–5057.

22 **Gray, D., Abramson, J., Benoist, C. and Mathis, D.**, Proliferative arrest and rapid turnover of thymic epithelial cells expressing Aire. *J. Exp. Med.* 2007. **204**: 2521–2528.

23 **Nishikawa, Y., Nishijima, H., Matsumoto, M., Morimoto, J., Hirota, F., Takahashi, S., Luche, H. et al.**, Temporal lineage tracing of Aire-expressing cells reveals a requirement for Aire in their maturation program. *J. Immunol.* 2014. **192**: 2585–2592.

24 **Onder, L., Nindl, V., Scandella, E., Chai, Q., Cheng, H. W., Caviezel-Firner, S., Novkovic, M. et al.**, Alternative NF-kappaB signaling regulates mTEC differentiation from podoplanin-expressing presursors in the cortico-medullary junction. *Eur. J. Immunol.* 2015. **45**: 2218–2231.

25 **Anderson, G. and Jenkinson, W. E.**, Border control: Anatomical origins of the thymus medulla. *Eur. J. Immunol.* 2015. **45**: 2203–2207.

26 **Ucar, A., Ucar, O., Klug, P., Matt, S., Brunk, F., Hofmann, T. G. and Kyewski, B.**, Adult thymus contains FoxN1(-) epithelial stem cells that are bipotent for medullary and cortical thymic epithelial lineages. *Immunity* 2014. **41**: 257–269.

27 **Wong, K., Lister, N. L., Barsanti, M., Lim, J. M., Hammett, M. V., Khong, D. M., Siatskas, C. et al.**, Multilineage potential and self-renewal define an epithelial progenitor cell population in the adult thymus. *Cell Rep.* 2014. **8**: 1198–1209.

28 **Ohigashi, I., Zuklys, S., Sakata, M., Mayer, C. E., Hamazaki, Y., Minato, N., Hollander, G. A. et al.**, Adult thymic medullary epithelium is maintained and regenerated by lineage-restricted cells rather than bipotent progenitors. *Cell Rep.* 2015. **13**: 1432–1443.

29 **Ribeiro, A. R., Meireles, C., Rodrigues, P. M. and Alves, N. L.**, Intermediate expression of CCRL1 reveals novel subpopulations of medullary thymic epithelial cells that emerge in the postnatal thymus. *Eur. J. Immunol.* 2014. **44**: 2918–2924.

30 **Hamazaki, Y.**, Adult thymic epithelial cell (TEC) progenitors and TEC stem cells: models and mechanisms for TEC development and maintenance. *Eur. J. Immunol.* 2015. **45**: 2985–2993.

Abbreviations: **Aire**: autoimmune regulator · **Cld**: claudin · **cTECs**: cortical TECs · **mTECs**: medullary TECs · **PDPN$^+$j**: podoplanin$^+$ TECs at the corticomedullary junction · **RANK**: receptor activator of NF-κB · **TECs**: thymic epithelial cells · **TEPs**: thymic epithelial progenitors · **TRAs**: tissue-restricted antigens

Full correspondence: Dr. Nuno L. Alves e-mail: nalves@ibmc.up.pt

See accompanying articles:
http://dx.doi.org/10.1002/eji.201545995
http://dx.doi.org/10.1002/eji.201546253

Received: 14/2/2016
Revised: 14/2/2016
Accepted: 1/3/2016
Accepted article online: 6/3/2016